Chapter 1: Introduction

1.1 Class B scavenger receptors

Scavenger receptors were originally defined as receptors involved in the binding and uptake of chemically modified lipoproteins such as acetylated (Ac-) or oxidized (ox-) low-density lipoproteins (LDL). The class B scavenger receptor family comprises a number of highly glycosylated cell surface membrane proteins that demonstrate a shared topology with respect to the plasma membrane, bind a wide variety of ligands and demonstrate a high degree of amino acid sequence similarity. CD36 is the founding member of this family and it has important roles in lipid metabolism, as an adhesion molecule and in the recognition of apoptotic cells. Other members of this family include lysosomal integral membrane protein II (LIMP-II) and scavenger receptor class B, type I (SR-BI). SR-BI has a critical role in reverse cholesterol transport, the process whereby excess cholesterol is acquired from the periphery by high density lipoproteins (HDL) and delivered to the liver and steroidogenic organs for the purposes of bile acid synthesis and secretion and steroid production respectively (reviewed in Trigatti et al., 2000). *Croquemort,* another member of this family, has been identified in *Drosophila melanogaster* where it has a role in the recognition and removal of apoptotic cells by hemocyte/macrophages (Hart et al., 1993, Franc et al., 1996). A silk moth olfactory neuron membrane protein, SnmP-1, has been identified as another member of the family (reviewed in Krieger, 2001).

With respect to nomenclature, fatty acid translocase (FAT) has been identified as the rat orthologue of CD36 (Abumrad et al., 1993), while CD36 and LIMP-II analogous protein-1 (CLA-1) has been identified as the human orthologue of rodent SR-BI (Calvo and Vega, 1993). For the sake of simplicity, human CD36 and the rat orthologue will both be referred to as FAT/CD36 herein. Similary, SR-BI will be used to describe both human and rodent orthologues of the molecule. With respect to splice variants, an approximately 57 kDa splice variant of human CD36, whose function is unknown, has been identified in an erythroleukemia cell line (Tang et al., 1994). A splice variant of SR-BI, known as SR-BII, has an alternate C-terminal cytoplasmic tail but the primary function of this splice variant is unclear at present (Webb et al., 1998).

1.2 Membrane topology and post-translational modification of FAT/CD36

FAT/CD36 is an 88-kDa membrane glycoprotein that, like other members of the class B scavenger receptor family, is anchored to the plasma membrane at both amino- and carboxy-termini and consists of a large extracellular loop that is heavily glycosylated. Human FAT/CD36 is predicted to contain 10 potential N-linked glycosylation sites that may be processed differently in different cell types (Greenwalt et al., 1992, Oquendo et al., 1989, Alessio et al., 1991).

Several studies have addressed whether one or both termini of the molecule are membrane-anchored. An early study by Pearce *et al.* suggested membrane anchorage of only the C-terminus, based on the detection of FAT/CD36 in the supernatant of transfected cells expressing a C-terminal truncation mutant of FAT/CD36 (Pearce et al., 1994). This finding was later refuted by two independent studies. Firstly, Tao *et al.* showed that a similar C-terminal truncation mutant, lacking the predicted transmembrane domain, could not be detected in the culture medium of transfected cells but was easily detectable in whole cell lysates and membrane fractions (Tao et al., 1996). Similarly, Gruarin *et al.* transfected cells with constructs that encoded FAT/CD36 lacking either one or both hydrophobic terminal domains. They found that both termini were membrane anchored; a result that was supported by the fact that an N-terminal FLAG epitope tag on wildtype FAT/CD36 was only detectable by immunofluorescent microscopy and flow cytometry following fixation and permeabilization of transfected cells (Gruarin et al., 2000). Importantly, this research also demonstrated that the N-terminal transmembrane domain of FAT/CD36 was required for efficient transport of the molecule to the plasma membrane and that its absence resulted in accumulation of the molecule in Golgi-like structures.

Biochemical analysis of human FAT/CD36 in transfected cell lines has revealed that the molecule is palmitoylated at cysteine residues on both the N- and C-terminal cytoplasmic domains of the molecule. Palmitoylation involves posttranslational addition of palmitate, a 16-carbon saturated fatty acid, by esterification to a cysteine residue. It is distinct from myristoylation, the covalent attachment of myristate (a 14-carbon saturated fatty acid), in that it is essentially only found in association with the cytoplasmic face of the plasma membrane (Sefton and Buss, 1987). Palmitoylation can play a role in targeting of proteins to membranes, protein-protein interactions and protein-lipid interactions. Furthermore,

because palmitoylation can be reversed, the attachment or removal of palmitate can potentially regulate the subcellular localization and function of proteins.

Investigations by Tao *et al.*, using site-directed mutagenesis to generate single or multiple cysteine to serine amino acid substitutions at cysteine residues 3, 7, 464 and 466, revealed that all four cysteines were could be palmitoylated in transfected HEK293 cells (Tao et al., 1996). Gruarin *et al.*, using similar cysteine amino acid substitution constructs transfected into COS-7 cells, confirmed these observations (Gruarin et al., 2000). Recently Malaud *et al.* showed that alanine substitution of cysteine residues in the C-terminal cytoplasmic tail of the molecule did not affect cell-surface expression significantly in HEK293 cells, or oxLDL binding and uptake mediated by the receptor (Malaud et al., 2002).

Interestingly, FAT/CD36 has been shown to form homodimers and homomultimers in platelets, and in COS-7 cells transfected with human FAT/CD36 cDNA expression constructs (Thorne et al., 1997). Multimerization of the molecule was attributed to disulphide bridging between cysteine residues located in the extracellular domain of FAT/CD36, given that multimers could be dissociated by treatment with a reducing agent and that alanine substitution of cysteine residues 3, 7, 464 and 466 in the cytoplasmic tails of the molecule did not inhibit multimerization. Homodimerization and multimerization may have important consequences with respect to the subcellular localization of the molecule. Authors of this work suggested that multimerization might play a role in intracellular retention of FAT/CD36 and targeting of the molecule to plasma membrane microdomains such as caveolae.

Based on the similar electrophoretic mobility of FAT/CD36 under reducing and non-reducing conditions, early reports suggested that intra-chain disulphide bonds were not present in FAT/CD36 (Oquendo et al., 1989, Tandon et al., 1989). However, a more recent reassessment by Gruarin *et al.* has found that intracellular processing and transport of FAT/CD36 is dependent on formation of one or more intra-chain disulphide bonds within the molecule (Gruarin et al., 1997). Differences in electrophoretic mobility of reduced and non-reduced FAT/CD36 were only visible after complete deglycosylation of the molecule with *N*-glycosidase. Since the difference in mobility between reduced and non-reduced samples generally reflects the distance between the cysteine residues involved in intra-chain disulphide bonds, the small difference in mobility detected by Gruarin *et al.* suggests

that the intra-chain disulphide bonds that are formed are probably within the extra-cellular loop and not between cysteine residues at the opposing termini of the molecule (or between adjacent cysteine residues at either terminus). This suggestion was confirmed by the fact that the mobility shift between reduced and non-reduced samples was seen also in transfected cells expressing FAT/CD36 with either an N-terminal truncation or where cysteine residues 3 and 7 were substituted with serine. Furthermore, pulse-chase experiments demonstrated that the reducing agent dithiothreitol (DTT) prevented the processing of the 74kDa FAT/CD36 precursor into a less mobile species, presumably by preventing disulphide bond formation in the Golgi.

1.3 FAT/CD36 ligands and distribution

FAT/CD36 binds a diverse array of ligands, indicating a range of alternative functions at different physiological sites throughout the body. FAT/CD36 demonstrates high binding affinity for modified (acetylated or oxidized) LDL (Endemann et al., 1993); the native lipoproteins HDL, LDL and VLDL (Calvo et al., 1998); long chain fatty acids (Abumrad et al., 1993); collagens I and IV (Tandon et al., 1989); thrombospondin-1 (TSP-1) (Asch et al., 1987); retinal photoreceptor outer segments (Ryeom et al., 1996); *Plasmodium falciparum* malaria-parasitized erythrocytes (Oquendo et al., 1989); apoptotic cells (Ren et al., 1995); and anionic phospholipids such as phosphatidylserine (PS) an phosphatidylinositol (PI) (Rigotti et al., 1995).

A range of cells and tissues express FAT/CD36. These include adipocytes, red skeletal muscle, cardiac muscle, microvascular endothelium, certain epithelia (retinal, mammary, small intestinal, sebaceous gland, circumvallate papillus), cells of the red pulp and marginal zones of the spleen and certain cells of hematopoietic lineage (erythrocytes, platelets, dendritic cells, monocytes/macrophages and megakaryocytes) (reviewed in Febbraio et al., 2001). Interestingly, despite initial reports of its absence (Abumrad et al., 1993), FAT/CD36 has recently been identified at high levels in the liver and in steroidogenic organs such as the adrenal glands, ovaries and testes (Zhang et al., 2003, Stahlberg et al., 2004).

With respect to the involvement of FAT/CD36 in lipid metabolism, two major functions have been identified. As described below, these are uptake of oxidised low-density

lipoproteins (oxLDL) by macrophages and uptake of long-chain fatty acids (LCFAs) by muscle and adipose tissues. However, FAT/CD36 may be involved in lipid metabolism in other tissues and in the study described herein, particular focus has been given to a potential role in hepatic LCFA uptake. Furthermore, given that FAT/CD36 binds high-density lipoproteins with high affinity and can mediate selective uptake of cholesteryl ester from these particles, albeit inefficiently (Gu et al., 1998, Connelly et al., 1999), the possible involvement of FAT/CD36 in hepatic HDL-lipid uptake has been re-assessed.

1.4 CD36 and accumulation of oxLDL by macrophages: an early event in the development of atherosclerosis

Atherosclerosis is the major cause of heart disease and stroke and is thus a major cause of morbidity in Western societies. Risk factors include inflammation, gender, and plasma cholesterol and triglyceride levels (reviewed in Eaton, 2005). The development of atherosclerosis initially involves the migration of monocytes into the vascular subendothelium, where they differentiate into macrophages. It is when these macrophages accumulate excessive amounts of lipoprotein-derived lipid that they become foam cells, which are the major constituent of atherosclerotic plaques that can restrict blood flow. The transendothelial migration of monocytes/macrophages into the subendothelium of the vascular wall and the transformation of these cells into foam cells is now regarded as a key interaction between inflammation and the process of atherogenesis (reviewd in Getz, 2005). Importantly, CD36 appears to play an important role in the accumulation of lipid by the subendothelial macrophages (Endemann et al., 1993). The nature of CD36-mediated binding and uptake of oxLDL, and the factors involved in regulation of CD36 expression by macrophages is, therefore, the subject of intense investigation. Over the last decade it has become clear that the source of the lipid accumulated in foam cells are oxidised low density lipoproteins (oxLDL) and that the receptor CD36 has a critical role in mediating the endocytosis of these modified lipoproteins (reviewed in Nicholson, 2004). This process, which appears to lack feedback control, is a reason why CD36 is considered to be pro-atherosclerotic.

Several lines of evidence indicate that CD36 is involved in the process of oxLDL uptake and foam cell formation. Firstly, Endemann *et al.* showed that transfection of 293 cells with CD36 cDNA conferred specific and high affinity binding of oxLDL and this oxLDL

was found to internalised and degraded (Endemann et al., 1993). These workers also demonstrated that anti-CD36 antibody could reduce oxLDL binding to the macrophage-like cell line THP-1 by ~50%. Nicholson *et al.* demonstrated binding of oxLDL to human monocyte-derived macrophages and transfected cell lines and showed the importance of the lipid moiety of the lipoprotein in CD36 binding (Nicholson et al., 1995).

The importance of CD36 in oxLDL uptake by macrophages and the relevance of this to development of atherosclerosis have been most convincingly demonstrated by investigations using CD36-null mice (Febbraio et al., 1999, Febbraio et al., 2000). Peritoneal macrophages from these mice demonstrated reduced binding and uptake of oxLDL compared with those isolated from control wild-type mice. Importantly, when CD36-null mice were bred onto a pro-atherogenic ApoE-null background, the resulting double-knockout mice were significantly protected from development of atherosclerotic lesions when compared to controls (Febbraio et al., 2000). These results provided strong evidence that CD36 expression by monocytes and macrophages has a physiologically significant role in the early events of atherogenesis.

In humans, CD36 deficiency has been demonstrated in some individuals and this blood group polymorphism, known as Nak^a, may manifest as one of two types; platelet CD36 deficiency (type II) or platelet and monocyte CD36 deficiency (type I) (Yamamoto et al., 1990). The type 1 polymorphism, which is more common in Africans, Japanese and other Asian populations, has been shown to result in a 40-60% decrease in monocyte/macrophage oxLDL binding, with reduced internalisation and accumulation of cholesteryl ester as compared to CD36 expressing monocytes/macrophages (reviewed in Febbraio et al., 2001). Furthermore, it has been reported that the ability of macrophages to produce pro-inflammatory cytokines in response to exposure to oxLDL is significantly reduced in macrophages isolate from CD36-deficient individuals (Janabi et al., 2000); a finding that is consistent with the pro-atherogenic potential of CD36.

As described earlier, the anti-atherogenic effects of CD36 deficiency include reduced binding of oxLDL by monocytes and macrophages, leading to reduced formation of foam cells and reduced secretion of pro-inflammatory cytokines. These positive aspects are countered by significant abnormalities in plasma lipid profiles in CD36-deficient individuals. As has been described in CD36-null mice (Febbraio et al., 1999, Febbraio et

al., 2000), CD36 deficiency in humans appears to contribute to a range of metabolic abnormalities, including significantly higher plasma triglyceride levels, lower HDL cholesterol levels, higher glucose levels, higher free fatty acid levels and insulin resistance (reviewed in Hirano et al., 2003).

1.4.1 Other mediators of oxLDL uptake by macrophages

Other receptors that have been implicated in the binding and uptake of modified LDL by macrophages include scavenger receptor class A types I and II (SR-A), CD68, lectin-like oxidized LDL receptor (LOX-1), scavenger receptor expressed by endothelial cells (SREC), scavenger receptor class B type I (SR-BI) and scavenger receptor for phosphatidylserine and oxidized lipoprotein (SR-PSOX) (reviewed in Kunjathoor et al., 2002). Of these, only SR-A has a proven role in oxLDL uptake *in vivo*. Investigations in SR-A knockout mice have demonstrated that these animals display partial inhibition of oxLDL or AcLDL uptake by macrophages and reduced development of atherosclerosis in hypercholesterolemic mice (Suzuki et al., 1997). The relative contributions of SR-A and CD36 to oxLDL uptake by macrophages have been assessed in SR-A and CD36 double-knockout mice (Kunjathoor et al., 2002). This research showed that the two molecules account for 75-90% of AcLDL and oxLDL degradation. This work also addressed the impact of the type and degree of oxidation on oxLDL uptake by macrophages derived from mice lacking one or both of the receptors. It was shown that CD36 was the major mediator of binding and degradation of LDL that had been oxidised mildly by copper ions or by the myeloperoxidase/hydrogen peroxide/ nitrite system, while SR-A contributed predominantly to the binding and degradation of LDL that had been oxidised extensively by copper ions (Podrez et al., 2000). Since minimally oxidised LDL is probably more representative of oxidised LDL *in vivo* (Podrez et al., 2000), it can be argued that CD36 is more significant in physiological uptake of oxLDL by macrophages.

1.4.2 Regulation of CD36 expression in macrophages

The regulation, and possibly dysregulation, of CD36 expression by macrophages has the potential to contribute to the transformation of monocyte/macrophages into lipid-laden foam cells. For this reason, macrophages have been a significant focus in research investigating the factors involved in regulation of CD36 expression and potential targets of

therapeutic intervention. Many different extracellular factors have been shown to modulate expression of CD36 by macrophages and several different intracellular pathways are involved. Whilst the details are beyond the scope of this review of the literature, the interested reader is directed to a detailed discussion by Nicholson and Hajjar of the factors that regulate expression of CD36 in macrophages; in particular the involvement of oxLDL and PPARγ (Nicholson and Hajjar, 2004). Some aspects of regulation are summarized in Figure 1-1.

1.5 FAT/CD36 and long-chain fatty acid transport

1.5.1 Long-chain fatty acid biology

Long chain fatty acids (LCFAs) play an important role in many aspects of cell biology and physiology (Figure 1-2). They are important precursors for rapid energy production through β-oxidation in mitochondria and peroxisomes; a process that is particularly important in tissues with high energy requirements such as cardiac muscle. The ability for storage of long chain fatty acids as neutral triglycerides in cytoplasmic lipid droplets is another important property. They also act as important precursors for lipid components of membranes such as phospholipids, biological mediators like eicosanoids and lipid molecules involved in signal transduction such as phosphoinositides. Furthermore, LCFAs can serve as important transcription factors for nuclear receptors involved in regulation of expression of genes involved in metabolism.

Although LCFAs can be released by hydrolysis of triglycerides and membrane lipids, they are also synthesized endogenously. De novo synthesis of LCFAs predominantly occurs in the liver and adipose tissue and is tightly regulated by enzymes such as acyl-CoA carboxylase and fatty acid synthase (Kusunoki et al., 2006). While most cells are capable of de novo synthesis of fatty acids, cells which have high energy requirements such as cardiac myocytes are highly dependent on exogenous fatty acids as substrates for β-oxidation in mitochondria. Similarly, cells that have a high capacity for fatty acid storage as neutral triglycerides, namely adipocytes, also depend upon the efficient import of exogenous fatty acids.

Figure 1-1. Involvement of CD36 in cholesterol transport in macrophages (adapted from (Nicholson, 2004)). Low-density lipoproteins (LDL) can become oxidatively damaged by nitric oxide (NO)-, hydrogen peroxide (H_2O_2)- and myeloperoxidase-dependent mechanisms. Oxidised LDL (oxLDL) can then be bound by CD36 on the macrophage cell-surface and endocytosed. Lipid metabolites (oxysterols and oxidized fatty acids) resulting from oxLDL degradation can then directly interact with the transcription factors peroxisome proliferators-activated receptor γ (PPAR-γ) and liver X receptor α (LXRα). Ligand-activated PPAR-γ heterodimerizes with the transcription factor retinoid X receptor (RXR), and binds PPAR-responsive elements (PPRE) in the promoters of numerous genes involved in lipid metabolism, including CD36, PPAR-γ and LXRα. Similarly, ligand-activated LXRα heterodimerizes with RXR and regulates transcription of numerous genes involved in lipid metabolism, including ATP-binding cassette transporter-class A1 (ABCA-1), which mediates efflux of cholesterol from the cell to extracellular acceptors (e.g high-density lipoprotein, HDL). Interaction of HDL with scavenger receptor class B type I (SR-BI) initiates signalling events that inhibit PPAR-γ-mediated regulation of gene expression. Similarly, the 'statin' class of inhibitors of cholesterol synthesis also inhibit PPAR-γ-mediated regulation of gene expression. Another class of drugs, known as thiazolidinediones (TZDs), which act as insulin-sensitizing agents, are potent ligands of PPAR-γ.

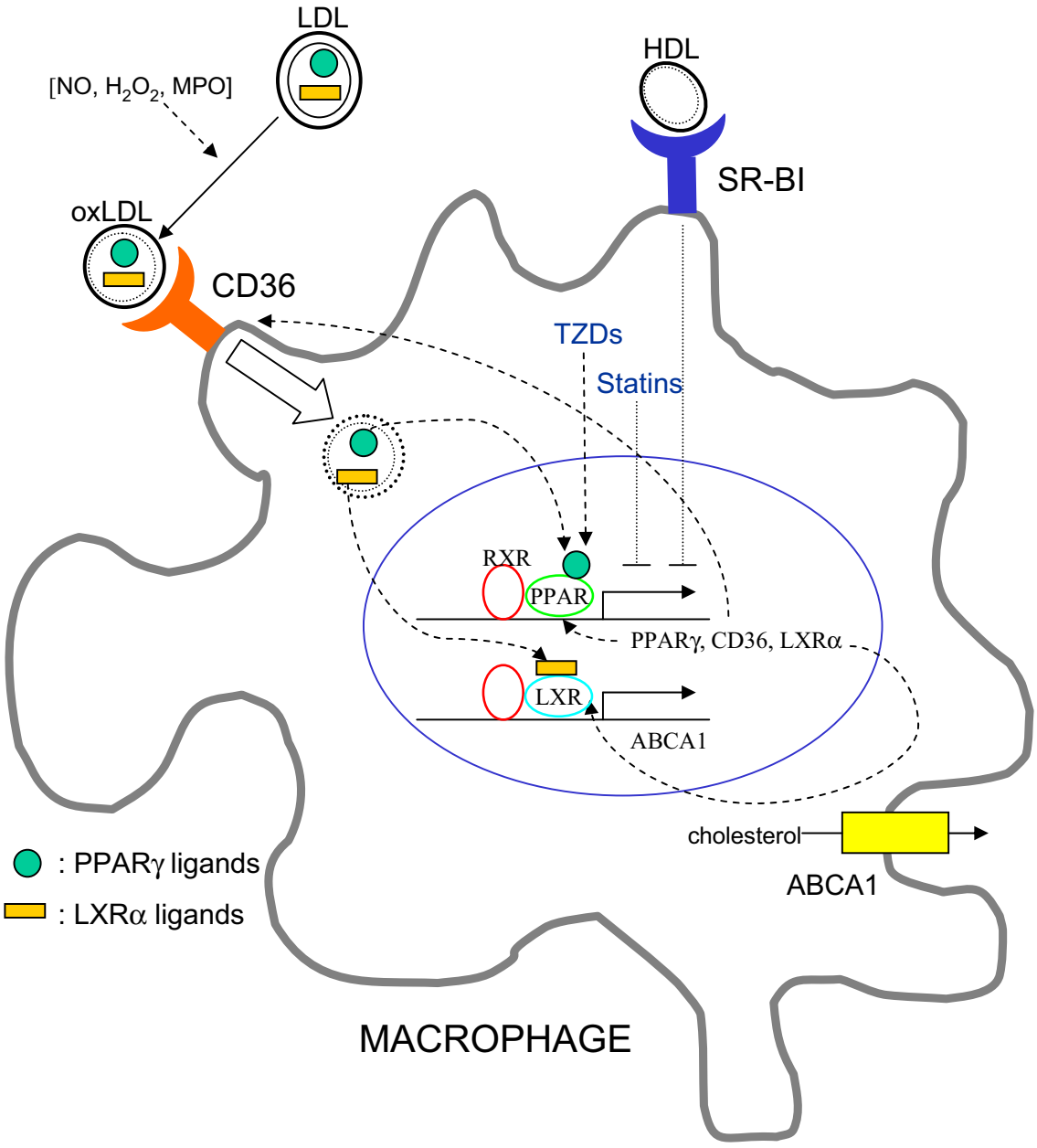
LDL
[NO, H_2O_2, MPO]
HDL
SR-BI
oxLDL
CD36
TZDs
Statins
RXR
PPAR
PPARγ, CD36, LXRα
LXR
ABCA1
cholesterol
ABCA1
: PPARγ ligands
: LXRα ligands
MACROPHAGE

Figure 1-1.

Figure 1-2. Model of protein-mediated long-chain fatty acid (LCFA) transport. Plasma membrane fatty acid binding protein (FABPpm) may bind LCFAs and facilitate their dissociation from albumin, such that passive diffusion or FAT/CD36-mediated transport across the plasma membrane ensues. Fatty acid transport protein (FATP1-6) may also transport LCFAs across the plasma membrane but also has acyl-CoA synthetase (ACS) activity. At the inner leaflet of the plasma membrane LCFAs likely associate with fatty acid binding proteins (FABPs) before their intracellular transport and esterification by acyl-CoA synthetases (ACS) to give acylCoAs. Long-chain fatty acylCoAs then serve as substrates in β-oxidation in mitochondria and peroxisomes, esterification of lipids (synthesis of triacylglycerol (TAG), phospholipids (PL) and cholesteryl esters (CE)), protein acylation (e.g. palmitoylation) and synthesis of biological mediators (e.g. eicosanoids).

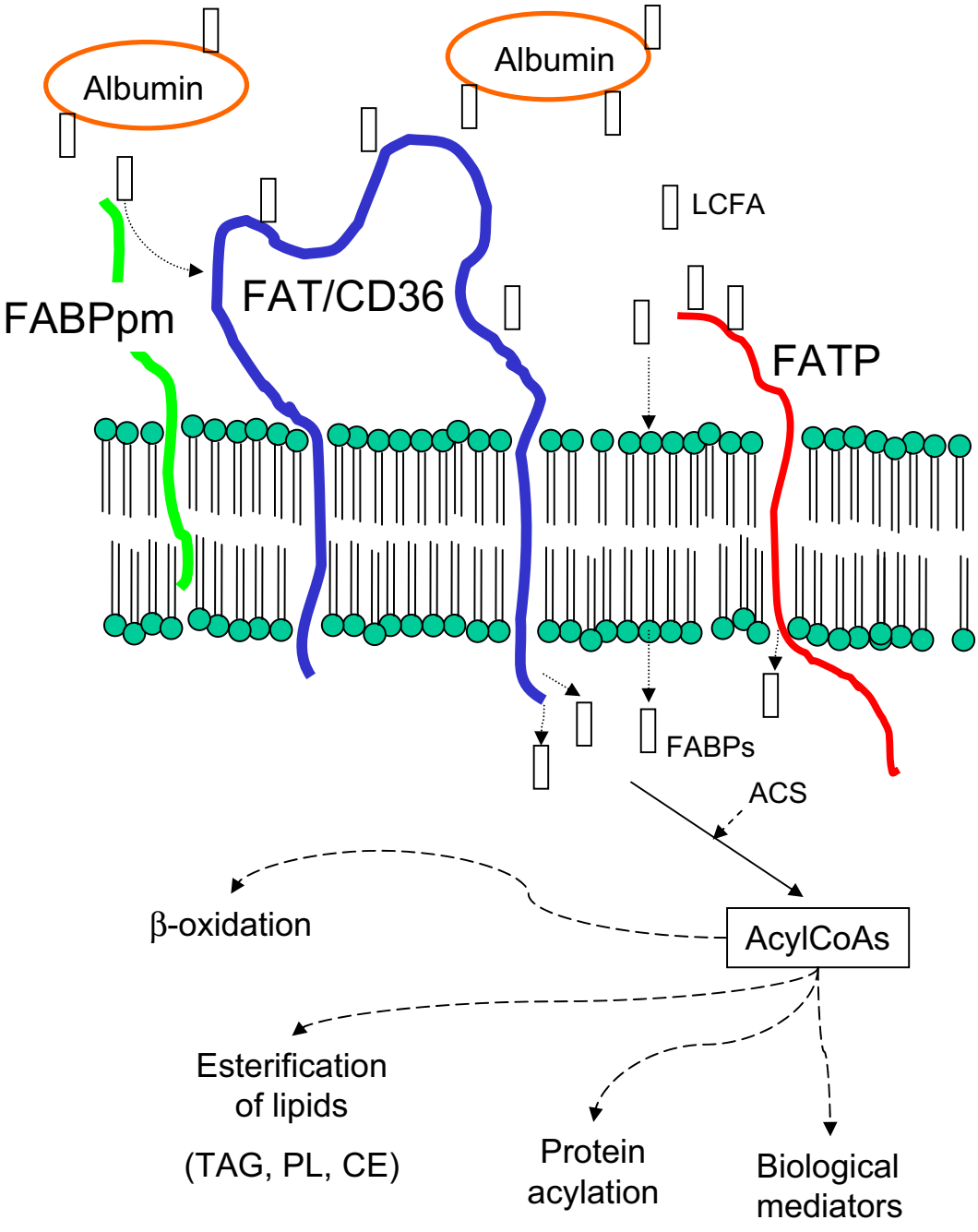
Albumin
Albumin
LCFA
FABPpm
FAT/CD36
FATP
FABPs
ACS
β-oxidation
AcylCoAs
Esterification
of lipids
(TAG, PL, CE)
Protein
acylation
Biological
mediators

Figure 1-2.

Since fatty acids are poorly soluble in aqueous environments, they are transported in the blood adsorbed to the surface of albumin or esterified to glycerol in the form of triacylglycerol in the core of lipoproteins. Upon release of fatty acids via dissociation from albumin or liberation from triglycerides by the action of lipases at the vascular endothelium, free fatty acids can be acquired by adjacent cells and utilized for energy production via β-oxidation in mitochondria or peroxisomes or they can be re-esterified to glycerol-3-phosphate for storage in cytoplasmic droplets as triglycerides. Alternatively, they may serve as substrates for the synthesis of membrane lipids or, less frequently, the synthesis of biological mediators such as eicosanoids. All of these outcomes require the initial conversion of fatty acid into acyl-CoA; a reaction catalysed by acyl CoA synthetases, which are localized at the inner leaflet of the plasma membrane (reviewed in Schaffer, 2002).

1.5.2 Passive diffusion of LCFA across the lipid bilayer

Several lines of evidence have demonstrated that LCFAs can enter cells through a receptor-independent process known as 'flip-flop' (Higgins, 1994). At physiological pH, LCFAs are readily ionized and movement of LCFA anions across lipid bilayers is slow (Schmider et al., 2000). However, movement of non-ionized fatty acids across lipid bilayers is rapid and mechanisms for protonation of LCFA anions at the membrane have been proposed (Hamilton and Kamp, 1999). Evidence of receptor-independent transport of LCFAs has probably been best provided by investigations using the fluorescent free LCFA indicator ADIFAB (Molecular Probes, Eugene, OR, USA). Two such studies used the indicator to demonstrate the rapid appearance of LCFAs in the aqueous phase of the interior of vesicles (models of lipid bilayers) and red blood cell ghosts (Kleinfeld et al., 1997, Kleinfeld et al., 1998). This transport was evident at high LCFA to BSA (carrier) ratios and showed no signs of saturation; further supporting the receptor-independent 'flip-flop' mechanism of LCFA transport. It should be noted that the process of LCFA uptake is only rendered unidirectional by the activity of acyl-CoA synthetase which catalyses the conversion of fatty acids into fatty acyl-CoA (reviewed in Schaffer, 2002).

1.5.3 Facilitated LCFA transport

Receptor-mediated or 'facilitated' transport of LCFAs is another mechanism whereby exogenous LCFAs can be acquired by cells. Early studies by Abumrad *et al.* were indicative of a receptor-mediated component of LCFA uptake (Abumrad et al., 1981, Abumrad et al., 1984). These experiments using isolated adipocytes demonstrated the presence of a saturable component of uptake that was specific for long-chain (>8-10 carbons) but not medium-chain fatty acids and was sensitive to proteases and phloretin, a potent inhibitor of membrane transport proteins. Similar studies investigating LCFA uptake in isolated rat hepatocytes suggested the presence of a receptor-mediated component of uptake that was saturable, energy-dependent and sensitive to inhibitors (Mahadevan and Sauer, 1974, Stremmel et al., 1986).

It is likely that both receptor-mediated and receptor-independent components of LCFA uptake represent separate pathways that serve different cellular requirements (Stump DD FanX 2001 JLR v42 p509). Overall, the component of LCFA uptake that is saturable and receptor-mediated is most significant at low LCFA to BSA molar ratios (<3). Conversely, when the ratio of fatty acid to albumin is greater than 3, LCFA uptake is predominantly the result of receptor-independent 'flip-flop' across the plasma membrane (reviewed in Schaffer, 2002). Given that lower ratios of fatty acid to albumin more closely represent physiological conditions it is appealing to suggest that receptor-mediated LCFA uptake is of greater physiological significance. Despite this, high free fatty acid levels have been observed in pathophysiological conditions and, at a given site, LCFAs released from lipoproteins by enzymes such as lipoprotein lipase may result in a local environment that is high in free fatty acids. Under these conditions passive diffusion or 'flip-flop' of LCFAs into cells may be of greater physiological relevance.

1.5.4 Proteins implicated in LCFA transport

1.5.4.1 FAT/CD36

FAT/CD36 was first identified as a fatty acid transporter in rats, based on its ability to bind a sulfosuccinimidyl LCFA derivative that inhibits LCFA uptake (Harmon and Abumrad, 1993). The molecule was covalently cross-linked to radiolabelled sulfosuccinimidyl-oleate

on the surface of rat adipocytes, purified and sequenced at its amino-terminal. The cDNA was then cloned and sequenced by Abumrad *et al.*, who showed that FAT was an orthologue of human CD36 and that its expression was induced during pre-adipocyte differentiation in culture (Abumrad et al., 1993). Research by Ibrahimi *et al.* later demonstrated that over-expression of FAT/CD36 in cultured fibroblasts resulted in increased LCFA uptake that was saturable, of high-affinity and sensitive to phloretin (Ibrahimi et al., 1996). However, a recent study by van Nieuwenhoven *et al.* demonstrated that LCFA uptake did not correlate directly with the levels of expression of FAT/CD36 in different clones after stable transfection of the rat heart muscle cell line H9c2 (Van Nieuwenhoven et al., 1998). This result suggested that expression of FAT/CD36 alone may not confer high-affinity LCFA uptake ability and that other cell-type specific factors may be necessary in this model.

Interestingly, recent research has identified a novel function for FAT/CD36 in the transfer of LCFAs into mitochondria (Campbell et al., 2004). While the carnitine-palmitoyl transferase (CPT) mechanism for transfer of long chain fatty acyl-CoA molecules across the mitochondrial membrane into the mitochondrial matrix is well established, it appears that FAT/CD36 may also contribute to this process, particularly when muscle energy requirements are elevated. This work showed that FAT/CD36 was present at high levels in purified skeletal muscle mitochondria and that its concentration in mitochondria correlated with the oxidative capacity of the muscle. Furthermore, addition of the FAT/CD36 inhibitor sulfo-*N*-succinimidyl oleate inhibited mitochondrial palmitate oxidation, while electrical stimulation of muscle increased the mitochondrial content of FAT/CD36.

The anatomical distribution of FAT/CD36 is consistent with an important role in LCFA metabolism. FAT/CD36 is found at high levels in adipose tissue, heart muscle and skeletal muscle; all of which have a high metabolic demand for fatty acids (Abumrad et al., 1993). Expression of the molecule in mammary gland epithelium may also reflect the high demand for LCFAs during lactation. Expression of FAT/CD36 by intestinal epithelium and microvascular endothelium is also consistent with a role in LCFA transport, given that each of these sites experiences flux of long chain fatty acids during absorption and delivery of fatty acids. Investigations using animal models of deficiency and over-expression of FAT/CD36, along with studies demonstrating acute regulation of FAT/CD36 localization to the plasma membrane in response to metabolic cues, provide the most

convincing evidence of the important role that the molecule plays in LCFA uptake and metabolism and these will be discussed in detail in subsequent sections.

1.5.4.2 FATP1

Another molecule that has demonstrated activity in fatty acid transport is fatty acid transport protein (FATP1). This 63kDa molecule was identified as a fatty acid transporter by Schaffer *et al.*, who used an expression/cloning strategy that involved transfection of a 3T3-L1 adipocyte cDNA library and screening of transfectants for enhanced uptake of a fluorescent LCFA analogue (Schaffer and Lodish, 1994). FATP1 consists of a least one transmembrane domain and multiple membrane-associated domains (Lewis et al., 2001). It is expressed predominantly in adipose tissue, skeletal muscle and cardiac muscle, all of which share a high capacity for fatty acid uptake either for storage or oxidation (Schaffer and Lodish, 1994, Abumrad et al., 1999).

FATP1 is the founding member of a family that now consists of six related proteins (FATP1-6) (reviewed in Stahl, 2004). Of this family, FATP4 is most similar to FATP1, with which it shares a similar tissue distribution (Stahl, 2004). It has been suggested that FATP4 may mediate basal fatty acid uptake while FATP1 may be involved in acutely regulated (i.e insulin regulated) fatty acid uptake. This is because FATP1 can rapidly translocate from intracellular sites to the plasma membrane following stimulation of adipocytes by insulin (Stahl et al., 2002) and FATP4 inactivation in mice results in embryonic or neonatal lethality (Gimeno et al., 2003a, Herrmann et al., 2003). FATP1 expression is also regulated at the level of transcription by the activity of peroxisome proliferator activated receptors α and γ (PPAR-α and -γ) (Martin et al., 1997, Motojima et al., 1998), further indicating that it plays the role of an acutely regulated fatty acid transporter. Of the remaining members of the FATP family, some are expressed exclusively in the liver (FATP2 and FATP5) and kidney (FATP5 only), while FATP3 is expressed in a broad range of tissues (Stahl et al., 2001). FATP6 is expressed exclusively in the heart (Gimeno et al., 2003b).

FATP1 shares approximately 40% amino acid sequence identity with the enzyme very long chain acyl-CoA synthetase (VLACS or ACSL), including an ATP binding motif that is common to all FATP isoforms and acyl-CoA synthetases (ACS) (Uchiyama et al.,

1996). Furthermore, site-directed mutagenesis of the ATP-binding motif of FATP1 abrogates its ability to mediate enhanced LCFA uptake in transfected cell lines (Stuhlsatz-Krouper et al., 1998, Stuhlsatz-Krouper et al., 1999). These and other results (reviewed in Schaffer, 2002) suggest that FATP1 might also have VLACS activity and that this could be its main activity, in that esterification of newly acquired fatty acids render their transport irreversible. Alternatively it may have both fatty acid uptake and esterification activity, as has been indicated by site-directed mutagenesis investigations involving its orthologue *FAT1* in *Saccharomyces cerevisiae* (Zou et al., 2002). Interestingly, recent studies have demonstrated that FATP1 and ACSL co-immunoprecipitate in 3T3-L1 adipocytes and that this interaction is probably constitutive because the degree of association between the molecules is not altered by manipulation of fatty acid uptake or lipolysis (Richards et al., 2006). This finding indicates that FATP1-mediated fatty acid uptake and FATP1- and/or ACSL-mediated acylation may be tightly inter-linked.

Finally, conclusive evidence of the importance of FATP1 in mediating fatty acid uptake/acylation has been provided by studies in FATP1-knockout mice. These mice, unlike FAT/CD36-knockout mice (Hajri et al., 2002), displayed no significant difference from wild-type controls in intramuscular fatty acid metabolite levels or skeletal muscle responsiveness to insulin, and neither did they display significant differences in plasma fatty acid or triglyceride levels (Kim et al., 2004). Furthermore, FATP1 KO mice displayed similar adiposity to wild-type controls when fed normal or high-fat diets. These mice were, however, protected from diet-induced diabetes and accumulation of intramuscular metabolites of fatty acids, suggesting a causal link between the two with FATP1 at the fulcrum. More recently, it has been demonstrated that insulin-induced LCFA uptake is lost in adipocytes of FATP1 KO mice and greatly reduced in skeletal muscle, while basal LCFA uptake was unchanged in both tissues (Wu et al., 2006). These effects were consistent with the finding that postprandial lipids were directed to liver in favour of muscle and adipose tissue in these mice.

1.5.4.3 $FABP_{PM}$

Plasma membrane fatty acid binding protein ($FABP_{PM}$) was first identified by Stremmel *et al.*, who purified the 40kDa protein from both rat liver plasma membrane and microvillous membranes of the small intestine, by exploiting affinity for [^{14}C]oleate (Stremmel et al.,

1985b, Stremmel et al., 1985a). A potential role in transport of LCFA import was suggested by purification of the molecule from plasma membranes of adipocytes and cardiac myocytes using the same technique (Potter et al., 1987). The protein was later shown to be identical to the mitochondrial enzyme mitochondrial aspartate aminotransferase (mAspAT) (Stump et al., 1993), which is found in both the mitochondrion and plasma membrane (Bradbury and Berk, 2000, Cechetto et al., 2002). Over-expression of mAspAT in fibroblasts has been shown to enhance saturable LCFA uptake (Isola et al., 1995). Further support for the role of $FABP_{PM}$ in LCFA uptake was provided by investigations demonstrating that an antibody directed against $FABP_{PM}$ inhibits LCFA uptake in isolated hepatocytes (Stremmel et al., 1986), cardiomyocytes (Luiken et al., 1999) and adipocytes (Zhou et al., 1992). Finally, regulation of $FABP_{PM}$ expression in skeletal muscle and adipose tissue is consistent with a role in LCFA uptake (reviewed in Brinkmann et al., 2002). Proof of the involvement of $FABP_{PM}$ in LCFA transport and metabolism *in vivo* was provided by a recent study demonstrating that over-expression of $FABP_{PM}$ in rat soleus muscle resulted in increased uptake of palmitate (Clarke et al., 2004). This increase was coincident with increased incorporation of palmitate into phospholipids and increased palmitate oxidation, while incorporation of palmitate into triacylglycerol was not affected.

1.5.4.4 Fatty acid binding proteins and fatty-acyl CoA synthetases

Although plasma membrane fatty acid transporters are a major focus of research into the mechanisms of cellular LCFA import, the contribution of cytoplasmic fatty acids binding proteins (FABPs) and fatty-acyl CoA synthetases (ACS) may be of equal importance. It is widely accepted that a component of cellular acquisition of LCFAs occurs via passive diffusion across the lipid bilayer (Figure 1-2). This process is rendered irreversible by the action of long chain fatty acyl CoA synthetases (ACLS) and fatty acid binding proteins (FABPs), which act as ‘sinks’ for LCFAs. By generating a concentration gradient of unesterified LCFAs across the plasma membrane, they may perpetuate diffusion of LCFAs into the cell. Similarly, enzymes involved in the downstream metabolism of LCFAs may also contribute to the transmembrane LCFA gradient and LCFA uptake, as has been demonstrated for 1-acyl-glycerol-3-phosphate acytransferase (Ruan and Pownall, 2001). The binding of LCFAs by FABPs and the esterification of LCFAs to acyl-CoAs at the inner leaflet of the plasma membrane are not only critical initial steps in the intracellular

transport and metabolism of LCFAs, but they also may prevent the accumulation of free fatty acids which can be toxic at high levels (reviewed in Atshaves et al., 2002).

To date, thirteen members of the cytoplasmic fatty acid binding protein ($FABP_c$) family have been identified (reviewed in van der Vusse et al., 2002). Of these, heart-type $FABP_c$ is the best characterized. The importance of $FABP_c$ in the uptake and utilization of LCFAs is highlighted by the impaired ability of cardiomyocytes from $FABP_c$-null to acquire and metabolise LCFAs (Binas et al., 1999, Schaap et al., 1999). It is thought that $FABP_c$ (and other FABPs) may bind LCFAs at the inner leaflet of the plasma membrane and participate in their transport to the mitochondrial outer membrane, where they are esterified and imported into the mitochondrial matrix for β-oxidation (Vork et al., 1997).

As discussed previously, esterification of LCFAs to (long-chain) fatty acyl-CoAs is the first step in the metabolism of fatty acids in mammalian cells. Within cells, acyl-CoAs may serve as substrates for β-oxidation, *de novo* synthesis or re-acylation of lipids (phospholipids, triacylglycerol and cholesteryl esters), fatty acylation of proteins or eicosanoid synthesis. Five different isoforms of long-chain acyl-CoA synthetase (ACSL) have been identified to date and these isoforms (ACSL1-5) differ somewhat in their tissue distribution, subcellular localization and substrate preference (chain length and degree of saturation) (Mashek et al., 2006). Given that the subcellular distributions of the isoforms do not overlap entirely, it has been suggested that regulation of their expression and/or activity may alter the intracellular fate of LCFAs (Mashek et al., 2004). Furthermore, cytoplasmic acyl CoA-binding protein (ACBP) may direct long-chain fatty acyl CoAs towards different metabolic pathways (Mashek et al., 2004). As described previously, very long-chain fatty acyl CoA synthetase (ACSVL) and FATP1 are other proteins with acyl-CoA synthetase activity that may impact on LCFA metabolism.

1.5.4.5 Caveolin-1, caveolae and lipid rafts

Whilst there is little evidence that caveolin-1 is a transporter of fatty acids *per se*, the possible importance of this molecule in fatty acid transport and metabolism has been difficult to assess, given the complex effects of caveolin-1 expression on plasma membrane fluidity, cholesterol homeostasis, vesicular transport and signal transduction. Although caveolin-1 is found at the inner leaflet of the plasma membrane, its ability to

bind fatty acids saturably (Trigatti et al., 1999, Pohl et al., 2004) has suggested that it may be involved in intracellular fatty acid handling (e.g transport to mitochondria or lipid droplets). Caveolin-1 is a 22-kDa integral membrane protein whose expression and oligomerization are both necessary and sufficient to induce the formation of morphological caveolae (Li et al., 1996, Fra et al., 1995). These plasma membrane microdomains, which are 50-100nm flask-shaped invaginations that are rich in cholesterol and sphingolipids, have been implicated in various aspects of lipid metabolism, including LCFA transport. Before considering the involvement of caveolae in LCFA transport and metabolism, however, it is important to first discuss similarities and differences between these structures and classical lipid rafts.

Caveolae represent a subset of classical lipid rafts, with which they share the properties of resistance to solubilization in low concentrations of non-ionic detergents (e.g Triton X-100, NP-40), a low buoyant density and enrichment with cholesterol, sphingolipids and Src-family tyrosine kinase signalling molecules (reviewed in Li et al., 2005). The biophysical properties of both structures constitute the basis for their biochemical isolation from cell membranes by lysis in non-ionic detergents, followed by flotation on sucrose density gradients (Brown and Rose, 1992, Simons and Ikonen, 1997). However, equating membrane fractions isolated by these procedures with lipid rafts / caveolae has drawn some criticism (Munro, 2003), because it is thought that this treatment could induce an artefactual aggregation of smaller raft membranes (Munro, 2003, Brown and London, 1998). For this reason, these membrane microdomains are often referred to as detergent-resistant membranes (DRMs), to distinguish them from 'native' rafts. Caveolae may be regarded as a subset of lipid rafts that have several important additional characteristics. Caveolae can be defined by their characteristic morphology, their enrichment with caveolin and their lack of glycosyl-phosphphatidylinositol (GPI)-anchored proteins (Smart et al., 1999). In contrast, classical lipid rafts lack a defined morphology and they are enriched in GPI-anchored proteins (Munro, 2003).

Cholesterol is thought to play an important role in determining structure and fluidity of biological membranes. For this reason, manipulation of caveolae and lipid raft function by either cholesterol-loading or cholesterol-depleting cells has provided a means to investigate the involvement of lipid rafts and/or caveolae in a variety of cell functions. Disruption of lipid rafts/caveolae by removal of cellular cholesterol with methyl-β-

cyclodextrin (MβCD) has been shown to result in reduced uptake of LCFAs by 3T3-L1 cells (Pohl et al., 2004) and HepG2 cells (Pohl et al., 2002). This effect is reversible because replenishment of cholesterol was found to re-instate the ability of the cells to mediate efficient LCFA uptake (Pohl et al., 2004). Similar inhibition of LCFA uptake results from treatment with the cholesterol binding agent filipin (Pohl et al., 2002), which, like other cholesterol binding agents such as nystatin, results in 'flattening' of flask-shaped caveolae (Rothberg et al., 1992). Moreover, this study found that 'loading' cells with cholesterol enhanced caveolin-1 expression and LCFA uptake (Pohl et al., 2004). Interestingly, a recent study by the same authors indicated that the inhibition of LCFA uptake in 3T3-L1 adipocytes treated with MβCD involved disruption of FAT/CD36 activity. The effects of specific inhibition of FAT/CD36 with sulfo-*N*-succinimidyl oleate (SSO) and depletion of lipid raft/caveolae by MβCD treatment were inter-active rather than additive (Pohl et al., 2005). This finding suggested that it may be the localization of FAT/CD36 to lipid rafts/caveolae, rather than the lipid rafts/caveolae *per se*, that is required for efficient protein-mediated LCFA uptake. This notion receives support from the demonstration that translocation of FAT/CD36 to the plasma membrane is prohibited in mouse embryonic fibroblasts (MEFs) derived from caveolin-1 knockout mice and that re-instatement of caveolin-1 expression in these cells resulted in translocation of FAT/CD36 to the plasma membrane and enhancement of LCFA uptake (Ring et al., 2006). Importantly, the effect of caveolin-1 deficiency and re-instatement could be correlated with changes in the localization and activity of FAT/CD36, because treatment of wild-type MEFs with the FAT/CD36-specific inhibitor sulfosuccinimidyl oleate (SSO) resulted in inhibition of LCFA uptake that was equivalent to that observed in caveolin-1-knockout MEFs.

With respect to the involvement of caveolae in cellular LCFA uptake, reduced uptake of radiolabelled oleate by HepG2 cells and 3T3-L1 adipocytes was observed after caveolus formation was inhibited by transfection with caveolin-1 antisense oligonucleotides or with a dominant negative caveolin mutant (Cav^{DGV}), respectively (Pohl et al., 2002, Pohl et al., 2004). This effect, however, may be an indirect result of disruption of caveolae and dysregulation of membrane cholesterol homeostasis, because the effect of Cav^{DGV} expression can be mimicked by MβCD treatment and reversed by cholesterol loading (Roy et al., 1999).

It is possible that the cholesterol content of the plasma membrane is a major determinant of cellular LCFA import and that it is the importance of caveolin-1 to membrane cholesterol homeostasis that connects caveolin indirectly to LCFA transport. Indeed, cellular cholesterol content correlates positively with caveolin-1 mRNA levels, suggesting that caveolin-1 may be a sensor of free cholesterol (Bist et al., 1997, Fielding et al., 1997). Interestingly, this correlation also extends to post-translational stabilization of caveolin-1 by cholesterol (Frank et al., 2002, Pohl et al., 2004). A recent study using transfected HEK 293 cell lines that express varying amounts of caveolin-1 demonstrated that caveolin expression correlated with cellular cholesterol levels and with the rate of fatty acid transport to the inner leaflet of the plasma membrane, possibly due to changes in the biophysical properties of the membrane (Meshulam et al., 2006). The rapid nature of fatty acid uptake and the lack of known putative fatty acid transporters in these cells suggested that diffusion was the primary mechanism of fatty acid import. These authors favoured a role for caveolin-1 in facilitating LCFA uptake by instigating the formation of cholesterol rich caveolae microdomains at the plasma membrane, across which LCFAs could diffuse more readily.

1.6 Animal models of FAT/CD36 deficiency and over-expression: Effects on LCFA metabolism

The generation and study of FAT/CD36-knockout and production of transgenic mice in which the molecule is over-expressed in muscle has demonstrated unequivocally the importance of FAT/CD36 in fatty acid metabolism. Firstly, investigations using FAT/CD36-null mice revealed that these mice had a significant increase in fasting plasma levels of non-esterified fatty acids and triglycerides when compared to age- and sex-matched wild type mice (Febbraio et al., 1999). Furthermore, adipocytes isolated from FAT/CD36-null mice demonstrated a significantly reduced uptake of radio-labeled oleate when compared to their wild-type counterparts. This difference was particularly evident at lower ratios of LCFA to albumin, suggesting that FAT/CD36 is important in the high-affinity component of LCFA uptake.

A more extensive investigation by Coburn *et al.* compared tissue deposition and metabolism of two iodinated LCFA analogues, 15-(*p*-iodophenyl)-3-(R,S)-methyl

pantadecanoic acid (BMIPP) and 15-(*p*-iodophenyl) pentadecanoic acid (IPPA), in FAT/CD36-null and wild-type mice (Coburn et al., 2000). These analogues were chosen for comparison because an earlier study showed a correlation between FAT/CD36 deficiency in humans and reduction of myocardial uptake of BMIPP (Tanaka et al., 1997). The 3-methyl group of BMIPP inhibits its β-oxidation, without affecting its incorporation into phospholipids, diglycerides and triglycerides, thus resulting in prolonged tissue retention. In comparison, IPPA is readily oxidized and behaves in a manner similar to native LCFAs. The results of this study showed that tissue deposition of both analogues was significantly reduced in heart (50-80%), skeletal muscle (40-75%) and adipose tissues (60-70%) from FAT/CD36-null mice as compared to wildtype controls. Conversely, tissue uptake of the analogues by other tissues from the FAT/CD36-null mice (liver, kidney, lung and small and large intestine) was either unaffected or greater. As might have been expected, the degree of reduction in BMIPP uptake in FAT/CD36-null muscle correlated with the known oxidative capacity of various muscles, such that uptake was most reduced in cardiac muscle and the muscle of the diaphragm.

An interesting additional finding in the FAT/CD36 knockout mice came from thin layer chromatographic (TLC) analysis of the incorporation of BMIPP into lipids extracted from heart, adipose and skeletal muscle tissues. There was a significant increase in radio-labelled diglycerides and a significant decrease of label in triglycerides in these tissues compared with those from wild-type mice. The authors suggested that, since the differences could not be attributed to changes in activity of microsomal enzymes diacylglycerol acyltransferase (DGAT) (responsible for conversion of diglycerides into triglycerides) or long chain acyl-CoA synthetase, FAT/CD36 in normal mice may contribute to channelling LCFAs towards metabolic pathways other than TAG synthesis. Since DGAT has a low affinity for acyl-CoA, then at lower levels of intracellular acyl-CoA the essential pathways of β-oxidation and phospholipid synthesis may normally be prioritised ahead of neutral lipid storage. This might explain why FAT/CD36-deficiency in these mice is essentially asymptomatic in under normal conditions.

The importance of FAT/CD36 in LCFA uptake and oxidation was further highlighted by investigations using muscle-specific over-expression of rat FAT/CD36 in transgenic mice (Ibrahimi et al., 1999). In these mice, expression of FAT/CD36 was controlled by the

muscle-specific creatine kinase promoter, leading to a 2-4-fold increase of FAT/CD36 in both cardiac and skeletal muscle. These mice had a slightly reduced body weight compared to age- and sex-matched wild-type controls and reduced adipose tissue as revealed by magnetic resonance spectroscopy. They also had reduced levels of plasma free fatty acids and triglycerides (in the VLDL fraction). Blood cholesterol levels were slightly reduced, although this was not attributable to a significant decrease in the cholesterol content of any of the major lipoprotein fractions. While blood glucose levels were significantly increased, insulin levels were not greatly affected and glucose tolerance curves were similar in transgenic and wild-type mice. Importantly, in isolated soleus muscle the contraction-induced increase in LCFA oxidation was greatly increased in transgenic mice (approximately 6-fold) compared to wild-type controls (approximately 2-fold). Overall, increased muscle uptake and oxidation of LCFAs in these mice probably resulted in lower plasma triglyceride levels, in part due to lower availability of fatty acids for hepatic triglyceride synthesis. Similarly, the increase in plasma glucose levels most likely resulted from a reduced requirement for glucose by the heart and skeletal muscle in the transgenic mice. The importance of FAT/CD36-mediated LCFA uptake in heart and skeletal muscle was further reinforced by recent assessment of the effect of transgenic rescue of FAT/CD36 expression in heart and skeletal muscle of FAT/CD36-null mice (Brinkmann et al., 2002). These mice are said to show almost completely normalized plasma levels of free fatty acid, triglyceride and glucose. Furthermore, assessment of fatty acid oxidation in soleus muscle from these mice showed normalization of both LCFA uptake and contraction-induced oxidation of LCFAs.

A recent investigation by Drover *et al.* assessed intestinal lipid secretion and clearance of chylomicrons from the blood by FAT/CD36-null and wildtype mice (Drover et al., 2005). Given that FAT/CD36 is expressed at high levels on the epithelium of the small intestine (Poirier et al., 1996), it was hypothesized that its absence would result in impaired uptake of dietary fatty acids and synthesis of triglycerides by enterocytes. Results showed that FAT/CD36-null mice fed a high-fat diet or given a fat bolus by gavage accumulated neutral lipid in the proximal intestine. Furthermore, direct measurement of lipid output suggested that lipoprotein secretion into mesenteric lymph was defective in FAT/CD36-null mice and that this defect most likely resulted from a reduced ability to synthesize triacylglycerols in the endoplasmic reticulum of enterocytes. This effect was overshadowed by reduced clearance of intestine-derived lipoproteins from the plasma by

FAT/CD36-null mice despite unaffected lipoprotein lipase activity. Overall this investigation demonstrated an important role for FAT/CD36 in dietary lipid absorption, efficient synthesis of triglycerides from dietary fatty acids and their packaging into chylomicrons.

Another rodent model, the spontaneously hypertensive rat (SHR), has also highlighted the contribution of FAT/CD36 to LCFA uptake. This strain of rat is the major animal model used in hypertension research and is reported to display a number of abnormalities with respect to lipid and carbohydrate metabolism including insulin resistance, hypertriglyceridaemia and abdominal obesity (reviewed in Aitman TJ Glazier AM 1999. Nature Genetics v21 p76). Research by Aitman *et al.* revealed that defects in both glucose and fatty acid metabolism mapped to the same locus on chromosome 4 (Aitman et al., 1997). FAT/CD36 was later identified as a defective gene on chromosome 4 in this strain. Importantly, FAT/CD36 protein could not be detected in adipocyte membrane preparations from SHR (SHR/NIH) rats. It should be noted that another SHR strain (SHR/Izm), which has been maintained in Japan, lacks the FAT/CD36 mutations described in the SHR/NIH strain but nonetheless develops insulin resistance (Gotoda et al., 1999). Interpretation of these findings is somewhat confused, however, by the fact that the two strains diverged long before they were inbred and a number of metabolic abnormalities have been observed in these rats.

The effect of FAT/CD36-deficiency in the SHR was further highlighted by investigations into the phenotype of rats in which a segment of chromosome 4 of the Brown Norway rat was transferred onto the SHR background (SHR-Brown Norway)(Pravenec et al., 1999). When compared to SHR, these rats demonstrated reduced hyperinsulinaemia, hyperlipidaemia, blood pressure and diet-induced glucose intolerance. Since these effects could not be directly linked to functional reinstatement of FAT/CD36 alone, Pravenec *et al.* also assessed the phenotype of rats resulting from transgenic gene-rescue of SHR FAT/CD36 (Pravenec et al., 2001). Results showed that these rats displayed a reduction in insulin resistance and reduced levels of plasma free fatty acids and insulin. These findings contributed to the growing appreciation of the link between FAT/CD36-deficiency and type 2 diabetes.

A more comprehensive assessment of fatty acid transport in the heart and adipose tissue of the SHR by Hajri T *et al.*, revealed that SHR demonstrated reduced tissue uptake of the LCFA analogue BMIPP in heart and adipose tissue when compared to rats of the SHR-Brown Norway strain (Hajri et al., 2001). More evident was the heightened tissue uptake of the radiolabelled glucose analogue ^{18}F-fluorodeoxyglucose (^{18}F-2-FDG) in the heart and diaphragm muscle of SHR. Given that heart and diaphragm muscle are highly reliant on exogenous fatty acids as a fuel source for β-oxidation, this increase in glucose uptake most likely reflected a compensation effect in the absence of FAT/CD36. These findings were also confirmed by *in vitro* assessment of LCFA and glucose uptake in isolated cardiomyocytes and adipocytes from these rats.

1.7 FAT/CD36 deficiency in humans and LCFA metabolism

FAT/CD36 deficiency is relatively common in Asian and African populations with different reports suggesting that between 0.3 and 11% of these populations carry null-mutations in the FAT/CD36 gene (reviewed in Brinkmann et al., 2002). FAT/CD36 deficiency in humans was originally identified as a blood group polymorphism known as Nak^a, which may manifest as one of two types; platelet FAT/CD36 deficiency (type II) or platelet and monocyte FAT/CD36 deficiency (type I) (Yamamoto et al., 1990). With respect to type II FAT/CD36 deficiency, a number of studies have demonstrated defective uptake of the radiolabelled LCFA analogue, BMIPP by the hearts of FAT/CD36-deficient subjects (Nozaki et al., 1999, Tanaka et al., 2001). Given that the heart is highly dependent on fatty acids as a source of energy, FAT/CD36 deficiency has been suggested as a contributing factor to development of cardiomyopathies (Tanaka et al., 1997).

FAT/CD36 deficiency in humans has also been linked to insulin resistance (reviewed in Hirano et al., 2003). Like FAT/CD36-null mice, FAT/CD36-deficient humans were found to demonstrate elevated plasma triglyceride and glucose levels and reduced HDL-cholesterol levels compared to age-matched controls (Miyaoka et al., 2001b, Kuwasako et al., 2003). Furthermore, FAT/CD36-deficient subjects were found to be insulin-resistant as demonstrated by tests involving the use of the hyperinsulinemic euglycemic clamp (Miyaoka et al., 2001a). Another abnormality in lipid metabolism that has recently been identified in FAT/CD36-deficient humans relates to an increase in small intestine-derived lipids associated with postprandial hyperlipidemia (Kuwasako et al., 2003). These results

were analogous to results obtained by Drover *et al.* in studies of intestinal LCFA uptake and metabolism in FAT/CD36-null mice (Drover et al., 2005), and suggest a relationship between FAT/CD36-deficiency and lipoprotein abnormalities that is related to defects in LCFA metabolism.

1.8 Regulation of FAT/CD36 expression and activity in muscle and adipose tissue

Expression of FAT/CD36 in muscle and adipose tissue is regulated at many levels. These may include transcriptional regulation, translational regulation, regulation of translocation of the molecule to the plasma membrane and regulation of post-translational modification of the protein. Furthermore, regulation of the functional activity of the molecule may also depend on its subcellular localization and the presence and activity of associated molecules in its microenvironment.

1.8.1 Transcriptional regulation of FAT/CD36 in muscle and adipose tissue

The initial identification of FAT/CD36 as a fatty acid translocase by Abumrad *et al.* also identified that its expression was upregulated during differentiation of pre-adipocytes into adipocytes (Abumrad et al., 1993); a change that coincides with increased uptake of long chain fatty acids (Abumrad et al., 1991). This change, however, cannot be attributed to increased FAT/CD36 expression alone, as other candidate fatty acid transporters $FABP_{PM}$ and FATP1 are also upregulated by this process (Zhou et al., 1992, Schaffer and Lodish, 1994). Indicative of a role in LCFA transport, FAT/CD36 mRNA expression was strongly induced in preadipocytes by both saturated and unsaturated LCFAs but not short-chain fatty acids (Sfeir et al., 1997). Importantly, this research demonstrated that fatty acid-induced FAT/CD36 expression was reversible by removal of the fatty acids and that a non-metabolized LCFA analogue, 2-bromopalmitate, could similarly mediate induction of FAT/CD36 mRNA expression. Similarly, LCFAs and thiazolidinediones (TZDs), which are potent activators for the nuclear receptor PPARγ, induce preadipocyte differentiation and upregulation of FAT/CD36 mRNA expression (Amri et al., 1995, Teboul et al., 1995).

Peroxisome proliferator-activated receptors (PPARs) are nuclear transcription factors that control expression of a number of genes involved in lipid metabolism. The PPAR family includes the receptors PPAR-α, PPAR-γ and PPAR-δ that have distinct but sometimes

overlapping tissue distribution patterns and functions related to lipid metabolism. PPARs heterodimerize with retinoid X receptors (RXRs) and regulate target gene transcription via binding to peroxisome proliferators responsive elements (PPREs) in promoter DNA (reviewed in Bonen et al., 2004). Activation of gene expression, however, requires the recruitment of coactivator molecules and this recruitment relies on PPAR activation by their ligands; saturated and unsaturated LCFAs and their derivatives. In this way regulation of expression of genes involved in lipid metabolism can be dictated by the level and nature of lipid metabolites via their interaction with PPARs. With respect to the tissue distribution of the members of the PPAR family, PPARγ is primarily expressed in adipose tissue, spleen, adrenal glands, colon, macrophages and T cells. PPARα is mainly expressed in liver, heart, kidney, adrenal glands, endothelial cells, macrophages and smooth muscle cells. PPARδ is found in a wide range of tissues and cell types (reviewed in Li and Glass, 2004).

Several lines of evidence have suggested that peroxisome proliferator-activated receptors (PPARs) play an important role in regulation of FAT/CD36 expression during adipocyte differentiation. Studies by Bastie *et al.* demonstrated that overexpression of a dominant-negative mutant of PPARδ inhibited LCFA-induced PPARγ induction, preadipocyte differentiation and induction of FAT/CD36 mRNA expression in 3T3C2 fibroblasts (Bastie et al., 1999). Conversely, they showed that overexpression of wildtype PPARδ enhanced LCFA-induced FAT/CD36 expression in the same cell type. Similarly, another study demonstrated that overexpression of PPARδ in fibroblasts conferred responsiveness to fatty-acid induced FAT/CD36 expression (Amri et al., 1995).

Structural and functional analysis of the proximal mouse FAT/CD36 promoter by promoter/reporter assays has revealed that FAT/CD36 expression in adipose tissue is dependent upon PPARγ and PPARδ-activated transcription (Teboul et al., 2001). This study identified two imperfect peroxisome-proliferator-responsive elements (PPREs) located at -245 to -233 base pairs and -120 to -108 base pairs from the transcriptional start site. Progressive deletion analysis of minimal FAT/CD36 promoter (-555 to +6) revealed that reporter activity was almost undetectable when constructs were transiently transfected into undifferentiated $C_2C_{12}N$ cells or $C_2C_{12}N$ cells directed to differentiate into myotubes. Reporter activity was, however, highly induced when constructs were transfected into

$C_2C_{12}N$ cells directed to differentiate in adipocytes and this activity was greatly diminished (3-fold) in constructs lacking the region between -309 and -170. Site-directed mutagenesis of the putative PPREs revealed that mutation of either of the sites greatly reduced reporter activity (>2-fold) while mutation of both sites resulted in a near-complete loss of reporter activity. Finally, reporter assays involving PPAR agonists, 2-bromopalmitate and BRL 49653 and electrophoretic mobility-shift assays using purified PPARγ- and PPARδ-RXR heterodimers confirmed the involvement of PPARs and the identified PPREs in induction of FAT/CD36 expression in adipocytes.

A more recent study reported the identification of two different transcription initiation sites located 16 kilobases apart in the mouse FAT/CD36 promoter which resulted in transcription of at least 3 different mRNA isoforms with different 5' non-coding regions (Sato et al., 2002). They also identified a new transcriptional initiation site and upstream promoter in the human FAT/CD36 gene that was approximately 14 kilobases upstream of the previously identified transcriptional initiation site. In contrast to the findings of Teboul *et al.*, this research found that only the distal upstream promoter responded to PPARα and PPARγ ligands in a cell type-specific manner. Furthermore, they could not identify PPREs in the promoter and concluded that PPARs may induce transcriptional activation of FAT/CD36 expression via an indirect mechanism. The identification of several different putative transcription factor binding sites, including sterol regulatory elements (SREs) and Sp-1 sites, in both the human and mouse distal upstream promoters may represent a means by which PPAR-independent mechanisms can regulate FAT/CD36 mRNA transcription.

Recently, the discovery of a fifth alternative promoter and (non-coding) first exon of the human CD36 gene and a comprehensive investigation of the tissue-specificity of expression of all five first exons in humans has shed light upon the complex nature of transcriptional regulation of *CD36* gene expression (Andersen et al., 2006). This study demonstrated that expression of the alternative first exons varied between tissues and cell types and that the upstream regions of each promoter differed with respect to the presence and nature of putative transcription factor binding sites. Interestingly, however, in macrophages expression of all five first exons was upregulated in response to exposure to oxLDL, suggesting that commonalities exist in the presence of certain regulatory elements or, alternatively, that control mechanisms for the entire locus exist.

In the heart, regulation of FAT/CD36 expression by PPARα has been indicated by the observation that expression of a number of genes involved in fatty acid uptake and oxidation, including FAT/CD36, is downregulated in the hearts of PPARα-null mice (Leone et al., 1999). Conversely, transgenic mice overexpressing PPARα in a heart-specific manner demonstrate heightened expression levels of FAT/CD36 and other genes involved in fatty acid uptake and utilization; a response that coincides with reduced rates of fatty acid oxidation (Finck et al., 2002).

1.8.2 Regulation of FAT/CD36 translocation to the plasma membrane of adipocytes and cardiac and skeletal myocytes

An emerging mechanism of regulation of FAT/CD36 activity at the cell surface is the identification of regulated translocation of FAT/CD36 from cytoplasmic pools to the cell surface. This mechanism, which has been identified in muscle, may allow for rapid changes in fatty acid uptake in response to changes in energy demand. This phenomenon was first identified by Bonen *et al.* who investigated changes in palmitate uptake and FAT/CD36 expression in contracting muscle (Bonen et al., 2000). They had previously shown that chronic muscle stimulation resulted in increased FAT/CD36 expression and increased LCFA uptake into giant sarcolemmal vesicles (Bonen et al., 1999). These vesicles are prepared from skeletal muscle and represent a useful model of LCFA uptake across the sarcolemma because uptake is not coupled to metabolism (Roy et al., 1997). These investigations demonstrated heightened levels of palmitate uptake and plasma membrane FAT/CD36 expression in giant sarcolemmal vesicles prepared from contracting muscle as compared to vesicles prepared from resting muscle. This effect was evident after very short periods of muscle stimulation and was inhibited by sulfo-*N*-succinimidyl oleate, an inhibitor of FAT/CD36-mediated LCFA uptake. Density gradient fractionation of muscle samples revealed that the increase in plasma membrane FAT/CD36 levels coincided with a decrease in intracellular FAT/CD36 levels, an effect that is analogous to contraction-induced translocation of GLUT-4, a receptor involved in facilitated glucose import (Goodyear et al., 1991).

Translocation of FAT/CD36 from intracellular stores to the plasma membrane is also regulated by insulin. Investigations using perfused rat hindlimb muscles have revealed that

insulin treatment enhances palmitate uptake and incorporation into phospholipids, diglycerides and triglycerides but results in decreased oxidation (Luiken et al., 2002a). This effect coincided with a shift in FAT/CD36 protein from intracellular pools to the plasma membrane. Similarly, in isolated rat cardiomyocytes, insulin treatment results in dose-dependent upregulation of FAT/CD36 expression and translocation of FAT/CD36 protein from intracellular stores to the plasma membrane (Chabowski et al., 2004). Unlike FAT/CD36, results showed that FABPpm expression and localization was not effected by insulin.

A number of studies have investigated the signalling pathways involved in translocation of FAT/CD36 from intracellular stores to the plasma membrane of myocytes in response to insulin exposure or contraction. Interestingly, experiments comparing insulin-induced and (electrical) contraction-induced enhancement of palmitate uptake by cardiac myocytes demonstrated that the signalling pathways (PI-3 kinase-dependent) involved in insulin-induced translocation of FAT/CD36 and enhancement of LCFA uptake were not involved in contraction-induced enhancement of LCFA uptake and that the effects of these stimuli were additive (Luiken et al., 2002b). These results demonstrated that insulin- and contraction-induced enhancement of LCFA uptake involves different signalling pathways and different intracellular FAT/CD36 reservoirs. Furthermore, as might be expected, the metabolic fate of LCFA was found to differ between insulin-stimulated and contraction-stimulated cardiac myocytes, in that LCFA oxidation was only significantly enhanced by contraction while LCFA esterification was only significantly enhanced by exposure to insulin. Similarly, in isolated contracting muscle insulin causes further enhancement of LCFA uptake but causes a shift in LCFA metabolism away from utilization (oxidation) and towards storage (triacylglycerol synthesis) (Dyck et al., 2001). The signalling pathways involved in the translocation of FAT/CD36 from intracellular depots to the plasma membrane are summarized in Figure 1-3.

Recently, a comprehensive study by Coort *et al.* investigated the effects of insulin and contraction on the subcellular distribution of FAT/CD36, LCFA uptake and the fate of LCFAs in cardiac myocytes isolated from lean and obese Zucker rats (Coort et al., 2004). Compared to lean controls, cardiac myocytes isolated from obese Zucker rats demonstrated heightened LCFA uptake, LCFA esterification into triglycerides and translocation of FAT/CD36 to the plasma membrane. Overall, the permanent translocation

Figure 1-3. Contraction- and insulin-stimulated translocation of long-chain fatty acid (LCFA) transporters (FAT/CD36) and glucose transporters (GLUT4) from intracellular depots to the plasma membrane in muscle. Insulin binds the insulin receptor at the plasma membrane, inducing tyrosine phosphorylation of the insulin-receptor substrate (IRS) and a signalling cascade involving phosphatidylinositol 3-kinase (PI3-kinase) and Akt, which culminates in translocation of FAT/CD36 and GLUT4 from intracellular reservoirs to the plasma membrane (PM). Inhibitors of PI3-kinase signalling (LY-294002 and wortmannin) inhibit translocation of these membrane transporters to the plasma membrane. Contraction, and the contraction-mimetic oligomycin induce elevated intracellular cAMP levels which activate AMP kinase (AMPK). AMPK is also activated by AICAR, another contraction mimetic. AMP kinase-dependent signalling events culminate in the translocation of FAT/CD36 and GLUT4 from intracellular depots to the plasma membrane. The phosphodiesterase (PDE) inhibitor, dipyridamole (DPY), inhibits signalling events downstream of AMPK to inhibit translocation of FAT/CD36 and GLUT4. Adapted from (Luiken et al., 2004).

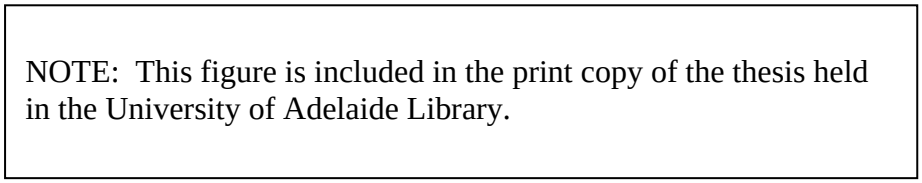
NOTE: This figure is included in the print copy of the thesis held in the University of Adelaide Library.

Figure 1-3.

of FAT/CD36 to the sarcolemma of cardiac myocytes in obese rats was thought to be responsible for excessive cardiac triglyceride accumulation and their resistance to further insulin-stimulated changes in LCFA uptake and metabolism. These results may indicate that the obesity and hyperinsulinemia of obese Zucker rats accelerates the development of cardiomyopathy due to a permanent shift of FAT/CD36 from intracellular reservoirs to the sarcolemma of cardiac myocytes.

Further evidence that contraction and insulin action differentially regulate the translocation of fatty acid transporters from intracellular depots to the plasma membrane was provided by a comprehensive study of the subcellular distribution of FAT/CD36, FABPpm and FATP1 in rat cardiac myocytes subjected to insulin or the contraction-mimetic AICAR (Chabowski et al., 2005). Results confirmed that insulin and AICAR induced translocation of FAT/CD36 to the plasma membrane, while only AICAR induced translocation of FABPpm and neither AICAR nor insulin induced FATP1 translocation in these cells. Parallel treatment of cardiac myocytes in conjunction with FAT/CD36-inhibition with SSO and analysis of palmitate uptake revealed that FABPpm appeared to enhance FAT/CD36-mediated LCFA uptake but alone was unable to enhance uptake. This finding suggested that FAT/CD36 and FABPpm act cooperatively in LCFA uptake in cardiac myocytes and contrasts another study demonstrating that FABPpm overexpression in skeletal muscle enhances LCFA uptake without concomitant changes in the content of FAT/CD36 in the plasmalemma (Clarke et al., 2004).

A transcription factor that has recently been implicated in regulation of FAT/CD36 translocation to the plasma membrane is the forkhead transcription factor FoxO1 (Bastie et al., 2005). FoxO1 is expressed in a number of tissues involved in lipid metabolism including liver, muscle and adipose tissue and its activity is suppressed by phosphorylation which results from insulin and insulin-like growth factor-I signalling pathways (Farmer, 2003). FoxO1-mediated regulation of fatty acid metabolism was further investigated using transfection of wildtype, constitutively active or null mutants of FoxO1 into the C2C12 myocyte cell line (Bastie et al., 2005). This research showed that FoxO1 activation results in the upregulation of a number of genes involved in fatty acid metabolism, including acyl CoA oxidase (ACO) and PPARδ. Furthermore, its activation caused an increase in fatty acid uptake and its oxidation and storage as triglyceride. While FAT/CD36 mRNA

expression was not significantly affected, FoxO1 activation caused enrichment of FAT/CD36 protein at the plasma membrane. The effects of the FAT/CD36 inhibitor sulfo-*N*-succinimidyl-oleate confirmed that FAT/CD36 translocation to the cell surface was responsible for the increased fatty acid and oxidation observed upon FoxO1 activation. Authors of this work postulated that FoxO1 activation was involved in the increased reliance of muscle on fatty acid metabolism during fasting.

1.9 Localization of FAT/CD36 in muscle and adipose tissues

While insulin- and contraction-induced translocation of FAT/CD36 from intracellular stores to the sarcolemma of muscle has been described in a number of studies, little is known about the subcellular localization of the molecule. Investigations into the distribution of FAT/CD36 in rats by Zhang *et al.* confirmed that FAT/CD36 is expressed at the sarcolemma of oxidative muscle fibres including those of the soleus and diaphragm muscles (Zhang et al., 2003). This study also found that FAT/CD36 was most evident on endothelial cells of capillaries, a finding that is consistent with a role for FAT/CD36 in transporting LCFAs across the endothelial membrane into the interstitial space as has been previously suggested (Van der Vusse et al., 1998). Interestingly this study could not identify the molecule in white fibres of the gastrocnemius muscle nor did it reveal any intracellular localization of the molecule in white or red skeletal muscle.

A recent study assessed the localization of FAT/CD36 in human type-1 and type-2 skeletal muscle fibres using immunofluorescence microscopy (Keizer et al., 2004). Results showed that FAT/CD36 was most easily detectable in capillary endothelium and was localized to the sarcolemma and intracellular regions of type-1 muscle fibres and, to a lesser extent, the sarcolemma of type-2 muscle fibres. Importantly, FAT/CD36 colocalized with caveolin-3, the muscle-specific isoform of caveolin. This may be of significance to the regulation and function of FAT/CD36 given that caveolin is the marker protein for plasma membrane microdomains known as caveolae which have implicated roles in LCFA metabolism (reviewed in Liu et al., 2002a).

A similar independent study by Vistisen *et al.* also found that FAT/CD36 expression was strongest on miscrovascular endothelial cells of human muscle and that expression levels were higher in type 1 than type 2 muscle fibres (Vistisen et al., 2004). Conversely, they

found that caveolin-3 expression levels were higher in type 2 fibres than type 1 fibres and that FAT/CD36 and caveolin-3 colocalized in the sarcolemma. Interestingly, this study could not provide any evidence of intracellular staining of FAT/CD36.

Several recent investigations have assessed the subcellular localization of FAT/CD36 and the nature of plasma membrane microdomains involved in LCFA uptake in adipocytes. While early studies demonstrated that FAT/CD36 localized to caveolae membrane microdomains in endothelial cells (Lisanti et al., 1994), more recent investigations have suggested that colocalization of FAT/CD36 and caveolin-1, the marker protein of caveolae, is cell type specific (Zeng et al., 2003). Given that adipose tissue demonstrates the highest levels of caveolin-1 expression and morphological caveolae of all tissues studied (Scherer et al., 1994), it has been hypothesized FAT/CD36 localization to these cholesterol and sphingolipid rich plasma membrane invaginations may facilitate LCFA import and intracellular processing by these cells (reviewed in Febbraio et al., 2001).

Many studies into adipocyte function and LCFA transport have employed the 3T3-L1 adipose cell line as a model. Differentiation of 3T3-L1 fibroblasts into adipocytes is accompanied by a several-fold increase in long chain fatty acid uptake (Abumrad et al., 1991) and expression of a number of proteins that may be important in LCFA import or intracellular traffic, including FAT/CD36 (Abumrad et al., 1993), FATP1 (Schaffer and Lodish, 1994), FABPpm (Zhou et al., 1992) and caveolin-1 (Fan et al., 1983, Scherer et al., 1994). Recent studies have demonstrated that FAT/CD36 and caveolin-1 cofractionate in detergent (CHAPS) resistant lipid rafts of 3T3-L1 adipocytes subjected to sucrose density gradient ultracentrifugation (Pohl et al., 2004). Despite this, FAT/CD36 was also found to strongly localize to detergent-soluble fractions that were devoid of caveolin-1. Interestingly, the distribution of radiolabelled LCFA across the gradient closely mirrored that of FAT/CD36.

An extensive study of FAT/CD36 function and localization in 3T3-L1 adipocytes by Pohl *et al.* demonstrated that FAT/CD36 was found in both detergent-resistant membranes (DRMs) and detergent-soluble membranes (DSMs) of these cells (Pohl et al., 2005). Contrastingly, caveolin-1 was only detectable in DRMs, while FATP1 and FATP4, the major representatives of the FATP family in adipose tissue, were only found in DSMs. Further analysis revealed that FAT/CD36 associated with DSMs was intracellular and that

FAT/CD36 exclusively localized to DRMs of the cell surface. This was supported by the demonstration that incubation of live cells with radiolabelled sulfo-*N*-succinimidyl oleate (SSO) and subsequent density gradient ultracentrifugation revealed that SSO was mainly associated with the DRM fraction and that FAT/CD36-associated SSO was almost exclusively associated with the DRM fraction. Importantly, homogenization of cells prior to incubation with SSO resulted in the association of SSO with FAT/CD36 in both DSM and DRM fractions, suggesting that detergent-soluble, intracellular FAT/CD36 was only made available for SSO binding upon homogenization.

Recently, a study of FAT/CD36 localization and function revealed that localization of the molecule to the plasma membrane was abrogated in embryonic fibroblasts (MEFs) isolated from caveolin-1 knockout mice (Ring et al., 2006). This study demonstrated that, in these cells, FAT/CD36 was retained in the Golgi and was prevented from insertion into lipid raft-derived detergent-resistant membranes (DRMs). Furthermore, LCFA uptake in caveolin-1-deficient MEFs was limited and this could be largely attributed to the intracellular retention of FAT/CD36. Finally, all of these phenotypes were reversed by re-instatement of caveolin-1 expression using an adenoviral vector encoding a fusion protein of caveolin-1 and green fluorescent protein (GFP).

1.10 Regulation, localization and function of FAT/CD36 in the liver

Several studies have found that mRNA transcripts encoding FAT/CD36 were not detectable in rat liver (Abumrad et al., 1993, Van Nieuwenhoven et al., 1999). In contrast, recent reports have demonstrated that the molecule is easily detectable in the livers of rats and humans, both at the levels of mRNA transcripts and protein (Zhang et al., 2003, Stahlberg et al., 2004). Furthermore, these latter studies demonstrated that expression levels were at least several-fold higher in female liver than in the livers of age-matched males. Because expression of FAT/CD36 in the liver is not commonly appreciated, little is known about its regulation, localization or function in that organ.

With respect to the localization of FAT/CD36 in the liver, Zhang *et al.* demonstrated, by immunohistochemical staining of rat liver cryosections, that FAT/CD36 expression was greatest in hepatocytes surrounding the central vein and that expression was weakest or not detectable in hepatocytes surrounding the portal triad (Zhang et al., 2003). This study also

demonstrated that FAT/CD36 was easily detectable at the plasma membrane of isolated hepatocytes. An early investigation employed immunoelectron microscopy to show that FAT/CD36 was localized to microvilli of human hepatocytes (Maeno et al., 1994). This study also reported intense staining of endothelial cells of the liver.

Little is known about regulation of FAT/CD36 expression in the liver. Beyond the effect of gender, Fitzsimmons *et al.* demonstrated that oophorectomy resulted in downregulation of FAT/CD36 expression in female rats, while castration resulted in upregulation of expression in male rats (Fitzsimmons, 2006). Furthermore, this study demonstrated that reinstatement of gonad-derived hormones (oestrogen and testosterone) in gonadectomized rats reversed the phenotypic changes in FAT/CD36 expression that accompanied gonadectomy. Finally, they provided evidence that these effects were indirectly mediated through the action of growth hormone (GH). Accordingly, microarray analysis of hepatic gene expression in male, female and GH-treated male rats demonstrated that the female-specific secretion of GH was the apparent cause of gender-biased expression of FAT/CD36 in the liver (Stahlberg et al., 2004).

Hepatic expression of mRNA transcripts encoding FAT/CD36 is increased by treatment of Syrian hamsters with lipopolysaccharide (LPS) and these effects were mimicked by treatment with the cytokines tumour necrosis factor (TNF) or interleukin-1 (IL-1) (Memon et al., 1998). While expression of FAT/CD36 is reportedly regulated by the nuclear transcription factor PPAR-α in the liver (c.f. PPAR-γ in adipose tissue and macrophages) (Motojima et al., 1998), the effects of PPAR-α activation on hepatic FAT/CD36 expression appear to be indirect, as demonstrated by reporter studies of the FAT/CD36 promoter (Sato et al., 2002).

With respect to the function of FAT/CD36 in the liver, little is known. The only direct investigation of the function of FAT/CD36 in the liver involved adenoviral vector-mediated overexpression of FAT/CD36 in the livers of mice and analysis of the cholesterol content of lipoprotein fractions (de Villiers et al., 2001). While adenoviral expression of SR-BI dramatically reduced the cholesterol content of all plasma lipoprotein fractions, especially HDL, overexpression of FAT/CD36 in the liver had no significant impact on plasma lipoprotein cholesterol profiles. These investigations were undertaken to address

the hypothesis that FAT/CD36 contributes to HDL-cholesterol uptake that is otherwise mediated by another class B scavenger receptor, SR-BI (reviewed in Trigatti et al., 2000). This hypothesis was based upon the observation that plasma cholesterol levels in FAT/CD36-knockout mice are elevated, particularly in the HDL fraction (Febbraio et al., 1999).

1.11 SR-BI: an atheroprotective class B scavenger receptor

Before considering a potential role for FAT/CD36 in hepatic HDL-cholesterol metabolism, one must consider what is known about the mechanism by which the proven HDL receptor, SR-BI, mediates cholesteryl ester uptake from HDL and the features of the molecule that may contribute to its activity. Given the importance of HDL cholesterol metabolism, numerous studies have employed mutational analysis of SR-BI to examine its post-translational modification and the amino acid residues and/or domains that are critical to its activity (see Table 1-1). SR-BI is an ~82kDa membrane glycoprotein that was originally identified based on its sequence homology to CD36, the founding member of the class B scavenger receptor family (Acton et al., 1994, Calvo and Vega, 1993). It was first identified as a receptor for high-density lipoproteins (HDL) by Acton *et al.* who demonstrated that its expression in LDL receptor-deficient CHO cells (ldlA cells) conferred high affinity and saturable binding of HDL (K_d ~30μg/ml) and heightened ability to acquire cholesteryl ester and other lipids from these particles without the concomitant uptake and degradation of entire HDL particle. This process, commonly known as selective uptake, has long been recognized as a physiologically relevant process (Pittman et al., 1987) and contrasts with the classical low-density lipoprotein (LDL) receptor pathway that involves internalization of the entire lipoprotein particle in clathrin-coated pits and subsequent degradation (Brown and Goldstein, 1986). Importantly, this study also found that the tissue distribution of SR-BI in mice was consistent with the predicted distribution of an HDL receptor in that its expression was greatest in adrenal glands, testis, ovary and liver; all of which are major destinations of HDL cholesterol (Glass et al., 1983, Glass et al., 1985). Since this initial discovery a myriad of research has investigated different aspects of SR-BI function and regulation, given the importance of regulation of HDL cholesterol metabolism to the development of conditions such as atherosclerosis.

Table 1-1

Mutation(s)	Phenotype	Reference
N108Q N173Q	Disruption of post-translational processing and low levels of surface expression	(Vinals et al., 2003)
Q402R / Q418R	Loss of HDL receptor activity. Normal LDL binding and lipid uptake from and cholesterol efflux to LDL.	(Gu et al., 2000a, Gu et al., 2000b, Chroni et al., 2005)
M158R	Reduced HDL and LDL receptor activities but normal AcLDL binding activity. Reduced efflux to lipid-associated ApoE.	(Gu et al., 2000a, Chroni et al., 2005)
C323G	Limited capacity to protect against nitric oxide-induced cytotoxicity.	(Li et al., 2006)
C462S / C470S	Loss of fatty acylation (palmitoylation). No effect on surface expression or HDL receptor activity.	(Gu et al., 1998)
Δ465-509	Inhibition of cell proliferation.	(Cao et al., 2004)
Δ509	Loss of cell-surface expression in hepatocytes (polarized) from SR-BIΔ509 transgenic mice. Commensurate changes in hepatic HDL metabolism. Unaffected surface expression in non-polarized cells.	(Silver, 2002)
G420H	Normal selective uptake of cholesteryl ester from HDL. Reduced ability to: (i) enlarge the cholesterol oxidase-sensitive cholesterol pool; (ii) mediated cholesterol efflux to HDL; and (iii) enhance cellular cholesterol accumulation.	(Parathath et al., 2004)
Epitope insertion mutagenesis	Various impacts on function and cell-surface expression.	(Connelly et al., 2003a)

1.11.1 Membrane topology and posttranslational modification of SR-BI

SR-BI is predicted to share a similar membrane topology to CD36 with a large extracellular loop that is heavily *N*-glycosylated and anchored to the plasma membrane at both termini by transmembrane domains with short cytoplasmic tails (reviewed in Krieger, 2001). Given the similarities in amino acid sequence and topology between SR-BI and FAT/CD36 it is predictable that the molecules undergo similar post-translational modifications. The mouse SR-BI amino acid sequence contains 11 potential sites of *N*-glycosylation (Asn-X-Ser/Thr) that are highly conserved between species. Furthermore, early studies showed that the initial *N*-glycosylation of the molecule occurs co-translationally, while maturation of the protein in the Golgi apparatus involves conversion of some of *N*-linked oligosaccharides into complex, endoglycosidase H-resistant forms (Babitt et al., 1997). Further research by the same group used site-directed mutagenesis of the 11 potential sites of *N*-glycosylation (positions 102, 108, 116, 173, 212, 227, 255, 288, 310, 330, 383) of murine SR-BI to demonstrate that all sites were glycosylated but only mutation of two sites, Asn-108 and Asn-173, resulted in disruption of post-translational processing of the molecule to endoglycosidase H-resistant forms and very low surface expression (Vinals et al., 2003). This suggested that glycosylation of the molecule at these sites is an important step in post-translational folding of the molecule in the endoplasmic reticulum and/or transport of the molecule to the cell surface. Furthermore, these mutants demonstrated high-affinity binding of HDL, when corrected for the level of surface expression, but a significantly reduced ability to mediate selective lipid uptake from HDL. As such, the role of *N*-glycosylation of the molecule in protein folding, surface expression and HDL-CE selective uptake appears to be independent of its ability to bind HDL with high affinity.

Like CD36, SR-BI is fatty acylated (Babitt et al., 1997). This property facilitates interaction with the cytoplasmic face of the plasma membrane and generally occurs at cytoplasmic cysteine residues that are proximal to membrane-embedded hydrophobic protein domains (Sefton and Buss, 1987). Site-directed mutagenesis of SR-BI revealed that cysteine residues at positions 462 and 470 of the mouse SR-BI amino acid sequence are the major sites of fatty acylation (Gu et al., 1998). Results showed that both of these sites could be fatty acylated with radiolabelled palmitate or myristate and that loss of fatty

acylation in point mutants of one or both of these cysteine residues did not affect surface expression of the molecule or HDL binding and efficient lipid transfer mediated by the molecule.

While dimerization of SR-BI has been observed in several studies (Azhar et al., 2002, Landschulz et al., 1996, Williams et al., 2000), it was most extensively studied by Reaven *et al.* who demonstrated that SR-BI formed homodimers and higher order multimers in a number of tissues and in transfected cell lines (Reaven et al., 2004). Western blot analysis of membrane proteins prepared from adrenal, liver, testes and ovaries of normal and hormone-treated rats and mice and whole cell lysates of transfected CHO, COS-7, HEK293 and Sf9 insect cells revealed the presence of SR-BI homodimers and multimers. While the degree of dimerization in a given tissue or cell type appeared to correlate with the efficiency of HDL-cholesteryl ester (HDL-CE) selective uptake, it also related to SR-BI expression levels such that dimerization was more evident in cells or tissues in which SR-BI expression was greatest.

1.11.2 SR-BI ligands and distribution

Like CD36, SR-BI has been shown to bind a range of ligands with high affinity including native and hypochlorite-modified HDL, modified (oxidized and acetylated) LDL, maleylated albumin, anionic phospholipids, advanced glycation end products, apoptotic cells and native LDL and VLDL (reviewed in Rigotti et al., 2003). Its major functions, however, appear to revolve around its ability to mediate selective uptake of cholesteryl ester from HDL and its physiologic distribution is consistent with this role. SR-BI is primarily expressed in the adrenal glands (on the surface of steroidogenic cells of the zona fasciculata and zona reticularis), liver, ovary (corpus luteal and thecal cells) and to a lesser extent, testis (Acton et al., 1996, Landschulz et al., 1996). This distribution is expected of an HDL receptor given that these sites are the major destinations of HDL cholesterol for purposes of bile acid synthesis (liver) and steroid hormone synthesis (steroidogenic tissues). The process of acquisition of cholesterol from the periphery by HDL and delivery to the liver and steroidogenic cells is known as reverse cholesterol transport (RCT) (Glomset, 1968) and has long been recognized as a critical mechanism of cholesterol homeostasis, given the inverse relationship between risk of developing atherosclerosis and plasma HDL levels (Miller and Miller, 1975).

SR-BI has also been detected at lower levels in the lactating mammary gland, absorptive cells of the proximal small intestine, embryo proximal decidual cells of the uterus, yolk sac visceral endoderm and trophoblasts of the developing embryo and macrophages (reviewed in Krieger, 2001). While SR-BI has been detected at low levels in heart and epididymal fat, these findings have not been consistent between separate studies (Acton et al., 1996, Landschulz et al., 1996).

1.11.3 SR-BI and HDL Cholesterol Metabolism

Since its initial identification as a receptor that is capable of mediating efficient transfer of cholesteryl ester from the core of HDL to cells (Acton et al., 1996), numerous other studies have confirmed that SR-BI expression confers efficient HDL-CE selective uptake on a number of different cell lines. Furthermore, the physiological relevance of SR-BI mediated HDL-CE selective uptake has been demonstrated *in vitro* by studies showing that steroid hormone synthesis is inhibited by antibody-mediated blockade of SR-BI-mediated HDL cholesteryl ester uptake in steroidogenic cell lines (Temel et al., 1997, Reaven et al., 1998). The physiological significance of SR-BI in HDL metabolism has since been demonstrated in several animal models of SR-BI-knockout and liver-specific transgenic mice and these will be discussed in later sections.

While the primary activity of SR-BI is accepted to be the selective removal of cholesteryl ester (CE) from HDL it has also been shown to mediate selective uptake of a number of other natural and synthetic lipids from HDL in cultured cell models. With respect to natural lipid components of HDL, SR-BI has also demonstrated the ability to mediate enhanced selective uptake of free cholesterol (FC) (Ji et al., 1997, Jian et al., 1998, Stangl et al., 1999, Ji et al., 1999), phospholipids (PL) (Urban et al., 2000), triglycerides (TG) (Greene et al., 2001) and α-tocopherol (vitamin E) (Goti et al., 2001). While SR-BI mediates significantly enhanced uptake of these lipids from HDL, cholesteryl ester uptake is probably of greatest physiological significance. Furthermore, comparative analysis of SR-BI-mediated uptake of various lipids has demonstrated that the efficiency of uptake is dictated by the hydrophobicity of the lipid, such that phospholipid uptake is less efficient (efficiencies of uptake: FC > CE > TG >> PL) (Thuahnai et al., 2001). Experimentally, a number of other lipid analogues and modified lipids can also be selectively removed from

HDL by SR-BI. These include DiI (a fluorescent lipid analogous to phospholipid) (Acton et al., 1996), BODIPY-cholesteryl ester (a fluorescent cholesteryl ester analogue) (Reaven et al., 2001), pyrene-labeled phospholipids (Urban et al., 2000) and cholesteryl ethers (non-hydrolyzable cholesteryl ester analogues) (Acton et al., 1996).

The composition and nature of HDL, with respect to its protein and lipid content, plays an important role in dictating the efficiency of selective cholesteryl ester uptake mediated by SR-BI. HDL consists of a mixture of particles that differ in composition, size and density (Cheung and Albers, 1984). The major protein component of HDL is apolipoprotein A-I (apoA-I) and cross-linking studies have demonstrated that it directly interacts with SR-BI via an amphipathic alpha-helix recognition motif that is common to class A apolipoproteins (Williams et al., 2000). This direct interaction of apolipoproteins with SR-BI was also demonstrated by Xu *et al.* who showed that, like anionic phospholipid vesicles, the HDL apolipoproteins apoA-I, apoA-II and apoC-III all bind SR-BI with high affinity either as lipid-free proteins or in the context of lipoproteins (Xu et al., 1997).

While SR-BI binds both lipoprotein-associated and lipid-free apoA-I with high affinity, it is becoming clear that the conformation of apoA-I in HDL significantly influences its interaction with SR-BI. Investigations by de Beer *et al.* demonstrated that SR-BI binding and cholesteryl ester uptake from HDL_2 was markedly greater than binding and uptake from HDL_3 which are smaller and have a lower cholesteryl ester content (de Beer et al., 2001a). Similarly they showed that larger recombinant HDL particles (9.6nm) were bound by SR-BI with an approximately 50-fold greater affinity than smaller recombinant HDL particles (7.8nm). Overall, these results demonstrated that SR-BI preferentially binds larger, cholesteryl ester-rich HDL, thereby enhancing reverse cholesterol transport.

Although apoA-I binds SR-BI with high affinity, research by Temel and colleagues showed that HDL isolated from apoA-I-knockout mice displayed a similar binding affinity to SR-BI as HDL from wildtype controls (Temel et al., 2002). Importantly, this research demonstrated that SR-BI-mediated HDL-CE selective uptake from apoA-I-deficient HDL was reduced (2-3 fold) compared to controls. Similarly, studies using HDL prepared with apoA-I mutants have demonstrated unaffected binding of HDL by SR-BI, but significantly inhibited selective lipid transfer mediated by SR-BI (Liu et al., 2002b). These results are consistent with many lines of research suggesting that high affinity binding of HDL and

efficient cholesteryl ester uptake are distinct steps of the selective uptake process that are mediated by separate domains of SR-BI.

With respect to the apolipoprotein components of HDL, early studies by Cheung *et al.* showed that HDL could contain apoA-I alone or both apoA-I and apoA-II (Cheung and Albers, 1984). This study also indicated that apoA-II plays a role in the regulation of HDL particle size, with apoA-II levels positively correlating with plasma free fatty acid and triglyceride levels. Unlike apoA-I, apoA-II is widely considered to be 'proatherogenic', given that transgenic mice overexpressing apoA-II display an increased rate of atherosclerosis development (Warden et al., 1993). These mice display elevated levels of large cholesteryl ester-rich HDL and triglyceride rich lipoproteins and are insulin resistant. In contrast, in apoA-II-null mice these phenotypic changes are reversed (Weng and Breslow, 1996).

While the proatherogenic nature of apoA-II has been attributed to inhibition of the activities of the enzymes hepatic lipase, lipoprotein lipase, cholesteryl ester transfer protein (CETP) and lecithin:cholesterol acyltransferase (LCAT) (reviewed in Kalopissis et al., 2003), there is a growing appreciation of its negative influence on SR-BI-mediated HDL-CE selective uptake (Pilon et al., 2000, de Beer et al., 2001b, Rinninger et al., 2003). Recently, research by de Beer *et al.*, using HDL isolated from apoA-II-null, apoA-II transgenic and wildtype mice, showed that the level of ApoA-II in HDL was inversely correlated with HDL binding and selective cholesteryl ester uptake by SR-BI and CD36 (de Beer et al., 2004). Although SR-BI mediated HDL-CE selective uptake is considerably more efficient than CD36-mediated uptake (Gu et al., 1998, Connelly et al., 1999), this study found that the inhibitory effect of ApoA-II on CD36-mediated HDL binding and HDL-CE selective uptake was more pronounced, such that CD36- and SR-BI-mediated HDL-CE selective uptake from HDL lacking apoA-II was comparable.

With respect to the effect that the conformation of HDL has on the ability of SR-BI to mediate efficient selective uptake of cholesteryl ester from HDL, it is likely that HDL remodelling by enzymes at the cell surface facilitates the formation of an 'active complex' between SR-BI and HDL. Several lines of evidence have indicated that hepatic lipase activity enhances SR-BI mediated HDL-CE selective uptake (Lambert et al., 1999, Collet et al., 1999). In support of this role, SR-BI expression is upregulated in the adrenal gland

of hepatic lipase knockout mice and in rats injected with antibodies directed against hepatic lipase (Vieira-van Bruggen et al., 1998, Wang et al., 1996). Similarly, lipoprotein lipase activity has been shown to significantly enhance SR-BI-mediated HDL-CE selective uptake in primary human hepatocytes and Hep3B cells by a mechanism involving cell surface heparan sulfate proteoglycans that anchor lipases to the cell surface (Rinninger et al., 1998). Remodelling of HDL by cholesteryl ester transfer protein (CETP), which mediates the transfer of cholesteryl esters from HDL to other lipoproteins in exchange for triglyceride, has also been shown to enhance SR-BI-mediated HDL-CE selective uptake both *in vivo* and *in vitro* (Collet et al., 1999). Likewise, hydrolysis of HDL phospholipids by phospholipase A_2 has also been found to enhance SR-BI mediated selective uptake, presumably by remodelling HDL particles into a form that is more amenable to lipid transfer by SR-BI (de Beer et al., 2000).

Despite the impact that HDL remodelling enzymes have on SR-BI mediated HDL-CE selective uptake, it is clear that they are not required for efficient uptake. Similarly, it is evident that SR-BI does not require the assistance of cytoplasmic factors to mediate efficient uptake of HDL-CE. These properties have been demonstrated by studies showing that isolated plasma membranes containing SR-BI and reconstituted phosphatidylcholine / cholesterol liposomes containing highly purified SR-BI alone are capable of mediating efficient HDL-CE selective uptake (Connelly et al., 2003b, Liu and Krieger, 2002, Shi et al., 1992).

The actual mechanism of SR-BI-mediated selective HDL-CE uptake is unclear, although it is widely accepted to be a two-step process involving high affinity binding of the HDL particle, followed by selective lipid uptake into the plasma membrane. One model of selective uptake suggests that the extracellular domain SR-BI forms a nonaqueous channel via homomeric interactions, such that hydrophobic cholesteryl ester can move down its concentration gradient from bound HDL particles into the cell membrane. This mechanism has been proposed by Rodrigueza *et al.* and supported by Connelly and colleagues who site the very low Arrhenius activation energy for selective uptake of HDL-CE in adrenocortical cells (Glomset, 1968) as an indication that transfer involves a nonaqueous concentration-dependent pathway (Connelly et al., 1999, Rodrigueza et al., 1999).

Another proposed mechanism of SR-BI-mediated HDL-CE selective uptake involves 'retroendocytosis'; a term used to describe endocytosis of HDL, cholesteryl ester liberation and hydrolysis, and recycling of cholesterol-depleted HDL to the plasma membrane (DeLamatre et al., 1990, Kambouris et al., 1990). This mechanism has also been supported by studies depicting endocytosis of SR-BI from the plasma membrane of hepatocytes and transfected CHO cells and MDCK cells (Silver et al., 2001, Burgos et al., 2004). Interestingly, Silver *et al.* demonstrated that HDL labelled with fluorescent tracers for protein (Alexa), phospholipid (DiI) and cholesteryl ester (BODIPY-CE) components were internalized by mouse hepatocytes, such that the fluourophores colocalized both at the surface and within cells (Silver et al., 2001). The process of retroendocytosis may be cell-specific in nature given that apoA-I is only detectable on the cell surface of cells of the rat adrenal gland zona fasciculata (Williams et al., 1995). Furthermore, the ability of SR-BI to mediate efficient HDL-CE selective uptake in reconstituted liposomes in which it is the only protein component present, however, contradicts the 'retroendocytosis' model of selective uptake (Liu and Krieger, 2002).

Although selective uptake of cholesteryl ester from HDL is the major physiological role of SR-BI, it has demonstrated an ability to mediate selective cholesteryl ester uptake from several classes of lipoproteins. While the majority of LDL clearance is mediated by the LDL-receptor pathway, in which the entire lipoprotein particle is endocytosed in clathrin-coated pits and degraded (Brown and Goldstein, 1986), several studies using isolated cell membranes, primary cells and cell lines have demonstrated that a proportion of LDL-CE is taken up selectively (Azhar et al., 1988, Shi et al., 1992, Rinninger et al., 1993, Rinninger et al., 1995). Since its identification as an HDL receptor, several studies have shown that SR-BI can mediate selective uptake of cholesteryl ester from LDL (Stangl et al., 1999, Swarnakar et al., 1999). Similarly, SR-BI has demonstrated an ability to mediate selective lipid uptake from VLDL although the physiological significance of this finding is unclear (Calvo et al., 1997). HDL mediates the majority of plasma cholesterol transport in rodents, since they lack the ability to transfer cholesteryl ester to other lipoproteins via the action of CETP (reviewed in Tall, 1993). In humans, however, LDL-CE transport is more significant. The LDL receptor pathway accounts for up to 80% of plasma LDL removal in humans, as determined by comparisons of clearance of radiolabelled LDL in patients with homozygous familial hypercholesterolaemia (defective in the LDL receptor pathway) with normal individuals (reviewed in Swarnakar et al., 1999). It is possible that SR-BI mediated

LDL-CE selective uptake accounts for the remainder of LDL-cholesterol removal. The involvement of SR-BI in LDL-CE selective uptake has also been indicated by the results of several *in vivo* studies involving SR-BI-knockout and transgenic mice and these will be discussed in more detail in subsequent sections. Despite these results and demonstration that SR-BI can bind LDL with high affinity, SR-BI binds HDL preferentially when both ligands are present, indicating that it's primary function centres around HDL metabolism (Acton et al., 1996, Gu et al., 2000b).

The immediate fate of cholesteryl ester delivered to the plasma membrane by SR-BI has recently become clearer. It is widely recognized that LDL-CE acquired via the LDL receptor pathway is hydrolysed to free cholesterol in lysosomes by an acid cholesteryl ester hydrolase (ACEH) (Brown and Goldstein, 1986). Cholesteryl ester delivered from HDL via selective uptake, however, is hydrolysed extralysosomally (Sparrow and Pittman, 1990). Comparable studies later demonstrated that extralysosomal hydrolysis of HDL-CE is mediated by a neutral cholesteryl ester hydrolase (NCEH) in rat hepatoma cells (Delamatre et al., 1993, Shimada et al., 1994). A recent study by Connelly and colleagues investigated hydrolysis of HDL-CE and LDL-CE selectively delivered to cells via SR-BI or CD36 (Connelly et al., 2003b). Results showed that HDL-CE delivered by SR-BI or CD36 was hydrolysed by a neutral cholesteryl ester hydrolase, although hydrolysis was more efficient when SR-BI was responsible for HDL-CE delivery. On the other hand selective uptake and hydrolysis of LDL-CE was similarly efficient in SR-BI and CD36 transfected cells. Interestingly, hydrolysis of LDL-CE delivered by SR-BI was via a neutral cholesterol ester hydrolase, while hydrolysis was via an acidic cholesterol ester hydrolase when LDL-CE delivery was mediated by CD36, suggesting that the receptors deliver LDL-CE to separate metabolic pathways.

An emerging function of SR-BI is its ability to mediate bidirectional flux of free cholesterol between cells and extracellular acceptors. This is of particular interest given that it has been detected in the periphery and on foam cells in atherosclerotic plaques. As such, SR-BI could participate in both ends of reverse cholesterol transport; (1) the efflux of cholesterol from peripheral cells to HDL acceptors and (2) the removal of cholesteryl esters and free cholesterol from HDL in the liver and steroidogenic tissues. The process of SR-BI-mediated free cholesterol (FC) flux was directly established by experiments demonstrating that expression of SR-BI enhanced FC efflux to the extracellular acceptors

HDL and phosphatidylcholine liposomes (de la Llera-Moya et al., 1999, Ji et al., 1997, Jian et al., 1998). Since then several studies have revealed that SR-BI mediated free cholesterol flux is bi-directional and concentration gradient-dependent (Kellner-Weibel et al., 2000, Yancey et al., 2000, de La Llera-Moya et al., 2001). As has been demonstrated for SR-BI-mediated HDL-CE selective uptake, studies using SR-BI/CD36 domain swap chimeras have demonstrated that the extracellular domain of SR-BI is essential to SR-BI-mediated bi-directional cholesterol flux (Connelly et al., 2001).

Several different properties of HDL composition have been identified that influence the efficiency and direction of SR-BI-mediated flux of cholesterol to and from HDL. Although lipid-free apoA-I binds to SR-BI with high affinity, this is not sufficient to instigate SR-BI mediated cholesterol efflux given the essential requirement for phospholipids in the acceptor (de la Llera-Moya et al., 1999). Furthermore, recent studies have demonstrated that the content and nature of phospholipids in the acceptor/donor particle has a significant influence on SR-BI-mediated free cholesterol flux (Jian et al., 1997, Yancey et al., 2000, Fournier et al., 1996, Fournier et al., 1997).

Although the mechanisms involved in SR-BI mediated cholesterol flux are unclear, it has been suggested that SR-BI simply enhances aqueous diffusion of cholesterol (reviewed in Phillips et al., 1987). While it is appealing to suggest that SR-BI enhances diffusional FC flux by mediating high affinity binding of acceptor particles at the cell surface, this hypothesis is refuted by the observation that expression of CD36, which binds HDL with high affinity, only minimally increases efflux to extracellular acceptor particles (de la Llera-Moya et al., 1999). Another mechanism whereby SR-BI may enhance cholesterol efflux is via changes to the accessibility of membrane cholesterol to extracellular acceptors. This has been indicated by studies showing that SR-BI expression enhances the susceptibility of membrane cholesterol to the enzyme cholesterol oxidase (de la Llera-Moya et al., 1999, Kellner-Weibel et al., 2000). Furthermore, kinetic analysis of free cholesterol efflux to cyclodextrin cholesterol acceptors has shown that SR-BI expression induces a shift in the distribution of cellular free cholesterol such that the fast pool size increases and the slow pool size decreases (Kellner-Weibel et al., 2000). These results suggest that SR-BI expression causes a redistribution of cholesterol in the plasma membrane, possibly making it more susceptible to extracellular acceptors. Localization of SR-BI to cholesterol and sphingomyelin rich plasma membrane domains know as

caveolae, as has been demonstrated in some cell types (Babitt et al., 1997, Graf et al., 1999), may therefore be of significance to SR-BI-mediated cholesterol redistribution given that caveolae may represent the fast pool of cholesterol and caveolae have been implicated in regulation of flux of free cholesterol (Fielding and Fielding, 1995).

1.11.4 Direct comparisons of the activity of SR-BI and FAT/CD36 and domain-swap chimeras of these receptors

Since the identification of SR-BI as a physiologically relevent HDL receptor (Acton et al., 1996), many studies have used mutational analysis to attempt to identify domains that are critical to SR-BI-mediated HDL binding, HDL-CE selective uptake and free cholesterol flux. An early study by Gu *et al.* found that while both mouse SR-BI (mSR-BI) and human CD36 (hCD36) are capable of mediating high affinity binding of HDL, SR-BI-mediated selective lipid uptake is considerably more efficient (Gu et al., 1998). Furthermore, using mSR-BI/hCD36 domain-swap chimeras, they demonstrated that the extracellular domain of SR-BI is essential for efficient selective lipid uptake and is capable of conferring efficient selective uptake to cells even when one or both of its terminal transmembrane domains and/or cytoplasmic tails are replaced with those of CD36. A similar study by Connelly *et al.* also found that mSR-BI and rat CD36 (rCD36) bind HDL with high affinity but SR-BI demonstrates a unique enhancement of selective cholesteryl ester uptake (Connelly et al., 1999). They also used SR-BI/CD36 domain-swap chimeras to show that the extracellular domain of SR-BI is critical to efficient selective uptake. Given that high affinity binding of HDL by CD36 is not sufficient to confer efficient HDL-CE selective uptake on transfected cells, the authors suggested that inefficient CD36-mediated HDL-CE selective uptake is simply a result of close tethering of HDL particles to the cell surface.

Despite the fact that the extracellular domain of SR-BI is necessary for efficient HDL-CE selective uptake, several studies have demonstrated that SR-BII, a splice variant of SR-BI that differs only in its cytoplasmic C-terminus, mediates selective uptake with a low efficiency despite demonstrating a similar binding affinity to HDL as SR-BI (Webb et al., 1998, Connelly et al., 1999). This splice variant results from a splicing event that skips the final exon of the SR-BI gene to produce an entirely different cytoplasmic C-terminus (Webb et al., 1997, Webb et al., 1998). Although it shares a similar distribution to SR-BI,

given that it is primarily expressed in the liver and steroidogenic tissues, its primary function remains unknown. *In vitro* studies have demonstrated that SR-BII is effectively targeted to the cell surface and has been observed to localize to caveolae in certain cell types. It is therefore unlikely that the alternative C-terminal tail prevents its targeting to lipid rafts of the plasma membrane (Webb et al., 1998, Connelly et al., 1999). Alternatively, it is possible that the C-terminal cytoplasmic tail of SR-BII is inhibitory to efficient HDL-CE selective uptake, possibly by negatively influencing the conformation of the extracellular domain or dimerization of the molecule. A third possibility is that the SR-BI C-terminal cytoplasmic domain enhances selective lipid uptake by interacting with cofactor(s) that facilitate uptake. From these studies, however, it is apparent that the C-terminal cytoplasmic tail of CD36 can perform a similar function given that chimeric SR-BI receptors featuring the C-terminal tail of CD36 mediate selective HDL-CE uptake with equal or greater efficiency to that of wildtype SR-BI (Gu et al., 1998, Connelly et al., 1999). Recently, PDZK1 or 'CLAMP' (C-terminal linking and modulating protein) has been identified as a cytoplasmic adaptor molecule that stabilizes SR-BI at the cell membrane, thereby facilitating HDL-CE selective uptake (Ikemoto et al., 2000, Silver, 2002, Kocher et al., 2003). The significance of the interaction between SR-BI and PDZK1 will be discussed in more detail in later sections.

With respect to SR-BI domains involved in other lipid transfer properties, Connelly *et al.* compared the abilities of SR-BI, CD36 and SR-BI/CD36 domain-swap chimeras to mediate HDL-CE selective uptake, free cholesterol (FC) flux between cells and lipoproteins and alteration in cholesterol mass and distribution (Connelly et al., 2001). Results showed that, as for HDL-CE selective uptake, the extracellular domain (ECD) of SR-BI is essential for efficient influx and efflux of free cholesterol between cells and HDL particles. Furthermore, the ECD was essential for receptor-dependent increases in total cellular cholesterol mass, efficient esterification of newly influxed cholesterol and cholesterol oxidase sensitivity (i.e. redistribution of membrane cholesterol). Similarly, research by the same group has indicated that efficient hydrolysis of receptor-delivered HDL-CE is reliant on the ECD of the molecule (Connelly et al., 2003b). Taken together, it is clear that multiple functions of SR-BI localize to its extracellular domain and that the transmembrane and cytoplasmic domains of the molecule do not greatly influence its function.

Several studies have employed site-directed mutagenesis and epitope-insertion mutagenesis to identify domains of SR-BI that are critical to its ability to bind HDL, mediate HDL-CE selective uptake and/or mediate flux of cholesterol between cells and HDL acceptors/donors. Residues and domains that contribute to the functional activity of SR-BI are indicated in Figure 1-4, as are sites of post-translational modifications and regions of the molecule that dictate its topology with respect to the plasma membrane (refer to Table 1-1 for the impact of mutagenesis of these residues).

1.11.5 In Vivo Studies of SR-BI-mediated HDL Metabolism

Manipulation of SR-BI expression in mice has provided much insight into the physiological significance of the receptor's functions identified *in vitro*. The effects of SR-BI-knockout and transgenic overexpression of SR-BI on lipid metabolism have confirmed the physiological importance of the receptor in reverse cholesterol transport. Furthermore, recent investigations involving cross-breeding of SR-BI knockout mice with several mouse models of atherosclerosis have demonstrated the importance of the molecule in protection against development of atherosclerosis.

To investigate the role of SR-BI in HDL metabolism, Rigotti *et al.* generated mice with a targeted null mutation in the SR-BI gene (Rigotti et al., 1997). This involved disruption of the first coding exon in the SR-BI gene with a neomycin resistance cassette such that heterozygous SR-BI mutants demonstrated approximately 50% of normal wildtype hepatic SR-BI expression, while homozygous SR-BI mutants lacked hepatic SR-BI expression altogether. They found that plasma cholesterol concentrations were elevated in SR-BI-null mice, with the increase in cholesterol being mainly associated with large ApoE-rich HDL particles. Further defects in the selective removal of cholesteryl ester from HDL in SR-BI-null mice were evidenced by drastic reductions in the cholesterol content of adrenal glands from these mice. Heterozygous knockout mice displayed similar but milder alterations in HDL-cholesterol metabolism.

Another SR-BI-knockdown mouse strain was generated by disruptive insertion in the mouse SR-BI promoter (Varban et al., 1998). This resulted in mice (SR-BIatt mice) that displayed attenuated expression of SR-BI in the liver (~50% reduction) but no apparent changes in expression of the molecule in steroidogenic tissues. These mice displayed

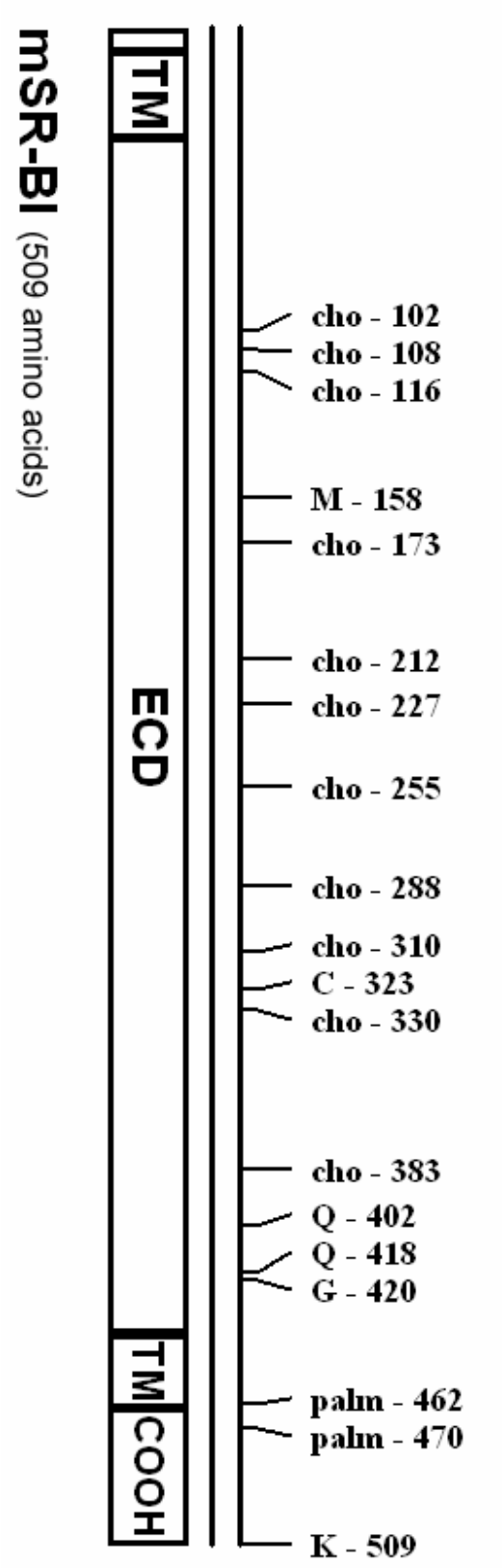

Legend

- cho: carbohydrate (*N*-glycosylation site)
- palm: palmitoylation (fatty acylation site)
- TM: transmembrane domain
- ECD: extracellular domain
- COOH: carboxy-terminal cytoplasmic tail
- M: methionine
- C: cysteine
- Q: glutamine
- G: glycine
- K: lysine

Figure 1-4. Schematic diagram of mouse SR-BI (mSR-BI).

increases in total plasma cholesterol levels and the size and cholesterol content of HDL, comparable to those effects observed in heterozygous SR-BI knockout mice. The increases in plasma HDL-cholesterol were consistent with demonstration of reduced clearance of HDL-cholesterol from plasma and reduced hepatic uptake of radiolabelled HDL-CE.

Further analysis of hepatic cholesterol metabolism in SR-BI knockout mice by Mardones *et al.* revealed that the absence of hepatic SR-BI expression results in reduced secretion of free cholesterol into the bile, but unaffected biliary bile acid or phospholipid secretion (Mardones et al., 2001). Given that the bile acid pool size and composition were also found to be unaffected in SR-BI knockout mice, it appears that the major roles of SR-BI in the murine liver are selective uptake of HDL-cholesterol and secretion of free cholesterol into the bile. Interestingly, the hepatic cholesterol content of SR-BI-knockout mice was found to be similar to that of wildtype mice, suggesting that changes in the expression of genes involved in hepatic cholesterol homeostasis may compensate for the absence of SR-BI.

Although SR-BI has been identified in canalicular domains of hepatocytes (Kozarsky et al., 1997), suggesting a possible role in secretion of free cholesterol into bile, this finding is controversial (reviewed in Trigatti et al., 2003). In regards to this, a recent study investigated whether SR-BI contributes directly to free cholesterol secretion into bile and further investigated changes in hepatic HDL-CE uptake in SR-BI knockout mice (Van Eck et al., 2003). Given that hepatic cholesterol content is not significantly altered in these mice, they attempted to identify any compensatory changes in expression of genes involved in lipoprotein cholesterol uptake (LDL receptor (LDLR), LDL receptor-related protein (LRP), SR-A, CD36, apoE, ABCG1), cholesterol biosynthesis (HMGCoA, Cyp7A1) and secretion of cholesterol into bile (ABCA1, ABCG1, ABCG5, ABCG8). Results showed that SR-BI knockout mice experience a significant reduction in the hepatic expression of ABCG5 and ABCG8. Given that these molecules are implicated in biliary cholesterol secretion (Yu et al., 2002), it is possible that their downregulation contributes to both reduced biliary cholesterol secretion and maintenance of normal hepatic cholesterol levels.

Investigations involving hepatic overexpression of SR-BI have also demonstrated the importance of the molecule in HDL metabolism. Early studies by Kozarsky *et al.*

demonstrated that adenovirus-mediated hepatic overexpression of SR-BI in mice resulted in a massive reduction in plasma HDL cholesterol levels that coincided with increased biliary cholesterol secretion (Kozarsky et al., 1997). This increase in the cholesterol content of bile was attributed to enhanced removal of cholesterol and lipid from HDL, given that intravenous administration of DiI-labelled HDL resulted in increased secretion of DiI into bile in these mice. Interestingly, these studies also found that plasma apoA-I levels were reduced in these mice.

The generation and analysis of liver-specific SR-BI-overexpressing transgenic mice has further highlighted the role of SR-BI in HDL cholesterol metabolism. Tall and colleagues generated transgenic mice in which SR-BI transgene expression was controlled by a region of the human apoE promoter (Wang et al., 1998). Analysis of plasma lipid profiles from these mice revealed that levels of total cholesterol, free cholesterol, esterified cholesterol, phospholipids and triglycerides were all reduced in transgenics compared to wildtype controls. More specifically, both HDL and LDL cholesterol levels were significantly reduced in transgenics. While the observed increase in selective uptake of radiolabelled HDL-CE by the liver was expected, SR-BI-transgenic mice also demonstrated a marked increase HDL protein catabolism by the liver and kidney. This result was mirrored by increased clearance of both radiolabelled HDL cholesteryl ester and protein from plasma. Similarly, plasma levels of HDL apolipoproteins (apoA-I and apoA-II) and LDL and VLDL apolipoprotein (apoB) were reduced in transgenic mice compared to wildtype controls.

Similar reductions in plasma HDL and non-HDL cholesterol levels were observed in liver-specific SR-BI transgenic mice generated by Rubin and colleagues in which SR-BI cDNA expression was driven by the apoA-I promoter (Ueda et al., 1999). This research also demonstrated increased hepatic HDL cholesterol uptake and secretion of cholesterol into bile by SR-BI-transgenic mice compared to controls. Other studies using SR-BI transgenic mice have also confirmed that hepatic overexpression of the molecule results in enhanced HDL-CE clearance and secretion of cholesterol into bile (Ji et al., 1999, Sehayek et al., 1998). Taken together, these results highlight the important role of SR-BI in the final stages of reverse cholesterol transport via removal of cholesterol from HDL by the liver and secretion into bile. Somewhat unexpectedly, however, these results also indicate that

the molecule may also play a physiologically relevant role in turnover of apolipoproteins and metabolism of non-HDL cholesterol.

With respect to the metabolism of apoB-containing lipoproteins, the contribution of SR-BI is an emerging focus. The potential contribution of the molecule to metabolism of non-HDL lipoproteins was highlighted by the observation that transgenic overexpression of SR-BI in the mouse liver results in reduced plasma triglycerides, LDL cholesterol and VLDL and LDL apoB, compared with control mice (Wang et al., 1998). With respect to chylomicron metabolism, Out and colleagues demonstrated that association of chylomicron-like particles with hepatocytes from SR-BI knockout mice is significantly reduced, compared with hepatocytes from wildtype mice (Out et al., 2004). This study also showed that hepatic deposition of radiolabelled chylomicrons was reduced, as was clearance of chylomicron-like particles from plasma. Finally, adenoviral-vector mediated overexpression of SR-BI in the liver results in accelerated hepatic clearance of chylomicron-like particles from plasma (Out et al., 2005, Webb et al., 2004). The effects of SR-BI on chylomicron metabolism are thought to result from its ability to bind ('capture') chylomicrons and, therefore, facilitate clearance of these particles mediated by the LDL receptor (LDLr) / LDLr-related protein 1 endocytic pathways (reviewed in Cooper, 1997).

The importance of SR-BI to HDL-cholesterol metabolism and reverse cholesterol transport has been highlighted by a number of studies involving cross-breeding of SR-BI gene-targeted mice with well-characterized mouse models of atherosclerosis (e.g ApoE knockout and LDL-R knockout mice). The details of these investigations are beyond the scope of this study; suffice to say that SR-BI deficiency results in accelerated development of atherosclerosis while hepatic SR-BI expression slows the development of atherosclerosis. The interested reader is directed to a concise review by Trigatti and colleagues, for further discussion of the atheroprotective role of SR-BI (Trigatti et al., 2004).

1.11.6 Regulation of hepatic SR-BI expression

Expression of SR-BI by hepatocytes is regulated by a number of factors including dietary lipids, hormones and cytokines. With respect to diet, ligation of the bile duct in mice and

rats results in downregulation of hepatic SR-BI expression by cholestasis and bile acids (Voshol et al., 2001). In contrast, a diet rich in polyunsaturated fatty acids results in upregulation of hepatic SR-BI expression (Spady et al., 1999). Although this is suggestive of activation of PPARs, given that LCFAs can act as PPARγ ligands, no PPAR response elements have been identified in the SR-BI promoter (Rhainds and Brissette, 2004). The effect may therefore be indirect, as appears to be the case for PPARα ligand (fibrate)-mediated downregulation of hepatic SR-BI expression (Mardones et al., 2003). Similarly, although no farnesoid X receptor (FXR) elements have been identified in the SR-BI promoter, FXR ligands, including bile acids, cause increased hepatic SR-BI protein levels and, accordingly, hepatic SR-BI protein levels are reduced in FXR-knockout mice (Lambert et al., 2003). Another dietary factor that alters hepatic SR-BI expression is vitamin E, which does not affect SR-BI mRNA levels but reduces SR-BI protein (Witt et al., 2000).

Hormonal regulation of hepatic SR-BI expression is also complex and possibly indirect in action. Firstly, SR-BI expression is reportedly higher in the livers of male mice (Landschulz et al., 1996) and rats (Graf et al., 2001) than in female counterparts and, furthermore, ovariectomy causes increased SR-BI expression in females (Graf et al., 2001). Estradiol-induced downregulation of hepatic SR-BI expression was later shown to likely be the indirect result of estrogen-mediated effects on the pituitary gland and severely altered hepatic LDL-receptor expression (Stangl et al., 2002). Testosterone, on the other hand, has an opposite and apparently more direct effect on hepatic SR-BI expression, given that it induces significantly heightened levels of SR-BI protein in human HepG2 cells (Langer et al., 2002). Finally, adrenocorticotropic hormone (ACTH) administration suppresses hepatic SR-BI expression in rodents (Galman et al., 2002). This effect however is indirect and dependent on the presence of an intact adrenal gland.

The promoter region of the SR-BI gene contains numerous elements that may contribute to its regulation by hormones and dietary lipids. The promoter contains binding sites for a number of transcription factors that include CAAT/enhancer-binding proteins (C/EBPs), steroidogenic factor-1 (SF-1) and sterol regulatory element binding protein-1 (SREBP-1) (reviewed in Trigatti et al., 2000, Rhainds and Brissette, 2004). With respect to the liver, SF-1 is absent but the action of the orphan nuclear receptor, liver receptor homologue-1

(LRH-1) appears to be an important regulator of SR-BI transcription (reviewed in Rhainds and Brissette, 2004).

1.11.7 Post-translational stabilization of SR-BI by the cytoplasmic adaptor PDZK1

Since the initial discovery that the cytoplasmic carboxy-terminus of SR-BI interacts with the cytoplasmic adaptor molecule PDZK1 (CLAMP/Diphor-1/CA70/NaPi-Cap1) in rat liver (Ikemoto et al., 2000), the tissue-specific stabilization of SR-BI by this molecule has been an emerging focus of research. PDZK1 is a 70 kDa protein that contains four PDZ domains and is expressed predominantly in liver, kidney and small intestine (reviewed in Silver, 2004). Several approaches have demonstrated that its interaction with the C-terminus of SR-BI results in its stabilization at the hepatocyte plasma membrane. Firstly, hepatic overexpression of SR-BI lacking the C-terminal amino acid (SR-BIdel509) in mice resulted in elevated levels of SR-BI (SR-BIdel509) mRNA and protein but unaltered levels of SR-BI protein at the hepatocyte cell-surface and unaltered levels of HDL-CE uptake by isolated hepatocytes (Silver, 2002). This reduction in surface expression and activity was unique to polarized cells, however, as SR-BIdel509 and other truncated SR-BI mutants are capable of translocation to the cell-surface and mediating HDL-CE uptake in non-polarized transfected cell lines (Silver, 2002, Connelly et al., 2001). Secondly, PDZK1 knockout mice display an approximately 85% reduction in SR-BI protein levels and increased plasma HDL cholesterol levels, similar to those observed in SR-BI knockout mice (Kocher et al., 2003). It appears, therefore, that PDZK1 stabilizes SR-BI at the hepatocyte cell surface by interaction with its C-terminus, and given that PDZK1 contains four PDZ-domains, it may act as a scaffolding protein for other SR-BI molecules and PDZ-interacting proteins.

In light of these findings, an emerging focus of research into the regulation of hepatic SR-BI expression involves assessment of post-transcriptional regulation and investigation of the factors that regulate expression of PDZK1. For example the observation that PPARα (fibrate)-dependent reduction of hepatic SR-BI protein levels coincides with reduced PDZK1 levels has led to hypotheses that fibrate-mediated reductions in hepatic SR-BI protein are secondary to changes in PDZK1 expression (Mardones et al., 2003). This, however, has since proven not to be the case (Lan and Silver, 2005). Furthermore, another

PDZK1-interacting protein, MAP17, appears to indirectly regulate SR-BI protein levels by depleting PDZK1, possibly by targeting its degradation (Silver et al., 2003).

1.11.8 Subcellular localization of SR-BI

The subcellular localization of SR-BI is somewhat controversial. Initial reports indicated that SR-BI localized predominantly to caveolae in transfected CHO cells and in Y1-BS1 adrenocortical cells (Babitt et al., 1997, Graf et al., 1999). These conclusions were based upon the co-fractionation of SR-BI with caveolin-1 in caveolae-enriched membrane fractions (Babitt et al., 1997, Graf et al., 1999) and observed colocalization of SR-BI with caveolin-1 in transfected CHO cells as determined by confocal fluorescence microscopy (Babitt et al., 1997). Similarly, Frank and colleagues found that SR-BI and caveolin-1 colocalized considerably in co-transfected COS-7 cells as determined by confocal fluorescence microscopy (Frank et al., 2002). Recent studies of SR-BI localization in human HepG2 hepatoma cells, however, demonstrated that the receptor was enriched in biochemically-prepared lipid raft fractions that were devoid of caveolin-1 and, hence, were not caveolae (Rhainds and Brissette, 2004). A similar study of the subcellular localization of SR-BI in HepG2 cells and mouse hepatocytes demonstrated that SR-BI was enriched in biochemically prepared lipid rafts, where it co-fractionated and co-localized with carboxyl ester lipase (CEL), suggesting a direct association between SR-BI mediated HDL-CE delivery and CEL-mediated hydrolysis of newly acquired cholesteryl esters (Camarota et al., 2004).

At a cellular level, immunohistochemical analysis of SR-BI expression in the liver results in a diffuse staining pattern, mostly of parenchymal hepatic cells (Landschulz et al., 1996, Fitzsimmons, 2006). SR-BI has been detected on both apical (canalicular) and basolateral (sinuisoidal) hepatocyte membranes (Kozarsky et al., 1997), although this finding is controversial, given that recent studies have failed to detect the molecule on apical membranes (Mardones et al., 2003, Stangl et al., 2002). Within the hepatocyte, SR-BI is purportedly localized to perinuclear organelles that may represent the endosomal recycling compartment; given that these compartments are also stained with internalised transferrin conjugates (Silver et al., 2001).

With respect to steroidogenic tissues, SR-BI has frequently been detected at the plasma membrane in double-membraned microvillar channels that protrude from the cell surface and also extend from the plasma membrane into the cytoplasm. Localization of SR-BI to these plasma membrane structures has been observed in a number of cell types including rat ovary luteal cells (Reaven et al., 1998), rat Leydig cells (Reaven et al., 2000), Y1-BS1 adrenocortical cells and transfected WI38-VA13 (lung fibroblast) cells (Peng et al., 2004). Further biochemical analysis of the subcellular localization of SR-BI in transfected CHO cells, WI38-VA13 cells and COS-7 cells revealed that SR-BI was not tightly associated with classical detergent-resistant membranes (Peng et al., 2004). At the cellular level, SR-BI is expressed at high levels by cells of the zona fasciculata and zona reticularis cortical cells of the adrenal gland, corpus luteal cells and thecal cells of the ovary and Leydig cells and, to a lesser extent, Sertoli cells of the testis (Rhainds and Brissette, 2004).

1.12 Prelude to the study

The primary focus of this study was to investigate the potential contribution of FAT/CD36 to hepatic lipid metabolism. Expression of FAT/CD36 in the liver is rarely acknowledged and for this reason its function in that organ is largely unknown. This is despite recent demonstration of its presence at high levels in the livers of humans and rodents where its expression is regulated in a hormone-dependent manner (Zhang et al., 2003, Stahlberg et al., 2004, Fitzsimmons, 2006). Given the proven role of FAT/CD36 as a mediator of cellular long-chain fatty acid (LCFA) import by myocytes and adipocytes, it is possible that the receptor similarly contributes to LCFA import by hepatocytes. Alternatively, given that *in vitro* studies have demonstrated that FAT/CD36 binds high-density lipoproteins (HDL) with high affinity and mediates selective uptake of lipids from these particles, albeit inefficiently (Gu et al., 1998, Connelly et al., 1999), it is possible that FAT/CD36 contributes to hepatic HDL-lipid clearance; a process that is a critical endpoint to reverse cholesterol transport. These putative functions and the subcellular localization of FAT/CD36 and the importance of this localization to the activity of the receptor have been investigated using transfected cell lines. Furthermore, the generation of transgenic mice that display liver-specific overexpression of FAT/CD36 has been initiated in this work. Future characterization of the any phenotypic changes in lipid metabolism in these mice should provide valuable insights into the primary activity of the receptor in the liver.

Chapter 2: Materials and Methods

2.1 Molecular Biology Techniques

2.1.1 Synthetic oligonucleotides

All synthetic oligonucleotides were purchased from GeneWorks (Adelaide, South Australia) (see Table 2-1). The concentration of the synthesized oligonucleotides was calculated using the following formula and an average mononucleotide MW of ~ 330 daltons:

$$\text{Oligonucleotide concentration } (\mu M) = \frac{(\text{Concentration (mg/ml)} \times 10^6)}{\text{Length (nucleotides)} \times \text{mononucleotide MW}}$$

2.1.2 RNA extraction

Total RNA was prepared from cultured cell lines or rodent tissue using the RNeasy Protect Mini Kit (Qiagen, Hilden, Germany) as per manufacturer's instructions. Where necessary, coarsely diced tissue samples were stored in RNA Later (Qiagen) at -20°C for later RNA extraction.

2.1.3 Estimation of RNA concentration

To estimate the concentration of RNA in a given sample, optical density (OD) was measured at 260 nm using a UV spectrophotometer (SmartSpec 3000, Bio-Rad Laboratories, Hercules, CA, USA) and a cuvette with a 10mm light path. The formula used was as follows:

$$\text{RNA concentration } (\mu g/ml) = OD_{260nm} \times \text{dilution factor} \times 40$$

RNA purity was estimated by the OD_{260nm} / OD_{280nm} ratio, with a minimum acceptable ratio of 1.80.

2.1.4 Preparation of cDNA from mRNA by reverse transcription

cDNA was prepared from RNA by reverse transcription, using SuperScript II RNaseH$^-$ Reverse Transcriptase (Invitrogen, Carlsbad, CA, USA). 2 µL of oligo dT (10 µM) was first added to 2 µg of RNA in 10 µL of RNase-free MilliQ water, mixing and centrifuging

NAME	SEQUENCE (5' → 3')	APPLICATION
FAT FP1	ACT GGA GCC GTT ATT GGT GC	Seq.
FAT FP2	CCT TCA CTG TCT GTT GGC AC	Seq.
FAT FP3	TGT TCT TCC AGC CAA CGC CT	PCR, Seq., Clon.
FAT RP2	CCA ACA CCA AGT AAG ACC ATC TC	PCR, Seq.
CD36 RT FP1	TGC TGC ACG AGG AGG AGA AT	Seq.
CD36 RT RP1	GCA CCA ATA ACG GCT CCA GTA	Seq.
EGFP FP1	TAC CTG AGC ACC CAG TCC	Seq.
Cav1 FPf	CCG AAG CTT ATG TCT GGG GGT AAA TAC GTA GAC	Clon.
Cav1 RPf	GGA TCC CGT ATC TCT TCC TGC GTG CTG ATG	Clon.
Cav1 FP1	ATG TCT GGG GGT AAA TAC GTA GAC	PCR
Cav1 RP1	CTA TAT CTC TTC CTG CGT GCT G	PCR
Cav1 RP2	ATC TAT CTC TTC CTG CGT GCT G	Seq.
tTA FP1	ATC GCG ATG GAG CAA AAG TA	PCR
tTA RP1	TCG ATG GTA GAC CCG TAA TTG	PCR
rHL FP1	AAG CTT CGC ATG GGA AAT CAC CTC	PCR
rHL RP2	CCC AGG CTG TAC CCA ATT AAG	PCR
SRBI FP3	GCA CGG TTG GTG AGA TCC T	PCR
SRBI RP1	GGT GGA TGT CTA GGA ACA AGG	PCR
SRBI-myc FP	AAG CTT *ATG GAG CAG AAG CTG ATC AGC GAG GAG GAC CTG* GTC AGC TCC AGG GCA CGC	Clon.
SRBI RPrf	TCT AGA CTG GTC TGA CCA AGC TAT CAG G	Clon.
β-ACTIN FP1	CTG GAG AAG AGC TAT GAG	PCR
β-ACTIN RP1	AGG ATA GAG CCA CCA ATC	PCR
GAPDH FP	TCC TTG GAG GCC ATG TAG GCC AT	PCR
GAPDH RP	TGA TGA CAT CAA GAA GGT GAA G	PCR
IRES FP1	GAA GCC GCT TGG AAT AAG G	Seq.
IRES RP1	GAG GAA CTG CTT CCT TCA CG	Seq.
CD36 del5 RP	AGA CTC GAG CGC TAT CTG CAA GCA CAG TAT GAA ATC	Clon.
CD36 del10 RP	AGA CTC GAG CGC TAT CTG CAA GCA CAC TAT GAA ATC	Clon.
BGHp(A) RP	TAG AAG GCA CAG TCG AGG	Seq.
CD36peptop	AGC TTC TGG ATT T*AT GAT TTC ATA CTG TGC TTG CAG ATC TAA GAA TGG AAA ATA A*G	Clon.
CD36pepbot	GAT CC*T TAT TTT CCA TTC TTA GAT CTG CAA GCA CAG TAT GAA ATC AT*A AAT CCA GA	Clon.
CavKYWFYRtop	AGC TTC TGG *AAA ATA TTG GTT TTA CCG C*TA GG	Clon.
CavKYWFYRbot	GAT CCC TA*G CGG TAA AAC CAA TAT TT*T CCA GA	Clon.
CD36 Ntm top	TCG AG*A TGG GCT GCG ATC GGA ACT GTG GG*C G	Clon.
CD36 Ntm bot	AAT TCG *CCC ACA GTT CCG ATC GCA GCC CAT* C	Clon.

TABLE 2-1.

Underlined sequences are introduced restriction sites (or restriction site overhangs). Italicised sequences encode peptides to be introduced in cloning of fusion proteins. With the exceptions of tTA primers (specific for cDNA encoding TetR-VP16 fusion protein) and GAPDH primers (specific for mouse *GAPDH* gene, but cross-reactive with rat and human *GAPDH* genes), all primers used in PCR were specific for rat cDNA / DNA. Seq., sequencing; Clon., cloning; PCR, polymerase chain reaction.

briefly. The following PCR program was used [Step 1: 70°C for 10 minutes. Step 2: 42°C for 2 minutes. Step 3: 42°C for 50 minutes. Step 4: 70°C for 15 minutes].

Between steps 1 and 2, the program was paused and samples were placed on ice before adding 4 µL of 'First Strand Buffer' (5×) (provided), 2 µL of DTT (0.1 M) (provided) and 1 µL of dNTP (10mM), mixing and brief centrifugation. Between steps 2 and 3, the program was again paused and samples were placed on ice, before adding 1 µL of SuperScript II RNase H^- reverse transcriptase (200 U/µL), further mixing and brief centrifugation.

2.1.5 Genomic DNA extraction

Mouse tail biopsies (~0.5 cm) were obtained from 2-3 week old mice and stored at −20°C or processed immediately for DNA extraction. Tail biopsies were transferred to 1.5 ml microcentrifuge tubes to which were added 615 µl of TNES buffer (see appendix) and 20 µl of Proteinase K (Qiagen, 600 mAU/ml). For extraction of DNA from confluent cell monolayers in 100 mm cell culture dishes, the monolayers were washed twice with PBS prior to solubilization in TNES, transfer of lysates to 1.5 ml microcentrifuge tubes and addition of Proteinase K as above. Samples were incubated overnight at 55°C with gentle agitation. To each sample was added 167 µl of saturated (~6M) NaCl and the samples were mixed vigorously. Following centrifugation (14,000 ×*g*) for 5 minutes at room temperature, supernatants (700 µl) were carefully transferred to new tubes. DNA was precipitated by addition of one volume (700 µl) of cold 95% ethanol to each tube, mixing and centrifugation at 20,800 ×*g* for 10 minutes at 4°C. Supernatants were aspirated and the DNA pellets were washed with 500 µl of cold 70% ethanol by vortexing briefly and centrifuging as above for 10 minutes at 4°C. The resulting pellets were dried by vacuum centrifugation and resuspended in 200 µl of TE buffer (see appendix). DNA concentrations were measured by spectrophotometry and samples were stored at 4°C or used immediately for PCR-based genotyping.

2.1.6 Polymerase Chain Reaction (PCR)

All thermal cycling, including PCR, sequencing and reverse transcription reactions, were performed using a PTC-100 Programmable Thermal Controller (MJ Research, Cambridge,

MA, USA). 5µM stocks of each primer were prepared in MilliQ water from original stocks. Each reaction consisted of 13µL AmpliTaq Gold (Applied Biosystems, Foster City, CA, USA), 5 µl forward primer (5µM), 5µL reverse primer (5 µM) and 2µl template DNA (diluted genomic DNA [~300 ng], diluted plasmid DNA [~5 ng] or undiluted synthesized cDNA as specified). The following PCR program was used for most PCR amplifications, with minor variations in annealing temperatures (step 3 below) and extension times (step 4 below) as appropriate. [Step 1: 95°C for 10 min. Step 2: 95°C for 30 secs. Step 3: 56°C for 30 secs. Step 4: 72°C for 2 mins. Step 5: repeat steps 2-4 (×30). Step 6: 72°C for 5 mins. Step 7: 4°C for 15 mins].

2.1.7 DNA sequencing

Plasmid DNA was sequenced by the addition of 1 µl of plasmid DNA (~300 ng), 6 µl of BigDye Terminator v.3 (Applied Biosystems), 1 µl of oligonucleotide (5 µM) and 12 µl of MilliQ water. After mixing by vortexing and brief centrifugation, samples were subjected to thermal cycling according to the following PCR program [Step 1: 96°C for 2 minutes. Step 2: 96°C for 30 seconds. Step 3: 50°C for 15 seconds. Step 4: 60°C for 4 minutes. Step 5: repeat steps 2-4 (x 25). Step 6: 4°C for 15 mins].

To precipitate extension products, samples were transferred to 1.5 ml microcentrifuge tubes, mixed with 80 µl of isopropanol (75%) by vortexing briefly and incubation at room temperature for 15 minutes. Tubes were then centrifuged at 20800 ×*g* for 20 minutes and the pellets were washed by addition of 250µl of 75% isopropanol, brief vortexing and centrifugation at 20,800 ×*g* for 5 minutes. After careful aspiration of the supernatants, the samples were dried in a vacuum centrifuge for 10 minutes. The resulting samples were placed on ice and delivered to the DNA sequencing facility at the Institute of Medical and Veterinary Science (IMVS) for nucleotide sequencing using an automated sequence analyser (Applied Biosystems).

2.1.8 Preparation of competent bacteria for transformation

E.coli strain DH5α was grown overnight at 37°C after streaking on Luria agar plates. Single colonies were inoculated into 5 ml Luria broths and grown overnight at 37°C with shaking. The 5 ml broths were then subcultured into pre-warmed 100 ml Luria broths and

incubated at 37°C with shaking until an OD^{600} of ~0.6 was reached. Cultures were then transferred to 50ml Falcon tubes and chilled for 5 mins on ice before centrifugation at 20,800 ×*g* for 10min at 4°C. The cell pellets were then resuspended in cold Tfb-1 (see appendix) (40% of original volume), incubated on ice for 5mins and then centrifuged (20,800 ×*g*, 10mins, 4°C). The resulting pellets were resuspended in cold Tfb-2 (see appendix) (4% of original volume) and incubated on ice for a further 15 minutes. The final suspensions were dispensed into 200 µl aliquots and 'snap-frozen' in dry ice before storing at -70°C.

2.1.9 Transformation of competent bacteria with plasmid DNA

To transform competent bacteria, an appropriate volume of plasmid DNA was added to an aliquot of frozen competent bacteria and mixed, followed by incubation on ice for 20 min. The samples were then 'heat-shocked' at 42°C for 90 seconds before returning to ice for 10 minutes. After incubation at room temperature for 5 minutes, Luria broth (1 ml) was added and the samples were incubated for 45 minutes at 37°C. The transformed bacteria were recovered by centrifugation at 20800 ×*g* for 1 minute and resuspended in 120 µl of saline (0.85 % NaCl) and plated onto Luria agar plates containing ampicillin (50 µg/ml) or kanamycin (50 µg/ml) (as appropriate to select for transformed bacteria) using the spread plate technique. The plates were incubated overnight at 37°C.

2.1.10 Preparation of plasmid DNA

In all types of preparations, single colonies resulting from the transformation process were isolated from Luria agar plates and inoculated into 10 ml Luria broths containing ampicillin (50 µg/ml) or kanamycin (50 µg/ml) as appropriate and incubated at 37°C overnight with shaking. For applications that required high quality DNA, plasmid DNA was isolated as per the respective manufacturer's instructions using the UltraClean Mini Plasmid Prep Kit (Mo Bio Laboratories, Solana Beach, CA, USA) for small-scale preparations (< 5 ml overnight culture, expected yield: < 20 µg). The PureYield Plasmid Midiprep System (Promega, Madison WI, USA) was used for larger scale preparations (< 100 ml overnight culture, expected yield: 100-200 µg). For diagnostic purposes, 1.5 ml samples of bacterial culture were centrifuged at 20800 ×*g* for 2 minutes and the pellets were resuspended in 100 µl of P1 (see appendix). To the samples were added serially 100

µl of P2 (see appendix) and 100 µl of P3 (see appendix), with mixing by inversion after each addition. The samples were then centrifuged at 20800 ×*g* for 8 minutes and the supernatants were transferred to fresh tubes containing 750 µl of cold 100% ethanol. The precipitated DNA was recovered by centrifugation at 20800 ×*g* for 14 minutes at 4°C and the pellets dried at 37°C before dissolving in 50 µl of 10mM Tris-HCl (pH 8.0) and storage at 4°C.

2.1.11 Restriction digests of plasmid DNA

Restriction endonucleases, purchased from Roche Applied Bioscience (Indianapolis, IN, USA) or New England Biolabs (Beverly, MA, USA), were used at working concentrations of 10 U/µl. For diagnostic digests of plasmid DNA, 4 µl of mini-prep plasmid DNA (approx. 1-2 µg of DNA), 1µl of each restriction enzyme and 1 µl of the appropriate 10× reaction buffer (supplied by manufacturers) were mixed, MilliQ water was added to a final volume of 10 µl and the digests were incubated at 37°C for 1-2 hours. For preparation of fragments for ligation reactions, plasmid restriction digests were performed by mixing 10 µl of plasmid DNA with 3 µl of each restriction enzyme and 5 µl of the appropriate 10× reaction buffer. MilliQ water was then added to a final volume of 50 µl and the digests were incubated at 37°C for 1-2 hours. Where necessary, enzymes were heat inactivated at the end of the digestion period by incubation at either 65°C or 80°C for 15 minutes, as per manufacturer's instructions.

2.1.12 Agarose gel electrophoresis

Agarose gels were prepared by dissolving DNA grade agarose (Progen, Heidelberg, Germany) in TAE buffer (see appendix) to a concentration of 0.8-1.5% (w/v), depending on the expected size of the products to be electrophoresed and the resolution desired. Gels were cast in horizontal EasyCast Mini Gel Electrophoresis Systems (Owl Separation Systems, Portsmouth, NH, USA) as per manufacturer's instructions. Samples to be loaded were mixed with Orange G loading buffer (6×) (see appendix) at a ratio of 5:1. Similarly, 1 µg of an appropriate DNA ladder was diluted with MilliQ water and mixed with loading buffer as described above. Appropriate volumes of sample were then loaded into wells and subjected to electrophoresis until the desired separation was achieved. Gels were then stained with ethidium bromide (2,7-Diamino-10-ethyl-9-phenyl phenanthridinum bromide) (Sigma) (0.2% w/v) in TAE buffer for 10 minutes and de-stained for 5 minutes in water.

Alternatively, if greater staining intensity was required or DNA was to be extracted for downstream applications such as cloning, gels were stained for 10 minutes in SYBR Gold (Molecular Probes, Eugene, OR, USA) diluted to a 1× concentration (from a 10000× stock in DMSO) in TAE buffer, followed by de-staining for 5 minutes in water.

2.1.13 Gel extraction of DNA

To extract DNA from agarose gels after electrophoresis for downstream applications such as cloning, bands were excised using a scalpel blade. DNA was purified using either the QIAquick Gel Extraction Kit (Qiagen) or the Wizard SV Gel and PCR Clean-Up System (Promega), according to manufacturer's instructions.

2.1.14 Alkaline phosphatase treatment of digested DNA

Calf Intestinal Alkaline Phosphatase (New England Biolabs) was used to prevent re-circularisation of cloning vectors digested with a single restriction enzyme. After digestion, electrophoresis and gel extraction, DNA was treated as follows: 8µl of DNA was mixed with 1 µl of alkaline phosphatase (10 units/µl) and 1 µl of 10× reaction buffer (supplies). Tubes were vortexed and incubated at 37°C for 60mins, followed by heat-inactivation at 70°C for 15 mins. Treated DNA was then used directly for downstream ligation reactions or, if necessary, purified using the Wizard SV Gel and PCR Clean-Up System (Promega) prior to downstream ligation.

2.1.15 Annealing oligonucleotides for adaptor-duplex cloning

Cloning using adaptor-duplexes was performed under guidelines suggested by Roche Applied Science (Roche Applied Science, 2000). To this end, complementary oligonucleotides encoding the peptide of interest were designed. These oligonucleotides were also designed to contain single-stranded 'overhangs' to complement the insertion site in the appropriately digested destination plasmid. The purified single stranded oligonucleotides for the top and bottom strands were resuspended in MilliQ water to a concentration of 100 µM. These oligonucleotides were then mixed at a 1:1 ratio (to theoretically give 50 µM of double-stranded oligonucleotide). Oligonucleotide annealing was achieved using a PTC-100 Programmable Thermal Controller (MJ Research) and the following program [95°C for 30 seconds, 72°C for 2 minutes, 37°C for 2 minutes, 25°C

for 2 minutes, 4°C for 20 minutes]. Annealed double-stranded oligonucleotides were then used immediately for cloning or stored at -20°C for later use.

2.1.16 DNA ligation

Reactions for ligation of digested 'insert' DNA into similarly digested 'backbone' plasmid DNA were generally performed in 20 µl volumes. Insert DNA was mixed with backbone DNA at a ratio of 3:1 and diluted to a final volume of 17 µl. This solution was added to a thin-walled PCR tube, followed by 2 µl of 10× ligation buffer (supplied) and 1 µl of T4 DNA ligase. In the case of adaptor-duplex cloning, 1 µl of diluted annealed oligonucleotide (0.5 µM) was used for each ligation. Samples were mixed by vortexing and incubated at 14°C for 1 hour or 4°C overnight. Ligation products were then transformed into competent bacteria and plated onto selective Luria agar plates as described earlier. Parallel controls, in which 'insert' DNA was replaced with MilliQ water, were performed for each ligation.

2.2 Cell Culture Techniques

2.2.1 Tissue Culture Medium

Dulbecco's Modified Eagle's Medium (DMEM) and RPMI 1640 were purchased from GibcoBRL (Grand Island, NY, USA) as powder concentrates. Liquid medium, containing appropriate antibiotics, was prepared according to manufacturer's instructions. Cell lines were cultured in the appropriate medium (see Table 2-2) containing 10% foetal bovine serum (FBS) (Trace Biosciences, Castle Hill, NSW, Australia) and supplemented with 2 mM L-glutamine (Gibco BRL).

2.2.2 Maintenance of Cell Lines

Cells were cultured in 0.2 µm vented-cap tissue culture flasks (25, 75 or 175 cm^2), tissue culture dishes (35 or 100 mm) or tissue culture trays (96-, 24-, 12- or 6-well) (Falcon-Becton Dickinson, Franklin Lakes, NJ, USA) in a humidified 5% CO_2/air atmosphere at 37°C. Adherent cells were subcultured by aspirating growth medium, washing twice with PBS (see appendix) and incubating with a small volume of Trypsin-EDTA (see appendix) at 37°C for 5 minutes. Cells were dislodged by gentle tapping and resuspended in warm

Cell Line	Culture Media
COS-7	Dulbecco's modified Eagle's medium (DMEM), 10% foetal bovine serum (FBS), 2mM L-glutamine, 50 units/ml penicillin, 50 μg/ml streptomycin.
H4IIE	DMEM, 10% FBS, 2mM L-glutamine, 50 units/ml penicillin, 50 μg/ml streptomycin.
HuH-7	DMEM, 10% FBS, 2mM L-glutamine, 50 units/ml penicillin, 50 μg/ml streptomycin.
CHO	RPMI, 10% FBS, 2mM L-glutamine, 50 units/ml penicillin, 50 μg/ml streptomycin.

Table 2-2. Cell culture media. DMEM, RPMI, L-glutamine, penicillin and streptomycin were purchased from Gibco BRL (Grand Island, New York, USA). Foetal bovine serum was purchased from Trace Biosciences (Castle Hill, Sydney, Australia).

culture medium containing FBS. Cell concentrations were determined by enumeration using a haemocytometer and cell viability was determined by trypan blue exclusion (0.4%, w/v) (Sigma). Generally, cells were subcultured at a ratio of between 1:5 and 1:10.

2.2.3 Cryopreservation

Cryopreservation of cell lines was initiated by transferring cells to sterile tubes and centrifuging at 200 ×*g* for 10 minutes. Cells were then resuspended in medium to a concentration of between 5×10^6 and 1×10^7 cells/ml and an equal volume of cold freezing mix (50% medium, 30% FBS, 20% DMSO, filter-sterilized) was added drop-wise and mixed. Aliquots of 0.5-1 ml of the suspension were added to each sterile cryopreservation tube and tubes were transferred to a freezing chamber (Nalgene, Rochester, NY, USA) containing isopropanol. The chamber was then transferred to a -80°C freezer to achieve a cooling rate of -1°C / minute. For long-term storage, the frozen tubes were transferred to a cryopreservation system containing liquid nitrogen.

2.2.4 Resuscitation of Frozen Cells

Tubes containing frozen cells were thawed rapidly in a 37°C water bath, the contents transferred to a fresh sterile tube and an equal volume of warm culture medium was added drop-wise over 5 minutes. The diluted samples were then incubated at room temperature for 15 minutes, before adding a further equal volume of warm medium over 5 minutes. After another incubation at room temperature for 5-15 minutes, the cells were centrifuged at 200 ×*g* and the supernatant was aspirated. Cells were then washed twice in 10 mls of warm medium before performing cell counts to determine yield and viability. Cells were then transferred to culture flasks, adding warm medium to a minimum cell concentration of approximately 2×10^5 cells/ml. The flasks were incubated at 37°C in a 5% CO_2 incubator.

2.2.5 Transfection

Cells were transfected using FuGENE 6 Transfection Reagent (Roche Applied Science) as per manufacturer's instructions. Briefly, cells were seeded into 6-well trays at $1\text{-}3 \times 10^5$ cells/well, such that 50-80% confluency was achieved 24 hours later, at the time when the cells were to be transfected. Serum-free medium, transfection reagent and plasmid DNA were mixed in a sterile tube and incubated as per manufacturer's instructions. Transfection

complexes were added to cells drop-wise and assays were performed 24-72 hours later. Generation of stably transfected cell lines was achieved by addition of the appropriate antibiotic to transfected cells 24-48 hours post-transfection. Usually, initial selection was performed using G418 sulphate (Invitrogen) at 500 μg/ml, puromycin dichloride (Sigma) at 5 μg/ml or Blasticidin S (Invitrogen) at 5 μg/ml, as appropriate. After generation of stable antibiotic resistance, cells were maintained in normal culture medium containing a lower concentration of the appropriate antibiotic (G418: 200 μg/ml, puromycin: 3 μg/ml, blasticidin: 3 μg/ml). Clones were produced from stable cell lines by trypsinizing the cultures and re-seeding into 10 cm tissue culture dishes at a very low density (~200 cells/dish). After several days of growth, distinct colonies were 'picked' using a pipette tip and transferred to wells of a 24-well tissue culture tray. Cloned cell lines were screened for expression of the protein of interest when cell numbers were sufficient.

2.3 Flow Cytometry Techniques

2.3.1 Labelling Cell Surface Antigens

Surface antigens were labelled by indirect immunofluorescence, for assessment by flow cytometry. All procedures were performed at 4°C or on ice. Approximately 1×10^6 cells were transferred to each FACS tube (Becton Dickinson, San Jose, CA, USA), centrifuged at 200 ×*g* for 10 minutes and the cell pellets were washed by resuspending in 3ml of cold FACS wash buffer (see appendix). After re-centrifugation, the cells were resuspended in 50 μl of primary antibody (mAb supernatant containing 10% normal rat serum (NRS) (v/v) or purified antibody diluted to an appropriate concentration in PBS containing 10% NRS (v/v)) (see Table 2-3) and incubated on ice for 1 hour. After washing twice in cold FACS wash buffer, the cells were resuspended in 50 μl of an appropriate secondary antibody fluorescent conjugate (see Table 2-4), or in the case of biotinylated primary antibodies, a streptavidin-fluorochrome conjugate. Secondary antibodies were diluted in PBS containing 10% NRS. After incubation on ice for one hour in the dark, the cells were washed twice as described and resuspended in 0.5 ml of FACS fixative solution (see appendix). Tubes were stored in the dark at 4°C prior to analysis.

Specificity	Name	Nature	Dilution	Manufacturer / Reference
FAT/CD36 (r)	UA009	mAb (IgG_1) (hybridoma S/N)	Neat (IF, FACS)	(Zhang et al., 2003)
	Biotinylated UA009	Biotinylated purified mAb (IgG_1) (~0.13 mg/ml)	1:150 (IF, FACS)	N/A
FAT/CD36 (h, r)	MO25	Purified mAb (IgG_1) (~1.6 mg/ml)	1:2000 (WB)	(Tandon et al., 1989)
Caveolin-1 (h, r, m)	C060	Purified mAb (IgM) (0.25 mg/ml)	1:500 (WB)	BD Transduction Laboratories (610057)
Transferrin receptor (r)	OX-26	mAb (IgG_{2a}) (hybridoma S/N)	1:10 (WB)	(Jefferies et al., 1985)
GFP	Biotinylated anti-GFP	Biotinylated purified (IgG) goat polyclonal (1 mg/ml)	1:5000 (WB)	Rockland (600-106-215)
SR-BI (h, r, m)	anti-SR-BI	Purified (IgG) rabbit polyclonal	1:2000 (WB)	Novus Biologicals (NB 400-104)
SR-BI/BII (h, r, m)	anti-SR-BI/BII	unpurified rabbit antisera	1:200 (IF, FACS)	Novus Biologicals (NB 400-103)

Table 2-3.

Primary antibodies. Species specificity ~ h: human, r: rat, m: mouse. Applications ~ IF: immunofluorescent microscopy, FACS: fluorescence activated cell scanning, WB: Western blotting. The catalogue numbers of each commercially available primary antibody are indicated.

Conjugate	Specificity	Host Species	Dilution / Application	Manufacturer
Horseradish peroxidase (HRP)	Mouse Ig	Sheep [F(ab')$_2$]	1:50 (IH) 1:20000 (WB)	Amersham Biosciences (NA9310V)
Horseradish peroxidase (HRP)	Rabbit Ig	Goat	1:15000 (WB)	Pierce Biotechnologies (1858415)
Horseradish peroxidase (HRP)	Biotin	N/A (Streptavidin)	1:20000 (WB)	Amersham Biosciences
FITC	Mouse Ig	Goat	1:100 (IF, FACS)	BD Pharmingen
Cy3	Mouse Ig	Donkey	1:150 (IF, FACS)	Jackson Immunoresearch (715-165-151)
Cy3	Rabbit Ig	Donkey	1:150 (IF, FACS)	Jackson Immunoresearch (711-165-152)
Cy5	Rabbit Ig	Donkey	1:150 (IF, FACS)	Jackson Immunoresearch (711-175-152)
FITC	Biotin	N/A (Streptavidin)	1:50 (FACS)	BD Pharmingen (554 060)
PE	Biotin	N/A (Streptavidin)	1:200 (FACS)	BD Pharmingen (554 061)

Table 2-4.

Conjugated secondary antibodies. Abbreviations: HRP, horseradish peroxidase; FITC, fluorescein isothiocyanate; PE, phyco-erythrin; Cy, cyanine dyes; IH, immunohistochemistry; IF, immunofluorescent microscopy; FACS, fluorescence activated cell scanning; N/A, not-applicable.

2.3.2 Labelling Intracellular Antigens

To label intracellular antigens by indirect immunofluorescence, the cells were fixed in suspension and permeabilized prior to incubation with appropriate primary antibodies and secondary antibody fluorescent conjugates. Approximately 1×10^6 cells were transferred to each FACS tube and washed in 3 ml of serum-free DPBS (see appendix). The cells were resuspended in 1ml of cold DPBS, 1 ml of 10% buffered formalin was added to each tube and the tubes were incubated on ice for 6 minutes. A further 2 ml of cold intracellular FACS wash buffer (see appendix) was then added to each tube and tubes were centrifuged at 200 $\times g$ for 10 minutes at 4°C. The supernatant was aspirated and the cells were washed in 3 ml of cold intracellular FACS wash buffer. After another round of centrifugation, the cells were washed in 3 ml of cold intracellular FACS wash buffer containing 0.1% saponin (w/v) (Sigma) to permeabilize cells.

After centrifugation, the permeabilized cells were resuspended in 50 µl of primary antibody (mAb supernatant containing 10% NRS (v/v) and 0.1% saponin (w/v) or purified antibody diluted to an appropriate concentration in DPBS containing 10% NRS (v/v) and 0.1% saponin (w/v)). Samples were then incubated on ice for 1 hour before washing twice with cold intracellular FACS wash buffer containing saponin. The cell pellets were then resuspended in 50 µl of secondary antibody fluorescent conjugate diluted to an appropriate concentration in DPBS containing 10% NRS (v/v) and 0.1% saponin (w/v). A streptavidin fluorescent conjugate was used in the case of biotinylated primary antibodies. The samples were then incubated on ice in the dark for 1 hour before washing once with cold intracellular FACS wash buffer containing 0.1% saponin (w/v) and once with cold intracellular FACS wash buffer lacking saponin. Cell pellets were resuspended in 0.5 ml of FACS fixative solution (see appendix) and stored in the dark at 4°C prior to analysis.

2.3.3 Flow Cytometric Analysis of Lipid Uptake from DiI-HDL

A flow cytometric assay was adapted (Gu et al., 1998), to assess the ability of transfected cell lines to take up lipid from purified HDL_3 labelled with DiI. Cells were seeded into wells of 6-well tissue culture trays (in triplicate for each condition) at an appropriate density, such that cells would be ~90% confluent at the time of the assay. The monolayers were washed twice with PBS before addition of 1 ml of warm DMEM containing 0.5% BSA (Sigma) and HDL_3-DiI (10 µg/ml unless otherwise specified). The plates were then

incubated with the HDL_3-DiI for 2 hours (unless otherwise specified) under normal culture conditions. The HDL_3-DiI-containing medium was then aspirated and the monolayers were washed three times, each with 2 ml of PBS. They were then incubated at 4°C with 1 ml of cold PBS-B/E (see appendix) for 30 minutes. The released cells were then resuspended, transferred to FACS tubes and washed once with 3 ml of cold PBS-B/E. The resulting cell pellets were resuspended in 0.5 ml of PBS-B/E and cell-associated fluorescence was assessed immediately by flow cytometry, using the FL-2 laser line.

Following the above HDL_3-DiI incubation and wash steps, cells were labelled where applicable by indirect immunofluorescence (using FITC as the second colour). Pilot experiments demonstrated that this process had no significant influence on the fluorescence of DiI within the cells. Preliminary experiments also demonstrated that HDL-lipid uptake was specific, in that cell-associated DiI fluorescence was negligible when a 40-fold excess of unlabelled HDL was included in the uptake medium. Similarly, cell-associated DiI fluorescence was minimal when uptake from HDL_3-DiI was performed at 4°C.

2.3.4 Flow Cytometric Analysis

Flow cytometric analysis of cell-associated fluorescence was performed using a FACScan or FACSaria (Becton Dickinson) flow cytometer. Intact cells were gated based on their forward-scatter (FSC) (size) and side-scatter (SSC) (complexity) properties. Fluorescence settings were established using unlabelled cells or cells labelled with isotype-matched control antibody, as appropriate. Two-colour flow cytometry required compensation for fluorescence 'bleed-through' from one excitation/emission spectrum into the other. This was achieved by manipulating compensation settings such that labelling of cells with a single fluorophore did not alter the mean fluorescence of the population for the other fluorescence channel.

2.4 Fluorescence Microscopy Techniques

2.4.1 Indirect immunofluorescence labelling

Prior to immunofluorescence labelling, cells were seeded at 1-5 × 10^4 cells per well in 24-well cell culture trays containing sterile coverslips and incubated for 24-48 hours. The coverslips were washed twice with PBS, before the addition of 0.5 ml of cold 5% buffered formalin in DPBS. The cells were fixed for 6 minutes at 4°C and washed twice with cold DPBS containing 1% FBS. Cells on coverslips were labelled by incubation with 200 µl of primary antibody (neat culture supernatant or appropriately diluted purified antibody) (see Table 2-3) containing 10% heat-inactivated normal rat serum (NRS) for 1 hour at 4°C. After washing twice with cold intracellular FACS wash buffer (see appendix), bound primary antibody was detected by incubation for 1 hour in the dark at 4°C with an appropriately diluted secondary antibody fluorescent conjugate (see Table 2-4) in PBS containing 10% NRS. To detect intracellular antigens in fixed cells, saponin (0.1% w/v) was included in wash buffers and antibody preparations. Following labelling, samples were washed twice with cold intracellular FACS wash buffer, before addition of 0.5 ml of FACS fixative solution (see appendix). After incubation (at least 30 minutes) at 4°C, fixative solution was aspirated and replaced with PBS. Coverslips were mounted on glass slides with Vectashield mounting medium containing DAPI (Vector Laboratories, Burlingame, CA, USA).

2.4.2 Staining Lipid Rafts with CT-B

An Alexa594 conjugated-cholera toxin B subunit (CT-B) (Molecular Probes) was used to visualize lipid rafts. Cells were grown on coverslips as above but before fixation, the coverslips were washed twice with PBS and cultured for 1 hour with 200 µl of Alexa594-CT-B (0.5 µg/ml w/v) in serum-free culture medium. The coverslips were then washed twice with PBS before fixation and immunofluorescence labelling (where applicable), as above.

2.4.3 Cellular binding and uptake of HDL_3-DiI

For fluorescence microscopic analysis of HDL_3-DiI binding and DiI uptake, cells were grown on sterile coverslips. HDL_3-DiI was prepared as described in section 2.6.3. The coverslips were washed twice with PBS before addition of 0.5 ml of HDL_3-DiI (10 µg/ml of protein (unless otherwise indicated) in serum-free culture medium). After culture for 2

hours (unless otherwise indicated), coverslips were washed twice with PBS and the cells were visualized immediately by fluorescence microscopy.

2.4.4 Light fluorescence microscopy

Light fluorescence microscopy was performed using an Olympus BX40 microscope, equipped with an Olympus U-RFL-T burner. Images were acquired using an Olympus DP70 camera and Olympus DP Controller software.

2.4.5 Confocal fluorescence microscopy

Confocal fluorescence microscopy was performed at Adelaide Microscopy (Adelaide, Australia). Microscopy was performed using a Bio-Rad MRC-1000UV Confocal Laser Scanning Microscope System, equipped with Nikon Diaphot 300 inverted microscope and Krypton/Argon and UV-Argon lasers. Alternatively, a Leica SP5 Spectral Scanning Confocal Microscope System was employed. Images were acquired for a single focal plane using a Kalman setting of at least 3. Images were analysed using Confocal Assistant version 4.02 and/or Adobe Photoshop 5.5 software.

2.5 Protein Chemistry Techniques

2.5.1 Antibody biotinylation

Purified mAb UA009 (5.2 mg/ml) was biotinylated as follows. Azide and salts were removed from 1 mg of antibody using Centriprep columns (Amicon, Beverly, USA) according to manufacturer's instructions, using three washes with bicarbonate buffer (0.1M $NaHCO_3$ buffer (pH 8.4)). The concentration of antibody was then adjusted to 1 mg/ml in bicarbonate buffer. A stock solution of biotinylation reagent was prepared by dissolving 1 mg of EZ-Link^{TM} Sulfo-NHS-Biotin (Pierce Biotechnologies, Rockford, IL, USA) in 1ml of DMSO at room temperature. Biotinylation reagent was then added to the diluted antibody drop-wise, with gentle mixing, followed by incubation for two hours in the dark at room temperature on a rocking platform. The biotinylated antibody was then separated from non-conjugated biotin using a PD-10 Sepahdex G-25M column (Pharmacia Biotech, Uppsala, Sweden) that was equilibrated with PBS containing 0.01M sodium azide. The biotinylated antibody mixture was added, 25 fractions (1 ml each) were collected by elution with PBS/azide and absorbance was measured at 280 nm (lambda

report) using a Bio-Rad Smart Spec 3000 spectrophotometer (Bio-Rad Laboratories). The first major peak was expected to contain antibody and the concentration of protein in this fraction (fraction 4) was calculated to be 0.13 mg/ml, using the formula:

Antibody concentration (mg/ml) = Absorbance (280nm) / 1.4.

The appropriate working dilution of this biotinylated antibody for use in flow cytometry was determined by labelling H4IIE (5A) and H4IIE-FAT/CD36 (1A) cells (see 3.3.2) using a range of dilutions (1:20 to 1:200), followed by detection with streptavidin-conjugated PE (see Table 2-4). A dilution of 1:150 (0.9 μg/ml) was chosen for future use.

2.5.2 Sucrose density step-gradient ultracentrifugation

Detergent-resistant membranes (DRMs) were prepared as follows. Confluent cell monolayers in 10 cm tissue culture dishes were washed twice with PBS and lysed in 0.7 ml of 1% Triton X-100 (v/v) in TNE buffer (see appendix). Lysates were transferred to microcentrifuge tubes, passed through a 26-gauge needle 10 times and incubated on ice for 30 minutes. Samples were then centrifuged at 1000 x *g* to remove nuclear debris and 0.5 ml of the cleared lysate was transferred to a new tube, mixed with an equal volume of 80% (w/v) sucrose in TNE buffer and transferred to 4.5 ml SW60 centrifuge tubes (Beckmann). The sample was overlaid with 2.5 ml of 38% (w/v) sucrose, followed by 1ml of 5% (w/v) sucrose in TNE buffer. The tubes were then centrifuged at 38,000 rpm (148,305 x*g*) for 15 hours at 4°C. Twelve fractions were collected, commencing at the top. The protein concentration in each fraction was determined by the Bradford procedure and the density was calculated from the refractive index, measured using a refractometer. An equal volume from each fraction was separated by SDS-PAGE for immunoblotting (see sections 2.5.8 and 2.5.9).

2.5.3 Hypotonic lysis

Fractionation of cells into soluble and particulate fractions by hypotonic lysis and high-speed centrifugation was performed essentially as described by Woodman and colleagues (Woodman et al., 2002). Briefly, cells were grown to confluency in 60 mm cell culture dishes and washed twice with PBS before scraping into 5 ml of ice-cold PBS. The cells were then centrifuged and the pellets were resuspended in 0.5 ml of cold hypotonic lysis buffer (see appendix) containing protease inhibitor cocktail (Sigma). After incubation on

ice for 30 minutes, the samples were passed through a 26-gauge needle 10 times and centrifuged at 1000 ×*g* for 5 minutes. Post-nuclear supernatants were transferred to polycarbonate tubes (11 x 34 mm) and centrifuged at 41,000 rpm for 30 minutes in a TLS-55 rotor (Beckman) at 4°C. Supernatants were collected (soluble fraction) and after gently rinsing with 200 µl of cold hypotonic lysis buffer, the pellets were resuspended in an equal volume of 1% SDS. Equal volumes of soluble and particulate fractions were subjected to SDS-PAGE and immunoblotting.

2.5.4 Extraction of Triton-soluble proteins

Triton extraction was performed essentially as described by Woodman *et al.* (Woodman et al., 2002). Briefly, confluent cell monolayers grown in six-well cell culture trays were washed twice with ice-cold PBS before the addition of 350 µl of cold MBS (see appendix) containing 1% Triton X-100 and protease inhibitors. Soluble fractions were collected after incubation on ice for 30 minutes. The residual monolayers were then rinsed gently with cold MBS, before the addition of 350 µl of 1% SDS to collect the Triton X-100-insoluble fractions. Equal volumes of Triton X-100-soluble and -insoluble fractions were subjected to SDS-PAGE and immunoblotting.

2.5.5 Cell surface biotinylation and streptavidin-precipitation

Cell surface biotinylation was performed essentially as described by Lisanti and colleagues (Lisanti et al., 1989). Briefly, cells were grown to confluency in 60 mm cell culture dishes, washed three times with ice-cold PBS-C/M (see appendix) and then incubated with 1 ml of sulfo-NHS-biotin (Pierce Biotechnologies) (0.5 mg/ml in PBS-C/M) for 20 minutes at 4°C with gentle agitation. This buffer was discharged, and fresh biotinylation agent was added for a further 20 minutes. Cell monolayers were then washed once with ice-cold DMEM and three times with ice-cold PBS-C/M, before lysis on ice in TNE buffer (see appendix) containing 1 % Triton X-100 plus appropriately diluted protease inhibitor cocktail (Sigma). Post-nuclear supernatants were prepared by centrifugation and the protein concentration in each lysate was determined by the Bradford procedure (Bio-Rad Laboratories). For each streptavidin precipitation, 500 µg of cellular protein, adjusted to 0.5 mg/ml, was mixed with 20 µl of streptavidin-conjugated agarose beads (Sigma) and incubated at 4°C by end-over-end rotation for two hours. The beads were washed four times with lysis buffer before heating at 95°C for 5 minutes in 50 µl of 2× SDS-PAGE

loading buffer (see appendix). The streptavidin precipitates, together with 20 μg of protein from each lysate, were subjected to 12% SDS-PAGE and immunoblotting.

2.5.6 Cell surface biotinylation and streptavidin precipitation of DRMs

Confluent cell monolayers in 100 mm cell culture dishes were surface-biotinylated as described above. The biotinylated cells were then lysed in 0.7 ml of TNE buffer (see appendix) containing 1% Triton X-100 and post-nuclear lysates were subjected to sucrose density gradient fractionation as described above. DRM fractions (fractions 2-4) were pooled, as were fractions referred to collectively as 'non-raft' fractions (fractions 8-12). Protein in the DRM fractions was below the limits of detection by the Bradford procedure. These fractions (1 ml total) were, therefore, used undiluted for precipitation of biotinylated proteins using streptavidin-conjugated agarose (as above). In the case of the non-raft fraction, 500 μg of protein was diluted in TNE buffer containing 1% Triton X-100 to a final volume of 1 ml and this was used for streptavidin precipitation of non-raft transmembrane proteins. Streptavidin precipitates and 20 μl of the post-streptavidin supernatant ('wash') were subjected to 12% SDS-PAGE and immunoblotting.

2.5.7 Deglycosylation of proteins with *N*-glycanase (PNGase F)

Proteins were de-glycosylated using *N*-glycanase (Genzyme Corporation, Baulkham Hills, NSW) according to manufacturer's instructions. Briefly, cells were lysed in PBS containing 1% β-mercaptoethanol (v/v) and 0.5% SDS (w/v). Aliquots of each lysate were denatured at 100°C for ten minutes. Twenty micrograms of protein from each lysate was then transferred to a new tube and the volume was adjusted to 12μl with PBS. To each sample, 2μl of 10% NP-40 (v/v) was added and samples were mixed thoroughly, before addition of 0.25μl *N*-glycanase. Control digest reactions lacked enzyme. Samples were then incubated at 37°C overnight. To each tube 5μl of 5× SDS-PAGE sample buffer (see appendix) was then added, samples were heated at 95°C for five minutes and subjected to SDS-PAGE and Western blotting.

2.5.8 SDS-PAGE

SDS polyacrylamide gel electrophoresis was used to separate denatured proteins as follows. The Protean II Dual Slab Cell (Bio-Rad) was used to cast discontinuous polyacrylamide gels. Twelve percent acrylamide gels (separating) with 4% stacking gels

were used, unless otherwise indicated. The following table indicates the contents of separating and stacking gel.

	Separating Gel (0.375M Tris, pH 8.8)		Stacking Gel (0.125M Tris, pH 6.8)
	12%	**7.5%**	**4%**
Distilled water	3.35 ml	4.85 ml	6.1 ml
0.5M Tris-HCl (pH 6.8)	-	-	2.5 ml
1.5M Tris-HCl, (pH 8.8)	2.5 ml	2.5 ml	-
10% SDS (w/v)	100 µl	100 µl	100 µl
Acrylamide/Bis (30% stock) *	4.0 ml	2.5 ml	1.3 ml
10% ammonium persulfate (APS) **	50 µl	50 µl	50 µl
TEMED	5 µl	5 µl	5 µl
TOTAL MONOMER	10 ml	10 ml	10 ml

* Acrylamide/bis solution (37.5:1) was purchased from Bio-Rad.

** 10% ammonium persulfate was made fresh daily.

Where applicable, protein concentrations were determined by the Braford procedure (Bradford, 1976), using the Bio-Rad Protein Assay (Bio-Rad) and BSA standards (New England Biolabs) and unless otherwise specified, the quantity of protein loaded from each sample was 25 µg. If necessary, samples were diluted in the respective cell lysis buffer and then further diluted (4:1) with either SDS reducing buffer (see appendix) or, where indicated, with SDS non-reducing buffer (lacking β-mercaptoethanol). Molecular weight markers were from New England Biolabs (Prestained Protein Marker, Broad Range (6-175 kDa)). All samples, including markers, were heated at 95°C for 5 minutes before loading. Following assembly of the inner cooling core, inner and outer reservoirs of were filled

with running buffer (GTS, see appendix) and boiled samples were loaded and separated by electrophoresis (200 V, ~300 mA).

Following separation, gels were stained with Coomassie Brilliant Blue R-250 (0.025% (w/v) in 40% methanol (v/v), 10% acetic acid (v/v)) for approximately 2 hours, followed by de-staining in 10% methanol (v/v), 5% acetic acid (v/v) for several hours. Alternatively, they were equilibrated in cold transfer buffer (see appendix) prior to electrophoretic transfer.

2.5.9 Western blotting

Following equilibration of gels in cold transfer buffer (as described above) for approximately 15 minutes, proteins were transferred to PVDF membrane (Hybond-P, Amersham Biosciences) by electrophoresis (100V, 1 hour) in cold transfer buffer using the Mini Trans Blot Electrophoretic Transfer Cell (Bio-Rad), according to the manufacturer's instructions. Membranes were then blocked for 1-2 hours at room temperature using 7.5% BSA (w/v) in TBS (see appendix) containing 0.1% Tween-20 (v/v) (TBS-T) with gentle agitation. Membranes were then incubated with appropriately diluted primary antibody (see Table 2-4) in TBS-T containing 0.5% BSA (w/v) overnight at 4°C with gentle agitation.

The blocked membranes were washed with large volumes of TBS-T (3 changes, 15 minutes per wash) and incubated with appropriately diluted horseradish peroxidase-conjugated secondary antibody in TBS-T containing 0.5% BSA (w/v) for one hour at room temperature with gentle agitation. The membranes were then washed extensively with large volumes of TBS-T (6 changes, 10 minutes per wash), before detection of bound antibody using a chemiluminescent substrate (SuperSignal West Femto Maximum Sensitivity Substrate, Pierce Biotechnology) and X-ray film (Curix Ortho HT-G Medical X-ray Film, AGFA).

2.5.10 Staining of cryostat sections by the indirect immunoperoxidase technique

Rat liver samples were embedded in OCT mounting medium (Tissue-Tek, Sakura Finetek USA), frozen in liquid nitrogen-cooled isopentane and stored at -80°C. Cryostat sections (5 μm) were transferred to glass slides, air-dried and fixed at 4°C in 95% ethanol for 5

minutes. Sections were then re-hydrated in cold PBS before incubating for 1 hour at 4°C with 50 µl of hybridoma culture supernatant containing 10% heat-inactivated normal rat serum (NRS). The slides were rinsed three times in cold PBS, before a further 1 hour incubation at 4°C with horseradish peroxidase-conjugated anti-mouse IgG $F(ab')_2$ (Amersham Biosciences, Piscataway, NJ) diluted 1:20 in PBS containing 10% NRS. After rinsing three times in cold PBS, bound conjugate was detected by incubation for 10 minutes in 0.05 M Tris buffer (pH 7.6) containing 0.02% hydrogen peroxide and 5 mg/ml diaminobenzidine (DAB, Sigma). The sections were then rinsed, counterstained with Gill's haematoxylin (see appendix), dehydrated and cleared before mounting in DePeX medium (Gurr, BDH, England).

2.6 Lipid Chemistry Techniques

2.6.1 Fractionation of Human Plasma Lipoproteins using OptiPrep

Human blood (approximately 50 mls per preparation) was collected into 9 ml EDTA-coated tubes (Greiner (Vacuette), Frickenhausen, Germany). Plasma was separated from blood cells by centrifugation (2,000 ×*g*, 15 minutes, 4°C). Chylomicrons were removed from plasma by ultracentrifugation using a Beckman SW-60 rotor (100,000 ×*g*, 10 minutes, 4°C). Chylomicron-free plasma was collected by tube puncture and adjusted to 12% iodixanol (w/v) using OptiPrep (60% iodixanol (w/v), density: 1.32 g/ml) (Axis-Shield, Oslo, Norway). The samples were transferred to 3.9 ml Quick-Seal polyallomer tubes (Beckman Coulter, Fullerton, CA, USA) in aliquots of 2.8 ml and over each aliquot was layered sufficient Hepes-buffered saline (0.85% NaCl (w/v), 10 mM Hepes-NaOH, pH 7.4) to fill the tubes. Tubes were then sealed and subjected to ultracentrifugation (350,000 $\times g_{av}$, 3 hours, 16°C, slow acceleration / deceleration). Fractions (0.1-0.2 ml) were collected from the bottom by tube puncture, or from the top by upward displacement with a solution of 80% sucrose using a peristaltic pump (Gilson (Minipuls 2), Middletown, WI, USA). For some preparations, a 0.5 ml cushion of 20% iodixanol was added to each tube before addition of iodixanol-adjusted plasma. The protein concentration in each fraction was assessed by the Bradford procedure and the density was calculated from the refractive index (measured using a refractometer, according to a standard table provided by the

manufacturer). Proteins in the fractions were analysed by SDS-PAGE and Coomassie staining.

2.6.2 Purification of HDL_3 by Sequential Ultracentrifugation

Chylomicron-free plasma was prepared as described above. Density was calculated from refractive index (measured using a refractometer) according to the following formula:

$$\rho = a\eta - b$$

where 'ρ' is density (g/ml), 'η' is refractive index and 'a' and 'b' are constants (for KBr, a = 6.4786 and b = 7.6431 at 25°C).

The density of plasma was adjusted to 1.14 g/ml by adding solid potassium bromide. The adjusted plasma was then transferred into 16 mm diameter (4.2 ml) tubes, filled (if necessary) with 1.14 g/ml KBr in HEPES-buffered saline, sealed and centrifuged at 175,000 ×*g* in a 80 Ti rotor for 24 hours at 4°C. After centrifugation, yellow/brown bands were apparent at the top and bottom of each tube. The tops of the tubes were sliced and the upper fraction (~2mls) (VLDL, LDL, HDL_2) was removed carefully from each tube using a Pasteur pipette and set aside for analysis. The lower fraction (HDL_3, plasma proteins) was collected and the density was adjusted to 1.21 g/ml using solid KBr.

The latter samples were then transferred to centrifuge tubes as above, filled (if necessary) with 1.21 g/ml KBr in HEPES-buffered saline, sealed and centrifuged (175,000 ×*g* in a 80 Ti rotor, 40 hours, 4°C). The upper fraction (containing HDL_3) was collected from each tube, dialysed for 2-3 hours against 1.21 g/ml KBr in TBS and transferred to a new centrifuge tube. The lower fraction (lipoprotein-deficient plasma) was collected from each tube, dialyzed against TBS (see appendix) and stored at 4°C for later use. Centrifuge tubes containing semi-pure HDL_3 (adjusted to 1.21 g/ml) were filled (if necessary) with 1.21 g/ml KBr in HEPES-buffered saline, sealed and centrifuged as above (40 hours). Upper fractions (pure HDL_3), which were gold in colour, were collected and dialysed exhaustively against TBS. Purified HDL_3 were stored under nitrogen in the dark and were used within two weeks of their preparation. Protein (apolipoprotein AI) concentration was determined by the Bradford procedure for each preparation and purity was assessed by

12% SDS-PAGE and Coomassie blue staining. Pure HDL_3 was indicated by the presence of a single ~27 kDa band (ApoAI) after SDS-PAGE performed under reducing conditions.

2.6.3 Fluorescent (DiI) Labelling of Purified HDL_3

Labelling of pure HDL_3 with the fluorescent phospholipid analogue DiI-C_{18} (1, 1'-dioctadecyl-3, 3, 3', 3'-tetramethylindocarbocyanine perchlorate, Molecular Probes) was performed essentially as described by Pitas *et al.* (Pitas et al., 1981). Firstly, 2 mg of pure HDL_3 (prepared by sequential ultracentrifugation) was added to 4 ml of (dialysed) lipoprotein-deficient plasma (prepared as a bi-product of sequential ultracentrifugation) plus 100 µl of DiI (3 mg/ml in DMSO) and incubated at 37°C in the dark with gentle agitation. The density was then adjusted to 1.21 g/ml with KBr and samples were transferred to 16 mm / 4.2 ml tubes, filled (if necessary) with 1.21 g/ml KBr in HEPES-buffered saline (see appendix), sealed and centrifuged at 175,000 ×*g* in a 80 Ti rotor for 24 hours at 4°C. Upper fractions were collected and dialysed extensively in the dark against TBS. Purified DiI-labelled HDL_3 was collected and protein (apolipoprotein-AI) concentration was quantified by the Bradford procedure.

2.6.4 Assay of oleate uptake

Assays were performed essentially as described by Pohl *et. al.* with minor modifications (Pohl et al., 2002). Oleic acid solution was prepared by mixing trace amounts of [^{14}C]-oleic acid (~5 µCi) (Amersham) with non-radioactive oleic acid (Sigma) and dissolving in a solution of fatty acid-free BSA (173 µM, Sigma) in PBS to achieve an oleic acid:BSA molar ratio of 1. Cells were seeded at a density of 3×10^5 cells per well in 12-well tissue culture trays. After overnight culture, they were washed twice with warm PBS before addition of 300 µl of warm oleic acid solution. After incubation at 37°C for the appropriate times, the oleic acid solution was replaced with 1 ml of ice-cold stop solution containing 200 µM phloretin (Sigma) and 0.5% BSA in PBS. After one minute, the stop solution was aspirated and the cells were washed twice (1 minute each) with ice-cold PBS containing 0.5% BSA, once with ice-cold PBS and were then lysed in 250 µl of NaOH (2 mol/l). Aliquots of the NaOH lysate were used for protein determination by the Bradford procedure and for measurement of radioactivity. To measure radionuclide, 200 µl of lysate was added to 1.5 ml of OptiPhase HiSafe 3 liquid scintillation cocktail (PerkinElmer Life Sciences, Boston, MA) and samples were analysed using a Wallac 1409 liquid scintillation

counter (Wallac Oy, Finland). Measured quantities of radioactive oleic acid uptake solution were also added to scintillation vials to allow estimation of molar amounts of oleic acid from counts of radioactivity (counts per minute). Oleic acid uptake was expressed as picomoles of cell-associated oleic acid per milligram of protein per unit time. Results were expressed as means ± standard deviation.

2.6.5 Cellular lipid separation by thin layer chromatography (TLC)

Incorporation of [^{14}C]-oleic acid into cellular lipids was determined after incubation of cells with oleic acid solution for 15 minutes, as described above. However, instead of lysing cells, lipids were extracted by two incubations with 0.3 ml hexane-isopropanol (3:2). The extracts were pooled, the solvent was evaporated by vacuum centrifugation and the lipids were redissolved in chloroform-methanol (2:1). Samples and standards (including oleic acid, a known quantity of radioactive oleic acid (for quantitation purposes) and a mono-, di-, tri-glyceride mix (40 μg) (Sigma)) were spotted onto Silica Gel 60 plates (Merck, Darmstadt, Germany). The lipids were separated by TLC, using a hexane-diethyl ether-acetic acid (60:40:1) solvent system, and visualized after staining with iodine vapour. Lipid spots were identified and scraped into liquid scintillation cocktail for scintillation counting. Dry cell monolayers were dissolved in NaOH (2 mol/L) for protein determination by the Bradford procedure. The amounts of oleic acid incorporated into different lipid subclasses were expressed as picomoles of oleic acid incorporated, milligram of protein^{-1}, 15 minutes^{-1}.

2.6.6 Oil Red O staining

Oil Red O (ORO) staining was performed essentially as described by Koopman *et. al.*, with minor modifications (Koopman et al., 2001). Stock solutions of ORO were prepared by dissolving 100 mg of ORO (Sigma) in 20 ml of 60% triethyl phosphate (Sigma). Working solutions were prepared by dilution of the stock solution with 0.65 volumes of distilled water. Working solutions were filtered through 0.22 μm filters prior to use. Cells were grown on coverslips overnight prior to staining or alternatively, staining was performed on cell monolayers in 35 mm cell culture dishes. After two washes with PBS, the cells were fixed with 3.7% (v/v) formaldehyde for 10 minutes and washed twice with PBS. To each sample, 1ml of the ORO working solution was added and samples were incubated for 20 minutes at room temperature. Samples were then washed three times with

PBS (1 minute each) and coverslip preparations were mounted onto microscope slides. Alternatively, coverslips were placed atop cell monolayers (in cell culture dishes). Samples were immediately visualized and photographed.

Chapter 3: Investigations into the involvement of FAT/CD36 in LCFA uptake in transfected cell lines

3.1 Introduction

It remains controversial to what extent cellular acquisition of long-chain fatty acids (LCFAs) occurs via passive diffusion across the lipid bilayer or requires active transport involving the actions of transporter proteins (reviewed in Abumrad et al., 1998, Hamilton and Kamp, 1999). Nevertheless, it is generally accepted that a component of LCFA uptake is protein-mediated and that this pathway is of particular significance in tissues with high metabolic requirements for fatty acids and/or when the levels of free fatty acid (FFA) are low (Abumrad et al., 1984, Abumrad et al., 1993). A major candidate for protein-mediated LCFA uptake is FAT/CD36 and evidence that it is involved in LCFA uptake has been provided by a number of studies conducted both *in vitro* and *in vivo* (reviewed in Febbraio et al., 2002). However, the mechanism by which FAT/CD36 mediates enhancement of LCFA uptake has not been established. For this reason, it is unclear whether mere expression of FAT/CD36 confers enhanced cellular LCFA uptake. Circumstantial evidence suggests that FAT/CD36 may act in concert with other candidate mediators of LCFA uptake (FABPpm and FATP family members) (reviewed in Ehehalt et al., 2006, van der Vusse et al., 2002) and that localization of the molecule in specialized microdomains of the plasma membrane may contribute to its activity as a LCFA transporter (Pohl et al., 2005, Ehehalt et al., 2006).

Following the recent demonstration that FAT/CD36 is expressed at high levels in the livers of female rodents and humans (Zhang et al., 2003, Stahlberg et al., 2004), and its proven role as a contributor to LCFA uptake in adipose tissue and both cardiac and skeletal muscle, it was hypothesized that FAT/CD36 contributes to hepatic LCFA uptake. This putative function would be consistent with the high activity of hepatocytes in acquiring fatty acids from plasma for the purpose of lipid synthesis and oxidation (Noy et al., 1986). Furthermore other candidate fatty acid transporters, such as FABPpm, FATP2 and FATP5, have been detected at high levels in the liver (Stremmel et al., 1985, Stahl et al., 2001). A further consideration is the gender-biased expression of FAT/CD36 in the liver (Zhang et al., 2003, Stahlberg et al., 2004), which is consistent with observed differences in hepatic LCFA uptake between male and female rats (Ockner et al., 1979, Hung et al., 2003).

At a subcellular level, FAT/CD36 has been shown to localize to specialized plasma membrane microdomains known as lipid rafts (Dorahy et al., 1996, Thorne et al., 1997, Thorne et al., 2000, Kolleck et al., 2002, Zeng et al., 2003, Pohl et al., 2004, Pohl et al., 2005). Lipid rafts are sphingomyelin- and cholesterol-rich microdomains of the plasma membrane that, together with their lipid content, are characterized by resistance to solubilization in low concentrations of non-ionic detergents (e.g Triton X-100 and NP-40) at 4°C. These membrane domains have relatively low density, as evidenced by flotation when subjected to ultracentrifugation on sucrose density gradients. The resistance of these domains to solubilization in detergent and their low density are both thought to result from tight packing of cholesterol, sphingolipids and saturated phospholipids (Brown and Rose, 1992). Thus rafts prepared biochemically using low concentrations of non-ionic detergent are often referred to as "detergent-resistant membranes" (DRMs).

Caveolae are a specialized subset of classical lipid rafts. They share the biochemical properties of DRMs but they have a unique flask-shaped morphology (50-100 nm invaginations of the plasma membrane) and they contain oligomers of the protein caveolin (Parton and Simons, 1995, Simons and Ikonen, 1997). FAT/CD36 has been observed in caveolae of endothelium (Lisanti et al., 1994) and human skeletal muscle (Keizer et al., 2004, Vistisen et al., 2004). Furthermore, it is enriched in DRMs prepared from 3T3-L1 adipocytes (Pohl et al., 2004, Pohl et al., 2005) and in COS-7 cells (Thorne et al., 1997) and CHO cells (Zeng et al., 2003) transfected to express caveolin-1. Moreover, in each of these investigations FAT/CD36 and caveolin-1 co-fractionated in DRMs, but in the latter study confocal fluorescence microscopy and electron microscopy showed that FAT/CD36 was present also in lipid rafts that were distinct from caveolae (Zeng et al., 2003).

Little is known about the subcellular localization of FAT/CD36 in hepatocytes and hepatocyte-derived cell lines. However, recent studies have demonstrated the existence of both lipid rafts and caveolae in hepatocytes. These microdomains were found to share the biochemical properties of lipid rafts and caveolae identified in other tissues (Calvo and Enrich, 2000, Calvo et al., 2001, Balbis et al., 2004, Tietz et al., 2005, Mazzone et al., 2006).

The significance of the localization of FAT/CD36 to lipid rafts and caveolae, with respect to its ability to mediate enhanced LCFA uptake, is unclear. Depletion of lipid rafts (with methyl-β-cyclodextrin (MβCD) or filipin) and inhibition of caveolus formation (with a dominant-negative caveolin mutant or antisense inhibition of caveolin-1 expression) have been shown to reduce LCFA uptake by 3T3-L1 adipocytes (Pohl et al., 2002, Pohl et al., 2004, Pohl et al., 2005). Recently, it has been demonstrated that specific inhibition of FAT/CD36 with sulfosuccinimidyl-oleate (SSO) and depletion of lipid rafts using MβCD results in equivalent and non-additive inhibition of oleate uptake by 3T3-L1 cells (Pohl et al., 2005). These findings indicate a critical link between FAT/CD36 activity and lipid raft function in these cells. Whether this phenomenon is also true for other tissues is unclear at this time.

3.2 Hypotheses:

I. FAT/CD36 localizes to lipid rafts in hepatic cells (as in other cell types).

II. FAT/CD36 and caveolin-1 colocalize in caveolae of transfected hepatic and non-hepatic cells.

III. Over-expression of FAT/CD36 in hepatic and non-hepatic cell lines enhances LCFA uptake.

IV. The presence of functional lipid rafts and caveolae both enhance FAT/CD36-mediated uptake of LCFA by hepatic and non-hepatic cell lines.

V. LCFA uptake correlates with levels of FAT/CD36 expression in a CHO cell line with exogenously-inducible expression of FAT/CD36.

3.3 Generation of FAT/CD36-expressing stable cell lines

3.3.1 Generation of mammalian expression plasmid pcDNA3-FAT/CD36

An expression plasmid suitable for generation of stably transfected eukaryotic cell lines was prepared by sub-cloning cDNA encoding FAT/CD36 from the previously described plasmid pSG5-FAT (Ibrahimi et al., 1996) into pcDNA3 (Invitrogen, Carlsbad, CA) (Figure 3-1). The FAT-encoding cDNA in pSG5-FAT was originally derived from mRNA extracted from adipocytes of Sprague Dawley rats (Abumrad et al., 1993). It was cloned into the unique *Bam*HI site of the multiple cloning site of pSG5 (Stratagene, La Jolla, CA, USA) (Ibrahimi et al., 1996). This plasmid was a generous gift of Dr. Nada Abumrad

Figure 3-1. Map of plasmid pcDNA3 (Invitrogen). P_{CMV}, cytomegalovirus promoter; T7, T7 promoter; Sp6, Sp6 promoter; BGH pA, bovine growth hormone polyadenylation signal; SV40, SV40 virus promoter; Neomycin, neomycin resistance (phosphotransferase) gene; SV40, SV40 virus polyadenylation signal; Col E1, ColE1 origin of replication; Ampicillin, ampicillin resistance (β-lactamase) gene.

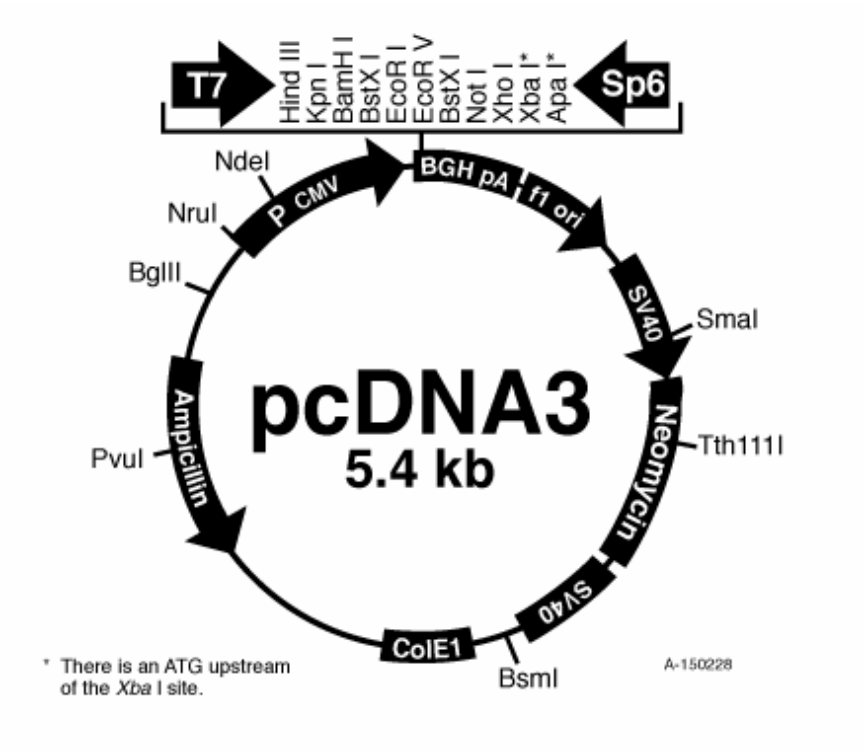
T7
Hind III
Kpn I
BamH I
BstX I
EcoR I
EcoR V
BstX I
Not I
Xho I
Xba I*
Apa I*
Sp6
NdeI
NruI
BglII
PvuI
P CMV
BGH pA
f1 ori
SV40
SmaI
Tth111I
Neomycin
SV40
ColE1
BsmI
Ampicillin
pcDNA3
5.4 kb
* There is an ATG upstream of the Xba I site.
A-150228

Figure 3-1.

(Department of Physiology and Biophysics, State University of New York at Stony Brook, USA) to Dr. Graham Mayrhofer (University of Adelaide, Australia). FAT cDNA was released from pSG5-FAT and subcloned by standard cloning techniques into pcDNA3 using unique *Eco*RI and *Xba*I restriction sites in both plasmids. Diagnostic restriction digests confirmed insertion of FAT/CD36 cDNA into pcDNA3 in the correct orientation (not shown). Furthermore, the integrity of the FAT/CD36 cDNA insert was confirmed by automated DNA sequencing.

3.3.2 Stable transfection of COS-7 and H4IIE cell lines

To generate stable COS-7 transfectants, COS-7 cells were transfected with pcDNA3 (empty vector control) or pcDNA3-FAT/CD36, as detailed (see 2.2.5). Antibiotic-resistant cells emerged after several weeks of selection with G418. COS-7 cells stably transfected with pcDNA3 were expanded as a heterogeneous mixture (COS-7-pcDNA3). However, COS-7 cells stably transfected with pcDNA3-FAT/CD36 were sub-cultured at low density and G418-resistant clonal colonies were isolated and expanded. Expression of FAT/CD36 by these clones was assessed by flow cytometry using mAb UA009 (anti-FAT/CD36) (Figure 3-2). One clone (#7) demonstrating high expression of FAT/CD36 at the cell-surface was chosen for further analysis. All stable transfectants were maintained in culture medium containing G418 at 200 μg/ml and were tested regularly for continued expression of FAT/CD36.

To generate stable H4IIE transfectants, cells were transfected with pcDNA3-FAT/CD36 as described above. After selection and sub-culture at low density, G418-resistant clones were assessed for cell-surface expression of FAT/CD36 by flow cytometry. A selection of clones is shown in Figure 3-3. One clone demonstrating no detectable expression of FAT/CD36 (later confirmed by RT-PCR and Western blotting; not shown) was chosen as a negative control cell line ("H4IIE (5A)"). Another clone demonstrating high-level expression of FAT/CD36 ("H4IIE-FAT/CD36 (1A)") was chosen for further analysis.

3.3.3 Generation of a CHO cell line in which FAT/CD36 expression can be manipulated exogenously by tetracycline

Figure 3-2. Assessment of FAT/CD36 expression by COS-7 cell clones stably transfected with pcDNA3-FAT/CD36 as determined by flow cytometry using anti-FAT/CD36 mAb UA009. mAb 1B5 was used as an isotype-matched negative control. Bound primary antibody was detected using FITC-conjugated anti-mouse IgG. Viable cells were gated on the basis of their forward (FSC) and side scatter (SSC) properties (not shown). Within the gated populations cells were analysed for their fluorescence in the FL-1 channel.

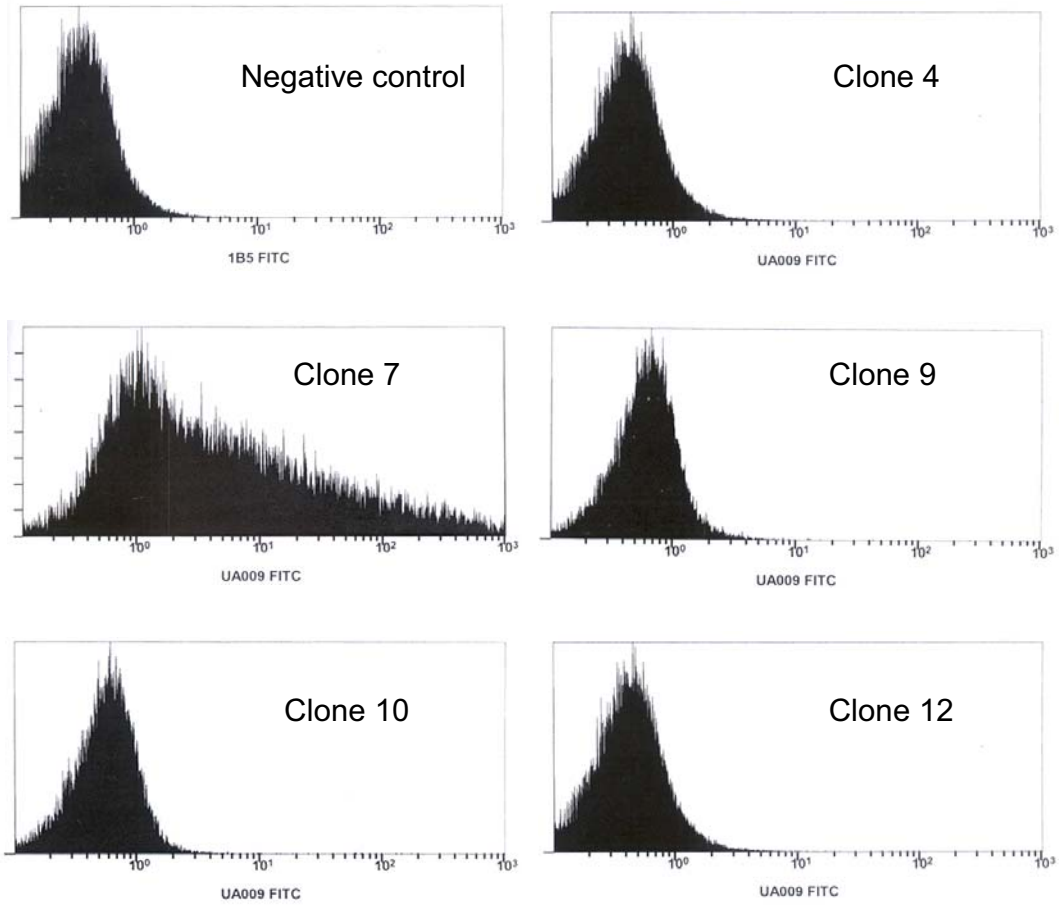
Negative control
1B5 FITC
Clone 4
UA009 FITC
Clone 7
UA009 FITC
Clone 9
UA009 FITC
Clone 10
UA009 FITC
Clone 12
UA009 FITC

Figure 3-2.

Figure 3-3. Assessment of FAT/CD36 expression by H4IIE cell clones stably transfected with pcDNA3-FAT/CD36 as determined by flow cytometry using anti-FAT/CD36 mAb UA009. mAb 1B5 was used as an isotype-matched negative control. Bound primary antibody was detected using FITC-conjugated anti-mouse IgG. Viable cells were gated on the basis of their forward (FSC) and side scatter (SSC) properties (top left). Within the gated populations cells were analysed for their fluorescence in the FL-1 channel.

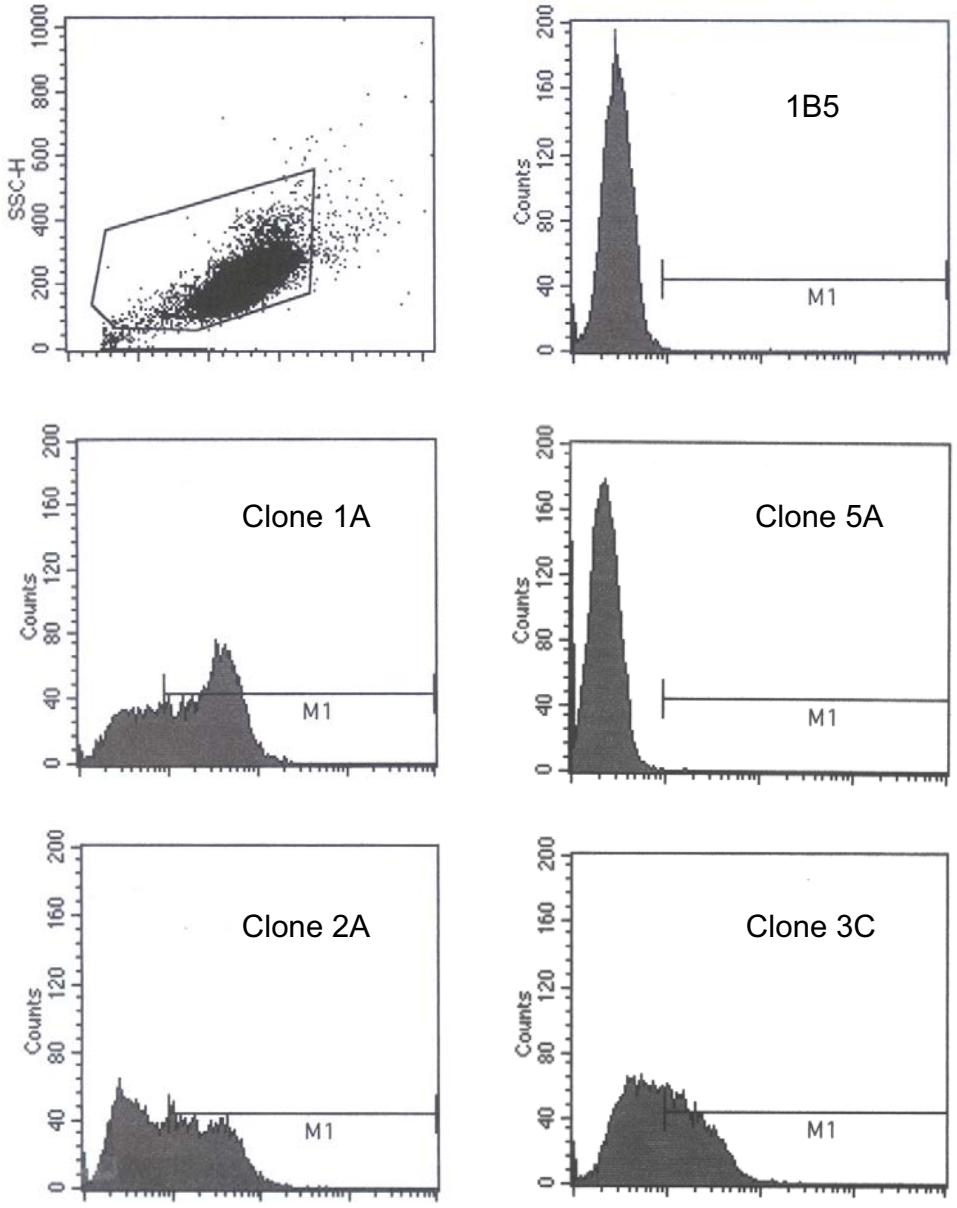
SSC-H
0
200
400
600
800
1000
1B5
Counts
0
40
80
120
160
200
M1
Clone 1A
Clone 5A
Clone 2A
Clone 3C

Figure 3-3.

3.3.3.1 The 'tet-off' system

Of a number of different systems in which gene expression can be regulated in mammalian cells (Lewandoski, 2001), the TetR-based system developed by Gossen and Bujard (Gossen and Bujard, 1992) has been characterized most thoroughly. This system was chosen to investigate whether levels of FAT/CD36 expression correlate with functional activity in LCFA uptake. DNA constructs were obtained and manipulated to allow exogenous modulation of FAT/CD36 expression using this system.

The TetR-based system consists of two components. The first component is a fusion protein consisting of the *E.coli* tetracycline repressor protein (TetR) plus the VP16 transactivation domain of herpes simplex virus. This fusion protein (TetR-VP16), commonly known as the tetracycline-controlled transactivator (tTA), binds to both the antibiotic tetracycline (or its derivatives) and the *tet* operon (19-bp *tetO* operator sequence). Binding of tTA to *tetO* results in recruitment of transcriptional machinery which, when upstream of a minimal promoter, drives expression of the gene that lies downstream. In the case of the 'tet-off' system, binding of tetracycline by tTA induces a conformational change in tTA such that it can no longer bind *tetO* and induce gene expression. This feature affords inducibility by removal of tetracycline.

3.3.3.2 Generation of a tTA-expressing stable CHO cell line

It was decided to use the 'tet-off' system of Clontech (Palo Alto, CA, USA) to regulate expression of FAT/CD36 in chinese hamster ovary (CHO) cells. The CHO cell line has been used successfully by others to study the function and subcellular localization of FAT/CD36 (Zeng et al., 2003). To generate a stable cell line that expresses tTA, CHO cells were transfected with the plasmid pTet-Off (Clontech) (Figure 3-4). After selection of stable transfectants with G418, antibiotic-resistant clones were expanded individually and assayed for tTA expression by RT-PCR (Figure 3-5). One clone (CHO-Tet-Off 1.2) that demonstrated detectable tTA mRNA expression was chosen for further analysis.

3.3.3.3 Generation of a tTA-responsive FAT/CD36 expression construct

To generate a construct in which expression of the FAT/CD36 gene would be regulated by tTA, FAT/CD36 cDNA was sub-cloned from pSG5-FAT into the *Bam*HI site of pTRE2 (Clontech) (Figure 3-6), downstream of the tTA-responsive promoter. Diagnostic restriction digest (with *Pst*I and *Not*I) and agarose gel electrophoresis was employed to

Figure 3-4. Map of plasmid pTet-Off (Clontech). P_{CMV}, cytomegalovirus promoter; tTA, tetracycline-controlled transactivator; SV40 polyA, SV40 virus polyadenylation signal; Col E1 ori, origin of replication; Amp^r, ampicillin resistance (β-lactamase gene); Neo^r, neomycin resistance (phosphotransferase) gene; P_{SV40}, SV40 virus promoter.

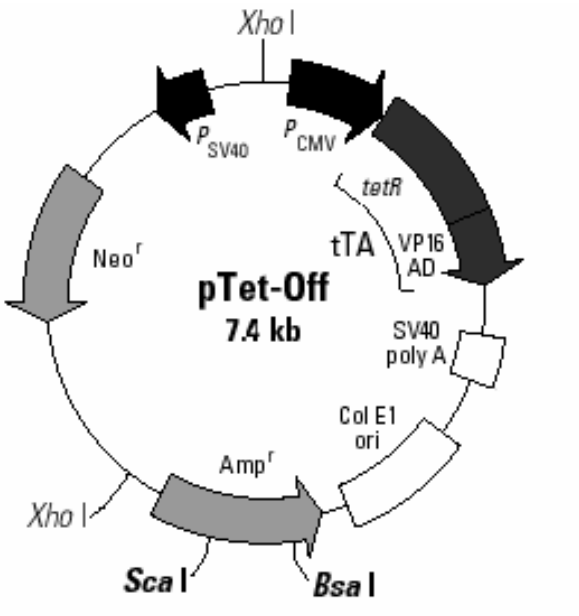
Xho I
P SV40
P CMV
tetR
tTA
VP16 AD
Neo r
pTet-Off
7.4 kb
SV40 poly A
Col E1 ori
Amp r
Xho I
Sca I
Bsa I

Figure 3-4.

Figure 3-5. Assessment of tTA expression by CHO cell clones stably transfected with pTet-Off as determined by RT-PCR. RNA was extracted from clones and used to prepare cDNA. RT-PCR was performed using primers specific for tTA transcripts (tTA FP1 / tTA RP1). PCR products were subjected to 1.5% agarose gel electrophoresis. Negative controls included PCR performed in the absence of template DNA (no-template control, NTC) and reactions performed using cDNA prepared from untransfected CHO cells. Reactions in which pTet-Off plasmid DNA was added as template DNA served as a positive control.

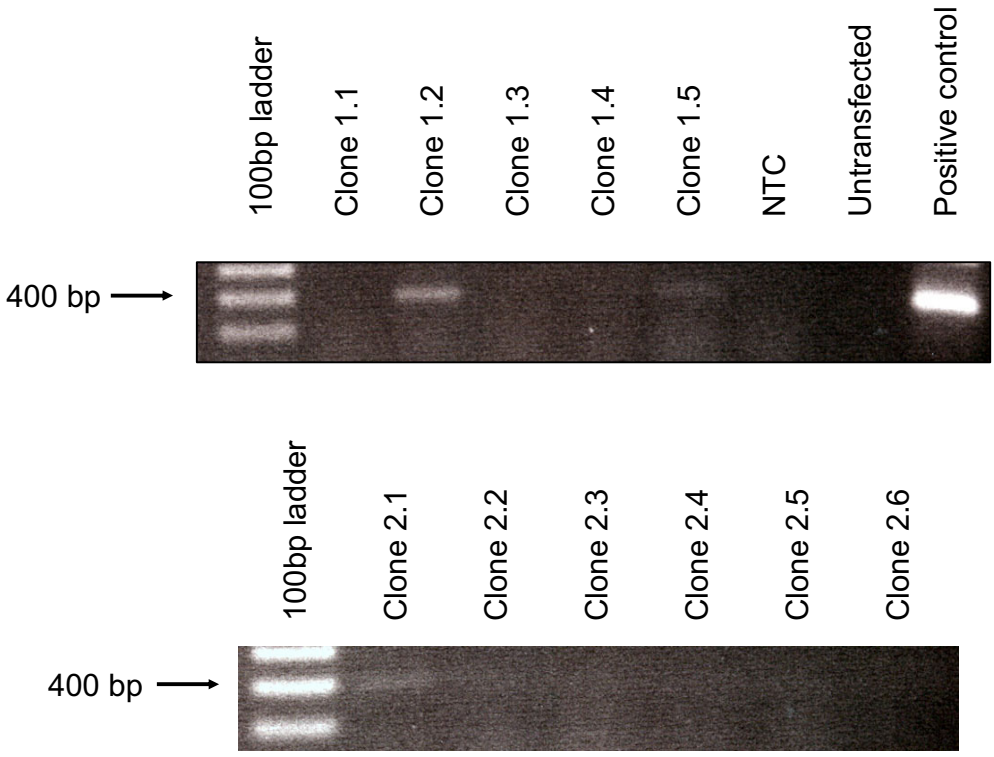
100bp ladder
Clone 1.1
Clone 1.2
Clone 1.3
Clone 1.4
Clone 1.5
NTC
Untransfected
Positive control
400 bp
100bp ladder
Clone 2.1
Clone 2.2
Clone 2.3
Clone 2.4
Clone 2.5
Clone 2.6
400 bp

Figure 3-5.

Figure 3-6. Map of plasmid pTRE2 (Clontech). TRE, Tet response element (seven *tetO* repeats); *P*minCMV, minimal cytomegalovirus promoter; MCS, multiple cloning site; β-globin polyA, β-globin polyadenylation signal; Col E1 ori, origin of replication; Amp^r, ampicillin resistance (β-lactamase) gene.

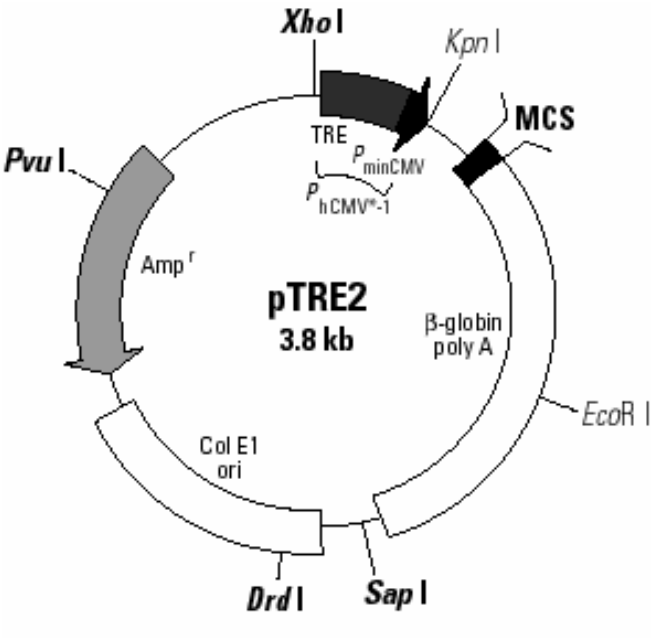
Xho I
Kpn I
MCS
TRE
P minCMV
P hCMV*-1
Pvu I
Amp r
pTRE2
3.8 kb
β-globin
poly A
EcoR I
Col E1
ori
Drd I
Sap I

Figure 3-6.

confirm the presence and correct orientation of the FAT/CD36 insert (not shown). Automated DNA sequencing showed that no undesired mutations were generated in the FAT/CD36 coding sequence.

Plasmid pTRE2-FAT/CD36 could be used for transient transfection of CHO-Tet-Off 1.2 cells. However, transient transfection is unsuitable for investigating the effects of tetracycline-regulated expression of FAT/CD36 because the time required to regulate tTA-induced gene expression can exceed the period of transient transfection (48-72 hours) (Clontech Laboratories, 2005). Therefore effective studies required stable transfection of this construct into CHO-Tet-Off 1.2 cells. Since pTRE2 does not contain a mammalian antibiotic resistance gene and CHO-Tet-Off 1.2 cells are resistant to G418, it was decided to insert a puromycin resistance (*puromycin dehydrogenase*) gene into the pTRE2-FAT/CD36 plasmid. Furthermore, due to a lack of compatible restriction sites between pTRE2-FAT/CD36 and the puromycin resistance gene cassette 'donor' pEF-IRES-puro6 (Figure 3-7), the entire TRE promoter-FAT/CD36 DNA fragment was sub-cloned from pTRE2-FAT/CD36 into the multiple cloning site of the promoter-less plasmid pIRES-puro6. This promoter-less plasmid was derived from pEF-IRES-puro6 by removal of the EF-1α promoter, as detailed elsewhere (Eyre, 2002). Briefly, the TRE2-FAT/CD36 fragment was sub-cloned into unique *Xho*I and *Not*I sites within the multiple cloning site of pIRES-puro6. Successful insertion of the TRE2-FAT/CD36 fragment into pIRES-puro 6 was confirmed by diagnostic digest (not shown). The integrity of FAT/CD36 in pTRE2-FAT/CD36-IRES-puro 6 was confirmed by automated DNA sequencing. It was anticipated that after transfection of this construct into tTA-expressing cells, the FAT/CD36 and puromycin dehydrogenase genes would be translated from a single bi-cistronic messenger RNA transcript. Expression of this bi-cistronic transcript would be under the control of the tTA-responsive TRE promoter.

3.3.3.4 Stable transfection of CHO-Tet-Off 1.2 cells with the tTA-responsive plasmid pTRE2-FAT/CD36-IRES-puro 6

CHO-Tet-Off 1.2 cells were transfected with pTRE2-FAT/CD36-IRES-puro 6 as described previously and selection for puromycin-resistant stable transfectants was commenced from 48 hours post-transfection. G418 selection was maintained throughout (final concentration of 200 μg/ml) but tetracycline (or doxycycline) was not included in

Figure 3-7. Map of plasmid pEF-IRES-puro6 (derived from pEFIRES-P (Hobbs et al., 1998)). pEF-1α, elongation factor 1α promoter; Intron, β-globin intron; MCS, multiple cloning site; IRES, internal ribosome entry site; 'pac, puromycin resistance gene; SV40 PA, SV40 virus polyadenylation signal; f1, origin of replication; AmpR, ampicillin resistance (β-lactamase) gene.

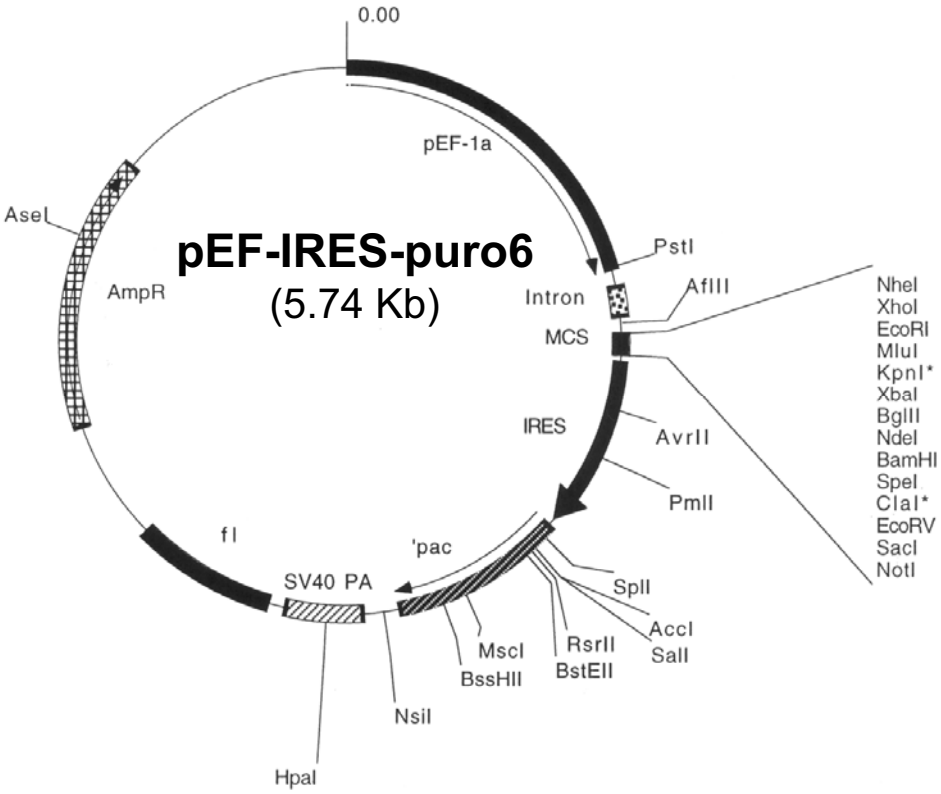
0.00
pEF-1a
AseI
pEF-IRES-puro6
(5.74 Kb)
AmpR
PstI
AflII
Intron
MCS
NheI
XhoI
EcoRI
MluI
KpnI*
XbaI
BglII
NdeI
BamHI
SpeI
ClaI*
EcoRV
SacI
NotI
IRES
AvrII
PmlI
f1
'pac
SV40 PA
SplI
AccI
SalI
MscI
BssHII
RsrII
BstEII
NsiI
HpaI

Figure 3-7.

the culture medium, thus allowing expression of puromycin dehydrogenase (and FAT/CD36).

The sensitivity of tTA-induced expression of FAT/CD36 to doxycycline was assessed in the un-cloned CHO-Tet-Off 1.2~TRE-FAT/CD36 cell line in several ways. To investigate doxycyline-induced repression of FAT/CD36 expression, doxycycline was added to wells to a final concentration of 1 μg/ml and culture continued for from 0-120 hours. Cells were harvested from triplicate wells at each time point and FAT/CD36 expression was assessed by flow cytometry after labelling with mAb UA009 (Figure 3-8). Similarly, to investigate induction (de-repression) of FAT/CD36 expression, cells were seeded in 6-well trays in medium containing doxycycline at 1 μg/ml. At various time-points, doxycycline was removed from the culture medium by washing the cell monolayers twice with PBS and replacing with warm culture medium lacking the antibiotic. Cells were then harvested from triplicate wells and FAT/CD36 expression was assessed by flow cytometry (Figure 3-8). The concentration of antibiotic (1 μg/ml) and time frame used in the experiments were chosen based on the results of similar experiments reported by the manufacturers (Clontech Laboratories, 2005). During the course of these experiments (and in all experiments involving doxycycline-mediated down-regulation of FAT/CD36 described hereafter), puromycin was excluded from the culture medium. As can be seen, FAT/CD36 expression by the CHO-Tet-Off 1.2~TRE-FAT/CD36 cells could be controlled effectively by the addition or removal of doxycycline from the culture medium. However, expression of FAT/CD36 by these cells was not uniform and the level of 'leaky' or basal expression of FAT/CD36 by cells cultured in the presence of high levels of doxycycline (i.e in the repressed state) was significant. To reduce the risk that the FAT/CD36-expressing, doxycycline-responsive cells, would be outgrown by non-expressing and/or non-responsive cells, clones were produced.

Expression of FAT/CD36 and regulation of FAT/CD36 expression by doxycycline was tested on G418- and puromycin-resistant clones. The cells were cultured in the presence or absence of doxycycline (1 μg/ml) for 48 hours prior to measurement of cell-surface FAT/CD36 expression by flow cytometry (Figure 3-9). FAT/CD36 expression by these clones was variable, ranging from no detectable expression of FAT/CD36 in the presence or absence of doxycycline (e.g clone C4), to high-level expression of FAT/CD36 that was

Figure 3-8. Doxycycline-dependent regulation of FAT/CD36 in the heterogenous CHO-Tet-Off 1.2~TRE-FAT/CD36 cell line as determined by flow cytometry. Cells were cultured in the presence of doxycycline (1 μg/ml) for 72 hours before seeding in six-well trays and removing doxycycline from the medium at the indicated time-point (dashed line). Alternatively, cells were cultured for 72 hours in the absence of doxycyline before seeding in six-well trays and adding doxycycline (to a final concentration of 1 μg/ml) at the indicated time-points. FAT/CD36 expression was assessed by flow cytometry after indirect immunofluorescent labelling using biotinylated mAb UA009 and streptavidin-conjugated PE. Data are means ± SD (n=3) for the mean fluorescence of the gated population.

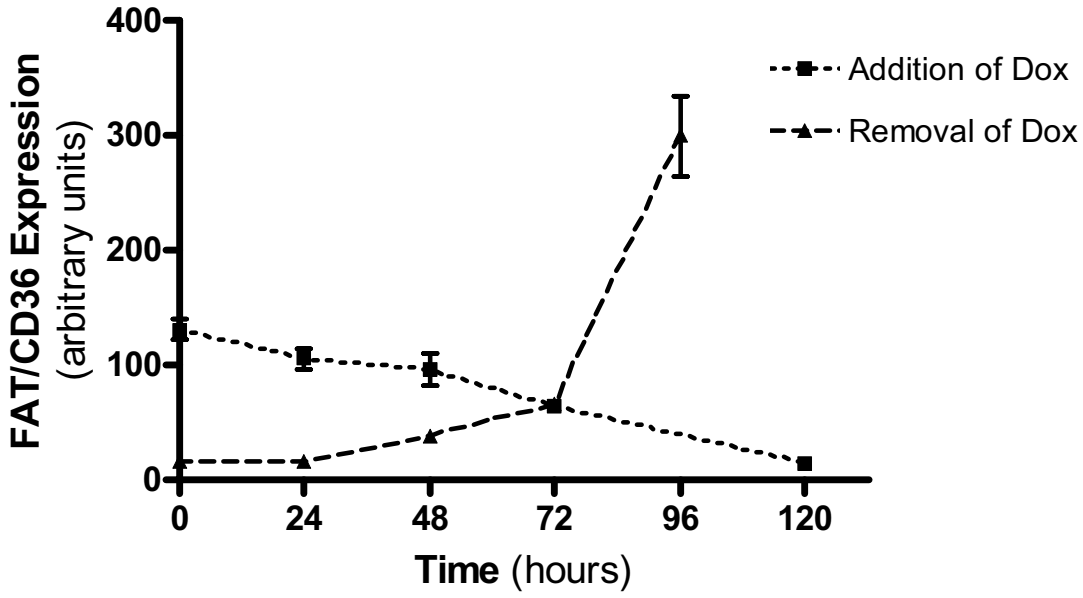
400
300
200
100
0
FAT/CD36 Expression
(arbitrary units)
0
24
48
72
96
120
Time (hours)
Addition of Dox
Removal of Dox

Figure 3-8.

Figure 3-9. Assessment of FAT/CD36 expression and sensitivity of FAT/CD36 expression to doxycycline in clones of the CHO-Tet-Off 1.2~TRE-FAT/CD36 cell line. Cells were seeded in six-well trays and cultured for 48 hours in the presence (open bars) or absence (diagonally striped bars) of doxycycline (1 μg/ml). Expression of FAT/CD36 was then assessed by flow cytometry following indirect immunofluorescent labelling with biotinylated mAb UA009 and streptavidin-conjugated PE. Data are the mean fluorescence of the gated population.

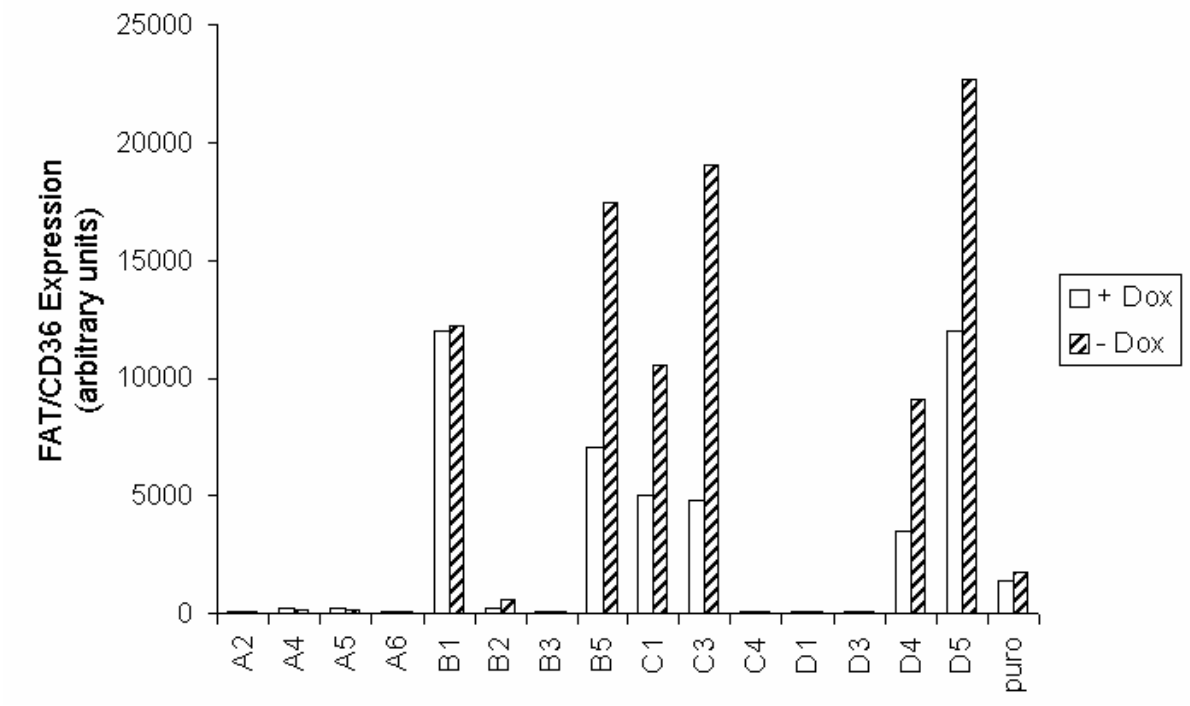
FAT/CD36 Expression
(arbitrary units)
25000
20000
15000
10000
5000
0
A2
A4
A5
A6
B1
B2
B3
B5
C1
C3
C4
D1
D3
D4
D5
puro
+ Dox
- Dox

Figure 3-9.

essentially insensitive to doxycycline (e.g clone B1), or high-level expression of FAT/CD36 that was highly sensitive to doxycyline (e.g clone C3). The desired features were high expression of FAT/CD36 in the 'induced' state (i.e in the absence of doxycycline) and high sensitivity of FAT/CD36 expression to doxycycline (i.e minimal 'leakiness' of FAT/CD36 expression in the 'off' state). For this reason the clone C3 (1.2C3) was chosen for further analysis as it represented the best compromise of high FAT/CD36 expression and high inducibility.

3.3.3.5 Dose-dependent regulation of FAT/CD36 expression by doxycycline in clone 1.2C3 of the CHO-Tet-Off 1.2~TRE-FAT/CD36 cell line

Expression of FAT/CD36 was investigated in cells from clone 1.2C3 after culture for 120 hours in the presence of a range of concentrations of doxycycline (0, 0.01, 0.1, 1, 10 and 100 ng/ml). These concentrations were chosen on the basis of results of similar experiments detailed in the manufacturer's handbook (Clontech Laboratories, 2005) and pilot experiments using clone 1.2C3 cells. Every 48 hours, the doxycycline-containing culture medium was replaced in order to minimize the influence of doxycycline turnover on tTA activity. Control cell lines for these experiments included the parent CHO-Tet-Off 1.2 cell line and/or the FAT/CD36 negative clone 1.2C4. After 120 hours in the presence of doxycycline, cell-surface expression of FAT/CD36 was assessed by flow cytometry (Figure 3-10). The results show that in the range from 0.01-1.0 ng/ml, there was a log-linear relationship between the concentration of doxycycline and the level of expression of FAT/CD36. There was, nevertheless, some 'leaky' expression of FAT/CD36 by cells cultured in the presence of higher levels of doxycycline. Even at 100 ng/ml of doxycycline, there was low level expression of FAT/CD36 by essentially all cells of the clone (not shown).

In similar experiments using Western blot analysis of FAT/CD36 protein in whole cell lysates, FAT/CD36 expression by clone 1.2C3 cells was repressed at concentrations of doxycycline greater than 1 ng/ml (Figure 3-11).

3.3.3.6 Time-dependent induction / repression of FAT/CD36 expression in clone 1.2C3 cells in response to doxycycline

The kinetics of FAT/CD36 down-regulation in response to addition of doxycycline to the culture medium of clone 1.2C3 cells was examined essentially as described for studies on

Figure 3-10. Dose-dependent regulation of FAT/CD36 expression in the CHO 1.2C3 clonal cell line. Cells were seeded in triplicate in six-well trays and cultured for 120 hours in the presence of doxycycline at the indicated concentration. FAT/CD36 expression was then assessed by flow cytometry following indirect immunofluorescent labelling with biotinylated mAb UA009 and streptavidin-conjugated PE. Data are means ± SD (n=3) for the mean fluorescence of the gated population.

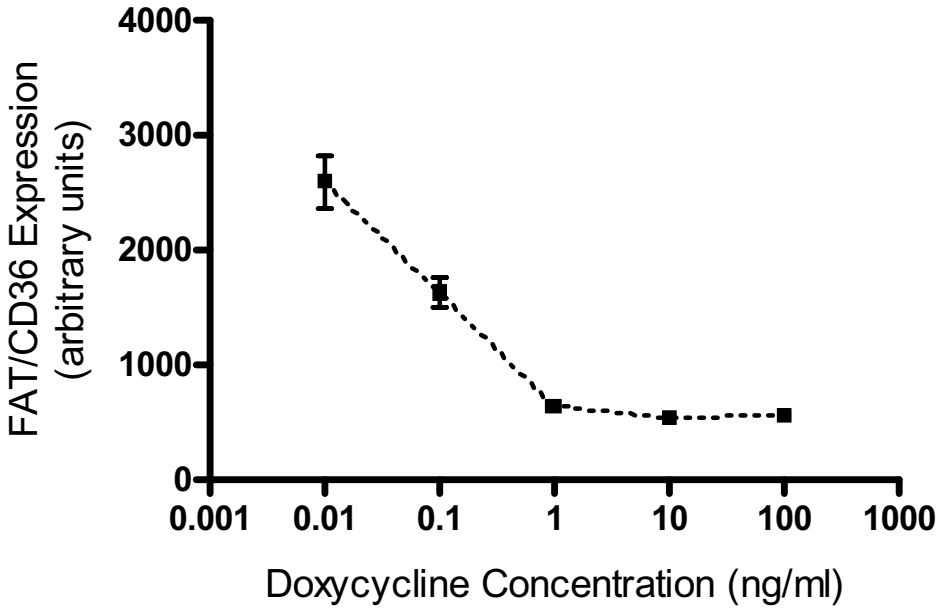
4000
3000
2000
1000
0
FAT/CD36 Expression
(arbitrary units)
0.001
0.01
0.1
1
10
100
1000
Doxycycline Concentration (ng/ml)

Figure 3-10.

Figure 3-11. Dose-dependent regulation of FAT/CD36 expression in the CHO 1.2C3 cell line as determined by Western blotting. CHO 1.2C3 cells or negative control CHO 1.2C4 cells were cultured for 120 hours in the presence of doxycycline (Dox) at a range of concentrations (1: CHO 1.2C4, 2: CHO 1.2C4 + 100 ng/ml Dox, 3: CHO 1.2C3, 4: CHO 1.2C3 + 0.01 ng/ml Dox, 5: CHO 1.2C3 + 0.05 ng/ml, 6: CHO 1.2C3 + 0.1 ng/ml Dox, 7: CHO 1.2C3 + 1 ng/ml Dox, 8: CHO 1.2C3 + 10 ng/ml Dox, 9 CHO 1.2C3 + 100 ng/ml Dox). **A**; Cells were then lysed and 20 μg of protein from each post-nuclear lysate was subjected to 12% SDS-PAGE and Western blotting using anti-FAT/CD36 mAb MO25 or anti-β-actin mAb as indicated. **B**; FAT/CD36 expression was normalized to β-actin (house keeping gene) and data are expressed as arbitrary units.

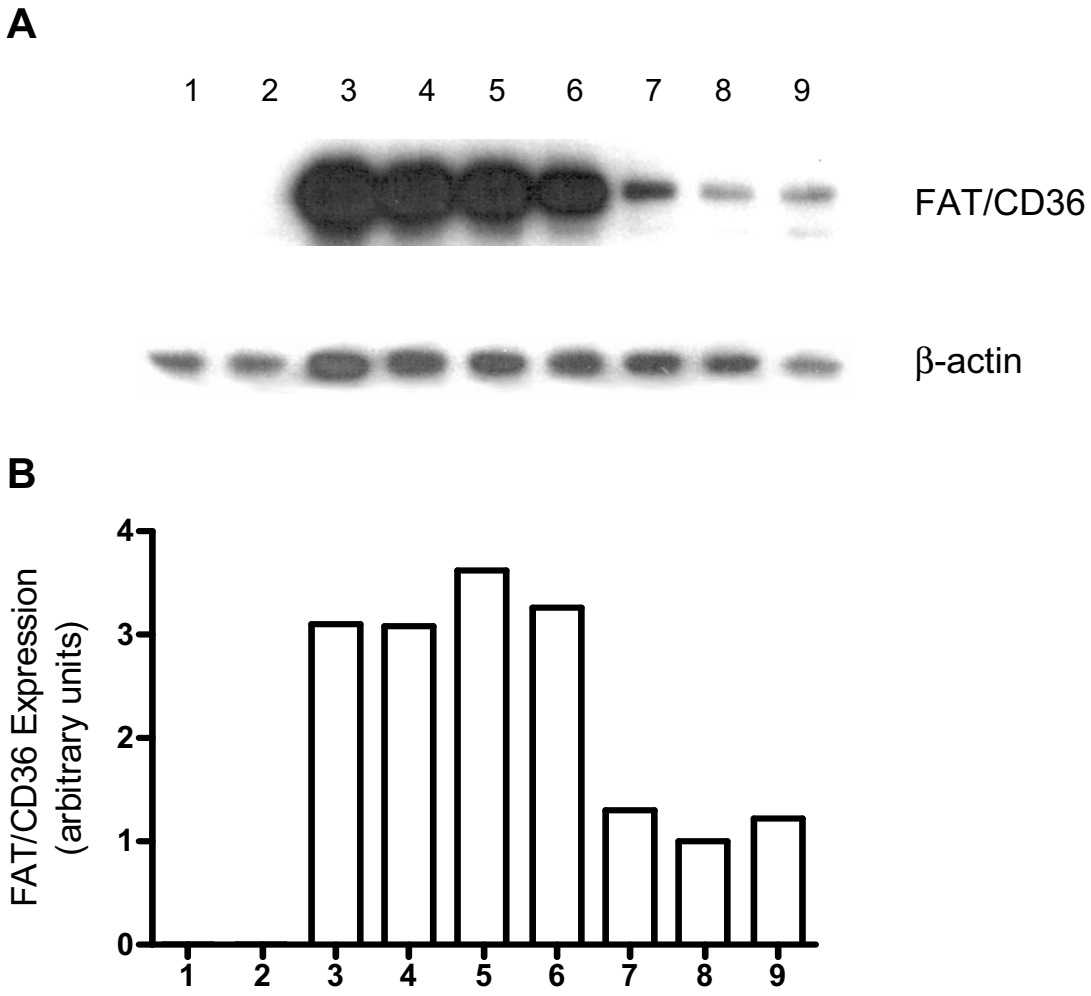
A
1 2 3 4 5 6 7 8 9
FAT/CD36
β-actin
B
FAT/CD36 Expression
(arbitrary units)
0
1
2
3
4
1 2 3 4 5 6 7 8 9

Figure 3-11.

the CHO-Tet-Off / TRE-FAT/CD36 cell line. Briefly, clone 1.2C3 cells were cultured in the absence of doxycycline prior to being seeded in six-well trays. Doxycycline (1000 ng/ml) was then added to culture medium and cells were harvested from triplicate wells at appropriate time-points and expression of FAT/CD36 was assessed by flow cytometry. The results show that the decline of FAT/CD36 expression was essentially linear with time and approached basal levels after 96 hours of culture with doxycyline (Figure 3-12). The down-regulation of cell-surface FAT/CD36 protein is relatively slow, although this is probably due to the rate of turnover of the membrane glycoprotein.

The kinetics of induction (de-repression) of FAT/CD36 expression in clone 1.2C3 cells was assessed by flow cytometry following removal of doxycycline from the culture medium. Prior to the experiment, the cells were cultured for four days in the presence of doxycycline to ensure that FAT/CD36 expression was fully suppressed. Cells were then seeded in six-well trays in medium containing doxycycline. Recent studies have indicated that doxycycline is maintained in the extracellular matrix and that effective removal of the antibiotic requires trypsinization, washing and re-plating of cells (Rennel and Gerwins, 2002). For this reason, removal of doxycycline was achieved by trypsinization, washing and re-plating of cells. FAT/CD36 expression was assessed at times indicated by indirect immunofluorescence and flow cytometry (Figure 3-13). The results show that levels of FAT/CD36 at the cell-surface are increased from 48 hours after removal of doxycycline, and that from this time, cell-surface FAT/CD36 increases rapidly to levels approximately 20-fold greater than those of fully repressed cells. Extension of the time-course beyond 96 hours resulted in no further induction of FAT/CD36 expression (not shown).

These cells will allow effective investigation of the correlation (if any) between the level of FAT/CD36 expression and changes in long-chain fatty acid uptake and metabolism. They will also serve as a valuable tool with which to investigate the possibility that FAT/CD36 expression impacts upon cellular import of lipids from high-density lipoproteins (HDL). Finally, characterization of doxycycline-sensitive FAT/CD36 expression in these cells provides proof-of-concept for the use of derivatives of the DNA constructs introduced into these cells in *in vivo* investigations involving FAT/CD36 overexpression.

Figure 3-12. Time-dependent downregulation of FAT/CD36 expression in CHO 1.2C3 cells following addition of doxycycline. Cells were cultured for 72 hours in the absence of doxycycline prior to their seeding in triplicate in six-well trays and addition of doxycycline (1 μg/ml, final concentration) at the indicated time-points. At the end of the time-course, cells were harvested and FAT/CD36 expression was assessed by flow cytometry following indirect immunofluorescent labelling using biotinylated mAb UA009 and streptavidin-conjugated PE. Data are means ± SEM (n=3) for the mean fluorescence of the gated population.

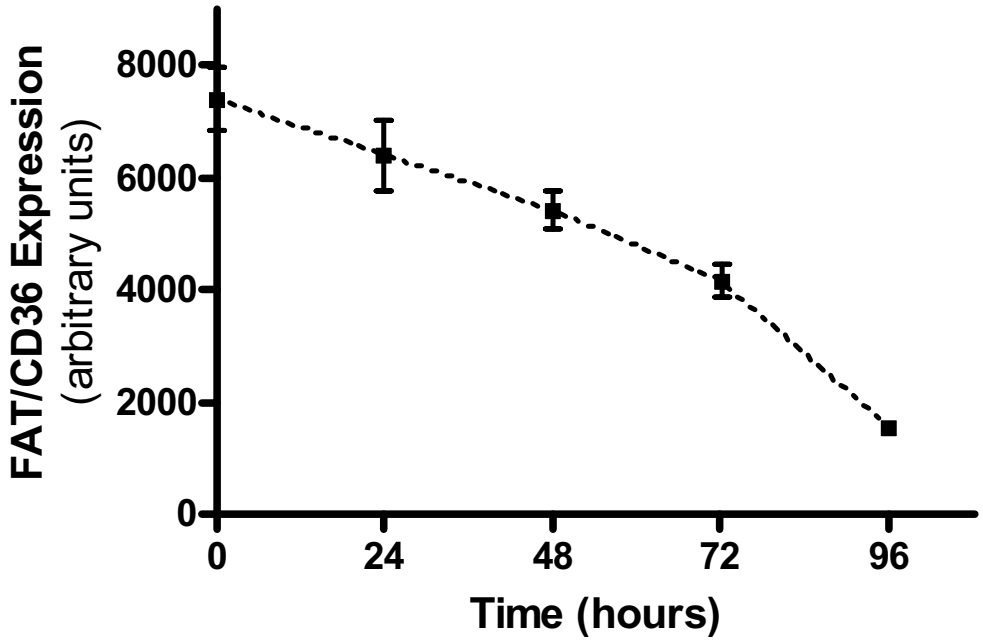
FAT/CD36 Expression
(arbitrary units)
8000
6000
4000
2000
0
0
24
48
72
96
Time (hours)

Figure 3-12.

Figure 3-13. Time-dependent upregulation (de-repression) of FAT/CD36 expression in CHO 1.2C3 cells following removal of doxycycline. Cells were cultured for 72 hours in the presence of doxycycline prior to their seeding in triplicate in six-well trays and removal of doxycycline (1 μg/ml, final concentration) at the indicated time-points. At the end of the time-course, cells were harvested and FAT/CD36 expression was assessed by flow cytometry following indirect immunofluorescent labelling using biotinylated mAb UA009 and streptavidin-conjugated PE. Data are means ± SEM (n=3) for the mean fluorescence of the gated population.

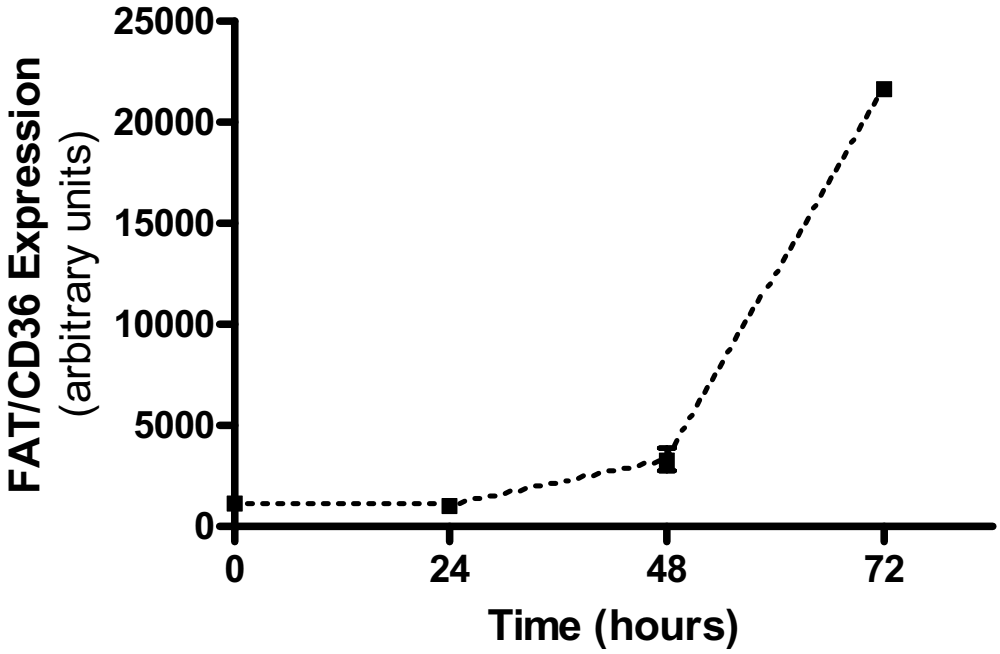
FAT/CD36 Expression
(arbitrary units)
25000
20000
15000
10000
5000
0
0
24
48
72
Time (hours)

Figure 3-13.

3.4 Investigations into the subcellular localization of FAT/CD36 in transfected cell lines and rat liver.

In the work that follows, several techniques were used to examine the subcellular localization of FAT/CD36 in rat liver and in transfected cell lines. The first technique involved the biochemical preparation of lipid rafts or detergent-resistant membranes (DRMs). The equating of DRMs with native lipid rafts has, however, received recent critical scrutiny (Munro, 2003). Firstly, DRMs are thought to represent artificial aggregates of raft domains (Brown and Rose, 1992). Secondly, the low temperatures used in preparing DRMs may alter membrane fluidity dramatically (Munro, 2003). Finally, the detergent itself may induce the formation of liquid-ordered (l_o) or 'raft' microdomains in lipid bilayers (Heerklotz, 2002). For these reasons, use of this technique to investigate the presence of FAT/CD36 within lipid rafts in tissue culture cells was combined with microscopic analysis of FAT/CD36 localization, using confocal fluorescence microscopy. This involved visualization of FAT/CD36 by indirect immunofluorescence (mAb UA009), with reference to the lipid raft marker GM_1 or the caveolae marker protein caveolin-1.

The glycosphingolipid GM_1 is a known marker of caveolae and lipid rafts, in which it is highly enriched (Parton, 1994, Iwabuchi et al., 1998). This sphingolipid is commonly detected using the B subunit of cholera toxin (CT-B); a non-toxic pentamer that binds GM_1 with high affinity and is internalised by raft- and/or caveolae-mediated endocytosis by live cells, after which it accumulates in the Golgi (Harder et al., 1998, Janes et al., 1999, Le and Nabi, 2003). To visualize GM_1, cells were cultured with an Alexa-594 conjugate of CT-B prior to fixation, labelled by immunofluorescence (where applicable) and examined by confocal fluorescence microscopy.

As discussed previously, caveolae represent a specialized subset of lipid rafts that are defined morphologically and by the presence of caveolin (reviewed in Cohen et al., 2004). Although caveolae can be separated from DRMs on the basis of their (subtly) differing biochemical properties, the similarities in lipid content, detergent insolubility and buoyancy between the two types of microdomain make this process difficult (reviewed in Hooper, 1999). Although caveolin is used commonly as a marker protein of DRMs and DRMs are often referred to mistakenly as 'caveolae' because they contain caveolin (reviewed in Anderson, 1998), the presence of caveolin in DRM fractions indicates merely that a *proportion* of lipid rafts are caveolae.

Caveolin is a 22 kDa cholesterol-binding integral membrane protein (Murata et al., 1995), whose expression is both responsible and required for formation of morphological caveolae (Li et al., 1996, Fra et al., 1995). It has, therefore, been used commonly as a marker for caveolae (reviewed in Cohen et al., 2004). In the studies described herein, an anti-caveolin-1 mAb (C060, Transduction Laboratories) has been used to assess the presence of caveolae within DRM preparations from those cells that express endogenous caveolin-1. As another marker of caveolin-1 (and hence caveolae), a mammalian expression plasmid encoding a fusion protein of caveolin-1 and enhanced green fluorescent protein (EGFP) has been generated and used to transfect tissue culture cells. Caveolin-1-EGFP fusion proteins have been used commonly to visualize caveolin-1 and caveolae and they appear to be represent native caveolin-1 accurately in their localization, enrichment in DRMs, palmitoylation and oligomerization (Volonte et al., 1999, Pelkmans et al., 2001, Thomsen et al., 2002). In the studies described herein, caveolin-1-EGFP was used as a marker for caveolae in studies of FAT/CD36 localization that involved confocal fluorescence microscopy. The fusion protein was also used as a marker for biochemically prepared DRMs in transfected cells that do not normally produce endogenous caveolin-1 (and hence caveolae).

3.4.1 Generation of Caveolin-1-EGFP expression plasmids

To generate a mammalian expression plasmid encoding a fusion protein of caveolin-1 and EGFP, the coding sequence of caveolin-1 (α-isoform) was first amplified by PCR from Dark Agouti rat liver cDNA, using sequence-specific oligonucleotides (Cav1 FPf / Cav1 RPf, Table 2-1). These oligonucleotides were designed such that, in the resulting PCR product, a *Bam*HI restriction site was introduced upstream of the start codon and a *Hind*III restriction site was introduced downstream of the mutagenised stop codon (Met → Arg). Furthermore, the reverse primer was designed such that the encoded caveolin-1 gene would be 'in-frame' with the coding sequence of EGFP in the destination plasmid, pEGFP-N1 (Clontech, Carlsbad, CA) (Figure 3-14). The PCR product was subjected to agarose gel electrophoresis and a band of the expected size (~550 bp) was identified, excised and purified. This PCR product was then digested with *Bam*HI and *Hind*III and cloned into similarly digested plasmid pEGFP-N1 (Figure 3-14), using standard cloning techniques. The integrity of caveolin-1-encoding DNA was confirmed in several positive

Figure 3-14. Map of plasmid pEGFP-N1 (Clontech). $P_{CMV\ IE}$, human cytomegalovirus (CMV) immediate early promoter; MCS, multiple cloning site; EGFP, enhanced green fluorescent protein gene; SV40 polyA, SV40 early mRNA polyadenylation signal; f1 ori, f1 single-strand DNA origin; *P*, bacterial promoter for expression of Kan^r gene; $P_{SV40\ e}$, SV40 early promoter; SV40 ori, SV40 origin of replication (requires host the expresses SV40 T antigen, e.g. COS-7); Kan^r / Neo^r, kanamycin / neomycin resistance gene; HSV TK polyA, herpes simplex virus thymidine kinase polyadenylation signal; pUC ori, pUC plasmid replication origin.

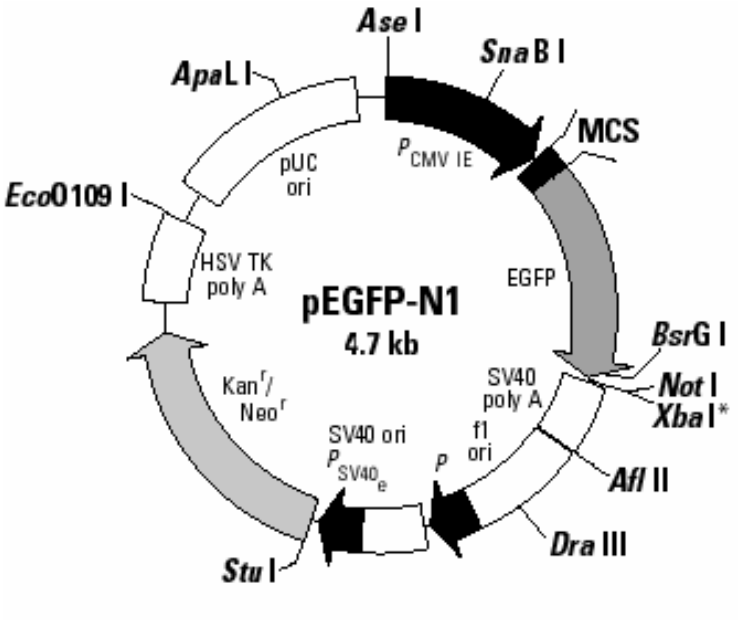
Ase I
Sna B I
ApaL I
MCS
P CMV IE
pUC ori
Eco0109 I
HSV TK poly A
EGFP
pEGFP-N1
4.7 kb
BsrG I
Not I
Xba I*
SV40 poly A
Kanr/ Neor
SV40 ori
P SV40e
f1 ori
P
Afl II
Dra III
Stu I

Figure 3-14.

clones by automated sequencing and sequences were found to be identical to other published rat caveolin-1α mRNA-encoding sequences (Genbank accession number: NM_031556).

The pCaveolin-1-EGFP plasmid described above contains a mammalian antibiotic selection marker (neomycin phosphotransferase) suitable for use in the generation of stably transfected cell lines. However, since the intended use of caveolin-1-EGFP expression was to assist in the localization of FAT/CD36 to caveolae, in H4IIE rat hepatoma cells stably transfected with the pcDNA3-FAT/CD36 plasmid which contains the same resistance marker, the entire caveolin-1-EGFP fusion protein coding sequence was sub-cloned from pCaveolin-1-EGFP into pEF-IRES-puro 6 (Figure 3-7) using *Xho*I and *Not*I restriction sites. The coding sequence of caveolin-1 and the linker region between caveolin-1 cDNA and EGFP cDNA were fully sequenced to confirm that no mutations had been introduced into the DNA encoding caveolin-1 and that the two coding sequences were in-frame.

3.4.2 Subcellular localization of FAT/CD36 in rat liver

3.4.2.1 Introduction

Contrary to initial reports (Abumrad et al., 1993), recent studies indicate that FAT/CD36 is expressed at high levels by rat and human hepatocytes (Zhang et al., 2003, Stahlberg et al., 2004). The reported low levels of expression of FAT/CD36 in liver was due to the exclusive use of male rats and the striking gender dimorphism in FAT/CD36 expression in this organ. FAT/CD36 is expressed in the livers of female rats and humans at levels up to 20-fold greater than in their male counterparts (Zhang et al., 2003, Stahlberg et al., 2004, Fitzsimmons, 2006). Because male rats are used in many studies of lipid metabolism, the level of FAT/CD36 expression in males may have been below the limits of detection by Northern blotting (Abumrad et al., 1993). Furthermore, strain-specific differences have been reported in hepatic FAT/CD36 expression in rats (Zhang et al., 2003) and this may also have contributed to variation in the levels of FAT/CD36 reported in the liver.

Little is known about the subcellular distribution of FAT/CD36 in hepatocytes, or about its function. Immunohistochemical detection of FAT/CD36 by indirect immunoperoxidase staining of isolated primary rat hepatocytes with mAb UA009 indicated that FAT/CD36 is

present on the surface of the plasma membrane (Zhang et al., 2003). While lipid rafts and caveolae have been reported in primary hepatocytes (Calvo et al., 2001, Calvo and Enrich, 2000, Tietz et al., 2005), localisation of FAT/CD36 to these lipid-enriched microdomains has not been studied.

3.4.2.2 Hepatic expression of FAT/CD36 in rats

To confirm previous findings and to further examine the subcellular localization of FAT/CD36 in hepatocytes, 5 μm cryosections were prepared from liver of male and female F344 strain rats and stained to detect FAT/CD36 using mAb UA009, according to the indirect immunoperoxidase technique (see 2.5.10). As a negative control, the irrelevant isotype control mAb 1B5 was substituted as the primary antibody (Figure 3-15, lower panels). In sections of female liver, mAb UA009 stained the hepatocyte plasma membranes intensely (Figure 3-15, right panels). The pattern of staining had a centrilobular distribution, as described previously (Zhang et al., 2003). Furthermore, the marked difference in amount and distribution of FAT/CD36 between male and female rats was confirmed. Staining with mAb UA009 included most hepatocytes of the lobules in female liver, excepting those in the near vicinity of portal triads. In contrast, only hepatocytes in close proximity to central veins were labelled with mAb UA009 in liver sections prepared from male rats (Figure 3-15, left panels). Observation at higher magnification (×100, obj) revealed relatively homogenous staining of the plasma membrane by mAb UA009 (Figure 3-15, middle panels). To attempt higher resolution of the subcellular distribution of FAT/CD36, attempts were made to employ immunofluorescence labelling of rat liver cryosections. Unfortunately, levels of background autofluorescence were unacceptable in unstained sections and sections stained with the isotype control mAb (not shown).

Western blot analysis, using an alternative anti-FAT/CD36 mAb, was used to measure differences in hepatic FAT/CD36 expression semi-quantitatively. Lysates of rat liver were prepared from each of three male and three female Dark Agouti (DA) rats and 25 μg of protein from each post-nuclear supernatant sample was subjected to 12% SDS-PAGE and Western blotting with mAb MO25 (Figure 3-16A). The results demonstrate clearly the gender bias in FAT/CD36 expression. Relative to the house-keeping protein β-actin, quantification of bands demonstrated an approximately five-fold higher expression of

Figure 3-15. Distribution of FAT/CD36 in male and female rat liver (F344 strain). Cryosections (5μm) of liver from male and female F344 rats were fixed and stained with anti-FAT/CD36 mAb UA009 by the indirect immunoperoxidase technique. Control experiments in which the primary antibody was substituted with the irrelevant isotype-matched control mAb 1B5 revealed no detectable staining (lower panels). Nuclei were stained with Gill's hematoxylin. Sections were visualized using ×20 (upper panels), ×100 (middle panels) and ×10 objectives (lower panels) and photographed.

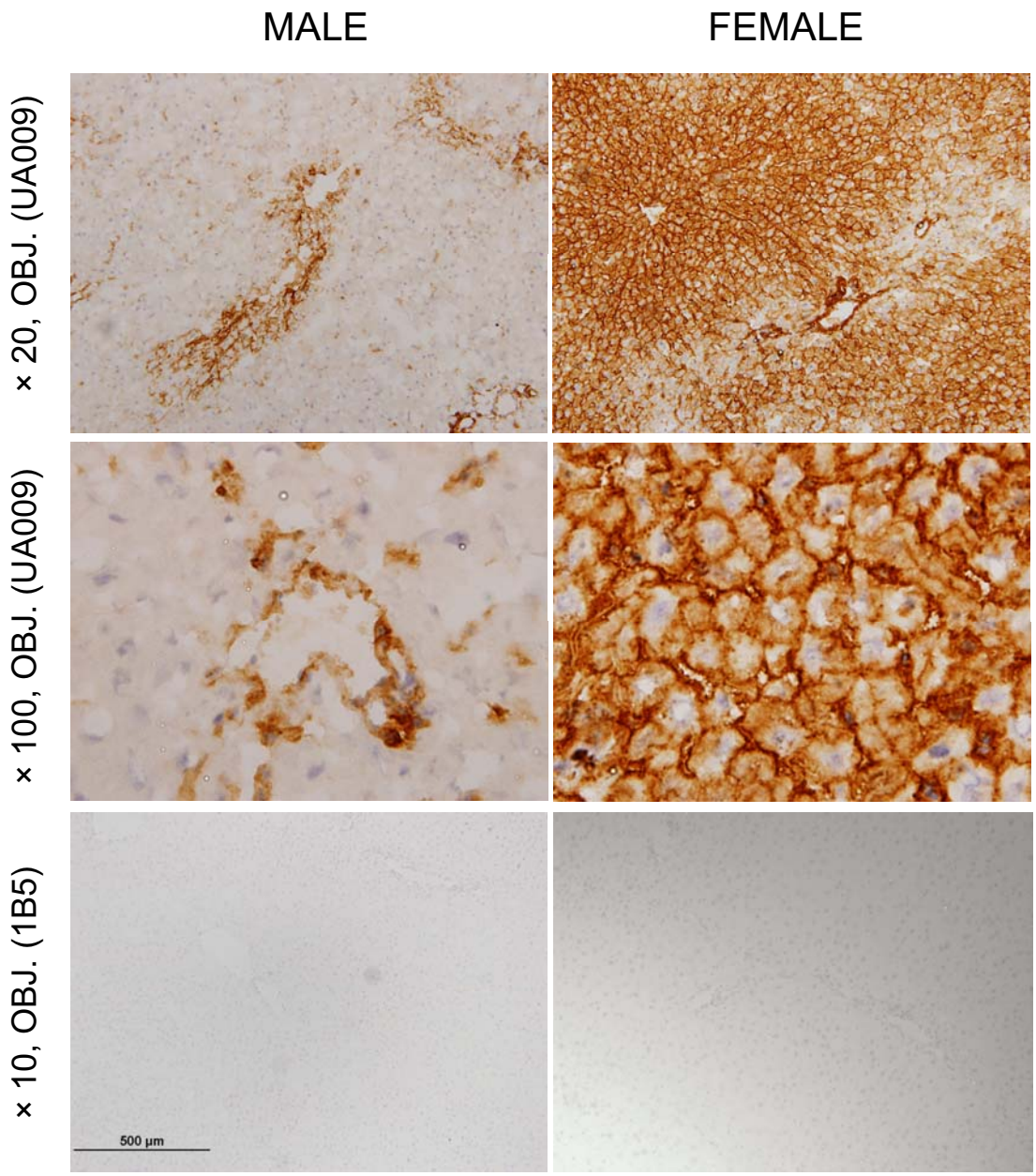

Figure 3-15.

Figure 3-16. Gender-biased expression of FAT/CD36 in rat liver. Lysates were prepared from liver samples from each of three male and three female DA rats. **A;** 25μg of protein from each lysate was subjected to 12% SDS-PAGE and Western blotting using anti-FAT/CD36 (mAb MO25) or anti-β-actin antibodies as indicated. **B;** Immunoreactive bands associated with FAT/CD36 were quantified by densitometric analysis and these values were standardized to signals associated with β-actin (house keeping loading control). Data are expressed as means ± SEM (n=3). *, $P < 0.05$.

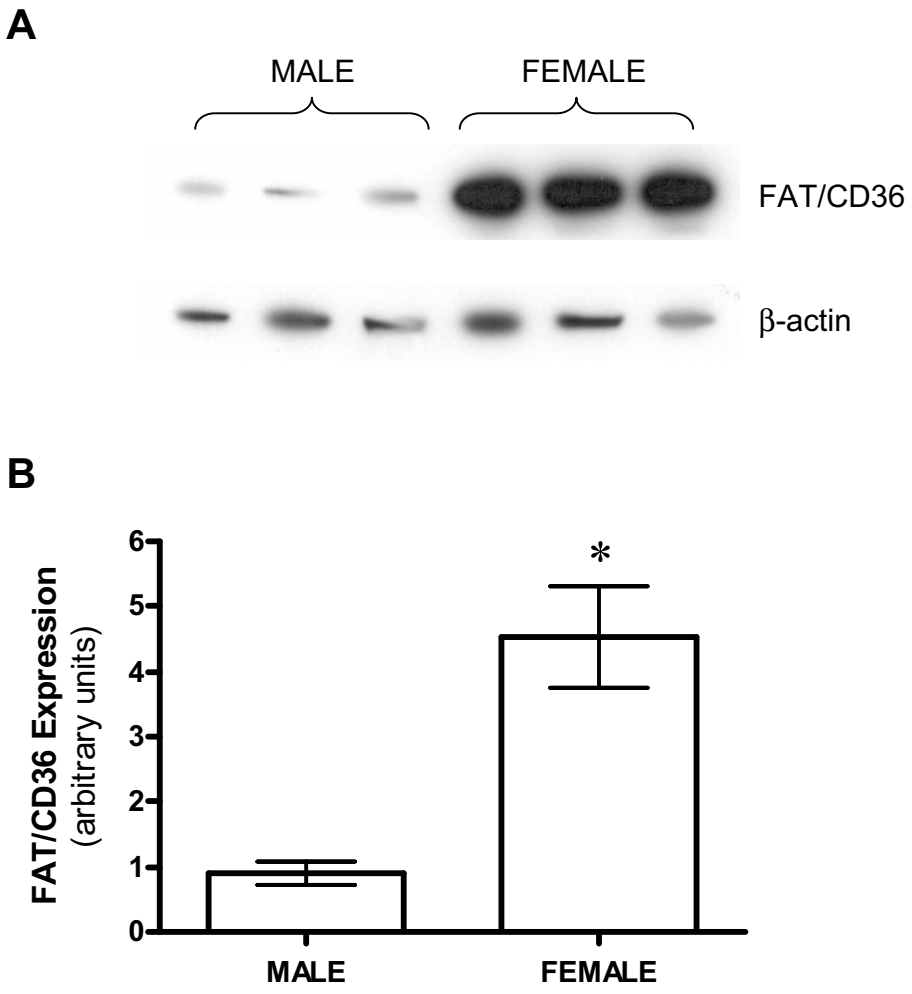
A
MALE
FEMALE
FAT/CD36
β-actin
B
FAT/CD36 Expression
(arbitrary units)
6
5
4
3
2
1
0
*
MALE
FEMALE

Figure 3-16.

FAT/CD36 protein in female liver (Figure 3-16B) than in male liver. The expression of caveolin-1 in rat liver was also assessed by Western blotting, using the same samples (Figure 3-17A). The results indicate that caveolin-1 protein is detectable in rat liver and that there is measurable difference in expression between males and females (Figure 3-17B). Detection of caveolin-1 protein in rat liver is consistent with detection of caveolin-1 mRNA expression by RT-PCR (see 4.3.1). While it is not clear whether the caveolin-1 detected was produced by hepatocytes, other studies indicate this to be the case (Calvo and Enrich, 2000, Calvo et al., 2001, Tietz et al., 2005, Mazzone et al., 2006). Other sources of caveolin-1 include vascular endothelial cells (Cohen et al., 2004) and it is possible that the amount of vascular tissue in the samples could have contributed to the large variation observed between animals. Future studies involving the purification of hepatocytes may reveal an effect of gender on caveolin-1 expression in these cells.

3.4.2.3 Biochemical analysis of FAT/CD36 localization to lipid rafts in rat liver

To investigate whether FAT/CD36 is associated with lipid rafts in hepatocytes, liver samples from male and female DA rats were lysed in 1% Triton X-100 at 4°C and subjected to sucrose step gradient fractionation as described previously (see 2.5.2). Analysis of the protein content of fractions revealed that > 95% of protein was contained within the final four (non-raft) fractions (Figure 3-18A). Furthermore, the sucrose content of various fractions resembled the corresponding fractions from gradients loaded with proteins prepared from cell lines (Figure 3-18A). Aliquots of each fraction (from a gradient prepared from female DA rat liver) were subjected to 12% SDS PAGE and Western blotting with mAb MO25 (anti-FAT/CD36), mAb OX-26 (anti-transferrin receptor) and mAb C060 (anti-caveolin-1) (Figure 3-18B). The results show that FAT/CD36 is enriched in DRM fractions prepared from rat liver. Furthermore, FAT/CD36 co-fractionated with caveolin-1 in the lipid raft-containing fractions, suggests that at least some of the FAT/CD36 in liver may localize to caveolae. However, as discussed above, DRMs cannot be equated with caveolae (Hooper, 1999) and some FAT/CD36 may be associated with DRMs that do not contain caveolin-1. Importantly the transferrin receptor was detected only in the final four (non-raft) fractions, indicating that DRM fractions were not contaminated with non-raft trans-membrane proteins.

Figure 3-17. Detection of caveolin-1 in homogenates of male and female rat liver. Lysates were prepared from liver samples from each of three male and three female DA rats. **A;** 25μg of protein from each lysate was subjected to 12% SDS-PAGE and Western blotting using anti-caveolin-1 or anti-β-actin antibodies as indicated. **B;** Immunoreactive bands associated with caveolin-1 were quantified by densitometric analysis and these values were standardized to signals associated with β-actin (house keeping loading control). Data are expressed as means ± SEM (n=3).

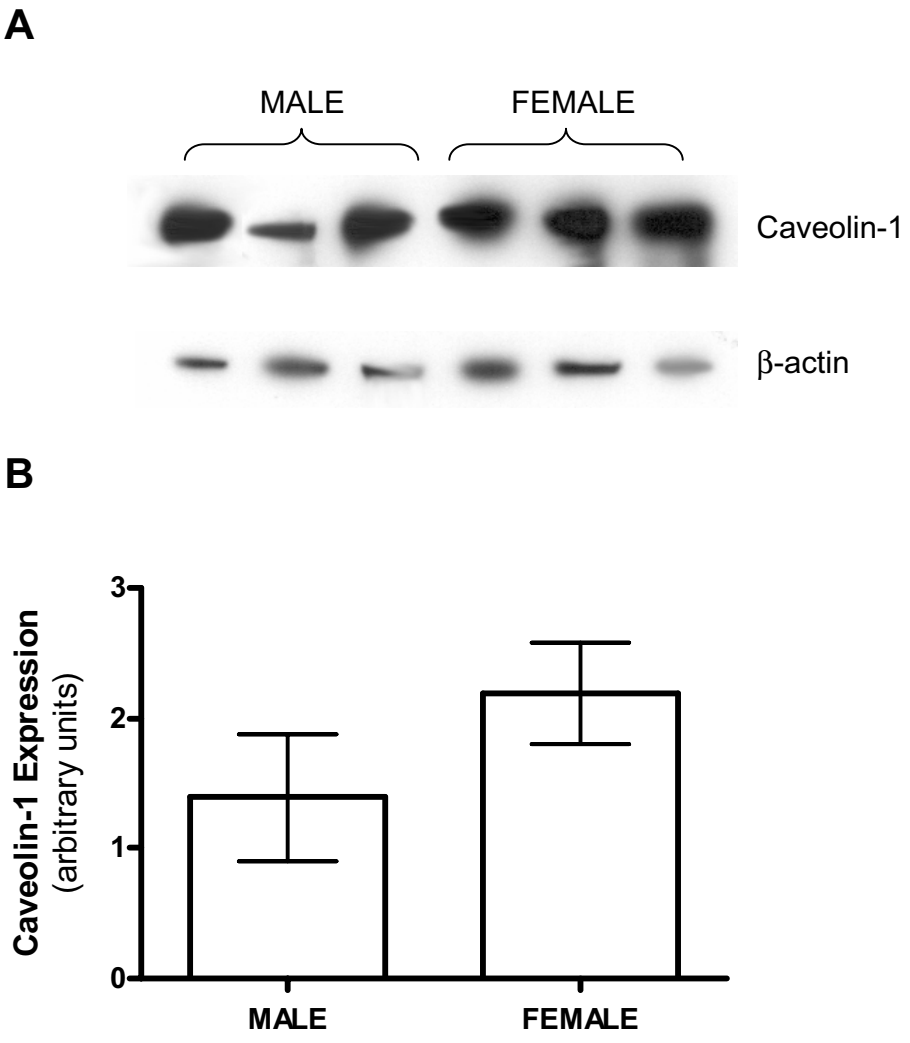
A
MALE
FEMALE
Caveolin-1
β-actin
B
Caveolin-1 Expression
(arbitrary units)
3
2
1
0
MALE
FEMALE

Figure 3-17.

Figure 3-18. Association of FAT/CD36 with lipid raft-derived detergent-resistant membranes (DRMs) prepared from rat liver. Portions of liver from female DA strain rats were lysed in 1% Triton X-100 at 4°C and samples were subjected to discontinuous 5-40% sucrose gradient centrifugation. Fractions were collected from the tops of the gradients. **A**; the protein and sucrose contents of each fraction (squares and triangles, respectively). **B**; aliquots of each fraction were subjected to 12% SDS-PAGE and Western blotting using anti-FAT/CD36 mAb MO25, anti-caveolin-1 mAb or anti transferrin receptor mAb OX-26 as indicated.

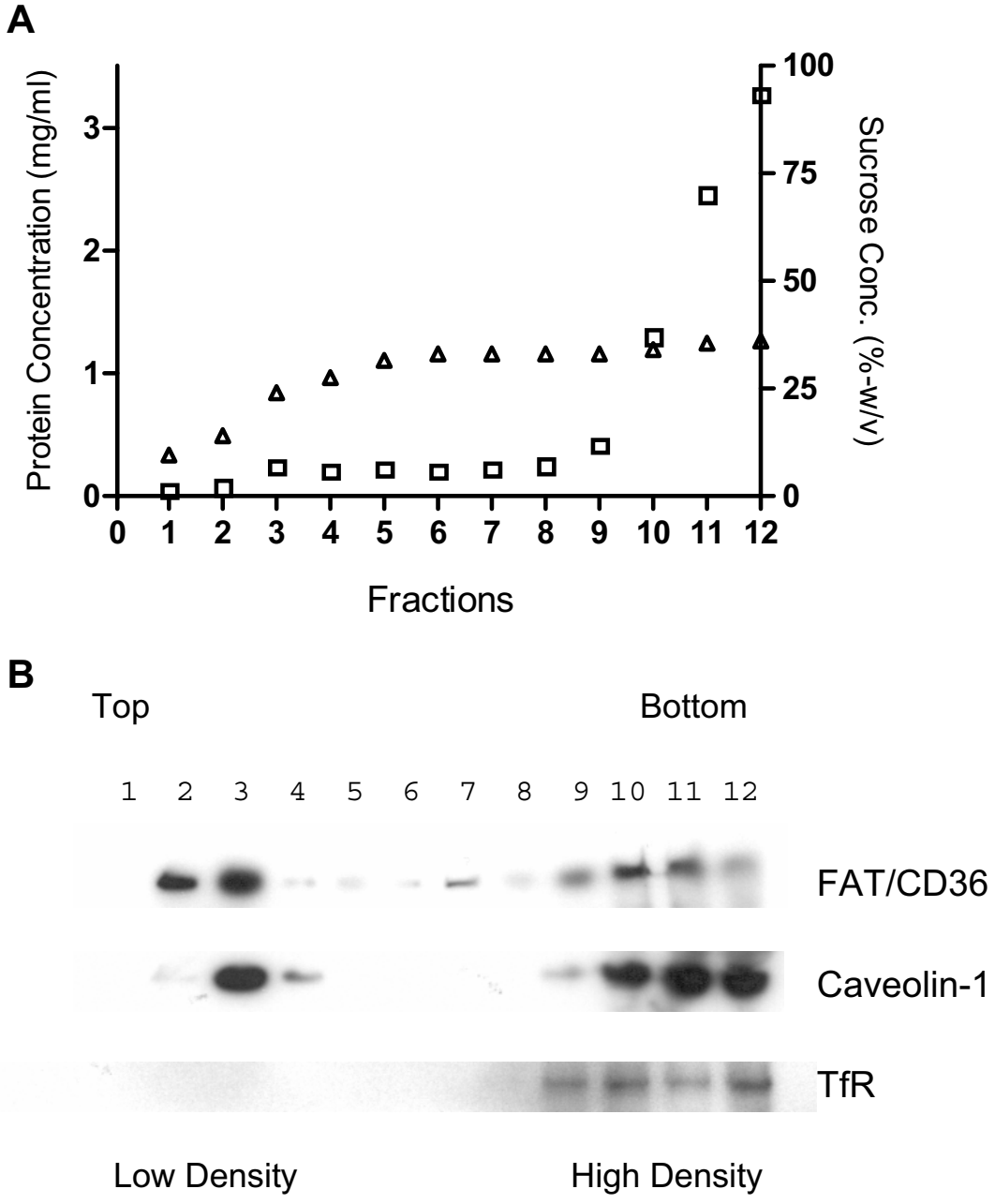
A
Protein Concentration (mg/ml)
Sucrose Conc. (%-w/v)
Fractions
B
Top
Bottom
1 2 3 4 5 6 7 8 9 10 11 12
FAT/CD36
Caveolin-1
TfR
Low Density
High Density

Figure 3-18.

To investigate whether incorporation of FAT/CD36 into lipid rafts in hepatocytes is gender-regulated, the FAT/CD36 content of sucrose gradient fractions prepared from male (n=3) and female (n=3) rat liver was measured using Western blotting and densitometry (Figure 3-19). As samples were not standardized for protein content, FAT/CD36 in a given fraction was calculated by densitometric analysis and expressed as a percentage of the sum of the FAT/CD36 in all fractions from the same gradient. In both genders, some of the immuno-reactive FAT/CD36 was associated with fractions expected to contain DRMs. However, there were some significant differences in the distribution of FAT/CD36 across gradients used to analyse lysates from male and female liver. The proportion of FAT/CD36 in DRMs was significantly greater in lysates prepared from female compared with male liver. The reasons for this difference are unclear. It may indicate that incorporation of FAT/CD36 into DRMs is associated with the mechanisms that differentially regulate expression of the molecule in hepatocytes of female and male rats. However, it is also possible that the lower proportion of hepatocytes that express FAT/CD36 in male liver elevates the contribution from other cell types such as endothelial cells, hepatic stellate cells and Kupffer cells and that the association of the molecule with DRMs is different in these cells.

3.4.3 Subcellular localization of FAT/CD36 in transfected COS-7 cells

The sub-cellular localisation of FAT/CD36 to DRMs in liver, and the possible effects of gender, raised questions about how the expression of the molecule in the plasma membranes of cells is regulated. COS-7 cells are readily transfectable, they do not express endogenous FAT/CD36 and they have been used previously to study aspects of FAT/CD36 expression (Thorne et al., 1997, Connelly et al., 1999). They were chosen as a non- hepatocyte cell line, for comparison later with the rat hepatoma H4IIE cell line.

3.4.3.1Biochemical analysis of FAT/CD36 localization to lipid rafts in transfected COS-7 cells

To assess whether FAT/CD36 in stably transfected COS-7 -FAT/CD36 cells resides in lipid rafts, the cells were lysed in 1% Triton X-100 at 4°C and the lysate was subjected to sucrose step-gradient fractionation (see 2.5.2). Analysis of the protein content of each fraction revealed that greater than 95% of the cellular protein was distributed in the final four fractions (Figure 3-20A), which are expected to contain cytosolic plus non-raft

Figure 3-19. Comparison of association of FAT/CD36 with lipid raft-derived detergent-resistant membranes (DRMs) prepared from male and female rat liver. Portions of liver from each of three male and three female DA strain rats were lysed in 1% Triton X-100 at 4°C and samples were subjected to discontinuous 5-40% sucrose gradient centrifugation. Fractions were collected from the tops of the gradients and equal volumes of each fraction were subjected to 12% SDS PAGE and Western blotting with anti-FAT/CD36 mAb MO25 (**A**). **B;** Association of FAT/CD36 with each fraction is expressed as a percentage of the total FAT/CD36 content across all fractions ± SEM (n=3). *, $P < 0.05$, statistically significant difference between male and females.

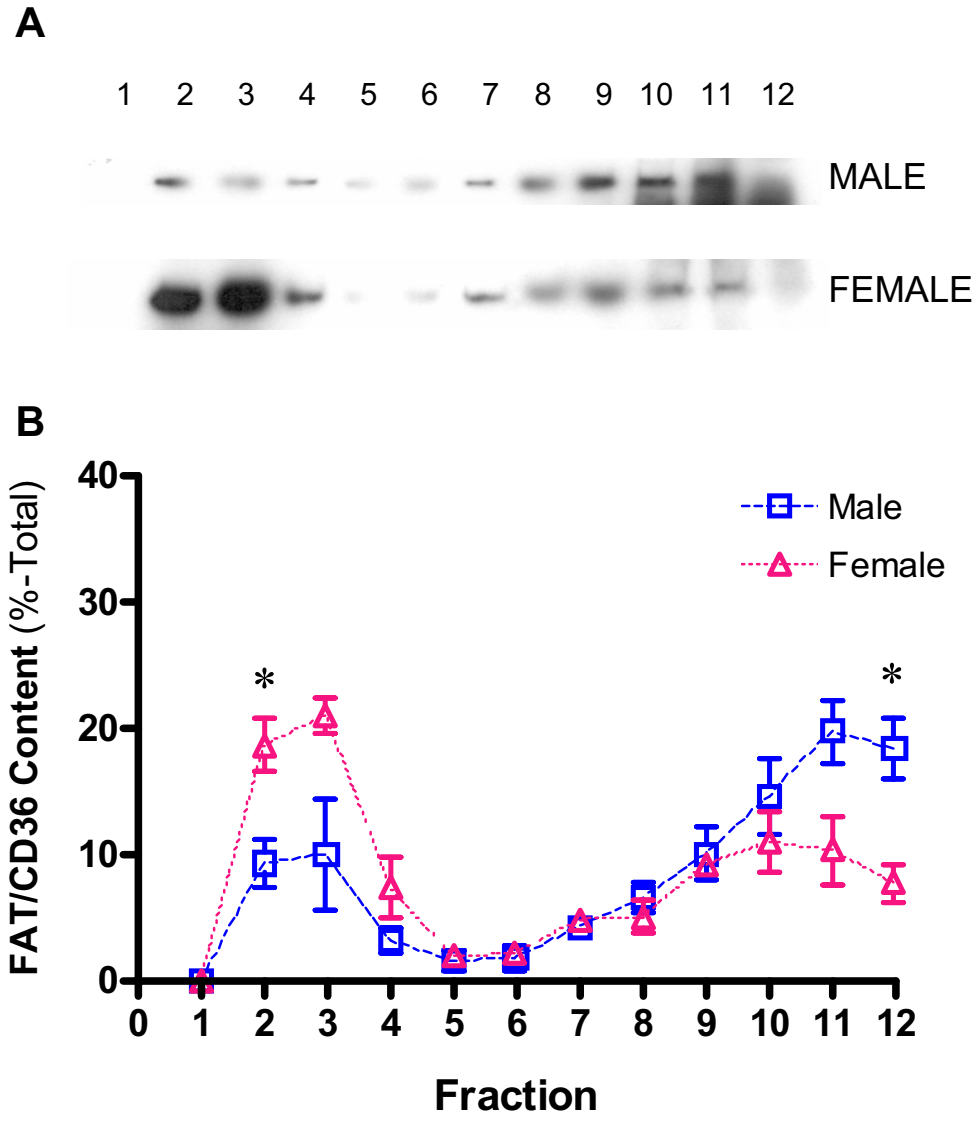
A
1 2 3 4 5 6 7 8 9 10 11 12
MALE
FEMALE
B
FAT/CD36 Content (%-Total)
40
30
20
10
0
Male
Female
*
*
0 1 2 3 4 5 6 7 8 9 10 11 12
Fraction

Figure 3-19.

Figure 3-20. Western blot analysis of FAT/CD36 and caveolin-1 in detergent-resistant mebrane (DRM) preparations from the clonal COS-7-FAT/CD36 cell line. After lysis in 1% Triton X-100 at 4°C, samples were subjected to discontinuous 5-40% sucrose gradient centrifugation. Fractions were collected from the tops of the gradients. **A**; the protein and sucrose contents of each fraction (squares and triangles, respectively). **B**; aliquots of each fraction were subjected to 12% SDS-PAGE and Western blotting using anti-FAT/CD36 mAb MO25 or anti-caveolin-1 mAb, as indicated.

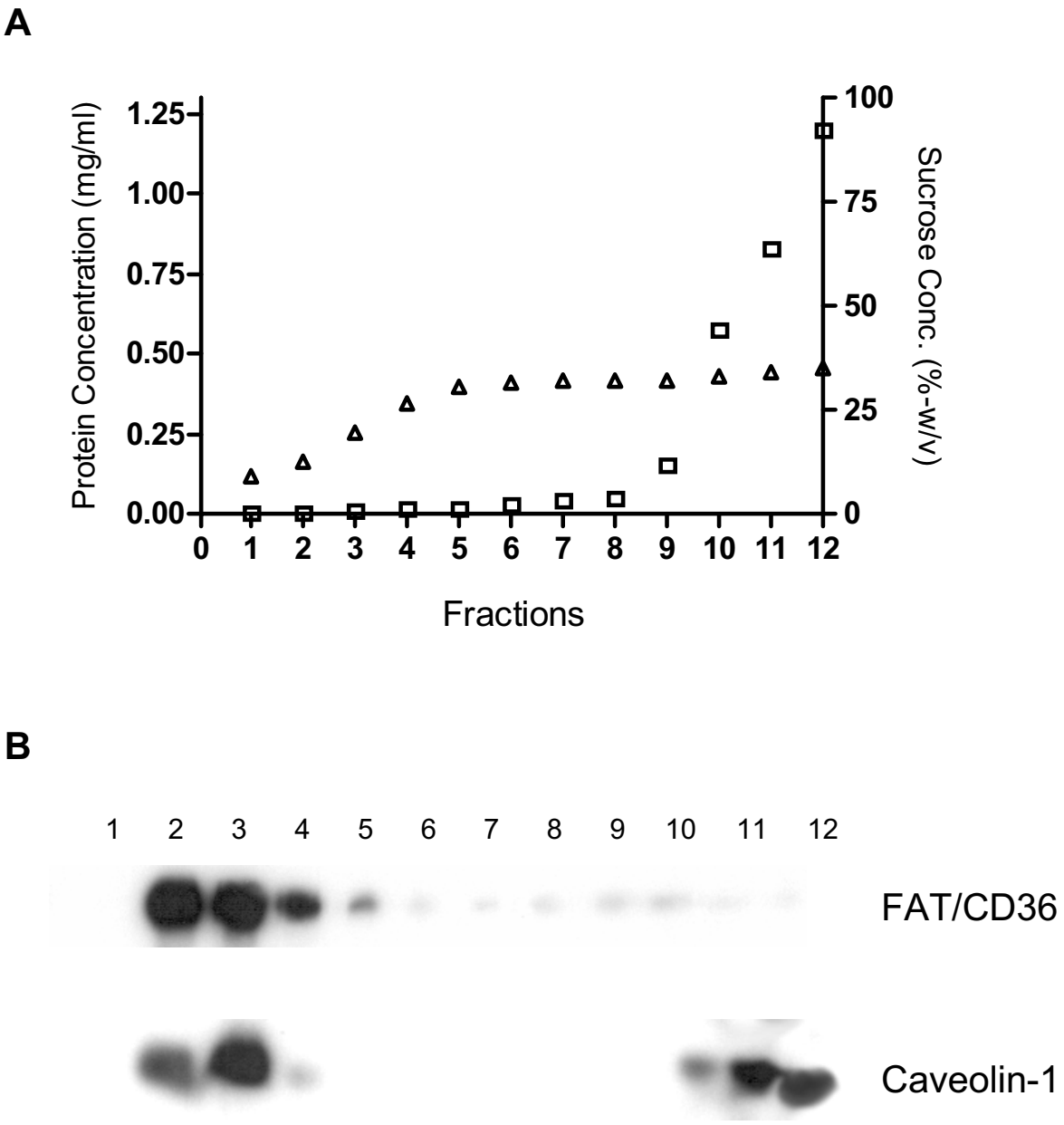
A
Protein Concentration (mg/ml)
1.25
1.00
0.75
0.50
0.25
0.00
100
75
50
25
0
Sucrose Conc. (%-w/v)
0 1 2 3 4 5 6 7 8 9 10 11 12
Fractions
B
1 2 3 4 5 6 7 8 9 10 11 12
FAT/CD36
Caveolin-1

Figure 3-20.

membrane proteins. The densities and sucrose concentrations of each of the fractions resembled those reported for DRM preparations from other cell types and from liver (see above). Aliquots from each fraction were subjected to 12% SDS-PAGE and Western blotting using antibodies against FAT/CD36 (mAb MO25) and caveolin-1 (mAb C060) (Figure 3-20B). The results indicate that FAT/CD36 is enriched in DRMs in these cells. Essentially all of the endogenous caveolin-1 was detected within the DRM-containing fractions and the partial co-fractionation of FAT/CD36 with caveolin-1 suggests that some of it may be located in caveolae. This finding is in accordance with similar investigations into the subcellular distribution of human FAT/CD36 in transfected COS-7 cells (Thorne et al., 1997). However, the asymmetrical distribution of caveolin-1 between fractions 2 and 3 of the gradient suggests that some FAT/CD36 is associated with lower density DRMs that are relatively caveolin-poor.

3.4.3.2 Localization of FAT/CD36 to lipid rafts/caveolae in transfected COS-7 cells, as determined by confocal fluorescence microscopy

To examine whether FAT/CD36 is associated with classical lipid rafts and/or caveolae in COS-7 cells, the subcellular localization of the molecule was assessed with reference to GM_1 and caveolin-1, using confocal fluorescence microscopy. FAT/CD36 and GM_1 were observed to overlap extensively in their subcellular distributions; both at the plasma membrane and within perinuclear Golgi-like organelles (Figure 3-21). To compare the subcellular localization of caveolin-1 and GM_1 and to confirm previous reports that caveolae represent a subset of classical lipid rafts, COS-7 cells were transiently transfected with pCaveolin-1-EGFP. They were then cultured with Alexa 594-conjugated CT-B, prior to fixation and examination using confocal fluorescence microscopy (Figure 3-22). As can be seen, the distributions of caveolin-1 and GM_1 overlap extensively, both at the cell surface and within the cell (especially in perinuclear Golgi-like organelles). There are, however, distinct micro-domains that are positive for the GM_1 marker but negative for caveolin-1-EGFP (arrow 1). Similarly, there are distinct micro-domains that are positive for caveolin-1 but negative for GM_1 (arrow 2). While the distinction between cell-surface and intracellular location of caveolin1-EGFP and CT-B cannot be made using this technique, it is apparent that these markers do not overlap perfectly. This suggests that caveolae do not all belong to the same subset of classical lipid rafts and that classical lipid rafts may consist of distinct sub-classes of plasma membrane microdomains. The results also suggest that not all GM_1–positive lipid rafts become caveolae after expression of

Figure 3-21. Co-localization of FAT/CD36 and lipid rafts by confocal fluorescence microscopic analysis of the COS-7-FAT/CD36 cell line. Cells were grown on coverslips and incubated at 37°C with an Alexa Fluor 594 cholera toxin subunit B (CT-B) conjugate (red) to allow binding and uptake. Cells were fixed (upper panels) or fixed and permeabilized with 0.1% saponin (lower panels). They were then labelled to detect FAT/CD36 using anti-FAT/CD36 (mAb UA009) and a FITC-conjugated secondary antibody (green). Yellow in the merged images indicates co-localization of FAT/CD36 and CT-B. ×63 objective plus ×2.5 zoom.

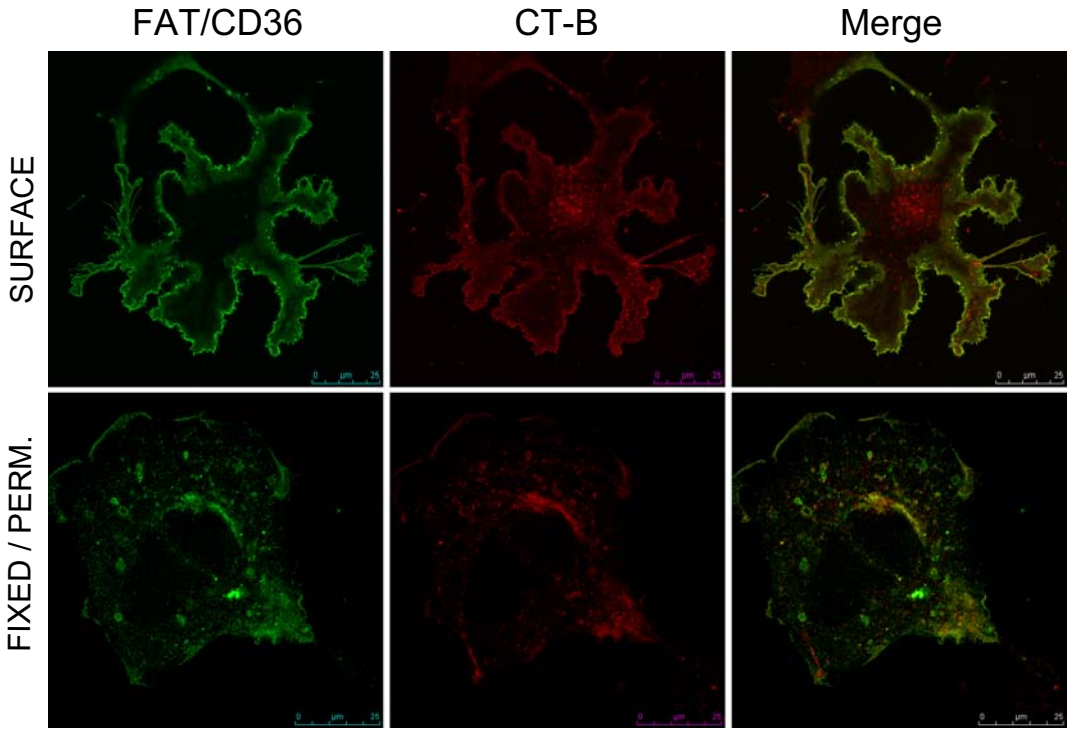

Figure 3-21.

Figure 3-22. Co-localization of caveolae (caveolin-1) and lipid rafts (GM_1) by confocal fluorescence microscopy. COS-7 cells were grown on coverslips and transiently transfected with pCaveolin-1-EGFP before incubating at 37°C with an Alexa Fluor 594 cholera toxin subunit B (CT-B) conjugate (red) to allow binding and uptake. Arrows indicate the presence of CT-B-positive / caveolin-1-EGFP-negative (arrow 1) or CT-B-negative / caveolin-1-EGFP-positive microdomains. Yellow in the merged image shows co-localization of CT-B (red) and caveolin-1-EGFP (green). ×63 objective plus ×2.5 zoom.

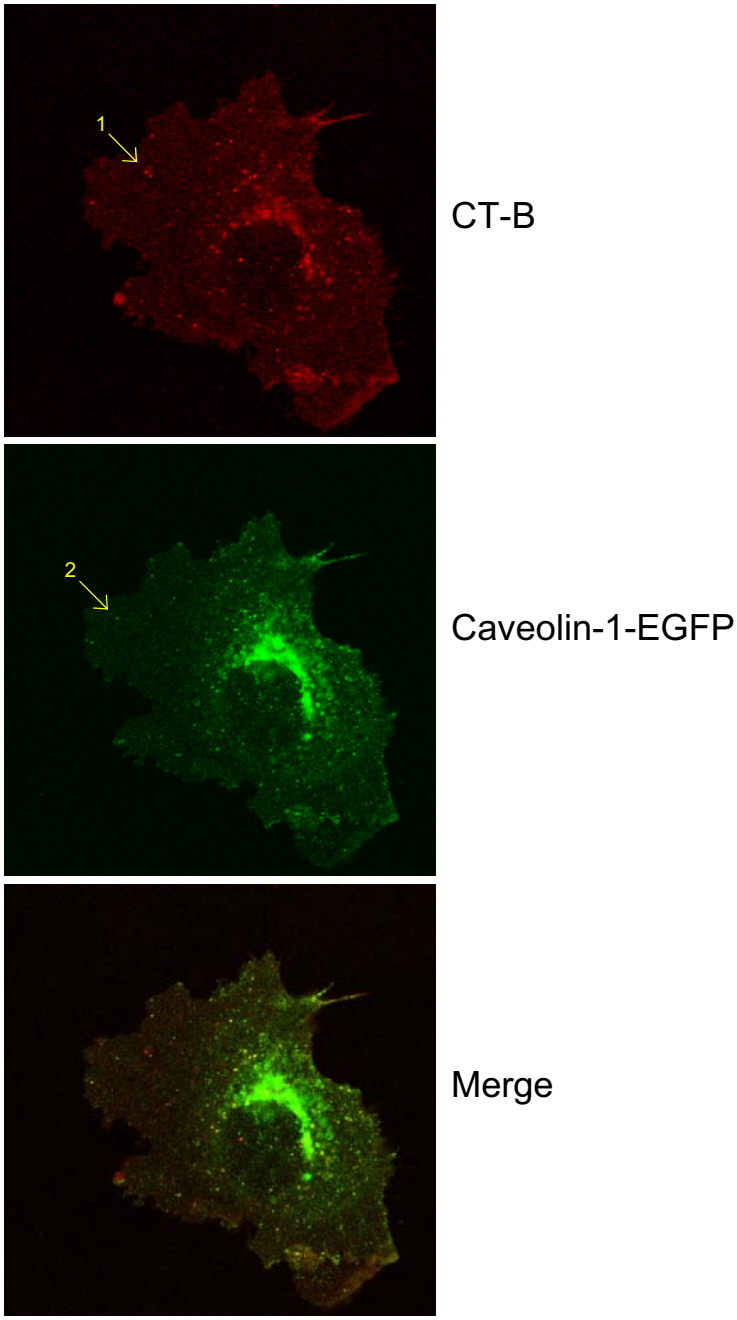

Figure 3-22.

caveolin-1. These interpretations must be tentative because it can be argued that some of the fluorescence that was detected is intracellular and that it could be associated with different cytoplasmic organelles that are engaged in traffic of the two molecules to the plasma membrane.

3.4.4 Subcellular localization of FAT/CD36 in transfected H4IIE cells

Expression of FAT/CD36 at the plasma membrane has been described in rat (Zhang et al., 2003, Stahlberg et al., 2004) and human (Stahlberg et al., 2004) hepatocytes. Therefore, as described previously (see 2.2.5), FAT/CD36-transfected H4IIE cell lines were generated to provide a model for FAT/CD36 localization and activity in hepatocytes. H4IIE cells lack endogenous FAT/CD36 expression as determined by flow cytometry, Western blotting and RT-PCR (see 3.3.2 and 4.3.1). They also lack caveolin-1 expression as determined by RT-PCR (see 4.3.1) and thus do not have caveolae, making them an ideal model with which to investigate possible interactions between caveolin-1 expression and formation of caveolae on the localization of FAT/CD36 and its activity in hepatocytes.

3.4.4.1 Biochemical analysis of FAT/CD36 localization to lipid rafts in transfected H4IIE cells

To investigate whether FAT/CD36 in H4IIE-FAT/CD36 (1A) cells (described in 3.3.2) is localized in lipid rafts, the cells were subjected to lysis in 1% Triton X-100 at 4°C and sucrose step gradient fractionation (see 2.5.2). The densities, sucrose content and protein content of fractions resembled those obtained for other DRM preparations using both this cell type and others (Figure 3-23A). Western analysis of fractions using an anti-FAT/CD36 antibody (mAb MO25) revealed that FAT/CD36 was enriched in the low-density DRMs (fractions 2-4) (Figure 4-23B). Importantly, the transferrin receptor (~97 kDa), commonly used as a marker representative of non-raft membrane proteins (Pohl et al., 2004, Pohl et al., 2005), was only detected in the final four high density fractions. These fractions are expected to contain cytosolic plus Triton X-100-soluble membrane proteins.

3.4.4.2 Stable expression of caveolin-1-EGFP in H4IIE (5A) and H4IIE-FAT/CD36 (1A) cell lines

To investigate the localization of FAT/CD36 in H4IIE cells that express caveolin-1, H4IIE-FAT/CD36 (1A) and H4IIE (5A) cell lines were stably transfected with the plasmid

Figure 3-23. Western blot analysis of FAT/CD36 in detergent-resistant mebrane (DRM) preparations from the H4IIE-FAT/CD36 (1A) cell line. After lysis in 1% Triton X-100 at 4°C, samples were subjected to discontinuous 5-40% sucrose gradient centrifugation. Fractions were collected from the tops of the gradients. **A**; the protein and sucrose contents of each fraction (squares and triangles, respectively). **B**; aliquots of each fraction were subjected to 12% SDS-PAGE and Western blotting using anti-FAT/CD36 mAb MO25 or anti-transferrin receptor mAb (OX-26), as indicated.

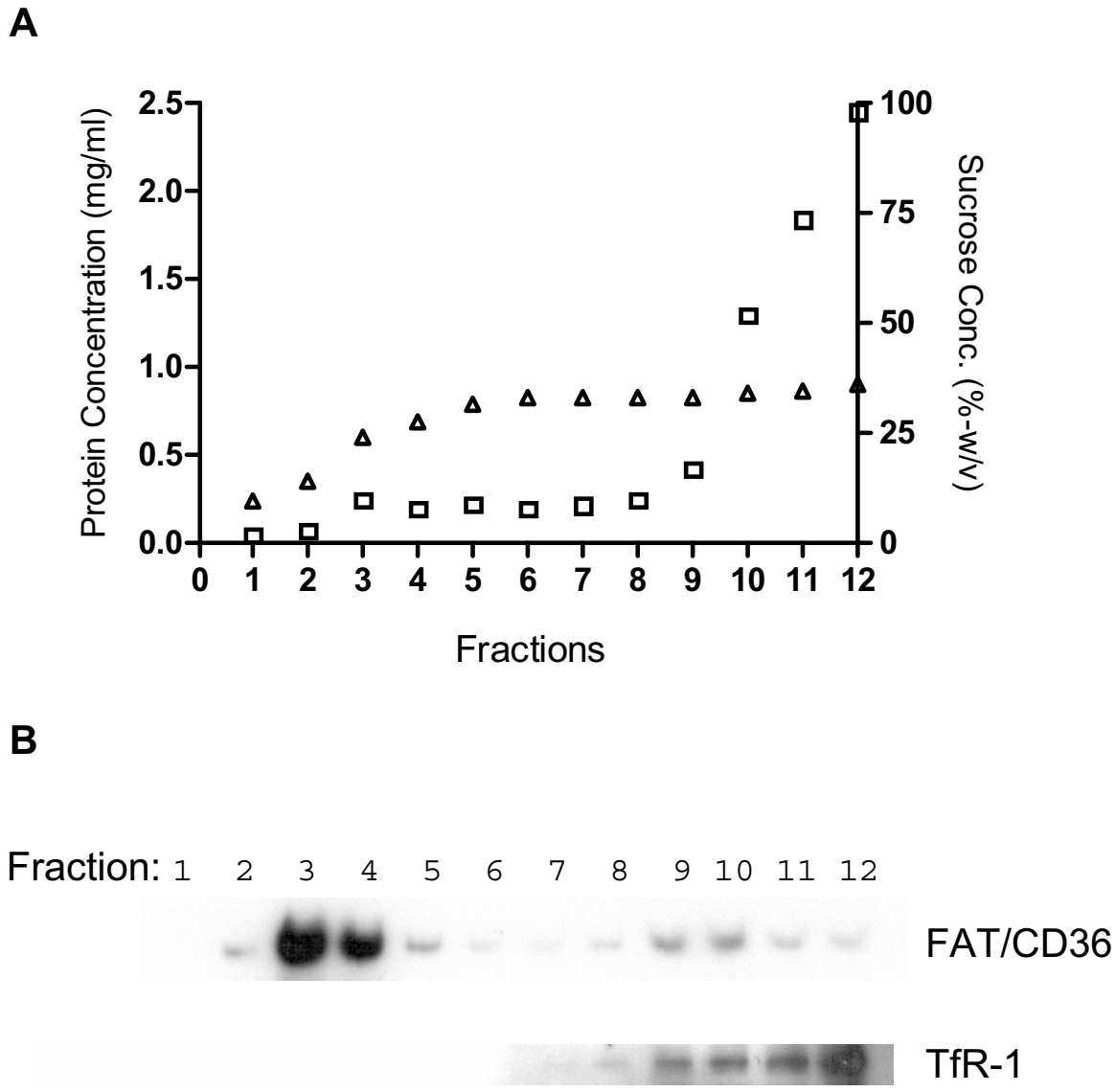
A
Protein Concentration (mg/ml)
2.5
2.0
1.5
1.0
0.5
0.0
100
75
50
25
0
Sucrose Conc. (%-w/v)
0 1 2 3 4 5 6 7 8 9 10 11 12
Fractions
B
Fraction: 1 2 3 4 5 6 7 8 9 10 11 12
FAT/CD36
TfR-1

Figure 3-23.

pEF-Cav1-EGFP-IRES-puro 6 (see 3.4.1). Following several weeks of selection with puromycin dihydrochloride (10 μg/ml), antibiotic-resistant cells that expressed caveolin-1-EGFP were enriched by fluorescence activated cell sorting (FACS) (see 2.3.4). The sorted cells were returned to culture and, after growth of sufficient stocks, FAT/CD36 and caveolin-1-EGFP expression were assessed by flow cytometry (Figure 3-24). As can be seen, cell-surface expression of FAT/CD36 was not affected by expression of caveolin-1-EGFP. Furthermore, caveolin-1-EGFP expression levels were similar between H4IIE (5A) + caveolin-EGFP and H4IIE-FAT/CD36 (1A) + caveolin-1-EGFP cell lines.

3.4.4.3 Enrichment of FAT/CD36 and caveolin-1-EGFP in DRMs prepared from co-transfected H4IIE cell lines

To investigate whether FAT/CD36 and caveolin-1 co-fractionate in lipid raft fractions of H4IIE cells, H4IIE-FAT/CD36 (1A) + caveolin-1-EGFP cells were subjected to lysis in 1% Triton X-100 at 4°C and sucrose step gradient fractionation. In parallel H4IIE (5A), H4IIE-FAT/CD36 (1A) and H4IIE (5A) + caveolin-1-EGFP cell lines were also subjected to DRM preparation. Analysis of fractions collected from each of these gradients revealed minimal differences in the sucrose and protein content of the corresponding fractions from each of the cell lines (Figure 3-25A). Western analysis of FAT/CD36 and caveolin-1-EGFP in fractions isolated from co-transfected cells revealed that both molecules were present in DRM fractions (Figure 3-25B). Furthermore, comparison of the distributions of FAT/CD36 and caveolin-1-EGFP across these fractions with their relative distributions across fractions prepared from H4IIE-FAT/CD36 (1A) and H4IIE (5A) + caveolin-1-EGFP cell lines, respectively, yielded similar results. It is apparent that the partitioning of caveolin-1-EGFP between DRMs and detergent-soluble fractions in H4IIE-FAT/CD36 (1A) + caveolin-1-EGFP hepatoma cells was similar to the partitioning of native caveolin in normal female rat liver. This suggests that the fusion protein in the cell line behaves in a fashion similar to native caveolin-1 in normal hepatocytes.

3.4.4.4 Localization of FAT/CD36 to lipid rafts/caveolae of transfected H4IIE cells as determined by confocal fluorescence microscopy

To further investigate whether FAT/CD36 is localized to plasma membrane lipid rafts in transfected H4IIE cells, as implied by the enrichment of FAT/CD36 in low-density DRMs, H4IIE-FAT/CD36 (1A) cells were cultured with Alexa-594 conjugated CT-B prior to

Figure 3-24. Expression of FAT/CD36 and caveolin-1-EGFP in stably transfected H4IIE cell lines as determined by flow cytometric analysis. H4IIE (5A) (lower left panel), H4IIE-FAT/CD36 (1A) (upper left panel), H4IIE (5A) + caveolin-1-EGFP (lower right panel) and H4IIE-FAT/CD36 (1A) + caveolin-1-EGFP (upper right panel) cell lines were labelled by indirect immunofluorescence using anti-FAT/CD36 (mAb UA009) and Cy3-conjugated anti-mouse secondary antibodies. Irrelevant isotype-matched anti-Giardia control antibody (mAb 1B5) was used as a negative control for non-specific labelling (not shown). Viable cells were gated on the basis of their forward- and side-scatter properties and cell-associated fluorescence of cells within the gate was assessed.

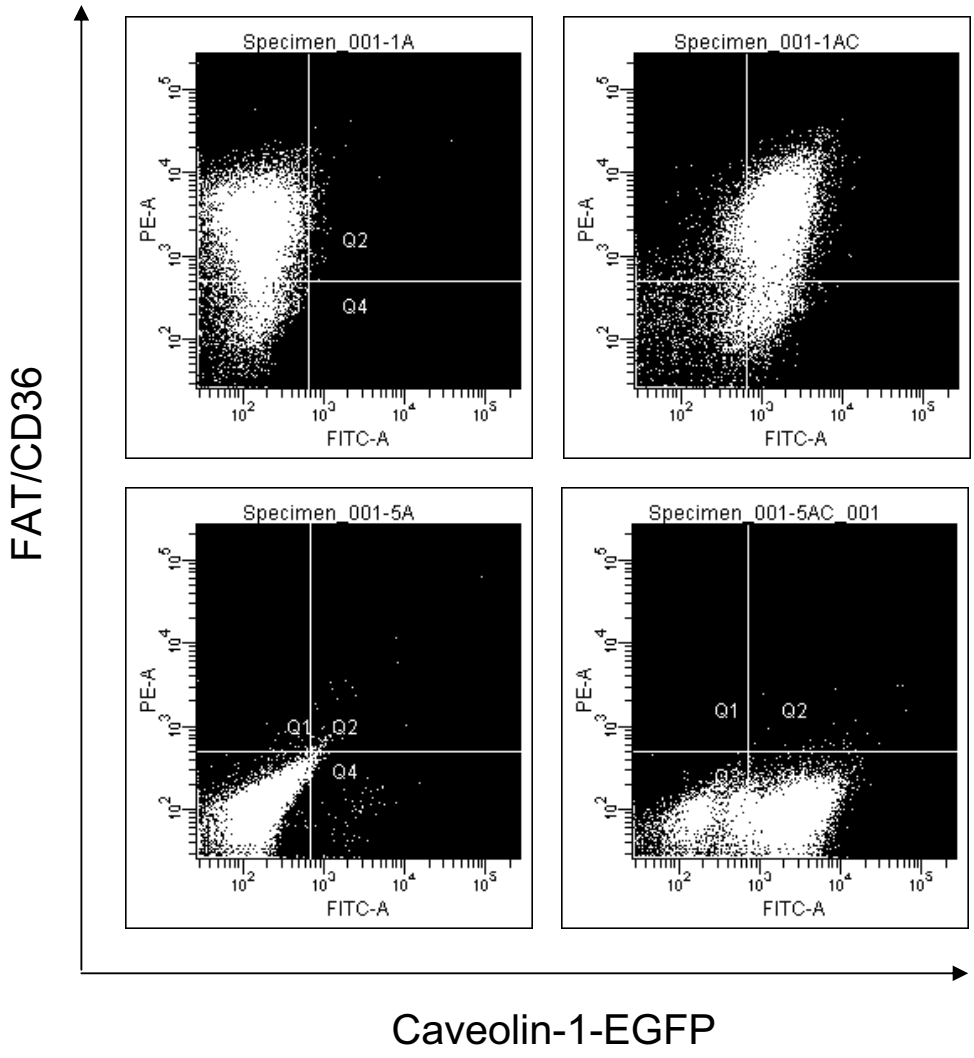
Specimen_001-1A
Specimen_001-1AC
Specimen_001-5A
Specimen_001-5AC_001
PE-A
FITC-A
Q1
Q2
Q4
FAT/CD36
Caveolin-1-EGFP

Figure 3-24.

Figure 3-25. Western blot analysis of FAT/CD36 and caveolin-1-EGFP in detergent-resistant membrane (DRM) preparations from transfected H4IIE cell lines (H4IIE-FAT/CD36 (1A) [I], H4IIE-FAT/CD36 (1A) + caveolin-1-EGFP [II, IV], H4IIE (5A) + caveolin-1-EGFP [III]). After lysis in 1% Triton X-100 at 4°C, samples were subjected to discontinuous 5-40% sucrose gradient centrifugation. Fractions were collected from the tops of the gradients. **A**; the protein and sucrose contents of each fraction (squares and triangles, respectively). **B**; aliquots of each fraction were subjected to 12% SDS-PAGE and Western blotting with anti-FAT/CD36 (mAb MO25) or anti-GFP antibodies as indicated. No immunoreactive bands were detected in fractions prepared from the H4IIE (5A) control cell line when either antibody was employed (not shown).

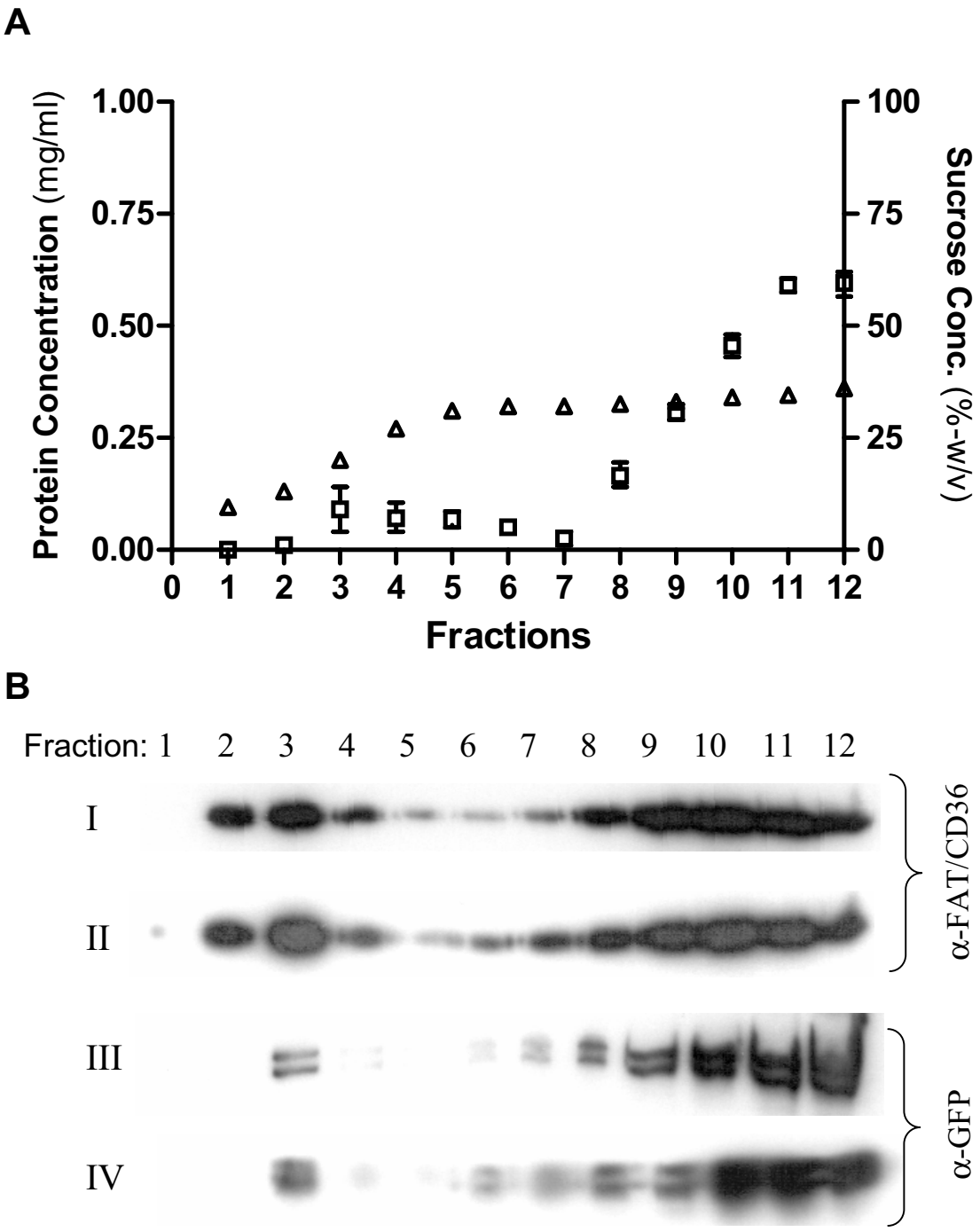
A
Protein Concentration (mg/ml)
1.00
0.75
0.50
0.25
0.00
100
75
50
25
0
Sucrose Conc. (%-w/v)
0 1 2 3 4 5 6 7 8 9 10 11 12
Fractions
B
Fraction: 1 2 3 4 5 6 7 8 9 10 11 12
I
II
III
IV
α-FAT/CD36
α-GFP

Figure 3-25.

fixation and labelling FAT/CD36 by immunofluorescence for confocal fluorescence microscopy. The results show that labelling of plasma membrane FAT/CD36 overlaps closely the labelling of GM_1 with CT-B (Figure 3-26, upper panels). In the same experiment, some of the H4IIE-FAT/CD36 (1A) cells that had been incubated with CT-B were fixed and permeabilized prior to immunofluorescence labelling of FAT/CD36. Confocal microscopic analysis of the permeabilized cells (Figure 3-26, lower panels) showed that FAT/CD36 and GM_1 were co-localized also within cytoplasmic organelles, especially within perinuclear Golgi-like organelles.

Co-fractionation of FAT/CD36 and caveolin-1 in DRMs could indicate that FAT/CD36 is present in caveolae in transfected H4IIE cells that express both molecules. However, previous studies have indicated that the presence of caveolin-1 cannot be taken as evidence that all of the DRMs in a preparation are caveolae (Hooper, 1999, Iwabuchi et al., 1998). Furthermore, studies on the localization of human FAT/CD36 in transfected CHO cells have indicated that FAT/CD36 can reside within plasma membrane lipid raft domains that are distinct from caveolae, despite similarities to caveolae in detergent-resistance and buoyant density (Zeng et al., 2003). H4IIE-FAT/CD36 (1A) + caveolin-1-EGFP cells were used to compare the localization of FAT/CD36 and caveolin-1 in cells of hepatic origin. The cells were cultured on coverslips, fixed and labelled by indirect immunofluorescence to stain FAT/CD36, with or without prior permeabilization. Confocal fluorescence microscopy revealed partial overlap of FAT/CD36 and caveolin-1-EGFP at the cell surface (Figure 3-27, upper panels). Furthermore, the two molecules could be seen to overlap closely in their intracellular distributions, particularly in Golgi-like perinuclear organelles (Figure 3-27, lower panels).

3.4.4.5 Localization of FAT/CD36 to lipid raft and non-raft micro-domains of the plasma membrane of transfected H4IIE cells

The biochemical studies described above have provided evidence of enrichment of FAT/CD36 in lipid rafts and this was consistent with the demonstration of co-localization of FAT/CD36 and GM_1 using confocal fluorescence microscopy. Further studies were needed to determine whether FAT/CD36 was confined to lipid rafts in these cells, as has been demonstrated 3T3-L1 adipocytes (Pohl et al., 2005). In the biochemical studies, it was not possible to assess whether the FAT/CD36 that was present in the detergent-soluble fractions included FAT/CD36 molecules derived from non-raft domains of the plasma

Figure 3-26. Co-localization of FAT/CD36 and lipid rafts by confocal fluorescence microscopic analysis of the H4IIE-FAT/CD36 (1A) cell line. Cells were grown on coverslips and incubated at 37°C with an Alexa Fluor 594 cholera toxin subunit B (CT-B) conjugate (red) to allow binding and uptake. Cells were fixed (upper panels) or fixed and permeabilized with 0.1% saponin (lower panels). They were then labelled to detect FAT/CD36 using anti-FAT/CD36 (mAb UA009) and a FITC-conjugated secondary antibody (green). Yellow in the merged images indicates co-localization of FAT/CD36 and CT-B. ×63 objective plus ×2.5 zoom.

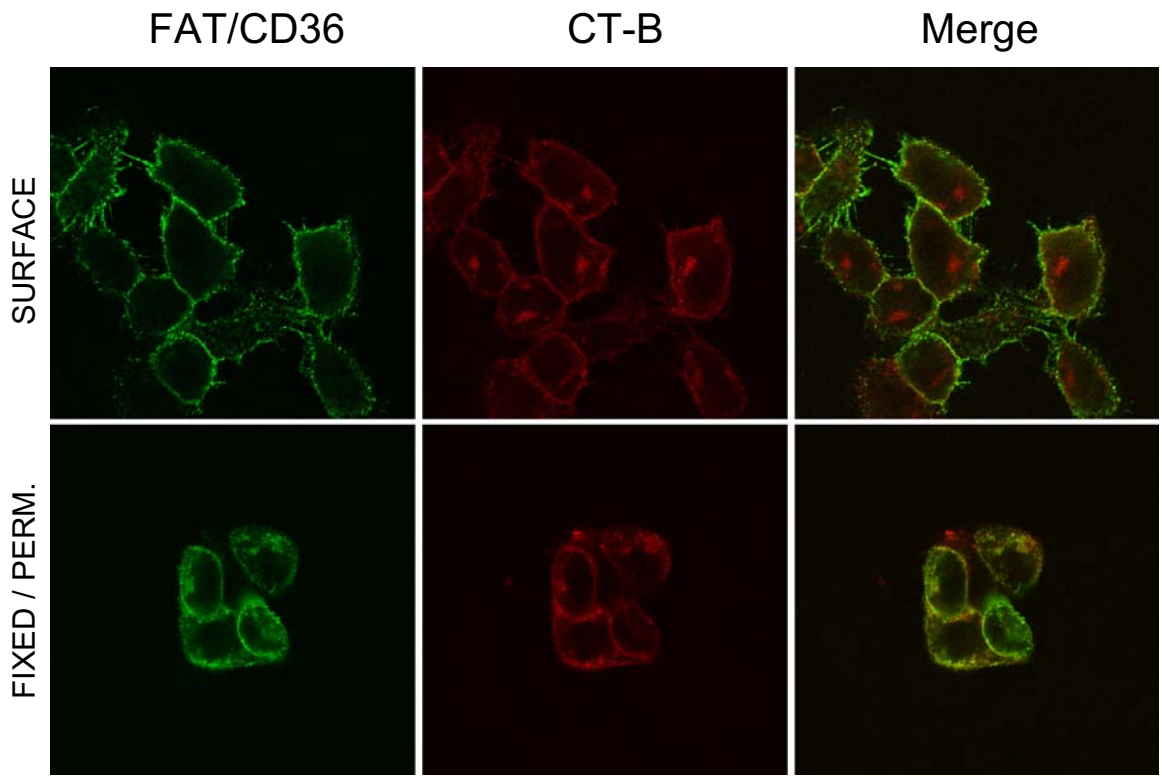

Figure 3-26.

Figure 3-27. Co-localization of FAT/CD36 and caveolin-1-EGFP in the H4IIE-FAT/CD36 (1A) + caveolin-1-EGFP cell line. Cells were grown on coverslips and either fixed (upper panels) or fixed and permeabilized (lower panels) before staining by indirect immunofluorescence, using anti-FAT/CD36 (mAb UA009) and Cy3-conjugated anti-mouse antibody (red). ×40 objective plus ×3 zoom.

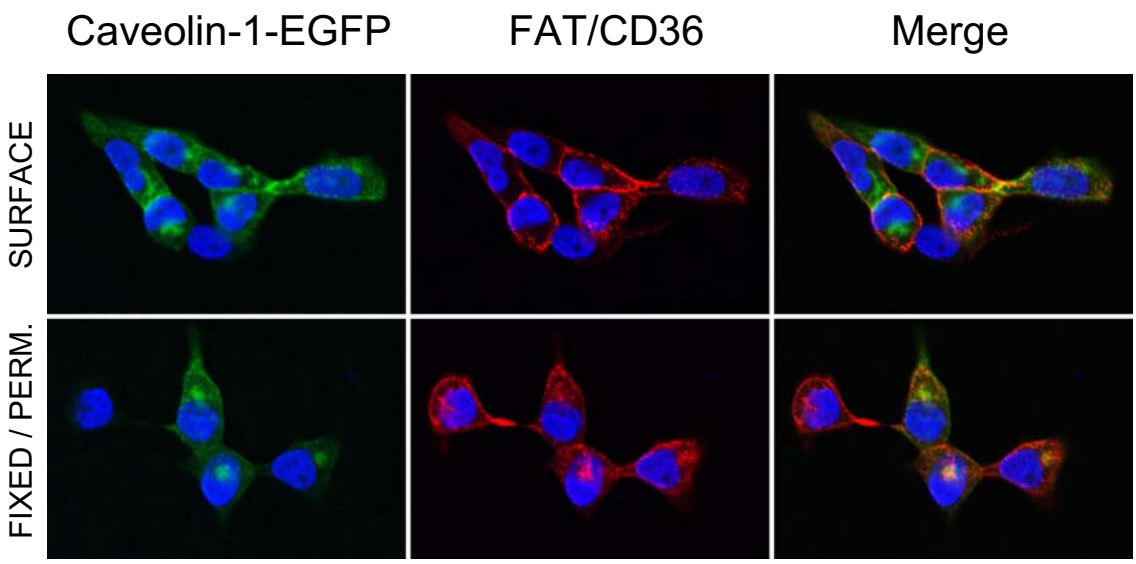

Figure 3-27.

membrane. To address this question, cell-surface proteins of the viable cells were biotinylated prior to preparation of the DRMs, thus allowing subsequent assessment of surface-labelled FAT/CD36 in the detergent soluble and detergent resistant fractions by probing Western blots with HRP-streptavidin and by precipitation of biotinylated proteins from sucrose gradient fractions with streptavidin-coated beads (see 2.5.6). This technique was adapted to study DRMs independently, but similar techniques have been described recently (Sprenger et al., 2006).

Briefly, H4IIE-FAT/CD36 (1A) cells were surface-biotinylated, lysed in 1% Triton X-100 and subjected to sucrose step gradient fractionation. Analysis of the protein and sucrose contents of fractions revealed profiles similar to those of other DRM preparations from this cell type (not shown). Aliquots of each fraction were subjected to 12% SDS-PAGE and the proteins were transferred electrophoretically to PVDF membrane. Following blocking, FAT/CD36 was detected by Western analysis (Figure 3-28A, upper panel). As in other DRM preparations from H4IIE-FAT/CD36 (1A) cells (Figure 3-23 and Figure 3-25), FAT/CD36 was detected in raft fractions (fractions 2 and 3) and non-raft fractions (fractions 8-12). Antibodies were then stripped from blots, which were then probed with streptavidin-conjugated horseradish peroxidase (Figure 3-28A, lower panel). As can be seen, biotinylated surface membrane proteins reside overwhelmingly in non-raft domains of the plasma membrane. In contrast, only two species were obvious in DRM fractions (~80 kDa and ~85 kDa), one of which could be FAT/CD36.

Lipid raft fractions (fractions 2-4) and non-raft fractions (fractions 8-12) were pooled separately. Biotinylated transmembrane proteins were then precipitated from each pool using streptavidin-conjugated agarose beads (see 2.5.6). FAT/CD36 was detected easily in streptavidin-precipitates of both lipid raft and non-raft fractions (Figure 3-28B, upper panel), indicating that FAT/CD36 resides in both raft and non-raft domains of the plasma membrane in these H4IIE transfectants. FAT/CD36 was also detectable in the wash fractions from both raft and non-raft streptavidin precipitations (Figure 3-28B, upper panel). It was unclear, however, whether this represented non-biotinylated FAT/CD36 that was associated with *intracellular* lipid rafts (DRM wash) or non-raft membranes. To clarify this, the supernatants were subjected to another round of streptavidin precipitation and precipitates and aliquots of each post-precipitation supernatant were subjected to 12% SDS-PAGE and Western blotting with anti-FAT/CD36 mAb MO25 (Figure 3-28C). As

Figure 3-28. Enrichment of FAT/CD36 in lipid raft and non-raft components of the plasma membrane. H4IIE-FAT/CD36 (1A) cells were surface-biotinylated, lysed in 1% Triton X-100 at 4°C and subjected to discontinuous 5-40% sucrose gradient centrifugation. **A;** Aliquots from each fraction were subjected to SDS-PAGE and immunoblotting with anti-FAT/CD36, using mAb MO25 (upper panel). Immunoblots were then stripped and re-probed with streptavidin-HRP (lower panel). **B;** Fractions 2-4 were pooled (DRM fraction), as were fractions 8-12 (non-raft fraction) and biotinylated plasma membrane (PM) proteins were precipitated from each. Precipitates and 20 µl from the un-precipitated washings were subjected to SDS-PAGE and immunoblotting with anti-FAT/CD36 (upper panel). Membranes were then stripped and re-probed with streptavidin-HRP (lower panel). **C;** Post-precipitation supernatants were subjected to a second round of precipitation of biotinylated proteins using streptavidin-conjugated agarose beads. Precipitates and 20µl of the un-precipitated washings were subjected to SDS-PAGE and Western blotting with anti-FAT/CD36.

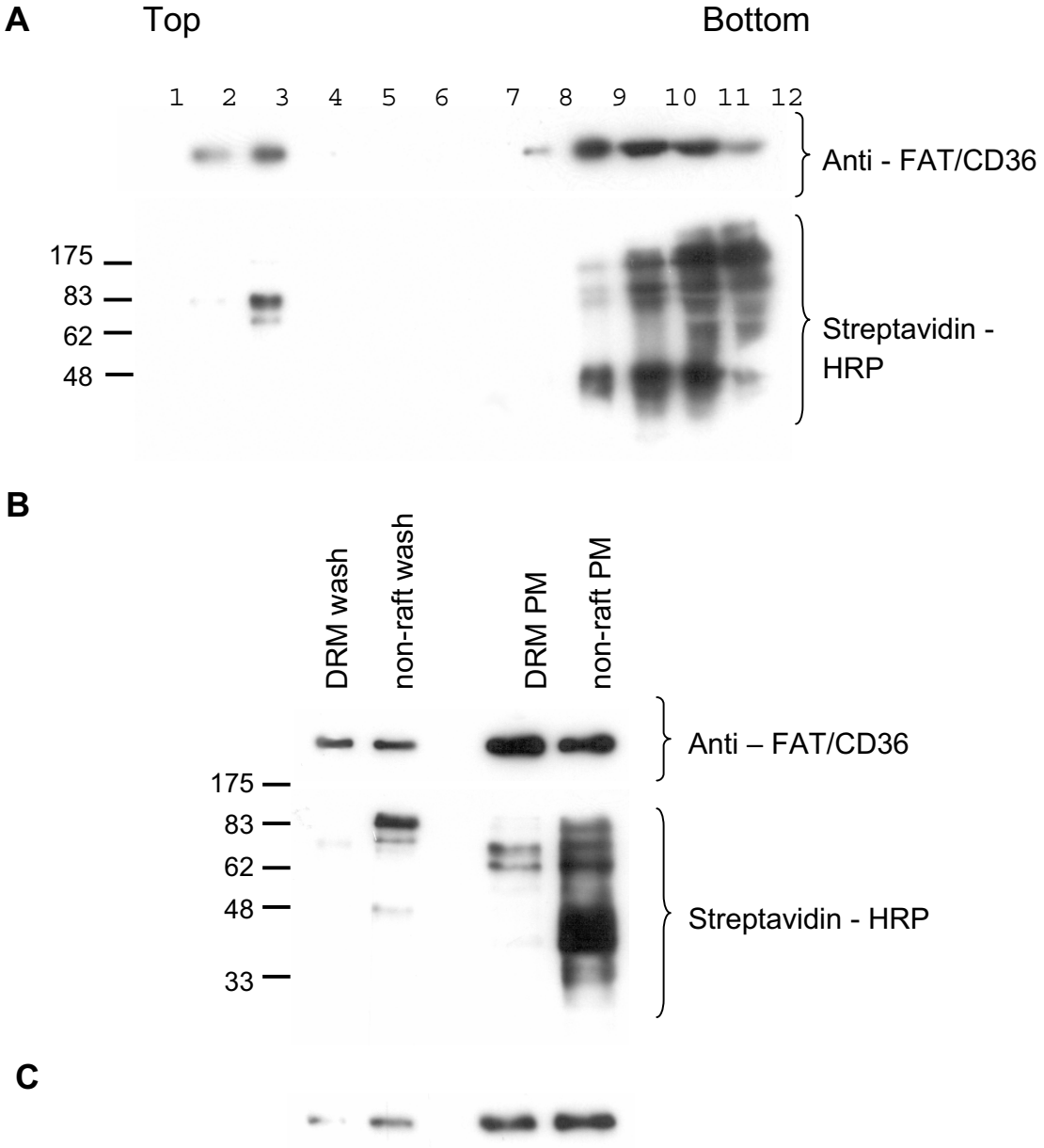
A
Top
Bottom
1 2 3 4 5 6 7 8 9 10 11 12
Anti - FAT/CD36
175
83
62
48
Streptavidin - HRP
B
DRM wash
non-raft wash
DRM PM
non-raft PM
Anti – FAT/CD36
175
83
62
48
33
Streptavidin - HRP
C

Figure 3-28.

can be seen, further biotinylated plasma membrane FAT/CD36 was precipitated from original supernatants, indicating that excess biotinylated proteins had remained after the first round of precipitation. However, FAT/CD36 was still detectable in the post-precipitation supernatants, suggesting that some FAT/CD36 is associated with both raft and non-raft intracellular membranes. This interpretation is consistent with the observation that some cytoplasmic FAT/CD36 does not co-localise with the raft marker GM_1 (see 3.4.4.4).

To further analyse lipid raft and non-raft domains of the H4IIE plasma membrane, blots used for detection of raft- and non-raft-associated plasma membrane FAT/CD36 (Figure 3-28B, upper panel) were stripped of antibodies and re-probed with streptavidin-HRP (Figure 3-28B, lower panel) to detect all surface-labelled proteins. Relatively few biotinylated plasma membrane proteins (~10) were detected in these DRMs. Of these, the major band at ~85 kDa was expected to represent FAT/CD36, given the ease of its detection in these samples by Western blot. If this is the case, FAT/CD36 may represent the major raft-associated transmembrane protein species in these cells. Unfortunately, attempts to resolve this matter by immuno-precipitation from DRMs with mAb UA009, followed by Western analysis with HRP-streptavidin, were not successful.

3.4.5 Subcellular localization of FAT/CD36 in transfected CHO cells

As discussed previously (see 3.3.3), the CHO 1.2C3 cell line was established for carrying out studies in which correlations will be sought between levels of FAT/CD36 expression and functional activity of the receptor. Previous studies in transfected CHO cells have indicated that FAT/CD36 may reside in lipid rafts that are distinct from caveolae (Zeng et al., 2003). It was important to re-investigate this observation before using the cells in functional studies and to compare the FAT/CD36-expressing CHO 1.2C3 cells with the other cell-types investigated above.

3.4.5.1 Biochemical analysis of FAT/CD36 localization in CHO 1.2C3 cells

CHO 1.2C3 cells were subjected to lysis in 1% Triton X-100 at 4°C and sucrose step gradient fractionation as described previously (see 2.5.2). The protein and sucrose content of fractions (Figure3-29A) revealed a similar pattern to those described above for liver, COS-7 cells and H4IIE cells. Aliquots of each fraction were subjected to 12% SDS-PAGE

Figure 3-29. Western blot analysis of FAT/CD36 and caveolin-1 in detergent-resistant mebrane (DRM) preparations from the CHO 1.2C3 cell line. After lysis in 1% Triton X-100 at 4°C, samples were subjected to discontinuous 5-40% sucrose gradient centrifugation. Fractions were collected from the tops of the gradients. **A**; the protein and sucrose contents of each fraction (squares and triangles, respectively). **B**; aliquots of each fraction were subjected to 12% SDS-PAGE and Western blotting using anti-FAT/CD36 mAb MO25 or anti-caveolin-1 mAb, as indicated.

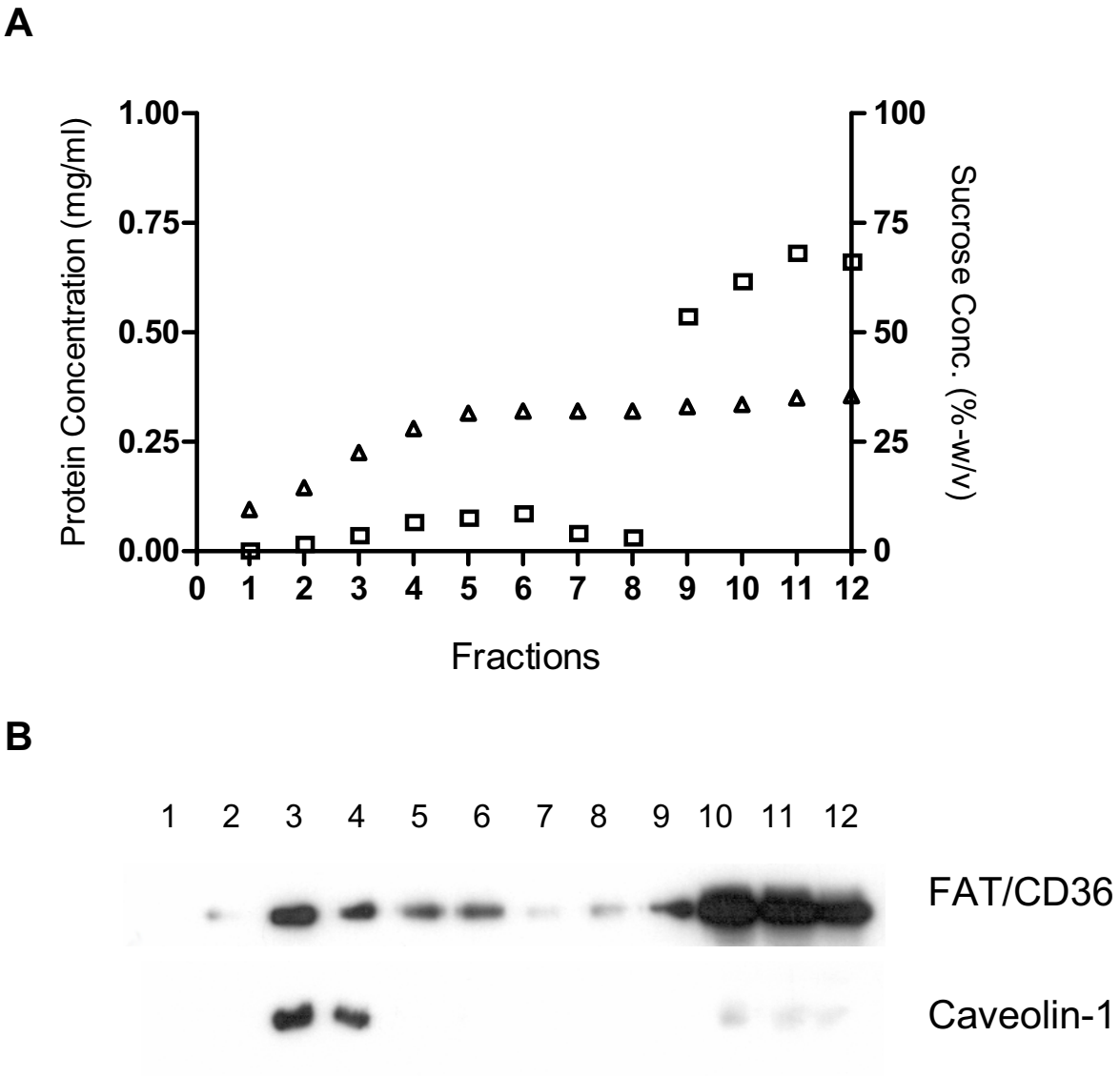
A
Protein Concentration (mg/ml)
1.00
0.75
0.50
0.25
0.00
100
75
50
25
0
Sucrose Conc. (%-w/v)
0 1 2 3 4 5 6 7 8 9 10 11 12
Fractions
B
1 2 3 4 5 6 7 8 9 10 11 12
FAT/CD36
Caveolin-1

Figure 3-29.

and immunoblotting with mAb MO25 (Figure 3-29B). FAT/CD36 was present in DRM fractions (fractions 2-4), while Western blotting shows that caveolin-1 localizes predominantly to DRM fractions (Figure 3-29B). These findings point to differences in the partitioning of FAT/CD36 and caveolin-1 between membrane compartments in different cell lines and also in liver. With respect to FAT/CD36, CHO 1.2C3 cells are similar to H4IIE-FAT/CD36 (1A) cells (Figure 3-25) and normal female rat liver (Figure 3-18), where the detergent-soluble fractions contain a considerable amount of the molecule. In contrast, little FAT/CD36 was found in the detergent-soluble fractions of COS-7-FAT/CD36 cells (Figure 3-20). With respect to caveolin-1, CHO 1.2C3 cells are different from H4IIE-FAT/CD36 (1A) cells and liver, and to a lesser extent from COS-7-FAT/CD36 cells, in having very little caveolin-1 associated with the detergent-soluble fractions. It appears, therefore, that CHO 1.2C3 cells contain very little caveolin-1 that is not associated with DRMs, while varying amounts of the molecule are associated with non-lipid raft membranes or the cytosol in some other cell types.

3.4.5.2 Subcellular localization of FAT/CD36 in CHO 1.2C3 cells, determined by confocal fluorescence microscopy

The localization of FAT/CD36 was assessed in CHO 1.2C3 cells, with reference to GM_1-staining with Alexa-594-conjugated CT-B. As in the case of FAT/CD36 transfected COS-7 and H4IIE cells, plasma membrane labelling of FAT/CD36 overlapped closely with that of GM_1 (Figure 3-30).

When transient transfection was used to express caveolin-1-EGFP in CHO 1.2C3 cells, the transfected cells exhibited the characteristic pattern of caveolin-1-EGFP fluorescence (punctate plasma membrane staining and intense staining of Golgi-like perinuclear organelles). There was partial overlap of caveolin-1-EGFP fluorescence and the punctate staining of FAT/CD36 in the plasma membrane (Figure 3-31, upper panels). When the cells were fixed and permeabilized prior to immunofluorescence labelling of FAT/CD36, there was little overlap between the intracellular fluorescence signals from caveolin-1-EGFP and FAT/CD36 (Figure 3-31, lower panels). These findings, together with the biochemical analysis, suggest that while both intracellular and plasma membrane caveolin-1 is associated with DRMs in CHO 1.2C3 cells, it is only at the plasma membrane that FAT/CD36 is likely to be associated with caveolin-1-associated DRMs in these cells.

Figure 3-30. Co-localization of FAT/CD36 and lipid rafts by confocal fluorescence microscopic analysis of the CHO 1.2C3 cell line. Cells were grown on coverslips and incubated at 37°C with an Alexa Fluor 594 cholera toxin subunit B (CT-B) conjugate (red) to allow binding and uptake. Cells were fixed and labelled to detect FAT/CD36 using anti-FAT/CD36 (mAb UA009) and a FITC-conjugated secondary antibody (green). Yellow in the merged images indicates co-localization of FAT/CD36 and CT-B. ×63 objective plus ×3 zoom.

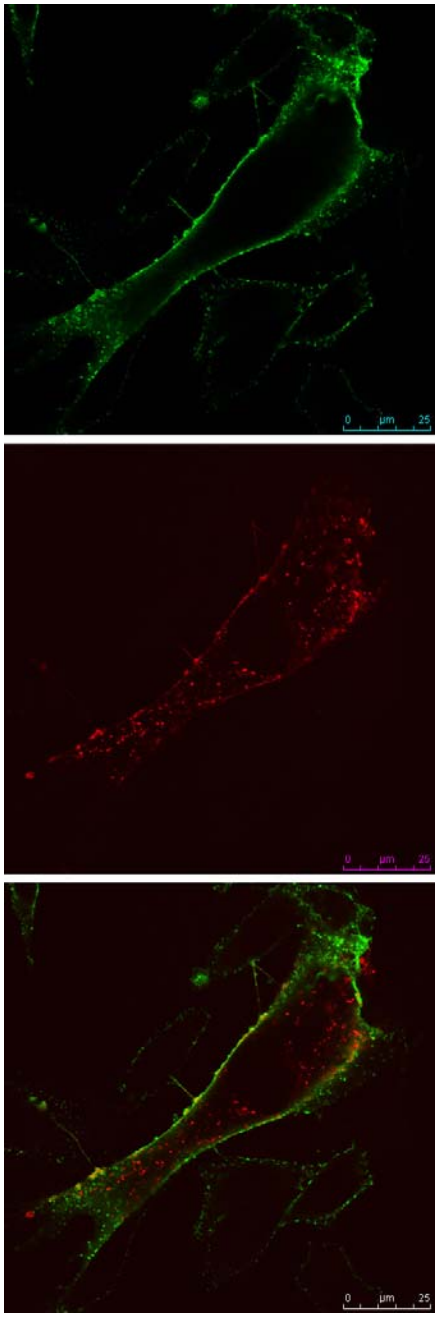

Figure 3-30.

Figure 3-31. Localization of FAT/CD36 and caveolin-1-EGFP in CHO 1.2C3 cells transiently transfected with pCaveolin-1-EGFP. Cells were grown on coverslips, transfected and either fixed (upper panels) or fixed and permeabilized (lower panels) before staining by indirect immunofluorescence, using anti-FAT/CD36 (mAb UA009) and Cy3-conjugated anti-mouse antibody (red). ×63 objective plus ×2 zoom.

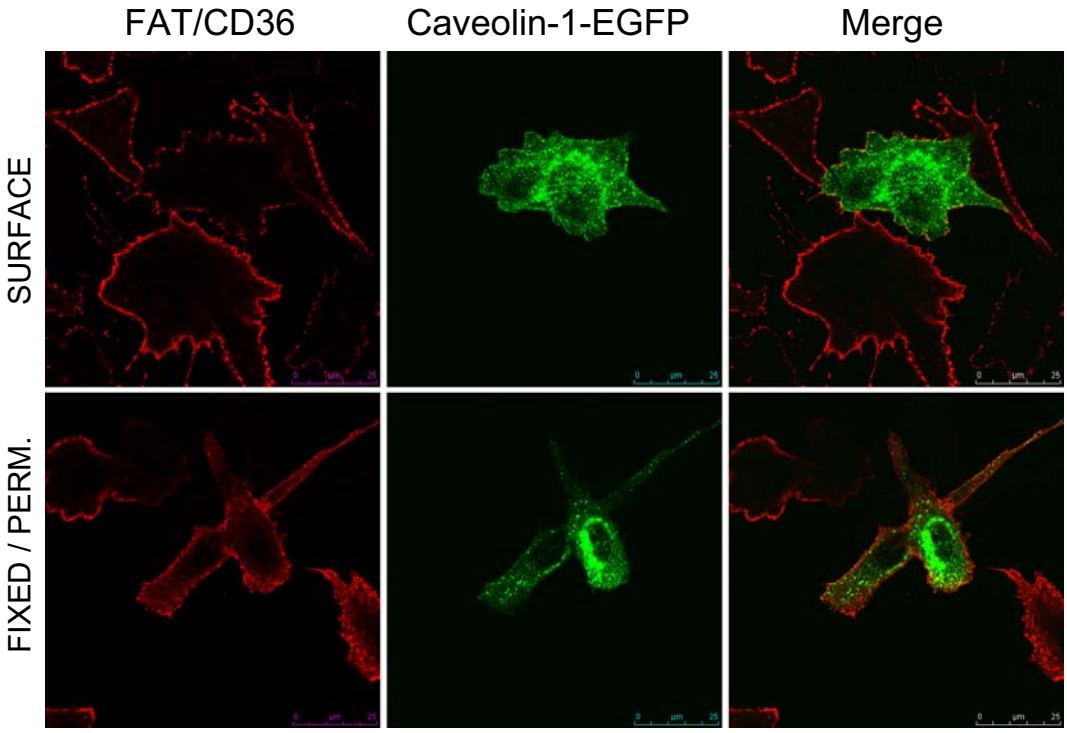

Figure 3-31.

3.5 Effects of FAT/CD36 on long-chain fatty acid uptake in transfected cell lines

3.5.1 Long-chain fatty acid uptake and metabolism by FAT/CD36-transfected H4IIE and COS-7 cell lines

Although some of the first reports of a saturable, protein-dependent component of long-chain fatty acid (LCFA) uptake were conducted in rat hepatocytes (Stremmel et al., 1985, Stremmel et al., 1986), the majority of research into protein-dependent LCFA uptake has focussed on heart and skeletal muscle and adipose tissue (reviewed in Bonen et al., 2002, Abumrad et al., 1999). Recent studies, however, have renewed interest in the mechanism(s) of hepatocellular LCFA uptake (Pohl et al., 2002, Rajaraman et al., 2005, Guo et al., 2006). In particular, recent demonstration of defective hepatic LCFA uptake in FATP5-knockout mice has highlighted the importance of protein-dependent mechanisms of LCFA import in the liver (Doege et al., 2006). However, there is debate about whether passive diffusion (Guo et al., 2006) or receptor-mediated transport (Rajaraman et al., 2005)is the major mechanism of LCFA uptake by hepatocytes. Nevertheless, it is apparent that the liver is a major destination of albumin-adsorbed LCFAs (Noy et al., 1986, Coburn et al., 2000), and for this reason the mechanism(s) of hepatocellular LCFA uptake warrants further investigation.

In this study, H4IIE rat hepatoma cells have been used as an *in vitro* model of LCFA uptake by hepatocytes. Moreover, over-expression of FAT/CD36 has been used to assess the contribution of the molecule to LCFA uptake and incorporation into cellular lipids by these cells, again as a model for normal hepatocytes. Finally, the impact of lipid raft function and caveolae on FAT/CD36-dependent and FAT/CD36-independent pathways of LCFA has been assessed using these cells and also in transfected cells of the non-hepatocyte-derived COS-7 and CHO cell lines.

3.5.1.1 Impact of FAT/CD36 over-expression on LCFA uptake by H4IIE cells

To investigate whether FAT/CD36 expression enhances LCFA uptake, H4IIE (5A) and H4IIE-FAT/CD36 (1A) cell lines (see 3.3.2) were cultured at 37°C in the presence of a solution containing [^{14}C]-oleic acid (trace amounts), non-radioactive oleic acid (173 μM) and fatty acid-free BSA (173 μM) in PBS (1:1, mol / mol) (see 2.6.4). At the times indicated, the uptake solution was aspirated from quadruplicate wells and after washing,

cell-associated radioactivity was assessed in NaOH cell lysates. Binding and uptake of oleate was standardized to the protein content of each sample (Figure 3-32). Cellular oleate uptake was significantly higher in cells expressing FAT/CD36 (H4IIE-FAT/CD36 (1A) cells), compared with the non-expressing H4IIE (5A) cells. Over this time-course, uptake of [^{14}C]-oleic acid uptake was essentially linear in both cell lines. The concentrations of oleic acid and BSA and the ratio of fatty acid to albumin used in these experiments were within accepted physiological ranges (Coburn et al., 2000). These results were typical of several similar experiments and they indicate that FAT/CD36 contributes to LCFA by hepatoma cells and that it may have a similar function in hepatocytes *in vivo*.

3.5.1.2 The impact of FAT/CD36 expression on metabolism of oleic acid by transfected H4IIE cells

Previous studies have demonstrated that over-expression of FAT/CD36 in muscle results in increased oxidation of LCFAs (Ibrahimi et al., 1999, Bastie et al., 2004, Garcia-Martinez et al., 2005) and can result also in increased incorporation of LCFAs into triglycerides (Bastie et al., 2004, Garcia-Martinez et al., 2005). It was hypothesized, therefore, that FAT/CD36 expression in H4IIE cells would alter the incorporation of [^{14}C]-oleate into cellular lipids. To investigate this hypothesis, incorporation of [^{14}C]-oleate into cellular lipids (polar lipids, diglycerides, triglycerides, free fatty acids and cholesteryl ester) of H4IIE (5A) and H4IIE-FAT/CD36 (1A) cells was determined by thin-layer chromatography (see 2.6.5). The results indicate that oleate is incorporated primarily into polar lipids (phospholipids, phosphatidic acid, monoacylglycerol 3-phosphate) and di- and tri-acylglycerides in these cells (polar lipids > triglycerides > diglycerides > free fatty acids) (Figure 3-33). These findings are consistent with other studies of LCFA metabolism by hepatic cell lines (Prip-Buus et al., 1992). Importantly, expression of FAT/CD36 in H4IIE cells resulted in significantly increased incorporation of [^{14}C]-oleate into diacylglycerol but significantly decreased incorporation into triacylglycerol. Incorporation of [^{14}C]-oleate into polar lipids, however, was not significantly altered by FAT/CD36 expression. Although fatty acid oxidation was not investigated as an end-point of cellular LCFA uptake, oxidation was not predicted to be a major metabolic destination of LCFA in these cells. Studies by others have indicated that LCFA oxidation is defective in H4IIE cells (and other hepatocyte cell lines) compared with primary rat hepatocytes. This is most likely the result of high malonyl-CoA concentrations and heightened sensitivity of carnitine palmitoyltransferase I (CPT I) to malonyl-CoA inhibition (Prip-Buus et al.,

Figure 3-32. Uptake of [^{14}C]-oleate acid H4IIE (5A) and H4IIE-FAT/CD36 (1A) cell lines (squares and triangles, respectively). Cells were incubated with [^{14}C]-oleate solution (173 μM) plus equimolar BSA for the times indicated. Fatty acid uptake was stopped by replacement of the radioactive oleate solution with ice-cold PBS containing 0.5% BSA and 200 μM phloretin. Cell monolayers were then washed and processed for measurement of radioactivity and protein content. Values are means ± SD for four replicates at each time-point. *, $p < 0.05$; **, $p < 0.005$; ***, $p < 0.001$ indicate significant differences in uptake compared to control cells. Results are typical of three replicate experiments.

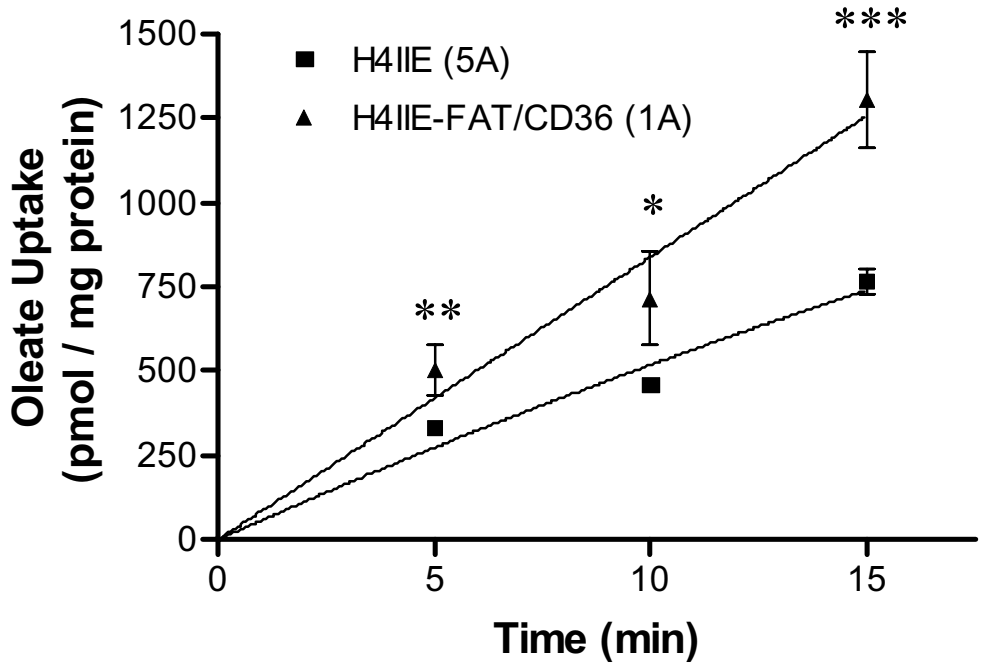
1500
1250
1000
750
500
250
0
Oleate Uptake
(pmol / mg protein)
H4IIE (5A)
H4IIE-FAT/CD36 (1A)
**
*
***
0
5
10
15
Time (min)

Figure 3-32.

Figure 3-33. Incorporation of [^{14}C]-oleate acid into complex cellular lipids in H4IIE (5A) and H4IIE-FAT/CD36 (1A) cell lines. Cells were incubated with [^{14}C]-oleate solution (173 μM) plus equimolar BSA for 15 minutes. Fatty acid uptake was stopped by replacement of the radioactive oleate solution with ice-cold PBS containing 0.5% BSA and 200 μM phloretin. Cell monolayers were then washed and lipids were extracted and separated using thin-layer chromatography (TLC). Radioactivity associated with free fatty acids (FFA), polar lipids (phospholipids, monacylglycerol 3-phosphate, phosphatidic acid), diacyglycerol (DAG) and triacylglycerol (TAG) was quantified. Data are means ± SD from a representative experiment performed in quadriplicate and are expressed as pmol oleic acid incorporated, mg protein^{-1}, 15 mins^{-1}. ***, $P < 0.0001$.

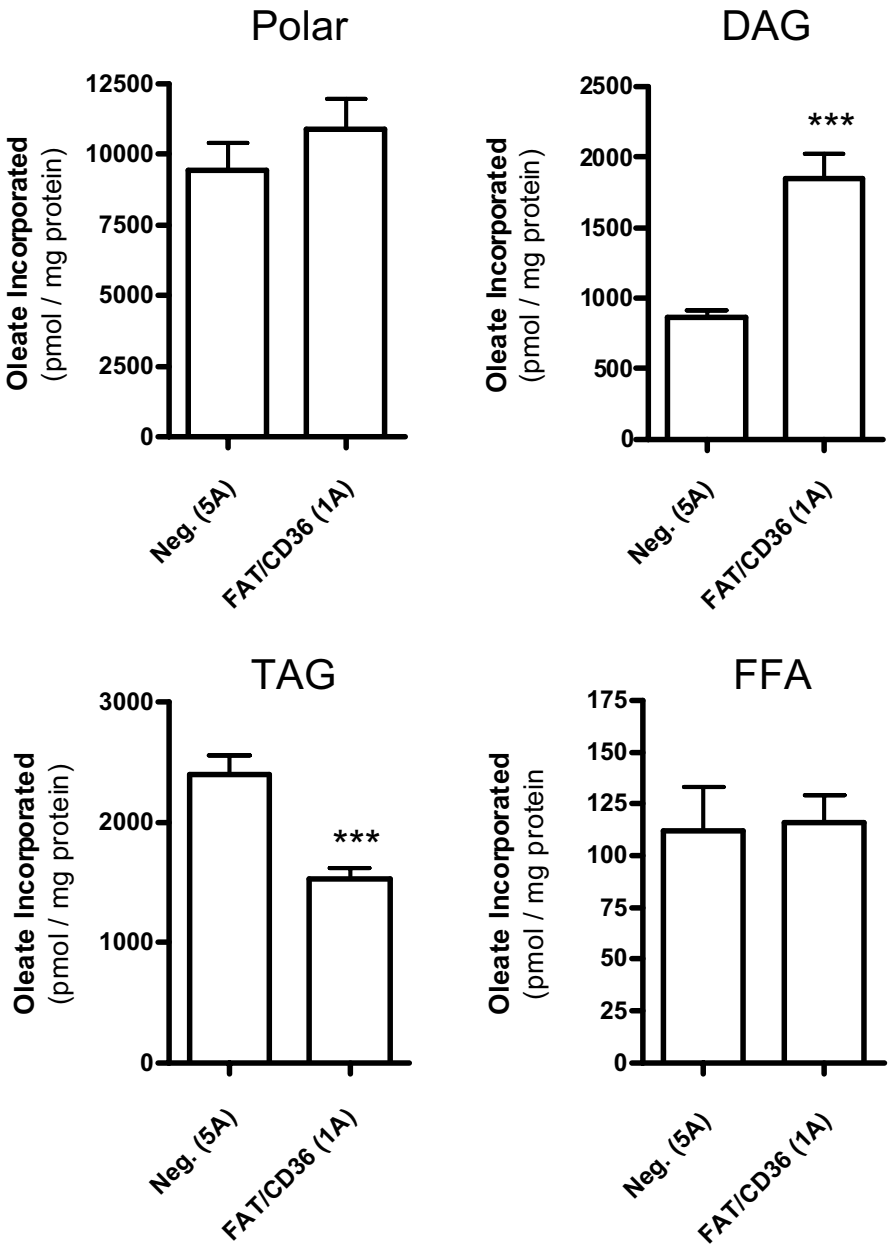
Polar
DAG
TAG
FFA
Oleate Incorporated
(pmol / mg protein)
12500
10000
7500
5000
2500
0
2500
2000
1500
1000
500
3000
175
150
125
100
75
50
25
***
Neg. (5A)
FAT/CD36 (1A)

Figure 3-33.

1992). The potential significance of these findings is discussed in more detail in later sections.

3.5.1.3 The effect of FAT/CD36 expression on neutral lipid accumulation in COS-7 cells

A chance observation in COS-7-FAT/CD36 cells provided an indication that in the longer term, expression of FAT/CD36 can alter the utilization and storage of LCFAs. Examination of FAT/CD36-transfected and empty vector-transfected COS-7 cells by light microscopy indicated that expression of FAT/CD36 was associated with an increase in the presence of cytoplasmic vacuoles that appeared similar to lipid droplets observed in adipocytes. To investigate this, COS-7-pcDNA3 and COS-7-FAT/CD36 cell lines were grown on coverslips and stained with the neutral lipid stain, Oil red O (see 2.6.6). As shown in Figure 3-34, COS-7-FAT/CD36 cells are stained more intensely than the control COS-7-pcDNA3 cells and some have distinct Oil red O-stained cytoplasmic vacuoles, indicating that COS-7-FAT/CD36 cells accumulate more neutral lipid than the FAT/CD36-negative controls. This observation suggests that cells that express FAT/CD36 can undergo changes that suggest storage of excess LCFA in the form of neutral lipid, most likely triglyceride.

Recent studies by Lee *et. al.* have shown that the complexity (granularity) of 3T3-L1 cells, as determined by flow cytometry (side scatter, SSC), increases as they differentiate into adipocytes. This was due to the associated accumulation of neutral lipids in cytoplasmic lipid droplets (Lee et al., 2004). To explore whether there was a similar difference in complexity between the COS-7-pcDNA3 and COS-7-FAT/CD36 lines, the cells were labelled with biotinylated mAb UA009 and streptavidin-conjugated PE and immediately subjected to flow cytometric analysis, without fixation (Figure 3-35). Analysis of COS-7-FAT/CD36 (lower panels) revealed that the FAT/CD36-positive cells (red) in the population were larger (~ 22 %) and more complex (~ 47 %) than the FAT/CD36-negative cells (green). Furthermore, as a whole population, COS-7-FAT/CD36 cells are larger and more complex than the COS-7-pcDNA3 controls. These observations are consistent with increased storage of neutral lipids in cytoplasmic lipid droplets in the COS-7-FAT/CD36 cells.

Figure 3-34. Neutral lipid staining of COS-7-pcDNA3 and COS-7-FAT/CD36 cell lines. COS-7-pcDNA3 and COS-7-FAT/CD36 cells were seeded at equal density and grown to approximately 80% confluency before staining of neutral lipids using oil red O (ORO). Stained monolayers were visualized using ×20 (upper panels) and ×100 objectives (lower panels) and photographed.

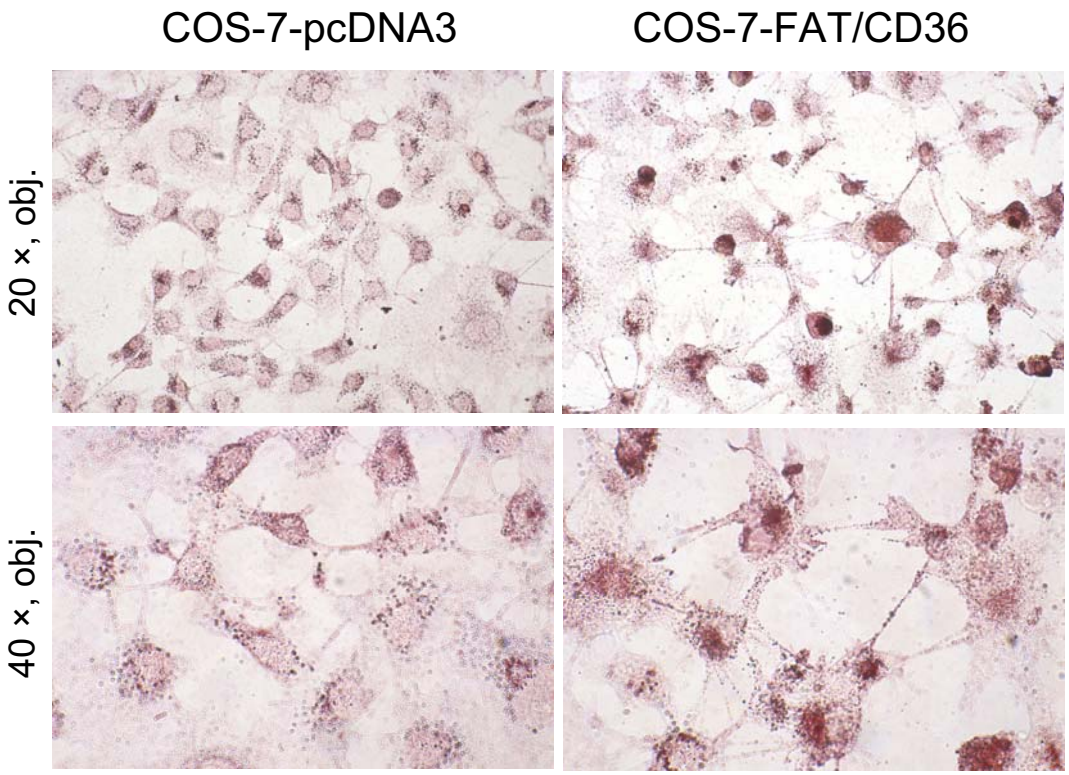

Figure 3-34.

Figure 3-35. FAT/CD36 expression in COS-7 cells increases their size and complexity. COS-7-pcDNA3 (upper panels) and COS-7-FAT/CD36 cell lines (lower panels) were labelled by indirect immunofluorescence using biotinylated mAb UA009 (anti-FAT/CD36) and streptavidin-conjugated PE and subjected to flow cytometric analysis. FAT/CD36-expressing cells (R1, red) and non-expressing cells (R2, green) were back-gated to assess their size and complexity as indicating by their forward scatter (FSC) and side scatter (SSC) properties, respectively. Results shown are representative of multiple repeat experiments.

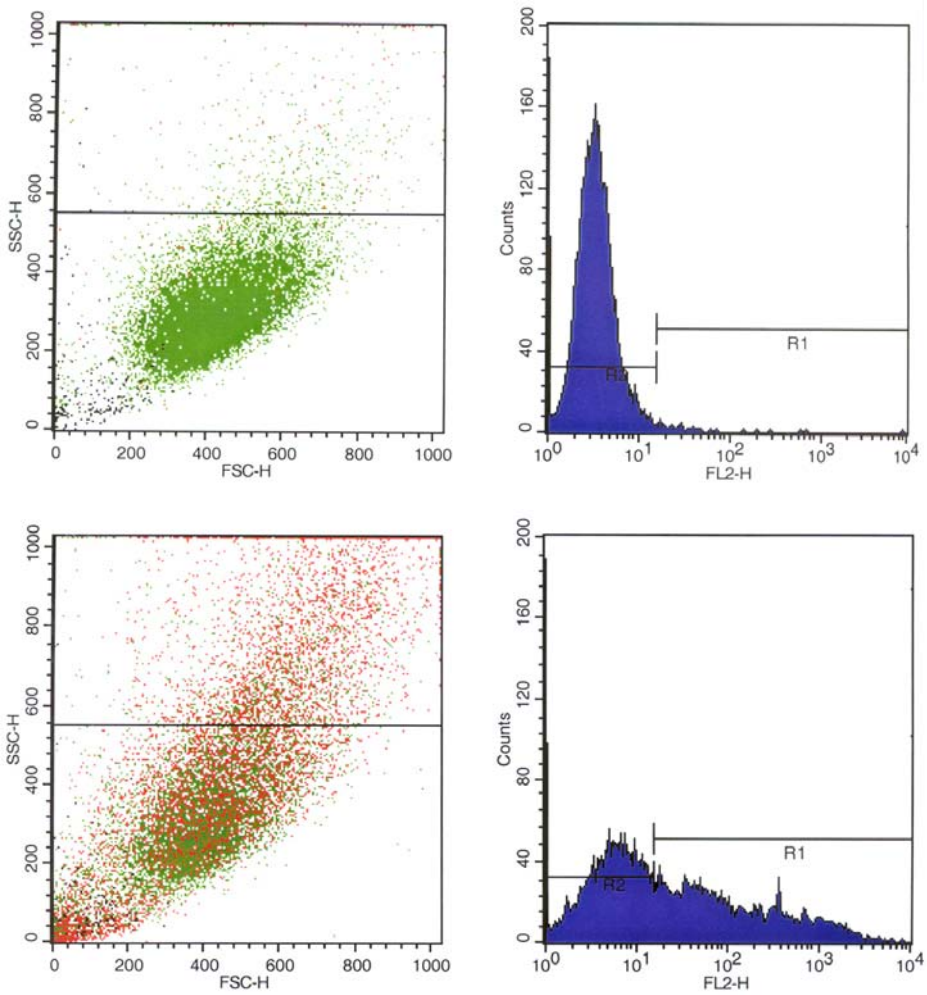

Figure 3-35.

3.5.1.4 The impact of lipid rafts on LCFA uptake by FAT/CD36-transfected COS-7 and H4IIE cell lines

To investigate whether lipid rafts contribute to FAT/CD36-dependent and/or -independent pathways of cellular LCFA uptake, the impact of lipid raft depletion on [^{14}C]-oleic acid uptake was assessed using COS-7-FAT/CD36 and H4IIE-FAT/CD36 (1A) cell lines and their respective negative control cell lines (COS-7-pcDNA3 and H4IIE (5A)). To do this each cell line was seeded in 12-well trays and after overnight culture, the cell monolayers were washed twice with PBS and returned to culture in either warm DMEM or warm DMEM supplemented with 10mM methyl-β-cyclodextrin (MβCD). After 30 minutes, assays of [^{14}C]-oleic acid uptake were performed as described elsewhere (see 2.6.4). The results indicate that depletion of lipid rafts with MβCD causes significant reduction in levels of [^{14}C]-oleic acid uptake in both H4IIE (5A) and H4IIE-FAT/CD36 (1A) cell lines (Figure 3-36B, right panels). Lipid raft depletion with MβCD also resulted in a significant reduction in uptake of [^{14}C]-oleic acid by both COS-7-pcDNA3 (control) and COS-7-FAT/CD36 cell lines (Figure 3-36A, right panels). These findings are in accordance with other reports of lipid raft-dependent components of LCFA uptake in other cell types (Pohl et al., 2002, Pohl et al., 2004, Pohl et al., 2005, Meshulam et al., 2006). Interestingly, even after lipid raft depletion, FAT/CD36-expressing cell lines maintained a heightened level of [^{14}C]-oleic acid uptake compared to their non-expressing counterparts. FAT/CD36-mediated LCFA uptake is, therefore, not exclusively dependent on lipid raft function.

MβCD depletes lipid rafts by sequestering cellular cholesterol and it can cause the total loss of morphological caveolae from adipocyte plasma membranes (Parpal et al., 2001, Pohl et al., 2004). A common use of MβCD is in examining the stability of the lipid raft association of putative raft proteins (for example see (Radeva et al., 2005), for review see (Lucero and Robbins, 2004)). However, it must be remembered that beyond its ability to deplete rafts of cholesterol, MβCD treatment may also induce cellular responses that are the result of changes in cholesterol homeostasis (Munro, 2003). Furthermore, the stable incorporation of proteins in lipid rafts can be resistant to MβCD treatment (Khan et al., 2003). To determine whether MβCD treatment had any effect on the localization of FAT/CD36 to the plasma membrane, parallel experiments were performed involving MβCD treatment of each of the cell lines (10 mM, 30 mins) and assessment of surface FAT/CD36 expression levels by flow cytometry. The results showed that MβCD treatment

Figure 3-36. Depletion of lipid rafts with methyl-β-cyclodextrin (MBCD) (10 mM, 30 mins) does not impact upon surface expression of FAT/CD36 in stably transfected (A) COS-7 and (B) H4IIE cell lines, as determined by flow cytometry (left panels). Black lines, irrelevant isotype control labelled cells; red lines, FAT/CD36 expression; blue lines, FAT/CD36 expression following MβCD treatment. While FAT/CD36 expression enhances [14-C] oleic acid uptake, lipid raft disruption with MβCD inhibits uptake in transfected (A) COS-7 and (B) H4IIE cell lines (right panels). Cells were untreated (empty bars) or treated with MβCD (thatched bars), as above, before measurement of oleic acid uptake. Data are means ± SEM for six replicates. *, $P < 0.01$ statistically significant difference compared to FAT/CD36-negative controls. #, $P < 0.01$ significantly different from non-treated controls (Student's t-tests (two-tailed)).

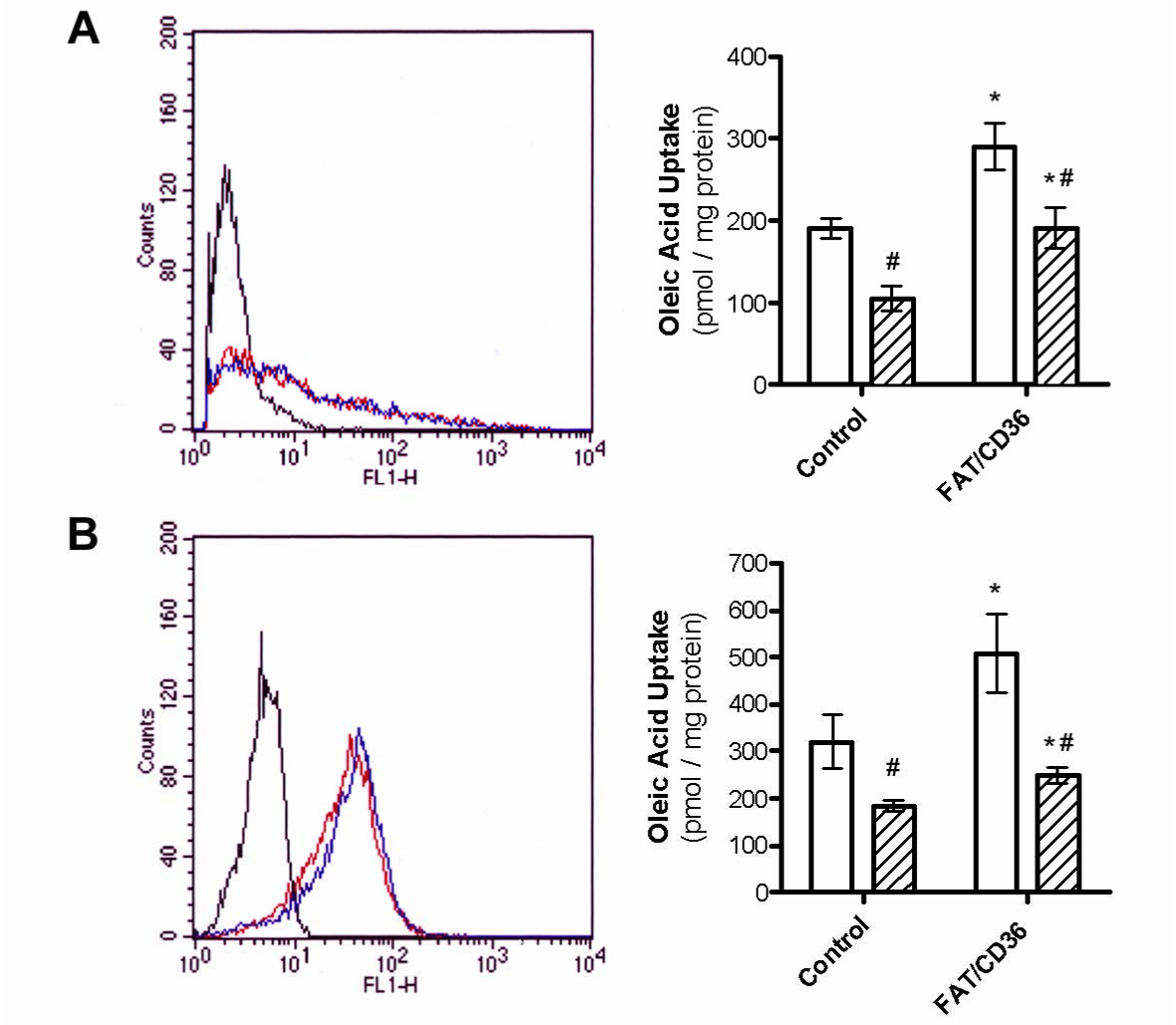
A
Counts
FL1-H
Oleic Acid Uptake
(pmol / mg protein)
Control
FAT/CD36
B
Counts
FL1-H
Oleic Acid Uptake
(pmol / mg protein)
Control
FAT/CD36

Figure 3-36.

had no effect of FAT/CD36 localization to the cell surface of FAT/CD36- and control-transfected COS-7 and H4IIE cell lines (Figure 3-36, left panels).

3.5.1.5 The impact of caveolin-1-EGFP expression on FAT/CD36-dependent and FAT/CD36-independent pathways of LCFA uptake

Disruption of lipid rafts with MβCD resulted in reduced LCFA uptake in COS-7 and H4IIE cell lines. However, it was unclear whether formation of caveolae is necessary for efficient uptake of LCFA. To investigate this, uptake of [^{14}C]-oleate was investigated in H4IIE cell lines expressing caveolin-1-EGFP and/or FAT/CD36. As detailed earlier, H4IIE cells lack endogenous caveolin-1 expression and hence lack caveolae. Accordingly, these cells make an excellent model in which to investigate the influence exogenous caveolin-1 expression and caveolae on hepatic LCFA uptake. [^{14}C]-oleate uptake was compared in the H4IIE (5A) + caveolin-1-EGFP and H4IIE (5A) cell lines over a 15 minute incubation period. The results demonstrated that the presence of caveolin-1-EGFP did not enhance cellular acquisition of oleate significantly under these conditions (Figure 3-37A).

To test whether expression of caveolin-1-EGFP and the localization of some FAT/CD36 to caveolae would enhance LCFA uptake, uptake of [^{14}C]-oleate was compared in the H4IIE-FAT/CD36 (1A) + caveolin-1-EGFP cell line (see 3.4.4.2) and the parent cell line H4IIE-FAT/CD36 (1A) over the course of 15 minutes. Co-expression of caveolin-1-EGFP and FAT/CD36 did not influence [^{14}C]-oleate uptake significantly (Figure 3-37B).

3.5.2 The influence of the level of FAT/CD36 expression on long-chain fatty acid uptake and metabolism by the CHO 1.2C3 cell line

3.5.2.1 The impact of modulation FAT/CD36 expression on oleic acid uptake by the CHO 1.2C3 cell line

Because expression of FAT/CD36 results in enhanced cellular LCFA uptake by transfected COS-7 and H4IIE cell lines (see above), it was hypothesized that uptake of [^{14}C]-oleate would correlate with the level of FAT/CD36 expression. To investigate this, CHO 1.2C3 cells (see 3.3.3.5) were cultured for 120 hours in the presence of doxycycline at various concentrations (0, 0.01, 0.1, 100 ng/ml). These concentrations of doxycycline, which are

Figure 3-37. The effect of caveolin-1 expression on cellular oleate uptake by transfected H4IIE cell lines. **A;** Comparison of [^{14}C]-oleate uptake by H4IIE (5A) and H4IIE (5A) + caveolin-1-EGFP cell lines (squares and triangles, respectively). **B;** Comparison of [^{14}C]-oleate uptake by H4IIE-FAT/CD36 (1A) and H4IIE-FAT/CD36 (1A) + caveolin-1-EGFP cell lines (triangles and squares, respectively). Cells were incubated with [^{14}C]-oleate solution (173 μM) plus equimolar BSA for the times indicated. Fatty acid uptake was stopped by replacement of the radioactive oleate solution with ice-cold PBS containing 0.5% BSA and 200 μM phloretin. Cell monolayers were then washed and processed for measurement of radioactivity and protein content. Values are means ± SD for four replicates at each time-point. *, $P < 0.05$, significantly different from control cells (H4IIE (5A)).

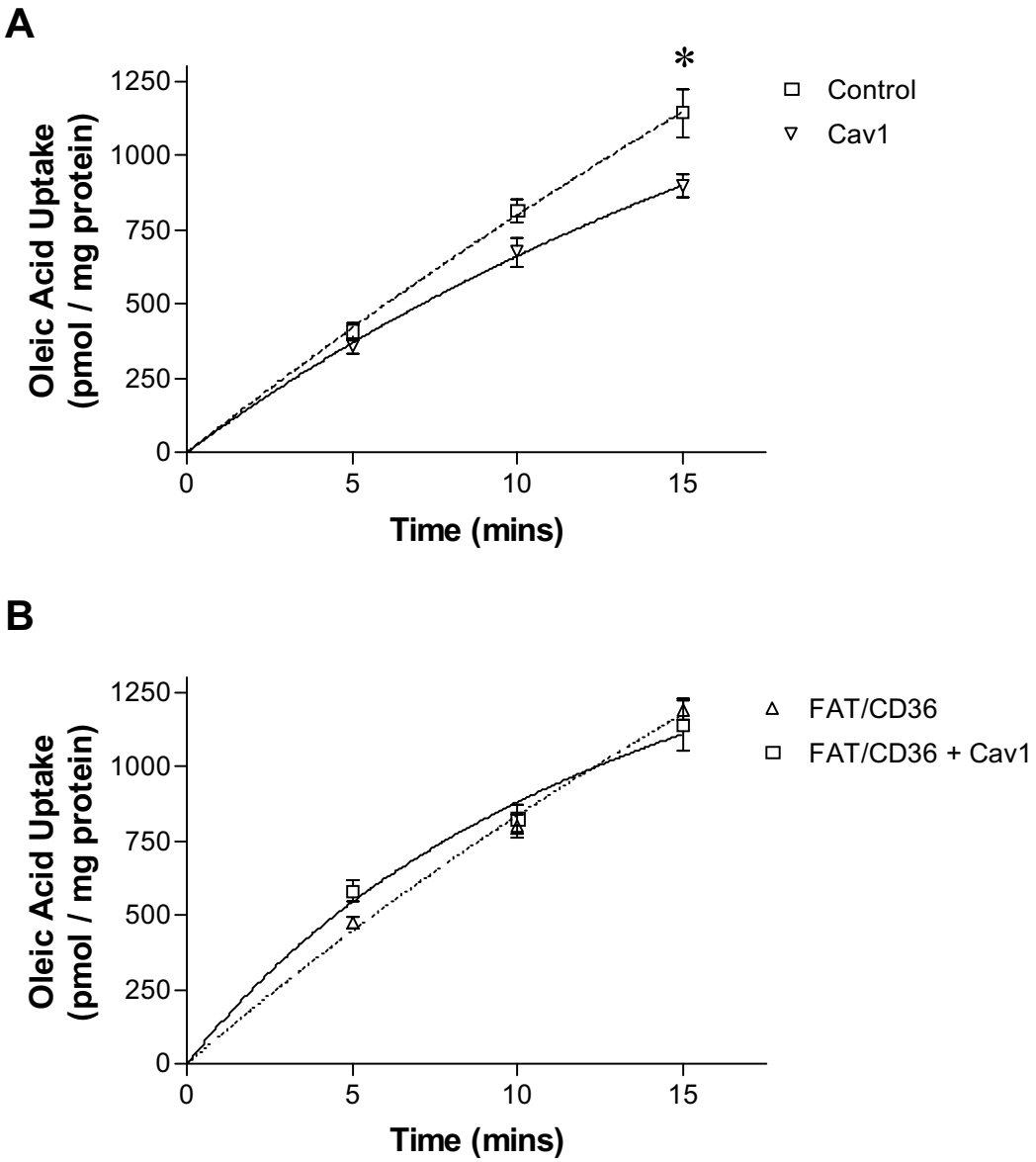
A
Oleic Acid Uptake
(pmol / mg protein)
1250
1000
750
500
250
0
0
5
10
15
Time (mins)
*
Control
Cav1
B
Oleic Acid Uptake
(pmol / mg protein)
1250
1000
750
500
250
0
0
5
10
15
Time (mins)
FAT/CD36
FAT/CD36 + Cav1

Figure 3-37.

below the fully suppressive dose, have been shown to result in a broad range of FAT/CD36 expression levels after 120 hours of culture (see 3.3.3.5). After this period, cells were seeded in 12-well cell culture trays and cultured overnight prior to measurement of uptake of [^{14}C]-oleate (Figure 3-38A). Expression of FAT/CD36 was assessed in parallel cultures by flow cytometry (surface expression) and Western blotting (total protein) (Figure 3-38A and 4-38B, respectively). Controls for these experiments included CHO-Tet-Off 1.2 cells (parent cell line, see 3.3.3.2) or CHO 1.2C4 cells (see 3.3.3.4). Correlation between levels of cell-surface FAT/CD36 and [^{14}C]-oleate uptake at 5 minutes was assessed by Spearman analysis (Figure 3-38A).

No significant correlation was detected between the level of FAT/CD36 expression and cellular [^{14}C]-oleate uptake at 5 minutes ($P > 0.05$, $R = 0.09$), despite an approximately 3-fold greater level of FAT/CD36 expression at the surface of CHO 1.2C3 cells cultured in the absence of doxycycline compared with those cultured in the presence of doxycycline (100 ng/ml). The difference in total FAT/CD36 between un-repressed and completely repressed cells (Western analysis) was even greater (at least 30 fold). Not surprisingly, there was no significant correlation between [^{14}C]-oleate uptake and total FAT/CD36 protein levels ($P > 0.05$, $R = 0.35$). Possible explanations for this lack of effect of FAT/CD36 in LCFA transport in CHO cells are discussed in greater detail in later sections.

3.5.2.2 The impact of the level of FAT/CD36 expression on oleic acid metabolism by the CHO 1.2C3 cell line

Previous studies have indicated that over-expression of FAT/CD36 in myocytes/myotubes results in increased oxidation and/or storage of LCFAs (as triglyceride) and that these changes are also dependent on the nature of the LCFA (saturated or unsaturated) acquired by the cell (Bastie et al., 2004, Garcia-Martinez et al., 2005, Gaster et al., 2005). Although uptake of [^{14}C]-oleate by CHO 1.2C3 cells was not significantly influenced by FAT/CD36 expression, it was hypothesized that FAT/CD36 expression by these cells might influence the intracellular fate of LCFAs. To investigate this hypothesis, CHO 1.2C3 cells and the control cell line CHO 1.2C4 were cultured in the presence of a range of doxycycline concentrations as described above. After 120 hours of culture, cells were re-seeded in 12-well trays and allowed to adhere. After incubation with [^{14}C]-oleate for 5 minutes, incorporation of radioactivity into different cellular lipids was measured by thin-layer chromatography followed by scintillation counting of the separated lipid bands (see 2.6.5).

Figure 3-38. FAT/CD36 expression levels do not correlate with cellular [^{14}C]-oleate uptake in CHO 1.2C3 cells. CHO 1.2C3 cells or CHO 1.2C4 cells (FAT/CD36-negative) were cultured for 120 hours in the presence of doxycycline at various concentrations (0, 0.01, 0.1 or 100 ng/ml) before re-seeding and incubation with [^{14}C]-oleate solution (173 μM plus equimolar BSA) for 5 minutes. Cell monolayers were then washed and processed for measurement of radioactivity and protein content. In parallel, cell-surface FAT/CD36 expression was assessed by indirect immunofluorescent labelling and flow cytometric analysis. **A;** The relationship between (cell-surface) FAT/CD36 expression and [^{14}C]-oleate uptake. Data are means ± SEM (n=4). Correlation was measured by Spearman analysis. $r = 0.09$, $P > 0.05$, no significant correlation. Results are representative of repeat experiments. **B;** Expression of FAT/CD36 in parallel cultures as determined by Western blotting. 20μg of protein from each lysate was subjected to SDS-PAGE and Western blotting using anti-FAT/CD36 and anti-β-actin antibodies (inset). FAT/CD36-associated signals were standardized to those associated with β-actin and expressed as arbitrary units.

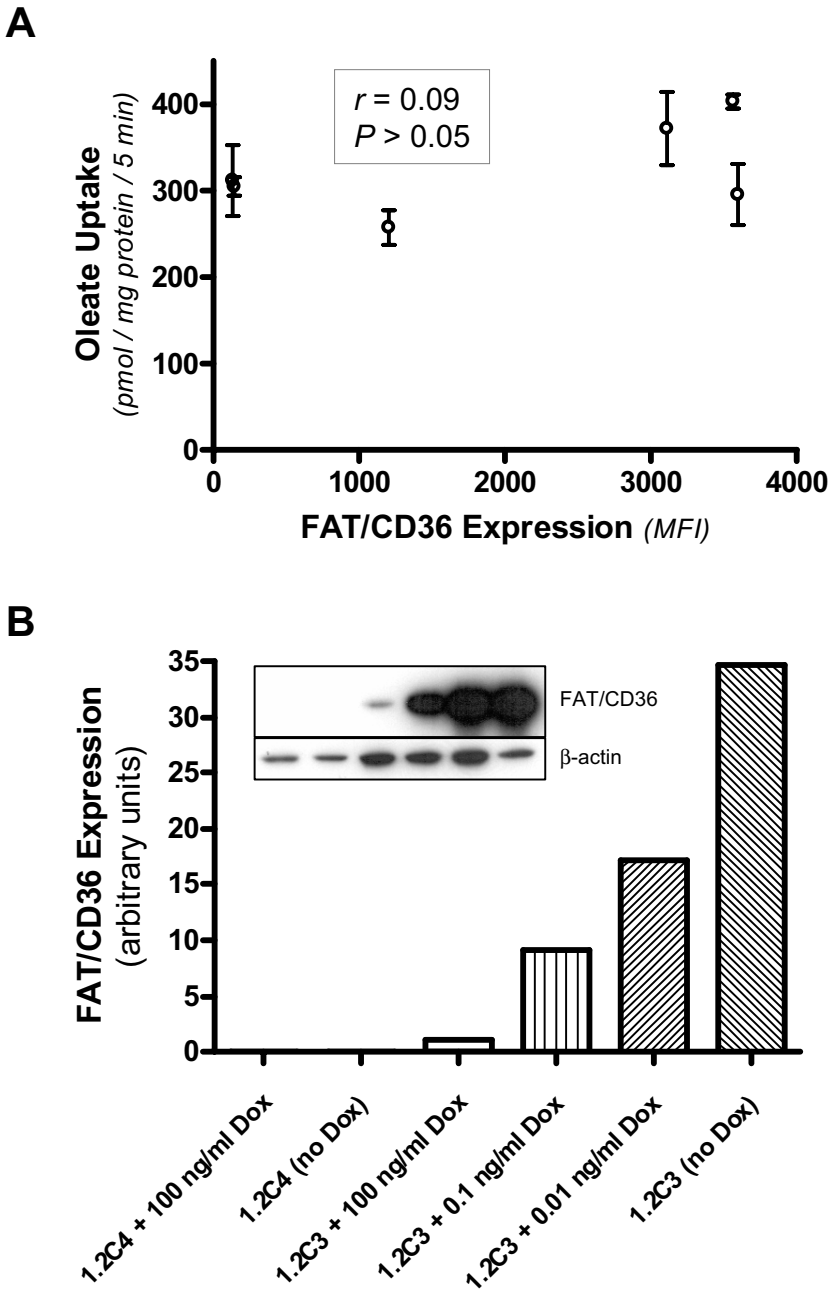
A
r = 0.09
P > 0.05
Oleate Uptake
(pmol / mg protein / 5 min)
400
300
200
100
0
0
1000
2000
3000
4000
FAT/CD36 Expression (MFI)
B
FAT/CD36 Expression
(arbitrary units)
35
30
25
20
15
10
5
0
FAT/CD36
β-actin
1.2C4 + 100 ng/ml Dox
1.2C4 (no Dox)
1.2C3 + 100 ng/ml Dox
1.2C3 + 0.1 ng/ml Dox
1.2C3 + 0.01 ng/ml Dox
1.2C3 (no Dox)

Figure 3-38.

FAT/CD36 expression at the cell-surface of parallel cultures was assessed by flow cytometry and the incorporation of [^{14}C]-oleate into each class of cellular lipid measured was expressed relative to FAT/CD36 expression levels (Figure 3-39). In CHO 1.2C3 and CHO 1.2C4 cells, oleic acid distributes to polar lipids (~ 45%), diglycerides (~ 20%), triglycerides (~ 15%) and free fatty acids (~ 10%). Correlation between FAT/CD36 expression levels and incorporation of [^{14}C]-oleate into each class of cellular lipid was assessed by Spearman analysis. The results indicate that expression of FAT/CD36 by CHO 1.2C3 cells had no significant influence on the incorporation of [^{14}C]-oleate into the different classes of cellular lipid.

3.5.2.3 Possible explanations for the lack of effect of FAT/CD36 on LCFA uptake by the CHO 1.2C3 cell line

There are several plausible explanations for the apparent lack of effect of FAT/CD36 on LCFA transport in the CHO 1.2C3 cell line. Firstly, it is possible that FAT/CD36 expression alone is not sufficient to enhance LCFA uptake by CHO cells. This could be because these cells might lack functional obligate partner proteins that are necessary to complement the action of FAT/CD36 in long-chain fatty acid transport (e.g. FABPpm, FATP), esterification (e.g. FATP, long-chain fatty acyl CoA synthetases) and/or intracellular fatty acid handling proteins (e.g. FABPs, caveolin). Of these putative partner proteins, caveolin-1 is unlikely to be limiting because the molecule has been detected in these cells, where it is enriched in lipid rafts/DRMs along with FAT/CD36.

Another potential difference between the effectiveness of FAT/CD36 in FAT/CD36-transfected CHO 1.2C3 cell line and FAT/CD36-transfected H4IIE and COS-7 cell lines might be the subcellular location of the molecule. Although the degree of enrichment of FAT/CD36 in DRMs prepared from each of the different transfected cell lines and the relative content of caveolin-1 in these fractions differs between cell types (CHO, COS-7 and H4IIE), these differences are not consistent with the relative capacities of these cell lines to mediate short-term uptake of oleic acid. Furthermore, FAT/CD36 is effectively targeted to the plasma membrane in each cell type where it overlaps in localization, at least partially, with markers of lipid rafts and caveolae.

It has been shown previously that FAT/CD36 forms covalently associated homo-dimers and -multimers in transfected COS-7 cells and it has been suggested that these post-

Figure 3-39. FAT/CD36 expression levels do not correlate with incorporation of [^{14}C]-oleate into complex lipids in CHO 1.2C3 cells. CHO 1.2C3 cells and CHO 1.2C4 cells (FAT/CD36-negative) were cultured for 120 hours in the presence of doxycycline at various concentrations (0, 0.01, 0.1, 100 ng/ml). After this period cells were re-seeded and incorporation of [^{14}C]-oleate into complex lipids was determined after incubation for 15 minutes at 37°C with a solution of [^{14}C]-oleate (173μM) adsorbed to equimolar amounts of fatty acid-free BSA. Fatty acid uptake was stopped, cell monolayers were washed and lipids were extracted and separated by thin layer chromatography (TLC). Radioactivity associated with free fatty acids (FFA), polar lipids (phospholipids, monacylglycerol 3-phosphate, phosphatidic acid), diacyglycerol (DAG) and triacylglycerol (TAG) was quantified. The amount of [^{14}C]-oleate incorporated into each class of cellular lipid (pmol, mg protein^{-1}, 15 mins^{-1}) and the level of FAT/CD36 expression at the cell surface are shown in scatter plots for each sample.

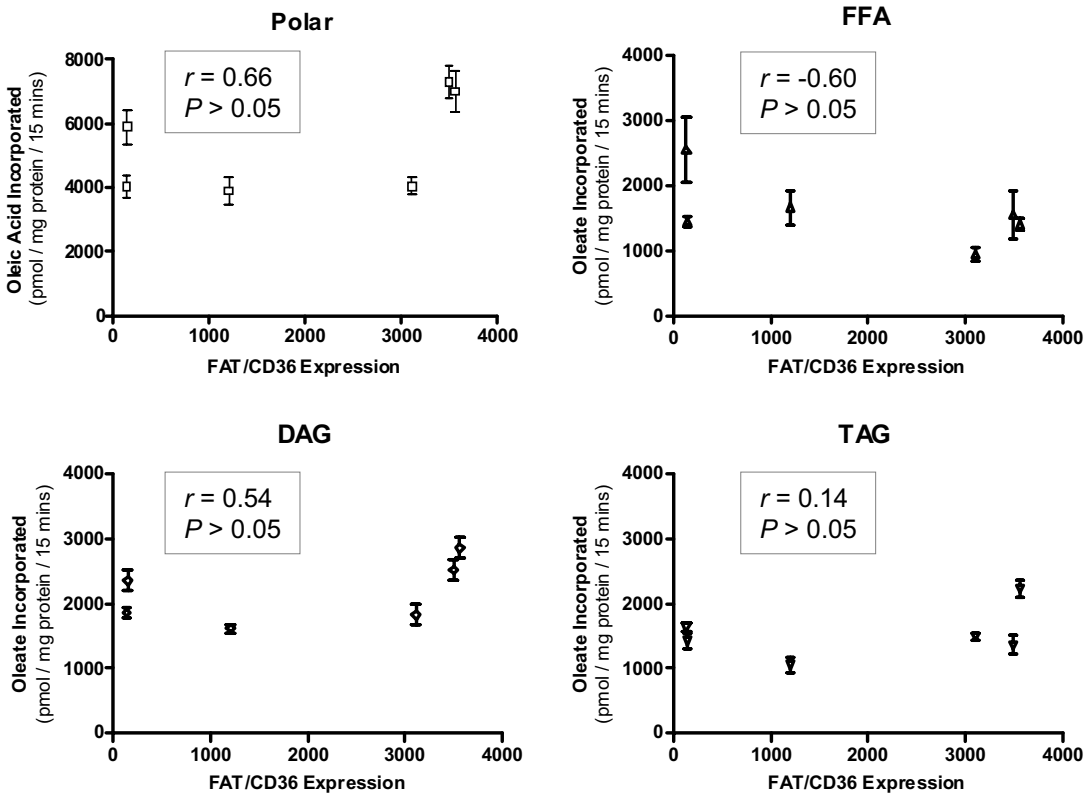
Polar
r = 0.66
P > 0.05
Oleic Acid Incorporated
(pmol / mg protein / 15 mins)
FAT/CD36 Expression
FFA
r = -0.60
P > 0.05
Oleate Incorporated
(pmol / mg protein / 15 mins)
FAT/CD36 Expression
DAG
r = 0.54
P > 0.05
Oleate Incorporated
(pmol / mg protein / 15 mins)
FAT/CD36 Expression
TAG
r = 0.14
P > 0.05
Oleate Incorporated
(pmol / mg protein / 15 mins)
FAT/CD36 Expression

Figure 3-39.

translational modifications may influence the activity of the receptor (Thorne et al., 1997). To determine whether FAT/CD36 undergoes homo-dimerization and/or multimerization in CHO 1.2C3 cells and whether defects in this process may contribute to the inability of FAT/CD36 expressed in these cells to enhance LCFA transport, lysates were prepared from CHO 1.2C3 cells, H4IIE-FAT/CD36 (1A) cells and female (DA) rat liver. These were subjected to 7.5% SDS-PAGE under reducing and non-reducing conditions and immuno-blotted to detect FAT/CD36 (Figure 3-40). The results did not provide any evidence of receptor dimerization/multimerization in any of the cell-types examined, although it is possible that dimerization/multimerization of FAT/CD36 masks the epitope that is recognized by mAb MO25. Interestingly, comparison of the bands of FAT/CD36 in these samples suggests that there may be some heterogeneity in the molecular weight of FAT/CD36 in CHO 1.2C3 cells, resulting in a smear of slightly higher molecular weight. This could be the result of differences in glycosylation of FAT/CD36 in CHO cells, perhaps due to incomplete 'trimming' and modification of N-linked glycans in the Golgi complex of these cells. Further investigation of the nature of FAT/CD36 glycosylation was beyond the scope of this project.

3.6 Summary

These investigations provide evidence that FAT/CD36 expression enhances long-chain fatty acid uptake by cells of hepato-cellular origin. This function may be of physiological significance, given that the receptor is expressed at high levels in the livers of female rodents and humans. Furthermore, it has been shown that localization of FAT/CD36 to lipid rafts is similar in transfected cell lines and in rat liver. Interestingly, these studies have provided the first evidence that FAT/CD36 is found in both lipid raft- and non-raft-domains of the plasma membrane. The functional significance of this is unclear but previous investigations have shown that lipid raft function may be required for FAT/CD36-mediated LCFA uptake (Pohl et al., 2005). Nevertheless, lipid raft association is not sufficient for FAT/CD36-mediated LCFA transport because its presence in DRMs from CHO 1.2C3 cells did not affect the ability of these cells to take up fatty acid.

While FAT/CD36 was found to co-fractionate with caveolin-1 in biochemically prepared lipid rafts in liver and transfected cell lines, the receptor was only partially co-localized with caveolin-1-EGFP in these cell lines when examined by confocal fluorescence microscopy. Furthermore, FAT/CD36 was found to localize to lipid rafts in transfected

Figure 3-40. FAT/CD36 in CHO 1.2C3 cells may be inappropriately glycosylated. Twenty micrograms of protein from lysates of female rat liver (DA strain) (1), CHO 1.2C3 cells (2) and H4IIE-FAT/CD36 (1A) cells were subjected to 7.5% SDS PAGE under reducing and non-reducing conditions (as indicated) and Western blotting with anti-FAT/CD36 mAb MO25. Single immunoreactive bands were detected for each sample and these are shown.

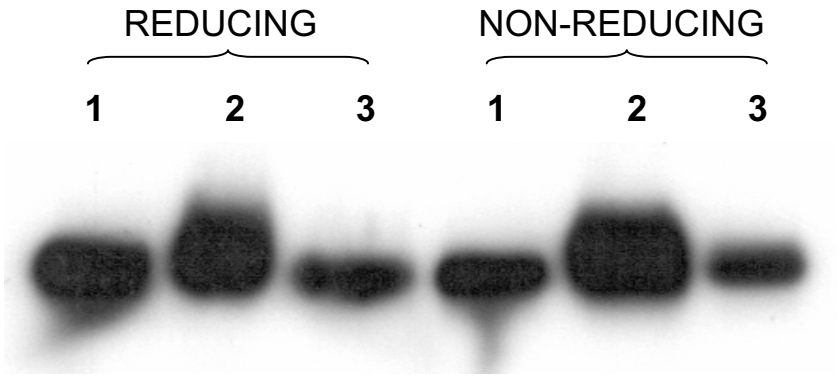

Figure 3-40.

H4IIE cell lines that lack caveolin-1 and caveolae. Taken together, these results indicate that FAT/CD36 does not require expression of caveolin-1 to localize to plasma membrane lipid rafts and to enhance uptake of LCFAs. Furthermore, caveolin-1-EGFP expression does not affect either FAT/CD36-dependent or FAT/CD36-independent LCFA uptake in H4IIE cell lines. However, lipid raft function contributes to a significant component of LCFA uptake.

An interesting finding of this study is the impact that FAT/CD36 expression has in the short term on the incorporation of radiolabelled oleate into complex cellular lipids in transfected H4IIE cells. Several studies have demonstrated that over-expression of FAT/CD36 in myocytes results in increased incorporation of LCFAs into triacylglycerol (TAG) and/or increased LCFA oxidation and that the metabolic fate differs between saturated (palmitate) and unsaturated (oleate) fatty acids (Ibrahimi et al., 1999, Bastie et al., 2004, Garcia-Martinez et al., 2005). The results described in this chapter show that expression of FAT/CD36 in H4IIE hepatoma cells results in decreased incorporation of [^{14}C]-oleate into triacylglycerol and increased accumulation of [^{14}C]-oleate in diacylglycerol (DAG); a finding that can be interpreted to indicate a shift away from storage of LCFAs as triglyceride and towards increased biosynthesis of phospholipids. DAG represents an accessible pool for phospholipid synthesis and β-oxidation is not reported to be a major metabolic pathway in these cells (Prip-Buus et al., 1992). We hypothesize that FAT/CD36 may indirectly influence the intracellular fate of LCFAs, possibly via activation of signal transduction pathways or direct interaction with acyl-CoA synthetases (ACS) or fatty acid binding proteins (FABP) mediated by the cytoplasmic C-terminus of FAT/CD36. However, in the longer term, the enhanced uptake of LCFA may lead to accumulation of excess lipid as triglyceride, and formation of cytoplasmic lipid vacuoles, as observed in the COS-7-FAT/CD36 cell line.

As discussed above, FAT/CD36 expression does not of itself appear to confer enhanced LCFA uptake. This has been indicated by previous reports (Van Nieuwenhoven et al., 1998) and studies of the CHO 1.2C3 cell line. Despite high-level expression of FAT/CD36 at the cell surface and its enrichment in lipid rafts, uptake and metabolism of [^{14}C]-oleate did not correlate with FAT/CD36 expression in CHO 1.2C3 cells. This could be the result of subtle differences in the post-translational modification of FAT/CD36 in these cells (i.e

glycosylation) or the absence of a critical co-factor(s) required for efficient FAT/CD36-mediated LCFA uptake. For instance, close association between FAT/CD36 and ACSs and/or FABPs might be required for vectorial transport of LCFAs by FAT/CD36. Alternatively, the function of FAT/CD36 in LCFA uptake could require association of the molecule with an adaptor protein, similar to the association between SR-BI and its adaptor protein (Silver, 2002, Kocher et al., 2003). Although the factors that dictate the ability of FAT/CD36 to mediate enhanced LCFA uptake remain unclear, localization of the molecule to plasma membrane lipid rafts is undoubtedly significant.

Chapter 4: Investigations into the involvement of FAT/CD36 in lipid uptake from HDL

4.1 Introduction

Reverse cholesterol transport (RCT) is the process whereby cholesterol is collected from the periphery by high-density lipoproteins (HDL) and delivered to the liver for excretion or recycling (reviewed in Rigotti et al., 1997a). This process is athero-protective because HDL acquire cholesterol from macrophages in the artery wall, thereby inhibiting transformation into the lipid-laden foam cells that are the primary constituents of atherosclerotic plaques. The athero-protective effects of HDL may also limit oxidative damage associated with foam cells and instigate anti-atherosclerotic signalling events by vascular endothelial cells (reviewed in Trigatti et al., 2003). The class B scavenger receptor SR-BI plays an intimate role in this process at several levels. Firstly, SR-BI accelerates bi-directional flux of free cholesterol between cells and HDL acceptors, although aqueous diffusion and the ATP-binding cassette transporter AI (ABCA1) also contribute (reviewed in Yancey et al., 2003). Secondly, expression of SR-BI is associated with increased cellular acquisition of α-tocopherol (vitamin E) from HDL and may therefore contribute to local protection against oxidative damage (Mardones et al., 2002, Pratico et al., 1998). Thirdly, interaction of HDL with SR-BI at the level of the vascular endothelium results in activation of endothelial nitric oxide synthase (eNOS) and other signalling events that culminate in vascular relaxation (reviewed in Rigotti et al., 2003). Finally, the ability of SR-BI to acquire cholesteryl ester selectively from HDL, particularly in the liver and steroidogenic tissues, allows re-utilisation of HDL for further rounds of cholesterol acquisition from the periphery (reviewed in Rigotti et al., 2003).

Once within HDL, free cholesterol is esterified to cholesteryl ester by the enzyme lecithin:cholesterol acyltransferase (LCAT) within the core of the lipoprotein. The acquisition of cholesterol by HDL and its conversion into CE is accompanied by changes in the physical properties of the lipoproteins by a process known as HDL maturation (reviewed in Fielding and Fielding, 1995). Accordingly, there are three major classes of HDL: small apolipoprotein A-I (apoA-I) complexes that are poor in lipid (pre-β-HDL); phospholipid- and free cholesterol-enriched nascent discoidal HDL (β-HDL); and larger spherical mature HDL (α-HDL), in which cholesterol is mainly in the esterified (CE)

form. It appears that as HDL mature, acquisition of free cholesterol from cells becomes less reliant on energy-dependent (ABCA1-mediated) efflux and more dependent on passive diffusion of free cholesterol and phospholipids from the cell membrane to the HDL(Wang and Tall, 2003). α-HDL (mature HDL) can be further sub-classified according to their size, density (HDL_2 and HDL_3) and apolipoprotein content (apo A-I or apo A-I/A-II) (reviewed in Assmann and Gotto, 2004). Selective uptake of CE is more efficient from smaller, apo A-I-containing β-HDL particles, compared to that from larger α-HDL (Liadaki et al., 2000). Accordingly, remodelling of HDL by lipid hydrolysing enzymes such as hepatic lipase and phospholipase A_2 may explain the association of these enzymes with enhanced (SR-BI-mediated) HDL-CE selective uptake (Lambert et al., 2000, de Beer et al., 2000).

The ability of SR-BI to mediate selective uptake of cholesteryl ester (CE) from HDL is well established (Acton et al., 1996, Krieger, 1999, Williams et al., 1999, Silver et al., 2001). The physiological significance of this activity has been highlighted by studies of genetically modified mice in which there is either targeted disruption of the gene encoding SR-B1, or over-expression of SR-BI in the liver (reviewed in Trigatti et al., 2004). SR-BI knockout mice display increased plasma cholesterol associated with large HDL-like particles, decreased neutral lipid storage in steroidogenic tissues and defective hepatic uptake of HDL-CE (Rigotti et al., 1997b, Trigatti et al., 1999, Van Eck et al., 2003). Similar, but milder, effects were reported in gene-targeted mice in which a modification in the promoter region of *SR-BI* resulted in attenuated expression of SR-BI protein in the liver but unaltered expression in steroidogenic tissues (Varban et al., 1998). On the other hand, hepatic over-expression of SR-BI results in decreased plasma cholesterol, in particular in HDL fractions, and increased levels of biliary cholesterol (Kozarsky et al., 1997, Wang et al., 1998, Ueda et al., 1999).

Numerous *in vitro* studies have demonstrated that both SR-BI and FAT/CD36 can bind HDL with high affinity (K_d: 10-20 μg/ml). However, SR-BI is several times more efficient than FAT/CD36 in mediating selective uptake of HDL-CE (Gu et al., 1998, Connelly et al., 1999, Connelly et al., 2001, Connelly et al., 2003b). Both of the receptors can bind to other native lipoproteins (LDL, VLDL) with high affinity and mediate selective lipid uptake from these particles (Acton et al., 1994, Calvo et al., 1997, Calvo et al., 1998,

Stangl et al., 1999, Swarnakar et al., 1999, Rhainds et al., 2003). The recent demonstrations that FAT/CD36 is expressed at high levels in female rodents and humans (Zhang et al., 2003, Stahlberg et al., 2004) stimulated an assessment of FAT/CD36-mediated lipid uptake from HDL by transfected cell lines of hepatic and non-hepatic origin. In particular, the possibility was explored that FAT/CD36 and SR-BI might co-localise when expressed simultaneously in cells and cooperate in selective uptake of HDL-CE.

4.2 Hypotheses:

I. FAT/CD36 and SR-BI co-localize in plasma membrane lipid rafts of transfected H4IIE cells and rat liver.

II. FAT/CD36 expression enhances selective HDL-lipid uptake in transfected cell lines of hepatic and non-hepatic origin.

III. FAT/CD36 enhances SR-BI-mediated uptake of lipid from HDL cooperatively.

IV. Caveolin-1 expression and formation of caveolae influences HDL-lipid uptake by hepatoma cells.

V. HDL-lipid uptake correlates positively with the level of FAT/CD36 expression and at high levels, lipid uptake mediated by FAT/CD36 can be comparable to that mediated by SR-BI.

4.3 Localization of FAT/CD36, SR-BI and lipid rafts

It is widely accepted that SR-BI, like FAT/CD36, consists of a large extracellular loop that is anchored to the plasma membrane at both amino- and carboxy-termini, each of which has short tails that extend into the cytoplasm (Connelly et al., 2001, Krieger, 2001). As in the case of FAT/CD36 (Chapter 3), the subcellular localization is controversial. Several reports, based on studies involving biochemical fractionation of cells (Babitt et al., 1997, Graf et al., 1999) and confocal fluorescence microscopy (Babitt et al., 1997), have indicated that SR-BI localizes to caveolae in Y1-BS1 murine adrenocortical cells and transfected CHO cells. Other studies in HepG2 human hepatoma cells (Rhainds et al., 2004) have indicated that the receptor is enriched in lipid rafts that are distinct from caveolae, while studies in transfected WI38-VA13 (human lung fibroblast), COS-7 or CHO cells (Peng et al., 2004) have indicated that SR-BI is not strongly associated with classical detergent-resistant lipid rafts at all. Examination of the subcellular distribution of

SR-BI by electron microscopy using transfected WI38-VA13 cells revealed that the molecule localized to microvillar extensions of the plasma membrane (Peng et al., 2004). This microvillar localization of SR-BI was also observed by Reaven *et al*, who used immunogold electron microscopy to demonstrate localization of SR-BI dimers to microvillar extensions and 'double-membraned' channels in transfected HEK293 cells and rat ovaries (Reaven et al., 2004).

As shown in Chapter 3, FAT/CD36 is enriched in classical lipid rafts and these overlap only partially with caveolae in transfected H4IIE, COS-7 and CHO cell lines. Furthermore, contrary to reports in 3T3-L1 adipocytes (Pohl et al., 2005), it is apparent that FAT/CD36 localizes to both raft and non-raft components of the plasma membrane in transfected H4IIE cell lines and that localization to the cell surface and to lipid rafts does not require expression of caveolin-1. Similarly, detergent-resistant membranes (DRMs) from rat liver contained both FAT/CD36 and caveolin-1. These results are consistent with the localization of FAT/CD36 to caveolae in liver. However, as discussed in Chapter 3 (reviewed in Rajendran and Simons, 2005), co-fractionation of a given protein with caveolin-1 in DRMs does not prove that all, or even some, of that protein is associated with caveolae.

The work described in this section investigates the localization of FAT/CD36 with respect to SR-BI and lipid rafts. It is a prelude to investigation of potential cooperativity between FAT/CD36 and SR-BI in selective HDL-lipid uptake.

4.3.1 Screening H4IIE cells for expression of SR-BI and other potential contributors to HDL-CE selective uptake

Prior to examination of HDL-lipid uptake by H4IIE rat hepatoma cells (and FAT/CD36- and/or caveolin-1-EGFP-transfectants of H4IIE cells) it was necessary to examine whether these cells express endogenous SR-BI. The opportunity was also taken to assess any endogenous expression of some other potential contributors to SR-BI-mediated selective uptake of HDL-CE by these cells. To this end mRNA was extracted from (un-transfected) H4IIE cells, cDNA was prepared and RT-PCR performed using gene-specific oligonucleotides (Table 2-1) to amplify fragments of *SR-BI* (primers SRBI FP3, SRBI RP1), *FAT/CD36* (primers FAT FP3, FAT RP2), *caveolin-1* (primers Cav1 FP1, Cav1 RP1), *hepatic lipase* (primers rHL FP1, rHL RP2) and *β-actin* (primers: β-ACTIN FP1, β-

ACTIN RP1) (Figure 4-1). Female DA rat liver cDNA was used as a positive template control, while amplification of a fragment of *β-actin* from H4IIE cDNA indicated that cDNA was of satisfactory quality. Negative control PCR reactions contained no template DNA. The results indicate that H4IIE cells lack endogenous transcripts encoding either FAT/CD36 or caveolin-1 but that they express endogenous transcripts encoding SR-BI (and/or SR-BII) and hepatic lipase.

To examine whether H4IIE cells express endogenous SR-BI protein and whether expression of FAT/CD36 and/or caveolin-1 affects expression of endogenous SR-BI, lysates were prepared from each of the transfected H4IIE cell lines (H4IIE (5A), H4IIE-FAT/CD36 (1A), H4IIE (5A) + caveolin-1-EGFP and H4IIE-FAT/CD36 (1A) + caveolin-1-EGFP). Twenty micrograms of protein from each post-nuclear supernatant was subjected to 12% SDS-PAGE and Western blotting using an SR-BI-specific antibody that does not recognize SR-BII (Figure 4-2). The results confirmed that these cells express endogenous SR-BI and indicate that expression of SR-BI was not affected detectably in cell lines expressing FAT/CD36 and/or caveolin-1-EGFP.

4.3.2 Localization of endogenous SR-BI with respect to FAT/CD36 and caveolin-1 in transfected H4IIE cell lines

To investigate whether SR-BI localizes to lipid rafts in H4IIE hepatoma cells, H4IIE-FAT/CD36 (1A) cells were subjected to lysis in 1% Triton X-100 at 4°C, followed by sucrose step gradient fractionation as detailed previously (see 2.5.2). Equal volumes of each aliquot from the sucrose gradient were subjected to 12% SDS-PAGE and Western blotting, using antibodies directed against FAT/CD36 (mAb MO25), SR-BI (rabbit polyclonal antibody) and the transferrin receptor (mAb OX-26) (Figure 4-3A). Aliquots of each fraction were also used to determine the protein content and density (expressed as %-sucrose [w/v]) of each fraction (Figure 4-3B). The results indicate that very little endogenous SR-BI is associated with the low density fractions containing DRMs (fractions 1-4), while FAT/CD36 is highly enriched in these fractions. Importantly, the transferrin receptor was only detected in the highest density 'non-raft' fractions, indicating that raft fractions were not contaminated with non-raft membrane proteins. The protein content and densities of fractions closely resembled those of other DRM preparations (Chapter 3). The distribution of SR-BI in sucrose gradient fractions from lysates of the other H4IIE cell

Figure 4-1. RT-PCR analysis of gene expression in H4IIE cells. RNA was extracted from H4IIE cells (untransfected) and used to prepare cDNA for PCR-based analysis of gene expression. For each primer pair (β-actin, SR-BI, FAT/CD36, caveolin-1 and hepatic lipase) reactions were performed using H4IIE cDNAas template (2). Positive control reactions (3) were performed using cDNA prepared from normal female (DA) rat liver (third lane of each gene analysed) as template DNA. Negative control reactions (1) lacked template DNA. Amplification of cDNA amplicons of the expected size (~300bp) for the house keeping gene β-actin confirmed suitable template cDNA quality.

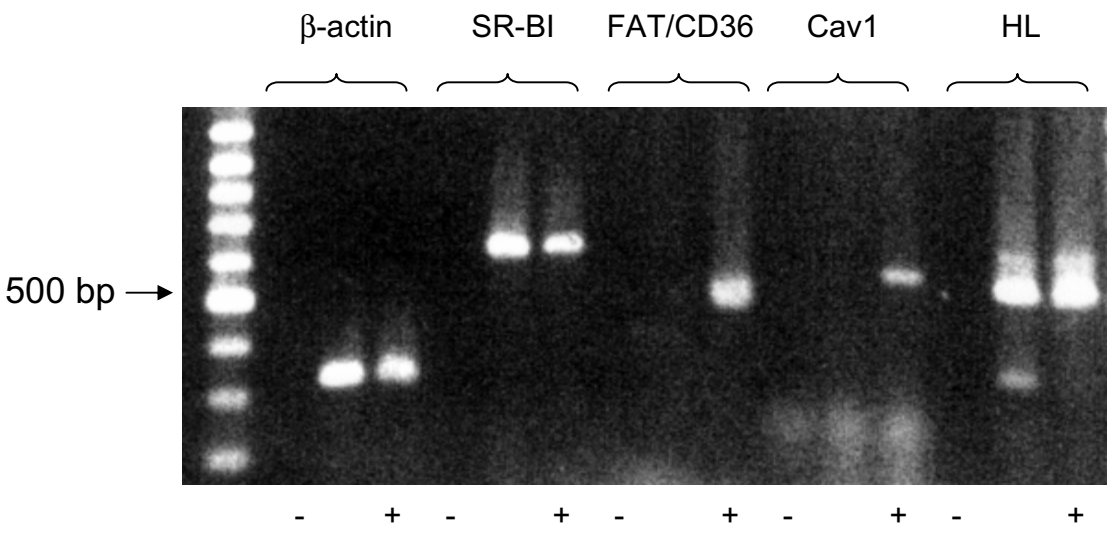

Figure 4-1.

Figure 4-2. Western analysis of endogenous SR-BI expression in H4IIE (5A), H4IIE-FAT/CD36 (1A), H4IIE (5A) + caveolin-1-EGFP and H4IIE-FAT/CD36 (1A) + caveolin-1-EGFP cell lines. Whole cell lysates were prepared from each of the cell lines (in duplicate) and 20μg of protein from each post-nuclear supernatants was subjected to SDS-PAGE and Western blotting with antibodies directed against SR-BI, caveolin-1 and β-actin, as indicated.

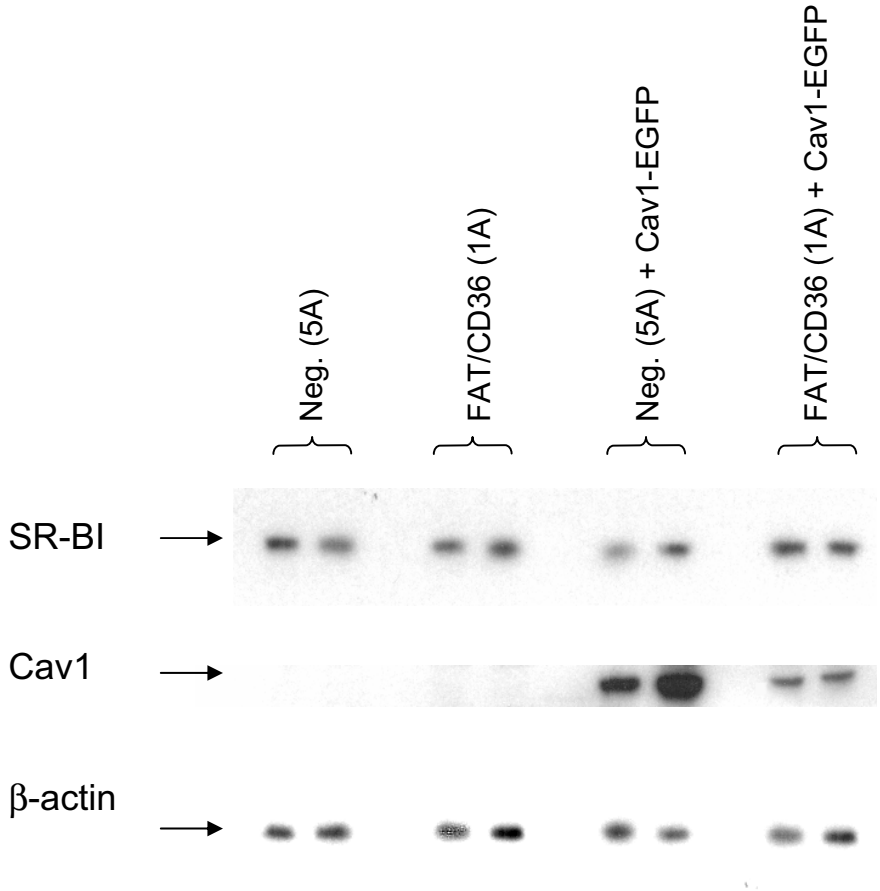
Neg. (5A)
FAT/CD36 (1A)
Neg. (5A) + Cav1-EGFP
FAT/CD36 (1A) + Cav1-EGFP
SR-BI
Cav1
β-actin

Figure 4-2.

Figure 4-3. SR-BI is not strongly associated with lipid raft-derived detergent-resistant membranes (DRMs) in H4IIE cell lines. H4IIE-FAT/CD36 (1A) cells were lysed in 1% Triton X-100 at 4°C and post-nuclear lysates were subjected to discontinuous 5-40% sucrose step gradient centrifugation. **A;** Twelve fractions were collected from the tops of gradients and equal volumes of each fraction were subjected to 12% SDS-PAGE and Western blotting with antibodies directed against SR-BI, FAT/CD36 and the transferrin receptor (Tfr-1), as indicated. **B;** The sucrose and protein contents of each fraction were measured by refractometry and Bradford analysis, respectively (triangles and squares, repectively).

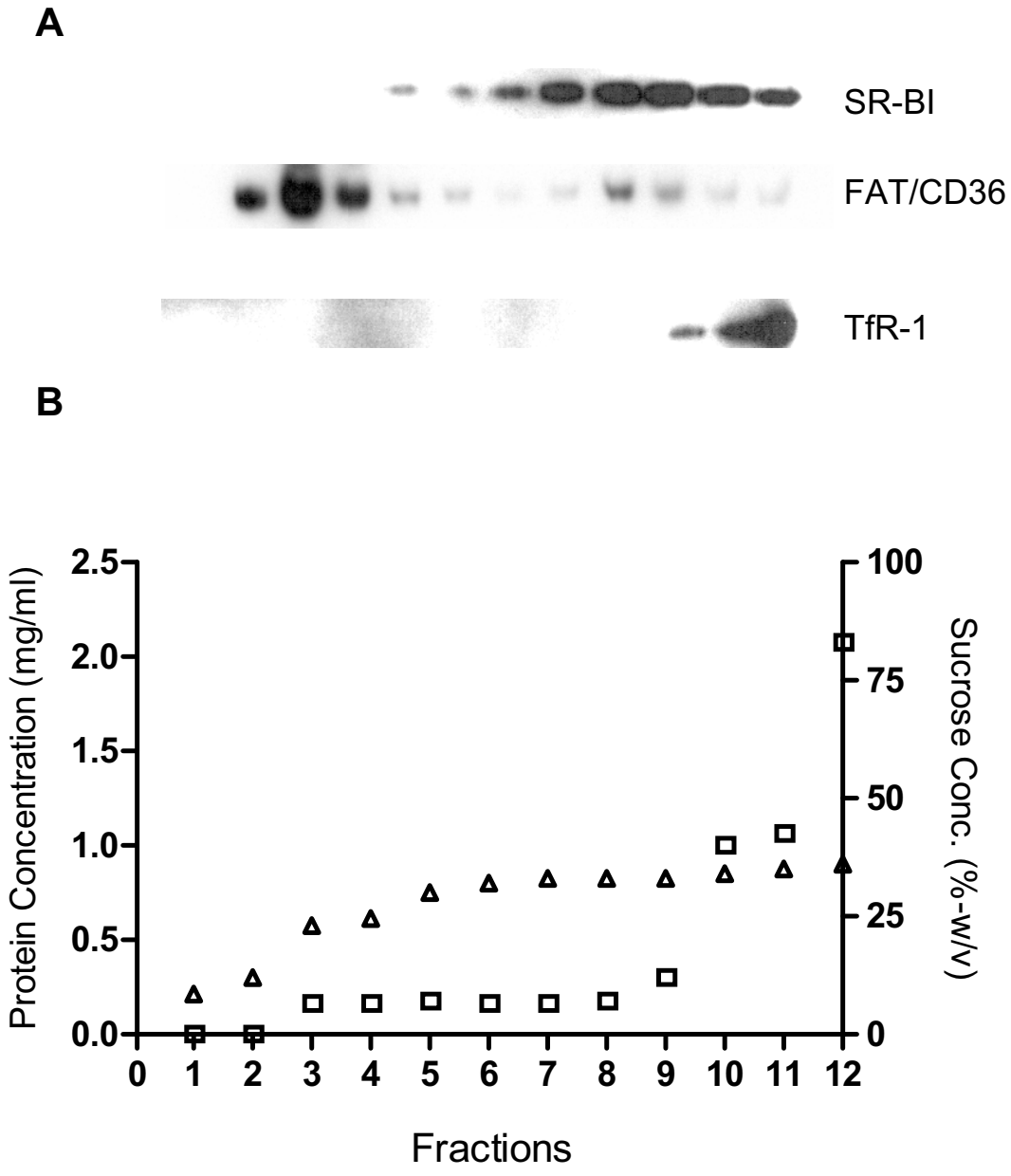
A
SR-BI
FAT/CD36
TfR-1
B
Protein Concentration (mg/ml)
2.5
2.0
1.5
1.0
0.5
0.0
100
75
50
25
0
Sucrose Conc. (%-w/v)
0 1 2 3 4 5 6 7 8 9 10 11 12
Fractions

Figure 4-3.

lines (H4IIE (5A) and H4IIE (5A) + caveolin-1-EGFP) (not shown) was similar to that obtained with H4IIE-FAT/CD36 (1A) cell lysates, indicating that expression of neither caveolin-1-EGFP nor FAT/CD36 altered the distribution of SR-BI to DRMs appreciably.

To assess the subcellular localization of SR-BI with respect to FAT/CD36 and caveolin-1-EGFP, H4IIE-FAT/CD36 (1A) + caveolin-1-EGFP cells were grown overnight on coverslips and fixed prior to labelling for immunofluorescence. SR-BI and FAT/CD36 were labelled at the cell-surface by indirect immunofluorescence using a polyclonal rabbit antibody directed against the extracellular domain of SR-BI (and SR-BII) and mAb UA009 respectively as primary antibodies (Figure 4-4). Confocal fluorescent images were acquired for caveolin-1-EGFP, FAT/CD36 and SR-BI and images for the same focal plane were merged. The results demonstrate that, as indicated previously (see 3.4.4.4), partial co-localization of FAT/CD36 and caveolin-1-EGFP at the cell-surface. There was, however, little overlap in the localization SR-BI and caveolin-1-EGFP. In contrast, there was frequent co-localization of SR-BI and FAT/CD36 at the plasma membrane. These findings, taken in conjunction with those obtained by examination of DRM biochemically, indicate that some FAT/CD36 is co-localized with caveolin-1 in caveolae (i.e DRM-associated FAT/CD36). In contrast, the co-localization of some FAT/CD36 and SR-BI by confocal microscopy and the low content of SR-B1 in DRMs biochemically suggests that SR-BI and some FAT/CD36 are associated in non-raft domains of the plasma membrane.

4.3.3 Expression of SR-BI in rat liver

It has been established clearly that hepatocytes of rodents and humans express SR-BI (reviewed in Krieger, 2001). Hepatic expression of SR-BI is regulated by a range of factors that include dietary lipids, cytokines and hormones (Rhainds and Brissette, 2004). With respect to the effects of gender, hepatic SR-BI expression is reported to be higher in male rats than in females (Graf et al., 2001). Accordingly, pharmacological doses of estrogen decrease expression of SR-BI in rat liver parenchymal cells (Fluiter et al., 1998), although this effect may be indirect because it is reliant on the presence of an intact pituitary gland (Stangl et al., 2002). To complicate matters further, estrogen treatment of rats results in upregulation of SR-BI by Kupffer cells (Fluiter et al., 1998). The effects of gender on hepatic expression of SR-BI by parenchymal and non-parenchymal cells were most clear in the studies by Brodeur *et. al*, who demonstrated that compared to age-

Figure 4-4. Subcellular localization of endogenous SR-BI with respect to FAT/CD36 and caveolin-1-EGFP in H4IIE-FAT/CD36 (1A) + caveolin-1-EGFP cells, as determined by confocal fluorescence microscopy. Cells were grown on coverslips overnight prior to fixation and labelling by indirect immunofluorescence. SR-BI/II was labelled using a (rabbit) polyclonal antibody directed against the extracellular domain of SR-BI and a Cy5-conjugated anti-rabbit Ig secondary antibody. FAT/CD36 was labelled using mAb UA009 and a Cy3-conjugated anti-mouse Ig secondary antibody. Epifluorescence associated with caveolin-1-EGFP was employed to visualize this protein. Upper panels show greyscale images for each of the individual labels. Lower panels show pseudo-coloured merged images for pairs of labels (lower left panel, caveolin-1-EGFP [green] and FAT/CD36 [red]; lower middle panel, caveolin-1-EGFP [green] and SR-BI [red]; lower right panel, FAT/CD36 [green] and SR-BI [red]).Control experiments using appropriate isotype-matched irrelevant primary antibodies (mAb 1B5 and polyclonal R127B8) demonstrated specificity of labelling (not shown). ×40 objective, ×3 zoom.

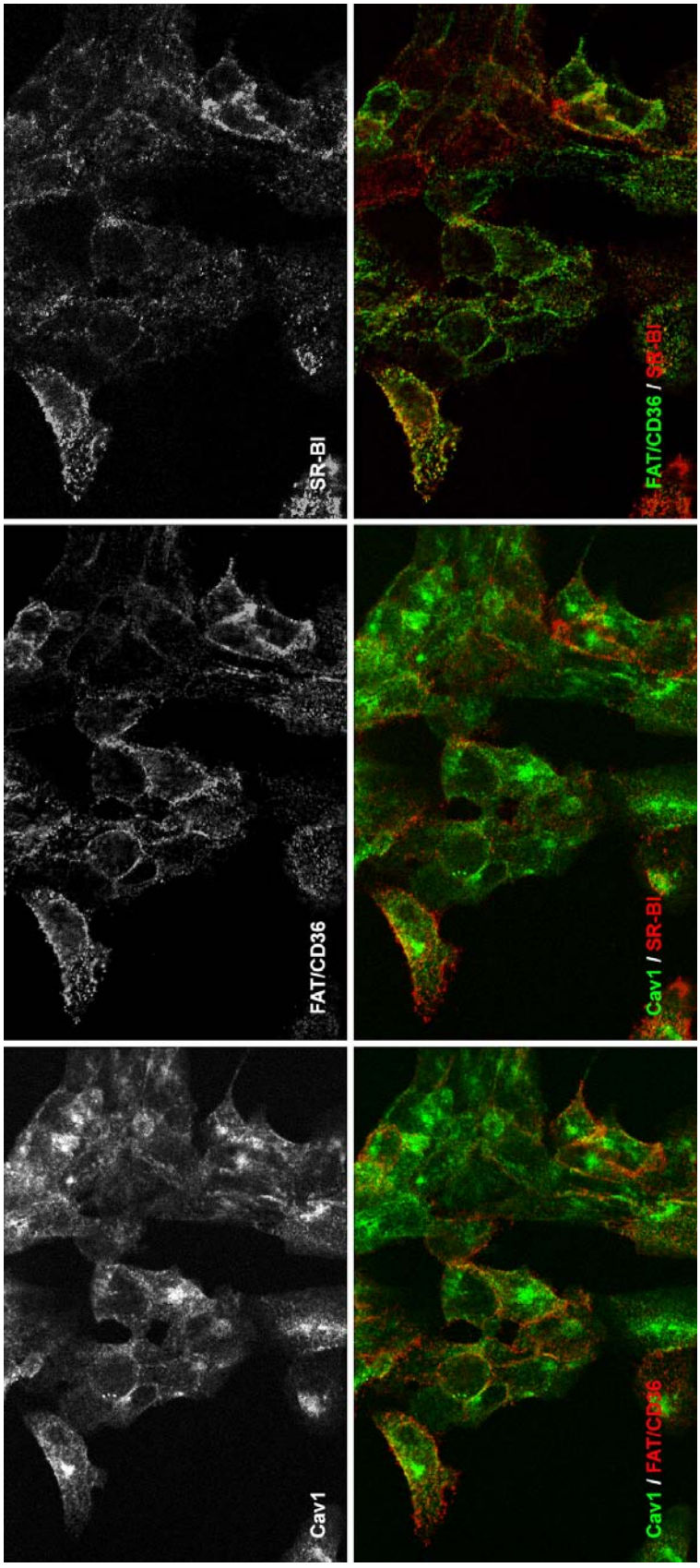

Figure 4-4.

matched female mice, expression of SR-BI is ~55% higher in the parenchymal cells of male liver but ~65% lower in the non-parenchymal cells (Brodeur et al., 2005).

As described in Chapter 3, expression of FAT/CD36 is several-fold higher in the liver of female rats compared with males. It was decided, therefore, to re-examine the gender-bias in hepatic expression of SR-BI in a rat strain in which there is a marked gender difference in expression of FAT/CD36. Lysates were prepared from male (n=3) and female (n=3) DA rats and 25 μg of protein from each post-nuclear supernatant sample was subjected to 12% SDS-PAGE and Western blotting (Figure 4-5A). Densitometric analysis revealed no significant difference in hepatic SR-BI expression between male and female rats ($P > 0.05$) (Figure 4-5B). These results contrast, therefore, with the moderately higher expression of SR-BI that has been reported for male rats (Graf et al., 2001), although further studies with a larger sample size may be required to examine whether subtle differences in hepatic SR-BI expression levels exist between the genders.

4.3.4 Subcellular localization of SR-BI in rat liver

To investigate whether SR-BI shares with FAT/CD36 enrichment within hepatocellular DRMs, female rat liver was homogenised in 1% Triton X-100 at 4°C and submitted to sucrose step-gradient fractionation. Sucrose gradient fractions were subjected to 12% SDS-PAGE and Western blotting, using anti-SR-BI antibodies (Figure 4-6). As in the case of H4IIE hepatoma cells, the results show that most of the SR-BI was not associated with DRMs. A small proportion was found in fractions 2 and 3 of the sucrose gradient but most was associated with the higher density non-raft fractions. Should there be cooperative interactions between SR-B1 and FAT/CD36 in selective CE uptake by hepatocytes, the findings indicate that that this could only involve a small proportion of the total hepatocellular SR-B1.

4.4 Assessment of FAT/CD36-mediated HDL-lipid uptake in transfected cell lines

Numerous studies, using transfected cell lines, have demonstrated that uptake of CE and other lipids from HDL is several-fold more efficient via SR-BI than via FAT/CD36, despite the comparable HDL-binding affinities displayed by the two receptors (Gu et al., 1998, Connelly et al., 1999, Gu et al., 2000, Connelly et al., 2001, de Villiers et al., 2001, Connelly et al., 2003a, Parathath et al., 2004). Furthermore, studies on the domains of SR-

Figure 4-5. Expression of SR-BI in rat liver is not significantly influenced by gender. **A;** Portions of liver from each of three male and three female Dark Agouti rats were homogenized in 1% Triton X-100 lysis buffer and 25μg of protein from each post-nuclear lysate was subjected to 12% SDS-PAGE and Western blotting with antibodies directed against SR-BI and β-actin, as indicated. **B;** Immunoreactive bands associated with FAT/CD36 and β-actin were quantified by densitometry and expression of SR-BI relative to that of the house keeping gene β-actin was calculated and expressed as arbitrary units (n=3). No significant difference between SR-BI expression in male and female rat liver was found ($P > 0.05$).

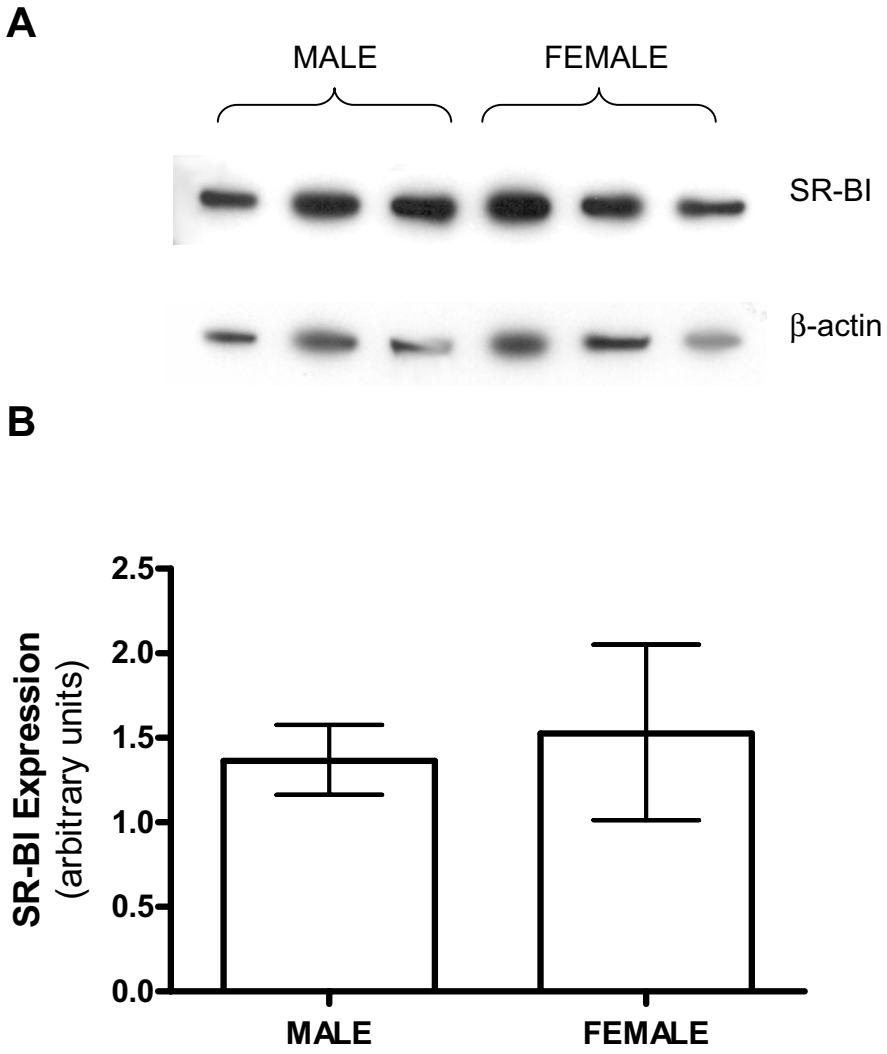
A
MALE
FEMALE
SR-BI
β-actin
B
SR-BI Expression
(arbitrary units)
2.5
2.0
1.5
1.0
0.5
0.0
MALE
FEMALE

Figure 4-5.

Figure 4-6. SR-BI is not strongly associated with lipid raft-derived detergent-resistant membranes (DRMs) in rat liver. Portions (~50mg) of liver from female Dark Agouti rats were solubilized in 1% Triton X-100 at 4°C and post-nuclear supernatants were subjected to discontinuous (5-40%) sucrose step gradient fractionation. Twelve fractions were collected from the tops of each gradient and equal volumes of each fraction were subjected to SDS-PAGE and Western blotting with antibodies directed against SR-BI, FAT/CD36, caveolin-1 and TfR-1, as indicated.

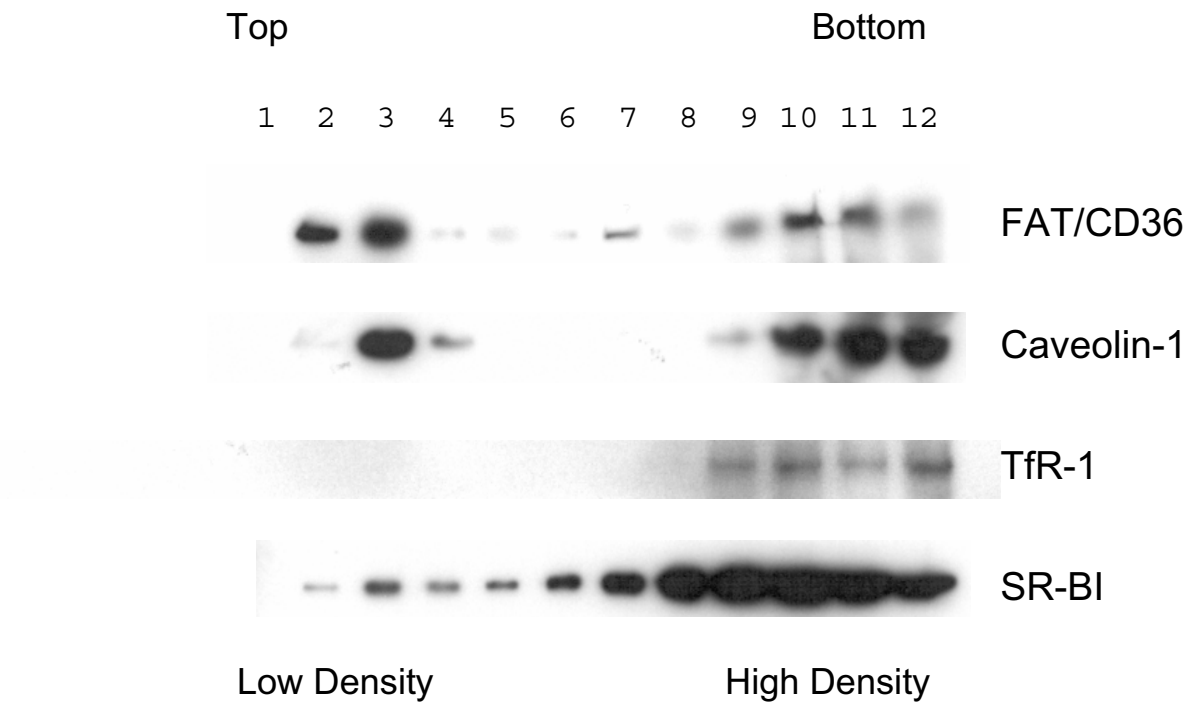
Top
Bottom
1 2 3 4 5 6 7 8 9 10 11 12
FAT/CD36
Caveolin-1
TfR-1
SR-BI
Low Density
High Density

Figure 4-6.

BI that are required for efficient selective uptake of HDL-CE, using SR-BI and FAT/CD36 'domain-swap' chimeras, have indicated that the extracellular domain of SR-BI is required for efficient HDL-CE selective uptake. Replacement of the N- or C-terminal cytoplasmic and/or transmembrane domains of SR-BI with those of FAT/CD36 did not limit uptake of HDL-CE (Gu et al., 1998, Connelly et al., 1999). However, there have been no reports to date on the influence of simultaneous expression of FAT/CD36 on SR-BI-mediated uptake of HDL-associated lipids. The aims of the studies described in this section were to investigate whether simultaneous expression of FAT/CD36 and SR-B1 potentiates uptake with evidence of cooperativity. Furthermore, the influence of the level of FAT/CD36 expression was investigated to examine whether higher levels of FAT/CD36 can overcome relative inefficiency of the molecule in mediating selective uptake of HDL-CE.

The influence of caveolin-1 on HDL-CE uptake is also controversial. Indeed, whether SR-BI is localized to lipid rafts/caveolae is itself controversial and the studies described above in rat liver and H4IIE cell lines (see 4.3) have indicated that SR-BI is not strongly associated with lipid rafts or caveolae. Expression of caveolin-1 and formation of caveolae have been associated with increased (Graf et al., 1999, Matveev et al., 1999), decreased (Matveev et al., 2001) or unchanged (Wang et al., 2003) selective uptake of HDL-CE in transfected cell lines. Some of these studies (Wang et al., 2003, Matveev et al., 2001), plus others (Frank et al., 2001a, Truong et al., 2006), have investigated the influence of caveolin-1 expression and formation of caveolae on flux of free cholesterol between cells and HDL acceptors. However, exploration of the latter activity is beyond the scope of the work described in this thesis. Little is known about the effects of caveolin-1 and formation of caveolae on selective uptake of HDL-CE by cells of hepatic origin specifically. Over-expression of caveolin-1 in primary mouse hepatocytes by transduction using a recombinant adenovirus vector has resulted in a small (~10%) but significant increase in HDL-DiI uptake (Frank et al., 2001b), while Truong *et. al.* showed that expression of caveolin-1 increased selective HDL-CE uptake by transfected HepG2 human hepatoma cells (Truong et al., 2006). To examine the impact of caveolin-1-EGFP expression on uptake of HDL-lipid in hepatoma cells, studies have been undertaken in transfected H4IIE cells.

4.4.1 Preparation, analysis and labelling of HDL_3 from human blood

4.4.1.1 Purification of lipoproteins using OptiPrep

HDL were required for to labelling with DiI and use to investigate uptake of HDL-lipid by cells *in vitro*. Initial attempts to purify HDL_3 from human serum used density gradient centrifugation employing a self-forming gradient of OptiPrep (Axis-Shield), according to manufacturer's instructions (see 2.6.1). Fractions of ~0.3 ml were collected from the bottom of gradients, using a fraction collector. The purity of lipoproteins in the resulting fractions was assessed by subjecting 10 μg of protein from each fraction to 12 % SDS-PAGE and Coomassie blue staining (not shown). HDL_3 is expected to contain only Apo A-I (Dr Kerry-Anne Rye, personal communication). However, the results indicated that all fractions were contaminated with serum proteins, especially with albumin (~45 kDa).

To improve the purity of HDL, the protocol was modified to include 0.2 ml cushions of 20% iodixanol at the bottom of the tubes. Furthermore, to minimize contamination of lipoprotein fractions with (high-density) serum proteins, small fractions (~150 μl) were collected from the tops of tubes by upward displacement using a solution of 80% sucrose (w/v) delivered by a peristaltic pump (Gilson, Minipuls 2). The protein content and density of each fraction was determined by Bradford analysis and refractometry, respectively (Figure 4-7A). SDS-PAGE and Coomassie blue staining (Figure 4-7B) showed that using these modifications fractions 35-37 contained Apo A-I with relatively little contamination with either albumin or ApoB. However, the amounts protein in these fractions was insufficient for the purposes of fluorescent labelling and *in vitro* investigations of HDL-lipid uptake.

4.4.1.2 Preparation of HDL_3 by sequential ultracentrifugation

Sequential ultracentrifugation was employed to purify larger amounts of HDL_3 (1.14-1.21 g/ml) as detailed (see 2.6.2). Briefly, plasma was adjusted to a density of 1.14 g/ml using solid KBr and subjected to high-speed ultracentrifugation (150,000 ×*g*, 24 hours, 4°C). Following centrifugation gold-coloured bands at the tops and bottoms of each tube were separated by a clear middle region. The upper fraction, which was expected to contain VLDL and LDL, was collected and stored at 4°C for future analysis. The lower fraction, expected to contain HDL_3 plus non-lipoproteins was adjusted to 1.21 g/ml and subjected to further ultracentrifugation (150,000 ×*g*, 40 hours, 4°C). The resulting lower fraction, expected to contain serum proteins, was collected and stored at 4°C for future analysis.

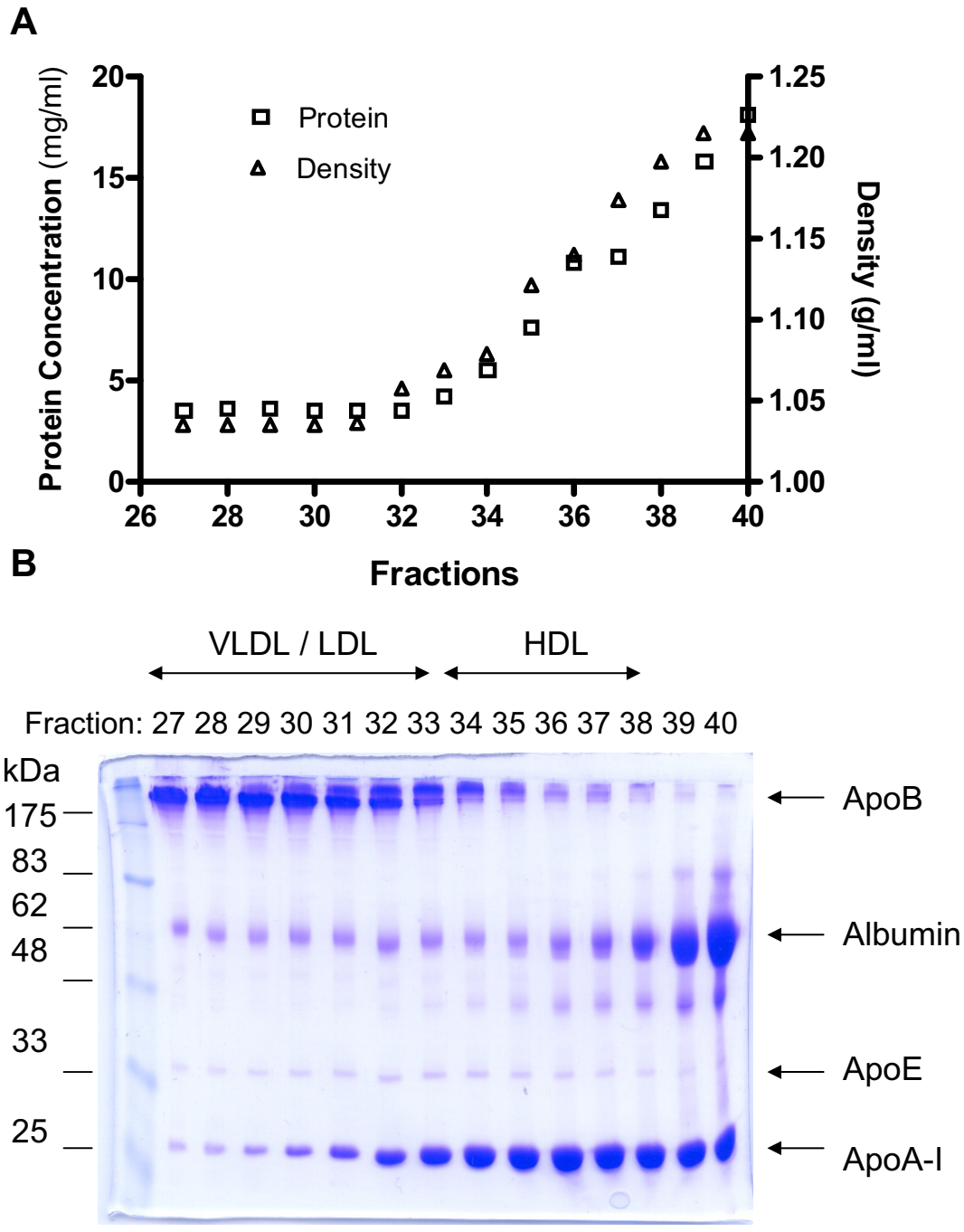
A
Protein Concentration (mg/ml)
Density (g/ml)
Protein
Density
20
15
10
5
0
1.25
1.20
1.15
1.10
1.05
1.00
26
28
30
32
34
36
38
40
Fractions
B
VLDL / LDL
HDL
Fraction: 27 28 29 30 31 32 33 34 35 36 37 38 39 40
kDa
175
83
62
48
33
25
ApoB
Albumin
ApoE
ApoA-I

Figure 4-7.

The upper fraction, expected to contain HDL_3, was dialysed against 1.21 g/ml KBr in TBS before a final round of ultracentrifugation (150,000 ×*g*, 40 hours, 4°C). The resulting upper fraction, expected to contain pure HDL_3, was dialysed extensively against TBS and stored under nitrogen in the dark at 4°C. The protein content from each fraction was determined and samples (10 µg of protein) were subjected to 12% SDS-PAGE and Coomassie blue staining (Figure 4-8). The results show that the upper fraction from the final ultracentrifugation contained essentially pure ApoA-I (~5 mg/ml of protein). Following establishment of the technique, the purity of resulting HDL_3 was checked routinely by SDS-PAGE and Coomassie blue.

4.4.1.3 Fluorescent labelling of HDL_3

For the purposes of measuring lipid uptake from HDL_3, the lipoproteins were labelled with the fluorescent phospholipid analogue DiI (see 2.6.3). This lipid analogue has been used extensively to measure lipid uptake from HDL and as a model for selective uptake of CE from HDL (Gu et al., 1998, Calvo et al., 1998, Gu et al., 2000). Following overnight labelling with DiI and re-isolation of the labelled product by ultracentrifugation (1.21 g/ml), HDL_3-DiI was dialysed extensively against TBS. The purified HDL_3-DiI was stored under nitrogen at 4°C in the dark and used within two weeks of preparation. SDS-PAGE and Coomassie blue staining was used routinely to confirm the purity of HDL_3-DiI (not shown).

4.4.2 HDL_3-DiI uptake by transfected cell lines

4.4.2.1 Uptake of HDL_3-DiI by transfected H4IIE cell lines

To investigate the influences of FAT/CD36 and caveolin-1-EGFP expression on uptake of DiI from HDL_3-DiI, H4IIE rat hepatoma cells (H4IIE (5A)), and the transfectants H4IIE-FAT/CD36 (1A), H4IIE (5A) + caveolin-1-EGFP and H4IIE-FAT/CD36 (1A) + caveolin-1-EGFP were grown on coverslips and cultured with 10 µg/ml of HDL_3-DiI for 2 hours at 37 °C. The cell preparations were then analysed immediately by fluorescence microscopy (see 2.4.3). Incubation of H4IIE cells with HDL_3-DiI resulted in punctate staining of the plasma membrane plus staining of intracellular vesicles (Figure 4-9). Importantly, specificity of lipoprotein binding by cells was indicated by the ability of excess (40-fold) unlabelled HDL_3 to inhibit HDL_3-DiI staining (not shown). Furthermore, exposure of cells

Figure 4-7. Preparation of lipoproteins from human plasma using OptiPrep (iodixanol) density gradient ultracentrifugation. Plasma was prepared from the blood from a healthy human donor and mixed with OptiPrep according to manufacturer's instructions, layered atop a cushion of 20% iodixanol and subjected to ultracentrifugation (353,000 ×*g*, 3 hours, 14°C). Fractions were collected from the tops of tubes by upward displacement. **A;** The protein content and density of each fraction was measured by Bradford analysis and refractometry, respectively. **B;** 20μg of protein from each fraction was subjected to 12% SDS-PAGE and gels were stained with Coomassie blue R-250. The molecular weights of markers (lane 1) are indicated, as are the predicted identities of certain plasma proteins (ApoB, albumin, ApoE and ApoA-I).

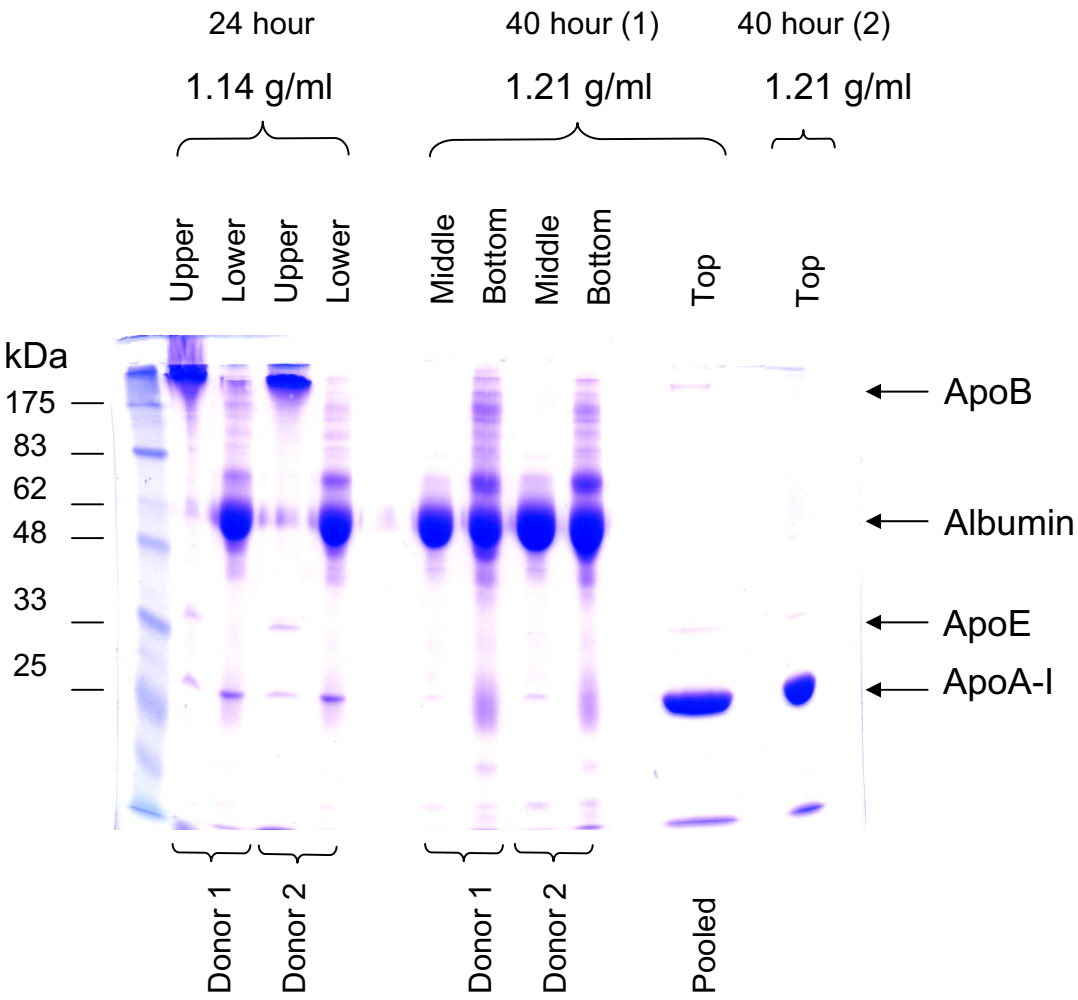
24 hour
40 hour (1)
40 hour (2)
1.14 g/ml
1.21 g/ml
1.21 g/ml
Upper
Lower
Upper
Lower
Middle
Bottom
Middle
Bottom
Top
Top
kDa
175
83
62
48
33
25
ApoB
Albumin
ApoE
ApoA-I
Donor 1
Donor 2
Donor 1
Donor 2
Pooled

Figure 4-8.

Figure 4-8. Preparation of highly purified HDL_3 by sequential ultracentrifugation (1.14-1.21 g/ml). Blood (~50 mls) was collected from two healthy donors and used to prepare plasma. After removal of chylomicrons by ultracentrifugation, the density of plasma was adjusted to 1.14 g/ml using solid KBr. Adjusted plasma was subjected to ultracentrifugation (175,000 ×*g*, 24 hours, 4°C) and upper and lower fractions were collected. The density of the lower fraction was adjusted to 1.21 g/ml and subjected to ultracentrifugation (175,000 ×*g*, 48 hours, 4°C). Upper, middle and lower fractions were collected. The upper fractions were pooled, adjusted to 1.21 g/ml and subjected to another round of ultracentrifugation (175,000 ×*g*, 48 hours, 4°C). The upper fraction was collected and dialysed exhaustively against TBS. 10 μg of protein from each fraction (indicated) was subjected to 12% SDS-PAGE and gels were stained with Coomassie blue. The molecular weights of markers (lane 1) are indicated, as are the predicted identities of certain plasma proteins (ApoB, albumin, ApoE and ApoA-I).

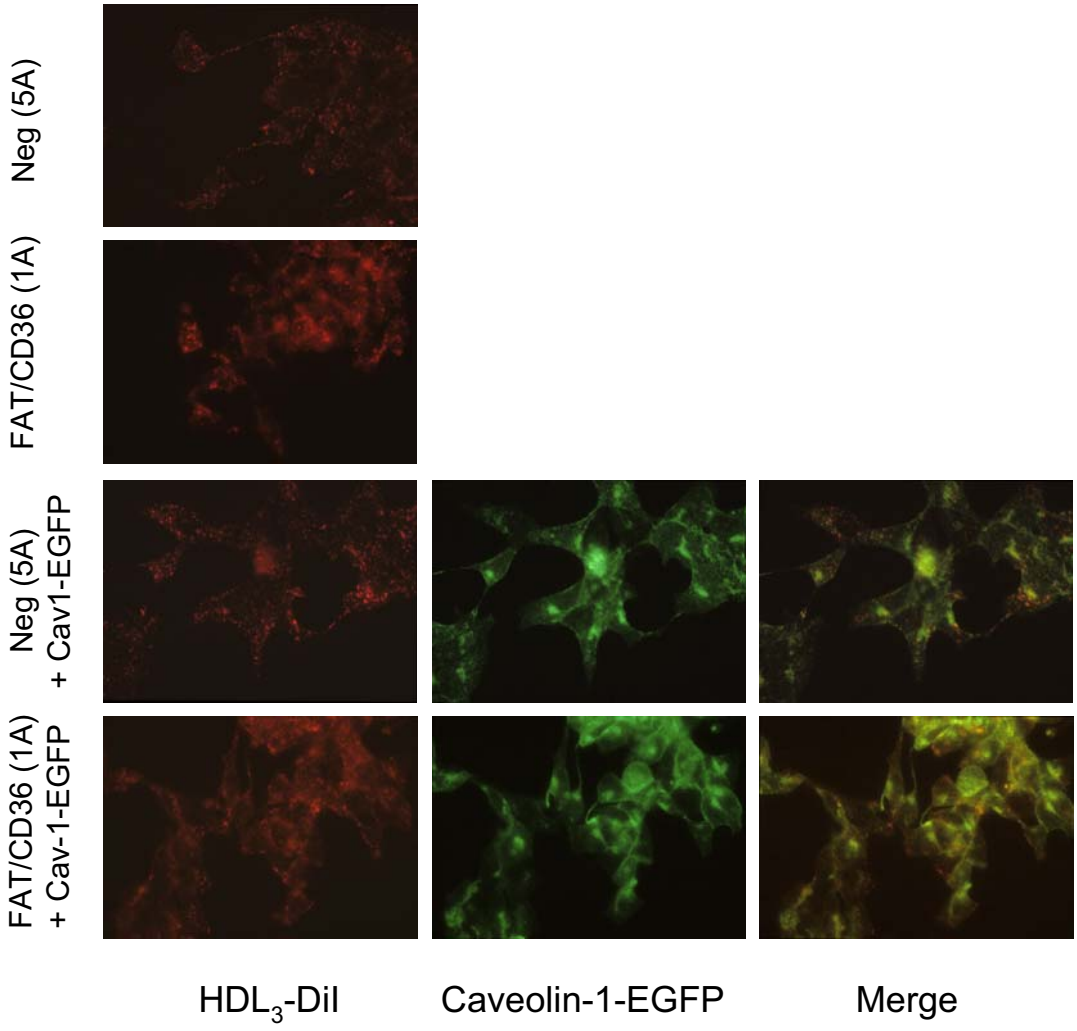
Neg (5A)
FAT/CD36 (1A)
Neg (5A) + Cav1-EGFP
FAT/CD36 (1A) + Cav-1-EGFP
HDL3-DiI
Caveolin-1-EGFP
Merge

Figure 4-9.

to HDL_3-DiI at 4°C or for short periods (10 minutes) at 37°C resulted in minimal fluorescence (not shown), indicating that most of the fluorescence seen after incubation at 37 °C is associated with internalised DiI, rather than bound HDL_3-DiI.

Expression of FAT/CD36 was associated with increased cellular DiI fluorescence and a more diffuse DiI-staining pattern. The former finding is consistent with the flow cytometric analysis of HDL_3-DiI uptake by these cell lines (see 4.4.2.2), while the latter suggests that, in contrast to SR-BI, FAT/CD36 may deliver DiI from HDL_3-DiI to a different metabolic pathway, as has been demonstrated for cholesteryl esters acquired from HDL_3 (Connelly et al., 2003b). To investigate further the subcellular localization of DiI after incubation with HDL_3-DiI, H4IIE (5A) + caveolin-1-EGFP and H4IIE-FAT/CD36 (1A) + caveolin-1-EGFP cell lines were examined for fluorescence of caveolin-1-EGFP and the images overlayed with DiI fluorescence (Figure 4-9). There was some overlap of fluorescence signal from caveolin-1-EGFP and DiI in both of these cell lines. However, the relatively diffuse fluorescence of both labels makes interpretation of the results difficult. Overlap at the plasma membrane could indicate that HDL_3-DiI is bound by SR-BI (and FAT/CD36 in the case of transfectants that express the molecule) in cell-surface caveolae, although the results in 4.3.2 and 4.3.4 indicated that only small amounts of SR-BI are associated with lipid rafts/caveolae (Peng et al., 2004). Intracellular co-localization of caveolin-1-EGFP and DiI could represent trafficking of caveolin-1 and internalised DiI lipid together within the same cytoplasmic organelles.

4.4.2.2 Kinetics of HDL_3-DiI uptake and the influence of FAT/CD36 and/or caveolin-1-EGFP expression.

The kinetics of uptake of HDL_3-DiI were examined in H4IIE (5A), H4IIE-FAT/CD36 (1A), H4IIE (5A) + caveolin-1-EGFP and H4IIE-FAT/CD36 (1A) + caveolin-1-EGFP cell lines. The cells were seeded in 6-well trays (three wells per point) and uptake of HDL_3-DiI (10 μg/ml) was measured by flow cytometry at 30, 60, 90 and 120 minutes after addition of the labelled lipoprotein (Figure 4-10). For all cell lines, uptake of HDL_3-DiI was essentially linear with time. Expression of FAT/CD36 resulted in a small but statistically significant increase in HDL_3-DiI uptake, consistent with previous reports of FAT/CD36-mediated uptake of CE and DiI uptake from HDL (Gu et al., 1998, Connelly et al., 1999).

Figure 4-9. HDL_3-DiI binding and uptake by transfected H4IIE cell lines as determined by fluorescence microscopy. H4IIE (5A), H4IIE-FAT/CD36 (1A), H4IIE (5A) + caveolin-1-EGFP and H4IIE-FAT/CD36 (1A) + caveolin-1-EGFP cells were grown on coverslips overnight and cultured with HDL_3-DiI (10μg/ml) (in DMEM containing 0.5% BSA) for 2 hours. Samples were mounted and immediately visualized using appropriate filter sets and photographed (60× objective). Control experiments showed that background fluorescence was minimal in the absence of caveolin-1-EGFP expression and HDL_3-DiI. Furthermore, DiI-associated fluorescence was minimal when cells were incubations with HDL_3-DiI were performed at 4°C or in the presence of a 40-fold excess of unlabelled HDL_3 (not shown).

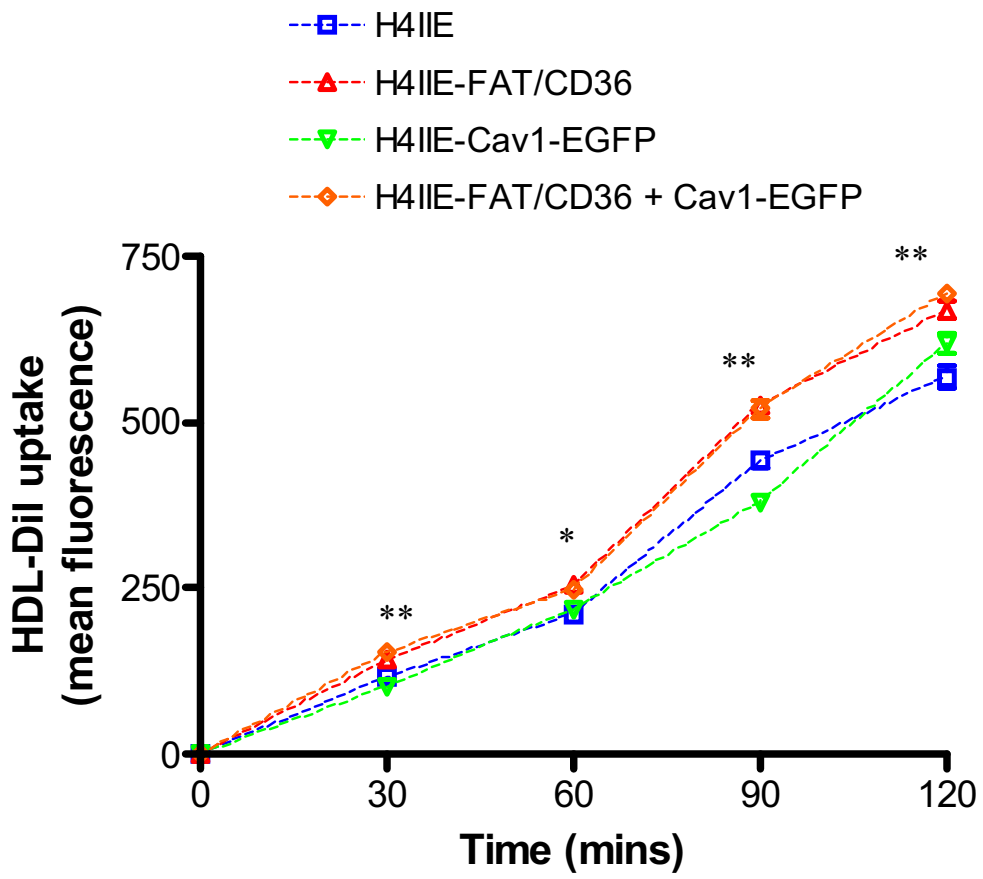
H4IIE
H4IIE-FAT/CD36
H4IIE-Cav1-EGFP
H4IIE-FAT/CD36 + Cav1-EGFP
HDL-DiI uptake
(mean fluorescence)
750
500
250
0
0
30
60
90
120
Time (mins)
**
*
**
**

Figure 4-10.

However, expression of caveolin-1-EGFP in H4IIE cells did not affect uptake of DiI from HDL_3-DiI.

To further examine the influence of FAT/CD36 expression on DiI uptake from HDL_3-DiI, H4IIE (5A) and H4IIE-FAT/CD36 (1A) cell lines were seeded in 6-well trays and uptake of HDL_3-DiI was measured in triplicate after 2 hours of culture with HDL_3-DiI at various concentrations (5, 10, 20, 40 μg/ml) (Figure 4-11). As reported by others using transfected cell lines (Acton et al., 1996, Gu et al., 1998, Calvo et al., 1998), uptake of DiI by H4IIE cells approached saturation at 40 μg/ml HDL_3-DiI and there was significantly greater uptake of DiI in H4IIE-FAT/CD36 (1A) cells than in control H4IIE (5A) cells at all concentrations of HDL_3-DiI.

4.4.2.3 The influence of variations in the level of FAT/CD36 expression on HDL_3-DiI uptake in CHO 1.2C3 cells

In the liver, FAT/CD36 is expressed at levels that are gender- and strain-dependent, against background of relatively constitutively expressed SR-BI. It was hypothesized that when FAT/CD36 is expressed at high levels, it could contribute significantly to selective CE uptake from HDL_3 by mass action. To investigate this hypothesis *in vitro*, CHO 1.2C3 cells (which do not express endogenous SR-B1) were cultured in the presence of a range of doxycycline concentrations that have been shown to affect the expression of FAT/CD36 in a dose-dependent manner (see 3.3.3.5). Uptake of DiI from HDL_3-DiI was measured by flow cytometry.

CHO 1.2C3 cells and CHO 1.2C4 cells (FAT/CD36-negative, control) were seeded in 6-well trays and cultured for 96 hours in the presence of doxycycline at 0, 0.01, 0.1, 1, 10 or 100 ng/ml. Medium, including doxycycline, was replaced every 48 hours to compensate for turnover of doxycycline. The cells were then washed twice and culture was continued for 90 minutes in RPMI containing 0.5% BSA plus 10 μg/ml HDL_3-DiI. The monolayers were then washed twice with PBS, harvested and transferred to FACS tubes. After labelling with biotinylated mAb UA009 followed by streptavidin-FITC, the cells were analysed by two colour flow cytometry to measure cell-associated DiI fluorescence and level of expression of FAT/CD36 simultaneously. Analysis of data by scatter diagrams (Figure 4-12A) showed that overall, there was no significant correlation between level of

Figure 4-10. Time-course of HDL_3-DiI uptake by H4IIE (5A), H4IIE-FAT/CD36 (1A), H4IIE (5A) + caveolin-1-EGFP and H4IIE-FAT/CD36 (1A) + caveolin-1-EGFP cell lines. Cells were cultured for the indicated times with HDL_3-DiI (10 μg/ml) before washing and harvesting of cells and immediate analysis of HDL_3-DiI uptake by flow cytometry. Data are means ± SD (n=3). *, $P < 0.05$; **, $P < 0.01$.

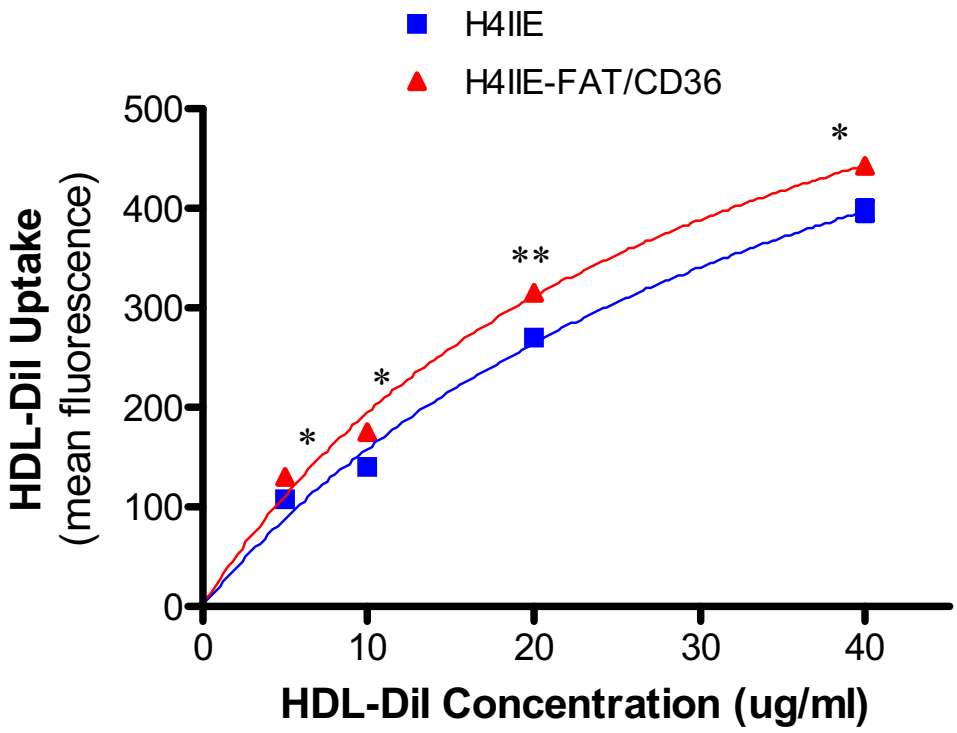
H4IIE
H4IIE-FAT/CD36
HDL-DiI Uptake
(mean fluorescence)
500
400
300
200
100
0
0
10
20
30
40
HDL-DiI Concentration (ug/ml)
*
*
**
*

Figure 4-11.

Figure 4-11. Saturation curves of HDL_3-DiI binding and uptake by H4IIE (5A) and H4IIE-FAT/CD36 (1A) cell lines at 37°C. Cells were cultured for 2 hours with the indicated concentration of HDL_3-DiI, before washing and harvesting of cells and immediate analysis of HDL_3-DiI uptake by flow cytometry. Data are means ± SD (n=3). *, $P < 0.05$; **, $P < 0.01$.

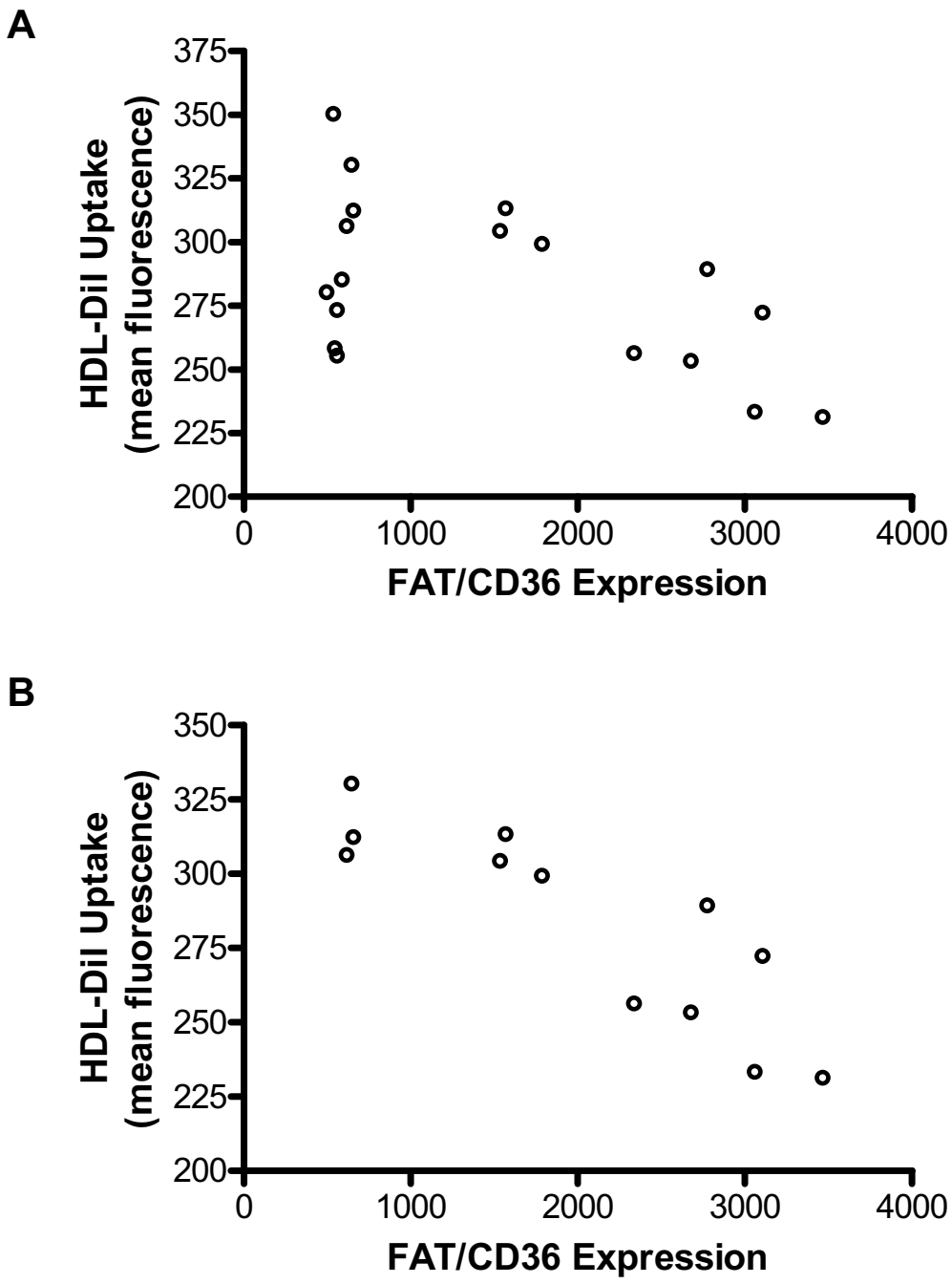
A
HDL-DiI Uptake
(mean fluorescence)
375
350
325
300
275
250
225
200
0
1000
2000
3000
4000
FAT/CD36 Expression
B
HDL-DiI Uptake
(mean fluorescence)
350
325
300
275
250
225
200
0
1000
2000
3000
4000
FAT/CD36 Expression

Figure 4-12.

FAT/CD36 expression and uptake of DiI (Spearman analysis, $P > 0.05$, $r = -0.34$). However, when the results obtained for CHO 1.2C4 cells (negative control) were excluded from the analysis, FAT/CD36 expression was negatively correlated with DiI uptake from HDL_3 (Spearman analysis, $P < 0.0005$, $r = -0.85$) (Figure 4-12B). In some respects the latter analysis may be more valid as all results were obtained for the same cell line (CHO 1.2C3), such that clone-specific differences are not influential.

4.4.2.4 The influence of FAT/CD36 expression on SR-BI-mediated HDL-lipid uptake in CHO 1.2C3 cells

While overall, there was no positive correlation between the level of FAT/CD36 expression and DiI uptake in CHO 1.2C3 cells, it was hypothesized that FAT/CD36 might enhance SR-BI-mediated HDL_3-DiI uptake in a cooperative manner. To investigate this possibility, uptake of DiI from HDL_3 by CHO 1.2C3 cells was measured in cells transiently transfected with an SR-BI expression vector or an empty control vector and cultured in the presence (↓ FAT/CD36) or absence (↑ FAT/CD36) of doxycycline (100 ng/ml). To accomplish this work, an SR-BI expression vector, pcDNA3~mycSR-BI, was produced using *SR-BI* cDNA obtained from rat liver cDNA by PCR-amplification (using the primers SRBI-myc FP, SR-BI RPrf. See Table 2-1). The resulting PCR product was cloned into the *Hind*III and *Xba*I restriction sites of the multiple cloning site of pcDNA3 (see Figure 3-1). The forward primer encodes a C-myc-epitope tag, such that the insert encodes recombinant SR-BI containing a C-myc epitope tag at its N-terminus. Automated sequencing was used to confirm that the *SR-BI* cDNA sequence matched published sequences for rat and that the C-myc epitope tag was in-frame with the *SR-BI* sequence.

Cells were seeded in 6-well trays and cultured with or without doxycycline (100 ng/ml) for 96 hours. At this point, they were transfected with pcDNA3 (empty vector control) or pcDNA3-mycSR-BI using FuGene 6 (see 2.2.5). Twenty-four hours later, HDL_3-DiI (10 μg/ml) was added and uptake after 2hours was measured (triplicate wells) by flow cytometry (Figure 4-13A). Expression of FAT/CD36 and myc-SR-BI by cells from parallel cultures was measured by Western blotting, using antibodies directed against FAT/CD36 (mAb MO25) or C-myc (mAb 9E10), respectively (Figure 4-13B). Control experiments demonstrated that approximately 15% of cells produced SR-B1 after

Figure 4-12. The correlation between FAT/CD36 expression levels and HDL_3-DiI uptake. **A;** CHO 1.2C3 cells and CHO 1.2C4 (control) cells were cultured for 96 hours in the presence of doxycycline at the indicated concentrations (0, 0.01, 0.1, 10 or 100 ng/ml) to give a range of FAT/CD36 expression levels. Cells were then washed and cultured for 90 minutes with HDL_3-DiI (10μg/ml). Cells then harvested and labelled by indirect immunofluorescence using biotinylated mAb UA009 and streptavidin-conjugated PE. Cells were immediately analysed by flow cytometry for DiI- and FAT/CD36-associated fluorescence. Satisfactory compensation and voltage settings for flow cytometric analysis were achieved by analysis of unlabelled, DiI-labelled and UA009/FITC-labelled cells, respectively. Pilot experiments demonstrated that DiI fluorescence was not significantly affected by immunofluorescent labelling or fixation (not shown). No significant correlation existed between FAT/CD36 expression and HDL_3-DiI uptake (Spearman analysis, $P > 0.05$, $r = -0.34$). **B;** However, when data obtained for CHO 1.2C4 cells (control) were excluded from the analysis, FAT/CD36 expression levels and DiI uptake were negatively correlated (Spearman analysis, $P < 0.0005$, $r = -0.85$).

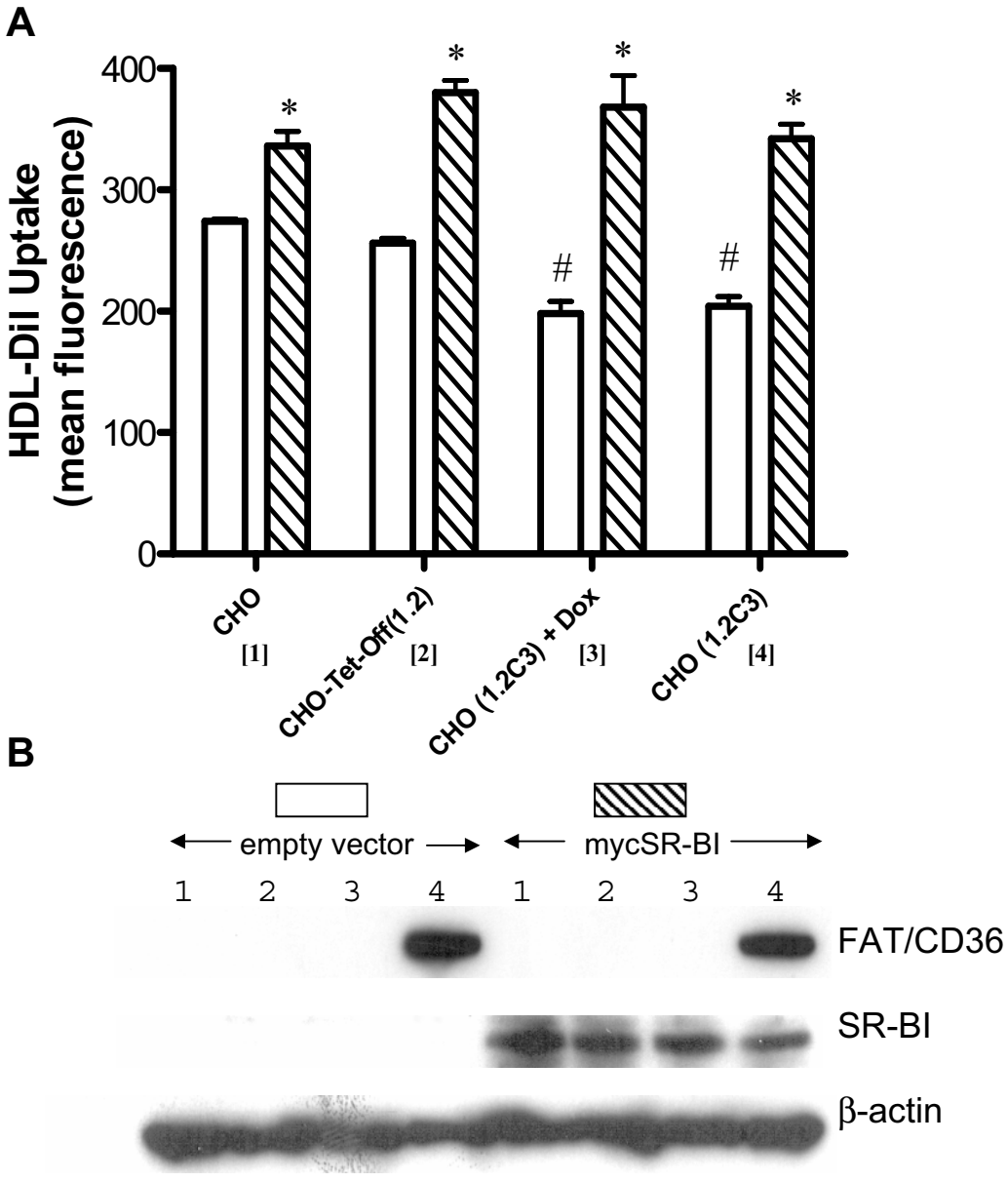
A
HDL-DiI Uptake
(mean fluorescence)
400
300
200
100
0
*
*
*
*
#
#
CHO
[1]
CHO-Tet-Off(1.2)
[2]
CHO (1.2C3) + Dox
[3]
CHO (1.2C3)
[4]
B
empty vector
mycSR-BI
1 2 3 4 1 2 3 4
FAT/CD36
SR-BI
β-actin

Figure 4-13.

transfection using this technique and that transfection efficiencies were not affected by doxycycline (not shown).

The results show that expression of SR-BI in the parent cell lines CHO and CHO-Tet-Off 1.2 and in CHO 1.2C3 cells enhanced uptake of HDL_3-DiI significantly. However, high-level expression of FAT/CD36 did not increase HDL_3-DiI uptake above that due to SR-BI alone. Interestingly, in cells that were not transfected to produce SR-BI, expression of FAT/CD36 reduced uptake of HDL_3-DiI significantly in comparison with the parent cell lines CHO and CHO-Tet-Off 1.2. This finding is consistent with the negative correlation observed between DiI uptake and FAT/CD36 when expressed at higher levels (Figure 4.12).

4.5 Summary

The work described in this Chapter investigated the hypothesis that FAT/CD36 contributes cooperatively in the process of SR-BI-mediated selective uptake of HDL-associated lipid in the liver. The first part of the investigation examined the subcellular localization of the two receptors, in liver, in the H4IIE hepatoma cell line and in transfected H4IIE derivatives. The results demonstrated that, in contrast to some reports (Babitt et al., 1997, Rhainds et al., 2004), most SR-BI is not associated with classical low-density, detergent-resistant lipid rafts. This finding is consistent with those of others using other cell lines including transfected CHO, COS-7 and WI38 (Peng et al., 2004). It appears, therefore, that the majority of SR-BI is not closely associated with either FAT/CD36 or caveolin-1 in lipid raft domains. Rather, most of the SR-B1 was found in sucrose density gradient fractions of intermediate to high density. This finding is consistent with the reported localization of SR-BI on microvilli rather than in caveolae in steroidogenic tissues (Reaven et al., 1998, Reaven et al., 2000, Azhar et al., 2002). However, it is unclear whether SR-BI localizes to microvilli in hepatocytes. The molecule has been found on both the apical (canalicular) and basolateral (sinusoidal) membranes of hepatocytes (Kozarsky et al., 1997), and in the intracellular endosomal recycling compartment (Silver et al., 2001). Canalicular localization of SR-B1 in hepatocytes has prompted the suggestion that the molecule might be involved directly in biliary cholesterol secretion (Silver et al., 2001), but this is controversial because other studies have failed to confirm its presence in

canalicular membranes (Mardones et al., 2003, Stangl et al., 2002). The subcellular distribution of FAT/CD36 has not been studied at the whole cell level in hepatocytes and it is unknown whether it is associated predominantly with apical and/or basolateral membranes. However, the biochemical study (Figure 4.6) indicates that there is minimal overlap with SR-BI in lipid rafts.

With respect to the putative role of FAT/CD36 as an additional mediator of HDL-CE selective uptake by the liver, expression of FAT/CD36 resulted in a moderate (~10%) but statistically significant increase in uptake of DiI from fluorescently labelled HDL_3 by H4IIE hepatoma cells. This contribution may be of some physiological significance but is not indicative of a cooperative effect on SR-BI-mediated HDL-lipid uptake. The observed increase in HDL_3-DiI uptake was consistent with previous reports of inefficient FAT/CD36-mediated HDL-CE and HDL-lipid uptake in transfected COS-7 and CHO cells (Connelly et al., 1999, Gu et al., 1998). Expression of caveolin-1-EGFP in these cells, however, did not significantly alter HDL_3-DiI uptake. This finding was consistent with some reports of unaffected (Wang et al., 2003), or minimally affected (Frank et al., 2001b) HDL-lipid uptake in cells overexpressing caveolin-1 and contrasts the results of other studies that report more profound effects of caveolin-1 on HDL-lipid metabolism (Graf et al., 1999, Matveev et al., 1999, Matveev et al., 2001, Truong et al., 2006).

The studies of HDL_3-DiI uptake in the CHO 1.2C3 cell line have strengthened the case against a major contribution of FAT/CD36 to HDL-lipid uptake. These results demonstrated FAT/CD36 expression did not enhance HDL_3-DiI uptake in these cells and, moreover, that FAT/CD36 expression was negatively correlated with HDL_3-DiI uptake when the results for HDL_3-DiI uptake by control cell lines were excluded from the analysis. This finding suggests that the relatively high affinity of HDL_3-binding by FAT/CD36 may compete with that of endogenous SR-BI, expressed at low levels by CHO cells, such that efficient SR-BI-mediated HDL_3-DiI uptake is impaired by high-level expression of FAT/CD36. Further, these studies demonstrated that FAT/CD36 expression did not enhance SR-BI-mediated HDL_3-DiI uptake in cells transiently transfected with an SR-BI expression vector. In these cells HDL_3-DiI lipid uptake was greatly enhanced (30-80%) by SR-BI expression, although only 10-15% of cells were transfected. It was apparent from these results that the levels of HDL_3-DiI uptake were significantly lower in

FAT/CD36 expressing 1.2C3 cells than in parental control cell lines, supporting the apparent ability of FAT/CD36 to compete with endogenous SR-BI for HDL_3-DiI binding.

Whilst FAT/CD36-deficient mice have significantly increased plasma HDL cholesterol levels (Febbraio et al., 1999), authors of this work postulated that this phenotype could be secondary to changes in fatty acid metabolism that result in increased VLDL-triglyceride levels which, in-turn, could cause elevated HDL-cholesterol levels. Alternatively, increased plasma HDL-cholesterol in these mice could result from reduced binding and clearance of HDL. Indeed, FAT/CD36 expression *in vitro* has been shown to increase HDL-CE uptake, albeit less efficiently than SR-BI (Gu et al., 1998, Connelly et al., 1999). To investigate whether FAT/CD36-mediated HDL-CE selective uptake is of physiological significance, de Villiers *et. al.* assessed lipoprotein cholesterol profiles of mice in which adenoviral vectors were used to deliver hepatic overexpression of FAT/CD36 or SR-BI (de Villiers et al., 2001). While hepatic SR-BI overexpression resulted in dramatically reduced lipoprotein cholesterol levels, particularly in HDL fractions, FAT/CD36 expression had no effect on lipoprotein cholesterol levels. Although these results and the findings of the study described above indicate that FAT/CD36 does not greatly contribute to HDL-lipid uptake, thorough investigation of lipid metabolism in an *in vivo* model of hepatic FAT/CD36 overexpression is required to determine the primary function of the receptor in the liver.

Figure 4-13. FAT/CD36 expression does not cooperatively enhance SR-BI mediated HDL_3-DiI uptake in CHO 1.2C3 cells. CHO 1.2C3 cells were cultured for 96 hours in the presence or absence of doxycycline (100 ng/ml). Control groups included FAT/CD36-negative parental cell lines (CHO and CHO-Tet-Off 1.2). Cells were then transfected with the SR-BI expression plasmid pcDNA3-C-myc-SR-BI or the empty plasmid pcDNA3. Twenty-four hours later HDL_3-DiI uptake (10μg/ml, 2hour incubation) was assessed by flow cytometry (**A**). Data are means ± SD (n=3). *, $P < 0.01$ significantly different from empty plasmid (pcDNA3) transfected equivalents. #, $P < 0.01$ significantly different from empty plasmid (pcDNA3) transfected CHO-Tet-Off 1.2 cells. **B;** Western analysis of expression of FAT/CD36 and SR-BI in parallel cultures. 20μg of protein from each post-nuclear whole cell lysate was subjected to 12% SDS-PAGE and Western blotting with antibodies directed against C-myc (mAb 9E10) (epitope tag for transfected SR-BI), FAT/CD36 (mAb MO25) or β-actin as indicated. FAT/CD36 was detectable in lysates of CHO 1.2C3 cells cultured in the presence of doxycycline upon longer exposure of PVDF membranes to X-ray film (not shown).